



Norwegian University of
Science and Technology

Pressure pulsations and thermodynamic efficiency measurements at Smeland power plant

Johannes Opedal Kverno
Vegard Selvåg Ulvan

Master of Energy and Environmental Engineering

Submission date: June 2018

Supervisor: Ole Gunnar Dahlhaug, EPT

Co-supervisor: Torbjørn Nielsen, EPT
Bjørn Winther Solemslie, EPT

Norwegian University of Science and Technology
Department of Energy and Process Engineering

EPT-M-2018-50

MASTEROPPGAVE

for

Student Johannes Kverno

Våren 2018

Trykkpulsasjoner ved Smeland Kraftverk
*Pressure pulsations at Smeland Power Plant***Bakgrunn**

Agder Energi har erfart kraftige vibrasjoner ved Smeland Kraftverk som ligger i Mandalsvassdraget i Vest-Agder. Vibrasjonene har en frekvens på ca. 2,8 Hz og det kan synes som at årsaken til dette kommer fra strømmingen i sugerøret. Turbinen er utstyrt med luftinnslipp til sugerøret og dette har muligens endret seg over tid. Det er ønskelig å gjennomføre både trykkpulsasjon- og virkningsgrads-måling på turbinen for å se om man kan finne årsaken til vibrasjonene. Hoved oppgaven vil fokusere på gjennomføringen av målinger på Smeland kraftverk i løpet av våren 2018.

Målingene ved Smeland Kraftverk gjennomføres i samarbeid med student Vegard Ulvan

Mål

Gjennomføre trykkpulsasjon-målinger ved Smeland Kraftverk og evaluere måleresultater fra Santa Rosa Kraftverk.

Oppgaven bearbeides ut fra følgende punkter:

1. Litteraturstudie
 - a. Evaluering av trykkpulsasjoner i Francis turbiner
2. Software
 - a. Labview skal benyttes for målinger i laboratoriet
 - b. Matlab skal benyttes til evaluering av resultater
3. Forberedelser i Vannkraftlaboratoriet
 - a. Gjør deg kjent med Francis turbin rigg
 - b. Gjennomføre statisk og dynamisk kalibrering av instrumenter som skal benyttes til trykk-måling på kraftverket
4. Måling på Smeland Kraftverk
 - a. Gjennomføre trykkmåling er på hele operasjonsområdet
 - b. Gjennomføre virkningsgradsmåling i samarbeid med Vegard Ulvan
 - c. Evaluering av måleresultater
5. Evaluering av måleresultater fra Santa Rosa kraftverk
6. Dersom studenten skal dra til Nepal på ekskursjon så skal tidligere arbeid fra prosjektet og det videre arbeidet i denne hovedoppgaven bli skrevet som en egen publikasjon og presentert på konferansen: 8th International symposium on Current Research in Hydraulic Turbines (CRHT-VIII) ved Kathmandu University i Mars 2018.
7. Dersom det er tid tilgjengelig skal det gjennomføres målinger på modell turbin i Vannkraftlaboratoriet
 - a. Trykkpulsasjonsmålinger på modell turbin med fokus på fullast
 - b. Evaluering av måleresultater

Senest 14 dager etter utlevering av oppgaven skal kandidaten levere/sendte instituttet en detaljert fremdrift- og eventuelt forsøksplan for oppgaven til evaluering og eventuelt diskusjon med faglig ansvarlig/veiledere. Detaljer ved eventuell utførelse av dataprogrammer skal avtales nærmere i samråd med faglig ansvarlig.

Besvarelsen redigeres mest mulig som en forskningsrapport med et sammendrag både på norsk og engelsk, konklusjon, litteraturliste, innholdsfortegnelse etc. Ved utarbeidelsen av teksten skal kandidaten legge vekt på å gjøre teksten oversiktlig og velskrevet. Med henblikk på lesning av besvarelsen er det viktig at de nødvendige henvisninger for korresponderende steder i tekst, tabeller og figurer anføres på begge steder. Ved bedømmelsen legges det stor vekt på at resultatene er grundig bearbeidet, at de oppstilles tabellarisk og/eller grafisk på en oversiktlig måte, og at de er diskutert utførlig.

Alle benyttede kilder, også muntlige opplysninger, skal oppgis på fullstendig måte. For tidsskrifter og bøker oppgis forfatter, tittel, årgang, sidetall og eventuelt figurnummer.

Det forutsettes at kandidaten tar initiativ til og holder nødvendig kontakt med faglærer og veileder(e). Kandidaten skal rette seg etter de reglementer og retningslinjer som gjelder ved alle (andre) fagmiljøer som kandidaten har kontakt med gjennom sin utførelse av oppgaven, samt etter eventuelle pålegg fra Institutt for energi- og prosesssteknikk.

Risikovurdering av kandidatens arbeid skal gjennomføres i henhold til instituttets prosedyrer. Risikovurderingen skal dokumenteres og inngå som del av besvarelsen. Hendelser relatert til kandidatens arbeid med uheldig innvirkning på helse, miljø eller sikkerhet, skal dokumenteres og inngå som en del av besvarelsen. Hvis dokumentasjonen på risikovurderingen utgjør veldig mange sider, leveres den fulle versjonen elektronisk til veileder og et utdrag inkluderes i besvarelsen.

I henhold til ”Utfyllende regler til studieforskriften for teknologistudiet/sivilingeniørstudiet” ved NTNU § 20, forbeholder instituttet seg retten til å benytte alle resultater og data til undervisnings- og forskningsformål, samt til fremtidige publikasjoner.

Besvarelsen leveres digitalt i DAIM. Et faglig sammendrag med oppgavens tittel, kandidatens navn, veileders navn, årstall, institutt navn, og NTNUs logo og navn, leveres til instituttet som en separat pdf-fil. Etter avtale leveres besvarelse og evt. annet materiale til veileder i digitalt format.

- Arbeid i Vannkraftlaboratoriet
- Feltarbeid

NTNU, Institutt for energi- og prosesssteknikk, 15. januar 2018


Ole Gunnar Dahlhaug
Faglig ansvarlig/veileder

Medveileder: Torbjørn Nielsen

EPT-M-2018-100

MASTEROPPGAVE

for

Student Vegard Ulvan

Våren 2018

Termodynamisk virkningsgradsmåling ved Smeland Kraftverk
*Thermodynamic efficiency measurements at Smeland Power Plant***Bakgrunn**

Agder Energi har erfart kraftige vibrasjoner ved Smeland Kraftverk som ligger i Mandalsvassdraget i Vest-Agder. Vibrasjonene har en frekvens på ca. 2,8 Hz og det kan synes som at årsaken til dette kommer fra strømmingen i sugerøret. Turbinen er utstyrt med luftinnslipp til sugerøret og dette har muligens endret seg over tid. Det er ønskelig å gjennomføre både trykkpulsasjon- og virkningsgradsmåling på turbinen for å se om man kan finne årsaken til vibrasjonene. Hoved oppgaven vil fokusere på gjennomføringen av virkningsgradsmålinger på Smeland kraftverk i løpet av våren 2018.

Målingene ved Smeland Kraftverk gjennomføres i samarbeid med student Johannes Kverno

Mål

Gjennomføre termodynamisk virkningsgradsmåling ved Smeland Kraftverk

Oppgaven bearbeides ut fra følgende punkter:

1. Litteraturstudie
 - a. Usikkerhets analyse av virkningsgradsmålinger i Francis turbiner
2. Software
 - a. Labview skal benyttes for målinger i felt
 - b. Matlab skal benyttes til evaluering av resultater
3. Forberedelser i Vannkraftlaboratoriet
 - a. Gjennomføre kalibrering av instrumenter som skal benyttes til virkningsgradsmåling på kraftverket
4. Måling på Smeland Kraftverk
 - a. Gjennomføre virkningsgradsmålinger er på hele operasjonsområdet
 - b. Gjennomføre trykkpulsasjonsmålinger i samarbeid med Vegard Ulvan
 - c. Evaluering av måleresultater
5. Dersom studenten skal dra til Nepal på ekskursjon så skal tidligere arbeid fra prosjektet og det videre arbeidet i denne hovedoppgaven bli skrevet som en egen publikasjon og presentert på konferansen: *8th International symposium on Current Research in Hydraulic Turbines (CRHT-VIII)* ved Kathmandu University i Mars 2018.
6. Dersom det er tid tilgjengelig skal det gjennomføres målinger på Ylja Kraftverk i samarbeid med student Trine Brath

Senest 14 dager etter utlevering av oppgaven skal kandidaten levere/sende instituttet en detaljert fremdrift- og eventuelt forsøksplan for oppgaven til evaluering og eventuelt diskusjon med faglig ansvarlig/veiledere. Detaljer ved eventuell utførelse av dataprogrammer skal avtales nærmere i samråd med faglig ansvarlig.

Besvarelsen redigeres mest mulig som en forskningsrapport med et sammendrag både på norsk og engelsk, konklusjon, litteraturliste, innholdsfortegnelse etc. Ved utarbeidelsen av teksten skal kandidaten legge vekt på å gjøre teksten oversiktlig og velskrevet. Med henblikk på lesning av besvarelsen er det viktig at de nødvendige henvisninger for korresponderende steder i tekst, tabeller og figurer anføres på begge steder. Ved bedømmelsen legges det stor vekt på at resultatene er grundig bearbeidet, at de oppstilles tabellarisk og/eller grafisk på en oversiktlig måte, og at de er diskutert utførlig.

Alle benyttede kilder, også muntlige opplysninger, skal oppgis på fullstendig måte. For tidsskrifter og bøker oppgis forfatter, tittel, årgang, sidetall og eventuelt figurnummer.

Det forutsettes at kandidaten tar initiativ til og holder nødvendig kontakt med faglærer og veileder(e). Kandidaten skal rette seg etter de reglementer og retningslinjer som gjelder ved alle (andre) fagmiljøer som kandidaten har kontakt med gjennom sin utførelse av oppgaven, samt etter eventuelle pålegg fra Institutt for energi- og prosesssteknikk.

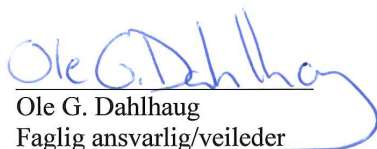
Risikovurdering av kandidatens arbeid skal gjennomføres i henhold til instituttets prosedyrer. Risikovurderingen skal dokumenteres og inngå som del av besvarelsen. Hendelser relatert til kandidatens arbeid med uheldig innvirkning på helse, miljø eller sikkerhet, skal dokumenteres og inngå som en del av besvarelsen. Hvis dokumentasjonen på risikovurderingen utgjør veldig mange sider, leveres den fulle versjonen elektronisk til veileder og et utdrag inkluderes i besvarelsen.

I henhold til ”Utfyllende regler til studieforskriften for teknologistudiet/sivilingeniørstudiet” ved NTNU § 20, forbeholder instituttet seg retten til å benytte alle resultater og data til undervisnings- og forskningsformål, samt til fremtidige publikasjoner.

Besvarelsen leveres digitalt i DAIM. Et faglig sammendrag med oppgavens tittel, kandidatens navn, veileders navn, årstall, institutt navn, og NTNUs logo og navn, leveres til instituttet som en separat pdf-fil. Etter avtale leveres besvarelse og evt. annet materiale til veileder i digitalt format.

- Arbeid i Vannkraftlaboratoriet
- Feltarbeid

NTNU, Institutt for energi- og prosesssteknikk, 15. januar 2018


Ole G. Dahlhaug
Faglig ansvarlig/veileder

Medveileder: Bjørn Winther Solemslie

*Til minne om Beste,
sivilingeniør Halldor Opedal (1928-2005),
som vekket interessen som har ført meg der jeg er i dag.*

-Johannes

Summary

In this master thesis, the cause and solution of a problem at Smeland power plant have been thoroughly investigated. The power plant has for years experienced severe pressure pulsations in their Francis turbine at full load, and the owner, Agder Energi, wanted to know why and what could be done to stop the pulsations.

In order to fully understand the problem, measurements of both the pressure pulsations and efficiency were made. The pressure pulsations were measured using five pressure transducers; two on the draft tube cone 180° apart, one before the main inlet valve, one on the inlet before the spiral casing, and one on the labyrinth leakage water. The efficiency was found using the thermodynamic method, mainly measuring the temperature increase and pressure drop before and after the runner. To find a solution to the problem, air injection was fully tested through a check valve that went through the runner in the centre. To measure the effect of air injection, two pressure transducers were placed on the draft tube cone as done previously. To measure the amount of air, an orifice plate was placed in the air pipe, and the pressure drop and temperature were measured. This allowed for a calculation of the air flow rate.

The hydraulic efficiency measurements showed a runner with seemingly unchanged efficiency from the commissioning measurements in 1985. This indicated that the pressure pulsations had no effect on the efficiency, or has been present in both measurements. Air injection had apparently no effect on the efficiency. The peak to peak pressure in the draft tube cone had a magnitude of about 20 % of the design head in the worst point of operation. Injecting 1,266 kg/min of air reduced the peak-to-peak pressure by about 97 %. The standing hypothesis is that the pressure pulsation problem at Smeland power plant stems from a full load vortex bubble oscillating and resonating with the penstock and/or outlet tunnel. Injecting air would change the bubble's volume, and therefore its eigenfrequency, pushing it out of resonance. To deal with the pressure pulsations, it is recommended that Agder Energi implement an air injection system at Smeland power plant, that pumps in an adequate amount of air around full load.

Sammendrag

I denne masteroppgaven er årsaken og løsningen til et problem hos Smeland kraftverk grundig undersøkt. Kraftverket har gjennom mange år opplevd kraftige trykkpulseringer i deres Francis turbin under fullast, og eieren Agder Energi ønsker å vite hvorfor og hvordan bli kvitt pulseringene.

For å få et helhetlig overblikk over problemet er det blitt gjort målinger på trykkpulseringene og turbinens hydrauliske virkningsgrad. Trykkpulseringene ble målt med fem trykktransdusere; to på sugerørskonusen 180° fra hverandre, én før innløpsventilen, én på innløpet før spiraltrømmen, og én på røret til labyrinthvannet fra turbinen. Virkningsgraden ble funnet via den termodynamiske metoden, hvor man hovedsakelig måler temperaturøkningen og trykkfallet over turbinen. På utkikk etter en løsning på problemet ble effekten av luftinjeksjon gjennom en enveisventil på løpehjulet omfattende testet. For å måle effekten av luftinjeksjonen ble to trykktransdusere plassert på sugerørskonusen som tidligere. For å måle mengden luft som ble injisert ble en plate med hull plassert i luftstrømmen, og trykkfallet samt temperaturen ble målt. Dette muliggjorde en beregning av luftstrømmen.

Den hydrauliske virkningsgraden viste et løpehjul med tilsynelatende uendret virkningsgrad fra igangsettelsesmålingene fra 1985. Dette indikerte enten at trykkpulseringene har vært tilstedeværende fra igangsettelsen, eller at de har ingen merkbar innvirkning på virkningsgraden. Luftinjeksjon hadde tilsynelatende ingen effekt på virkningsgraden. “Peak-to-peak” trykket i sugerørskonusen hadde en størrelse på rundt 20 % av nominell fallhøyde på verste driftspunkt. Injisering av 1,266 kg/min luft reduserte “peak-to-peak” trykket med 97 %. Den mest aktuelle teorien på trykkpulseringene på Smeland kraftverk er at det er en strømvirvel/gassboble under fullast som pulserer, og resonerer med svingesjakten og/eller utløpstunnelen. En innsprøytning av luft vil endre boblens volum og dermed dens egenfrekvens, og flytter den ut av frekvensområdet hvor resonans oppstår. For å stoppe trykkpulseringene er det anbefalt at Agder Energi implementerer et luftinjeksjonssystem som tilfører nok mengde luft når trykkpulseringene oppstår.

Preface

This master thesis was conducted at the Waterpower Laboratory at NTNU during the spring semester of 2018 as a continuation of the specialisation project completed in the fall semester 2017. The problem we have been working on, and solved, was given by Agder Energi, an energy company based in Kristiansand, Norway.

This master thesis' main work have been the problem given by Agder Energi. However, throughout the master thesis there has been both extra and additional work done. Extra work was done on Agder Energi's power plant, in the form of a new measurement, due to interesting finds on the first round of measurements. Additional work was done to supplement the master thesis. These were measurements and analysis done at an additional power plant, a paper written for a conference, and an analysis of data from a power plant in South America. These are found after the main work.

We would like to express our deep gratitude to Agder Energi and their employees, not only for allowing us to work on such a practical and exciting project, but for all their expertise, help, and hospitality, both on and off site. A special thanks to Inge Lines, discipline leader mechanical, Willy Åsland, engineer at Smeland power plant, and Bjørn Otto Mjåland, head of Skjerka power plant. It is a pleasure to thank our supervisor at the Waterpower Laboratory, professor Ole Gunnar Dahlhaug for all the help and support he has given us during the entire process. We would also like to thank the technical personnel at the Waterpower Laboratory for all their help throughout the semester. A special nod to prof. T.K. Nielsen, PhD (c) C. Bergan and postdoc B.W. Solemslie for taking the time to aid us when difficult problems arose.

Trondheim, June, 2018



Johannes O. Kverno



Vegard S. Ulvan

TABLE OF CONTENTS

| | |
|---|-------------|
| Summary | i |
| Sammendrag | ii |
| Preface | iii |
| Table of Contents | viii |
| List of Tables | x |
| List of Figures | xiii |
| Abbreviations | xiv |
| 1 Introduction and Background | 1 |
| 1.1 Background | 2 |
| 1.2 Problem and significance | 2 |
| 1.3 Response | 2 |
| 1.4 About Smeland Power Plant | 3 |
| 2 Theory | 5 |
| 2.1 Hydraulic efficiency | 5 |
| 2.2 Thermodynamic method for measuring efficiency | 6 |
| 2.2.1 Restrictions | 7 |
| 2.3 Affinity laws | 8 |
| 2.4 Pressure pulsations | 9 |

| | | |
|----------|--|-----------|
| 2.4.1 | Runner influence and draft tube flows | 9 |
| 2.4.2 | Waterway and pressure waves | 11 |
| 2.4.3 | Characteristic frequency of a suspended gas bubble | 12 |
| 2.4.4 | Signal processing and frequency analysis | 13 |
| 2.5 | Air injection | 19 |
| 2.6 | Uncertainty analysis | 23 |
| 2.6.1 | Useful rules | 23 |
| 2.7 | Uncertainty in measurements | 24 |
| 2.7.1 | Random error in repeatability of secondary instrument | 25 |
| 2.8 | Uncertainty in the thermodynamic method | 25 |
| 3 | Methodology | 27 |
| 3.1 | Programs and measuring equipment | 27 |
| 3.1.1 | Equipment | 28 |
| 3.2 | Measurements on Smeland power plant | 29 |
| 3.2.1 | Thermodynamic method | 30 |
| 3.2.2 | Pressure pulsations | 36 |
| 3.2.3 | Air injection | 38 |
| 3.3 | Data handling | 42 |
| 3.3.1 | Efficiency | 42 |
| 3.3.2 | Pressure pulsations | 42 |
| 3.3.3 | Assumptions made for the air mass flow rate calculations | 44 |
| 4 | Results | 45 |
| 4.1 | Hydraulic efficiency at Smeland | 45 |
| 4.2 | Pressure pulsations | 50 |
| 4.2.1 | Observed frequencies | 50 |
| 4.2.2 | Draft tube pressure | 53 |
| 4.2.3 | Spiral casing inlet | 56 |
| 4.2.4 | Leakage pipe | 57 |
| 4.2.5 | Sound recordings | 58 |
| 4.2.6 | RSI | 59 |
| 4.3 | Calculated system frequencies | 60 |
| 4.4 | Calculated suspended bubble volume | 61 |
| 4.5 | Air injection | 62 |
| 4.5.1 | Preliminary test | 62 |
| 4.5.2 | Orifice plate | 63 |

| | | |
|----------|---|-----------|
| 5 | Discussion | 67 |
| 5.1 | Hydraulic efficiency | 67 |
| 5.1.1 | Measuring conditions | 67 |
| 5.1.2 | Uncertainty | 67 |
| 5.1.3 | State of the Francis runner | 67 |
| 5.1.4 | Repetition points | 68 |
| 5.1.5 | Efficiency with air injection | 69 |
| 5.1.6 | Sources of error | 69 |
| 5.2 | Pressure pulsations | 71 |
| 5.2.1 | History and Agder Energi's observations | 71 |
| 5.2.2 | General observations | 71 |
| 5.2.3 | Possible causes | 72 |
| 5.2.4 | Air injection | 73 |
| 5.2.5 | Error sources | 75 |
| 6 | Conclusion | 77 |
| 7 | Further work | 79 |
| | Bibliography | 81 |
| | Appendix | A1 |
| A | Measured values, efficiency | A1 |
| B | Measured values, pressure pulsations | B1 |
| C | Graphs from pressure pulsation measurements in February 2018 | C1 |
| D | Hydraulic efficiency example calculation, $M-I$ | D1 |
| E | Hydraulic efficiency uncertainty example calculation, $M-I$ | E1 |
| F | Air mass flow rate example calculation, $M-XXI$ | F1 |
| G | CRHT VIII Paper | G1 |
| H | Inlet and outlet, additional drawings | H1 |
| I | Characteristic frequency of an air bubble in water | I1 |
| J | Evaluation of the Santa Rosa measurement data | J1 |

LIST OF TABLES

| | | |
|-----|--|----|
| 1.1 | General information about the power plant (Agder-Energi, 2015) | 3 |
| 2.1 | Component errors in the calibration of an instrument | 24 |
| 2.2 | Component errors in measurement with an instrument | 24 |
| 3.1 | Key components used for the measurements at Smeland power plant | 28 |
| 3.2 | Other components used for the measurements at Smeland power plant | 28 |
| 3.3 | Chosen points of operation during the measurement | 29 |
| 3.4 | Additional measurement points in February 2018 | 30 |
| 3.5 | Measurement points from the air injection test in April 2018. Note that M -XVII to M -XXI is with the intake at Monn open, while M -XXII to M -XXIV is with the intake closed. | 30 |
| 3.6 | Key dimensions for the measurement pipe and orifice plate | 40 |
| 4.1 | Main results in tabular form, adjusted for nominal head and flow | 45 |
| 4.2 | Nomenclature used in table 4.4 | 50 |
| 4.3 | Additional measurement points in February 2018 (left) and April 2018 (right). Note that M -XVII to M -XXI is with the intake at Monn open, while M -XXII to M -XXIV is with the intake closed. | 50 |
| 4.4 | Normalised measured frequencies and peak to peak pressures | 51 |

| | | |
|------|--|----|
| 4.5 | Normalised measured frequencies and peak to peak pressures during the various tests done in February 2018 at the same load as <i>M–XII</i> | 52 |
| 4.6 | Normalised measured frequencies and peak to peak pressures in the draft tube in April 2018 | 52 |
| 4.7 | Dominating frequencies obtained from the sound recordings . | 58 |
| 4.8 | Calculated system frequencies for Smeland normalised with the runner frequency | 61 |
| 4.9 | Results from the air injection measurements, both with the intake at Monn open (top), and closed (bottom) | 64 |
| 4.10 | Calculated air bubble volume change for each of the measurement points in April 2018 | 64 |
| 5.1 | Comparison of observed frequencies and calculated waterway pressure wave frequency | 72 |

LIST OF FIGURES

| | |
|---|----|
| 1.1 From left: Vegard Ulvan, Johannes Kverno, Rune Åsland, Bjørge Fossdal, Roger Thorsland, Job Willem De Vos, Reidar Åsland, Willy Åsland, Aanen Breilid (partially hidden) and Ole Thorsland. (Ole Gunnar Dahlhaug, 2018) | 1 |
| 1.2 Map showing the power plant location (Agder-Energi, 2015) | 3 |
| 1.3 Entrance to Smeland power plant | 4 |
| 2.1 Different places of measurement | 7 |
| 2.2 Flow profile in the draft tube at best efficiency, and off design. (Gogstad and Dahlhaug, 2016) | 9 |
| 2.3 Illustration of the vortex filament typically found at full load (left) and part load (right) (Brekke, 1999). | 10 |
| 2.4 Illustration of RSI (Kobro, 2010) | 11 |
| 2.5 Illustration of signal aliasing when $f_S = 1,5f_c$ | 14 |
| 2.6 Hilbert peak envelope superimposed over a recorded sound signal | 14 |
| 2.7 FFT results from both a regular sine wave, and a square wave with the same amplitude and frequency | 15 |
| 2.8 Example of windowing with overlap on a signal (Bergan, 2013) | 17 |
| 2.9 Example of a signal with a highly skewed distribution and histogram with a 99% confidence interval | 18 |
| 2.10 Picture of an orifice plate (left), and a cross section sketch with dimensions (right) | 21 |
| 2.11 Example sketch of an orifice plate mounted in a pipe with flanges | 22 |

| | | |
|------|---|----|
| 3.1 | Unloading the equipment at Smeland power plant | 28 |
| 3.2 | Setup for the thermodynamic method (Brede, 1985) | 32 |
| 3.3 | Sketch of frame | 34 |
| 3.4 | Probe on inlet (left), labyrinth water temperature measurement (right) | 35 |
| 3.5 | Frame used in outlet, 3 individual beams | 35 |
| 3.6 | Pressure sensor placements | 36 |
| 3.7 | Draft tube sensor placement | 37 |
| 3.8 | Check valve at the turbine cover (left), air vent in the runner centre (right). | 38 |
| 3.9 | Sketch showing where the air goes in the turbine (Andresen & Grøner AS, 1984b) | 39 |
| 3.10 | Air hose and valve mounted in place of the check valve | 39 |
| 3.11 | Sketch of the sensor placements on the air pipe | 40 |
| 3.12 | Cross section sketch of the air pipe and orifice plate arrangement | 40 |
| 3.13 | Arrangement used for air flow measurements | 41 |
| 3.14 | Window modified signal with Hann window function superimposed. Signal amplitude reduced to scale with window amplitude. | 42 |
| 3.15 | Pressure signal with the peak-to-peak edges superimposed. | 43 |
| 3.16 | Sound signal with the Hilbert envelope superimposed. | 43 |
| 4.1 | $\eta - Q$ plot with the air injection point superimposed at $H_n = 91$ m | 46 |
| 4.2 | $\eta - P_t$ plot with the air injection point superimposed at $H_n = 91$ m | 47 |
| 4.3 | Closeup of the repetition point in the $\eta - Q$ plot, at $H_n = 91$ m | 48 |
| 4.4 | Closeup of the repetition point in the $\eta - P_t$ plot, at $H_n = 91$ m | 48 |
| 4.5 | Comparison between the guaranteed efficiency, results from the Kværner report, and the calculated efficiency, at $H_n = 91$ m | 49 |
| 4.6 | 5 second samples of the measured pressure in the draft tube (DT 0°) at all the measured loads | 53 |
| 4.7 | Frequencies for the measurements in the draft tube (DT 0°) at all the measured loads | 54 |
| 4.8 | Frequencies for the measurements in the draft tube (DT 0°) at all the measured loads, with the x -axis limited to $0 - 16$, and the z -axis limited to $0 - 10$ kPa. | 54 |

| | | |
|------|--|----|
| 4.9 | Pressure signal and frequencies from the draft tube (DT 0°) at $M-XII$ | 55 |
| 4.10 | Pressure signal and frequencies from the spiral casing inlet (SC) at $M-XII$ | 56 |
| 4.11 | Pressure signal and frequencies from the leakage pipe (LP) at $M-XI$ (BEP) | 57 |
| 4.12 | Sound signal and frequencies of the envelope | 58 |
| 4.13 | Spiral casing inlet during operation at BEP, clearly showing the runner frequency, pump vane frequency (as in figure 4.11), and the RSI. | 59 |
| 4.14 | Schematic of the water way with lengths, not to scale | 60 |
| 4.15 | Calculated volume to frequency. Normalised with the draft tube cone volume (10.17 m ³) | 61 |
| 4.16 | Measured pressure in the draft tube during the air injection, both at the opening of the valve (top) and when the compressor was drained (bottom) | 62 |
| 4.17 | Measured draft tube pressure (DT 0°) normalised with design head, at various calculated air mass flow rates, intake gate at Monn open. | 63 |
| 4.18 | Measured draft tube pressure (DT 0°) normalised with design head, at various calculated air mass flow rates, intake gate at Monn closed. | 63 |
| 4.19 | Spectrogram of the pressure measurement in the draft tube, starting and ending with no air injection, illustrating the reduction in pulsation frequency as air is injected | 65 |
| 5.1 | Runner as seen from under | 68 |

Symbols & Abbreviations

Symbols

| | | |
|--------------|---|----------|
| A' | - Empirical coefficient | - |
| A_1 | - Inlet area | m^2 |
| A_2 | - Outlet area | m^2 |
| A_p | - Area inside probe | m^2 |
| C | - Discharge coefficient | - |
| D | - Pipe inner diameter | m |
| D_0 | - Initial diameter | m |
| D_1 | - Inlet diameter | m |
| D_p | - Diameter inside probe | m |
| E | - Specific energy | J/kg |
| E_h | - Specific hydraulic energy | J/kg |
| E_m | - Specific mechanic energy | J/kg |
| $E_{m,leak}$ | - Specific mechanic energy from leakage | J/kg |
| H | - Head | m |
| H_0 | - Nominal head | m |
| I | - Inertial factor | kg/m^4 |
| L | - Length | m |
| L_1 | - Relative length for sensor placement | - |
| L'_2 | - Relative length for sensor placement | - |
| L_{p1} | - Upstream pipe length | m |
| L_{p2} | - Downstream pipe length | m |
| M'_2 | - Empirical coefficient | - |
| $M- \#$ | - Measurement number | - |
| N | - Number of samples | - |
| P | - Power | MW |
| P_0 | - Nominal power | MW |
| P_{gen} | - Generator power | MW |
| P_h | - Hydraulic power | MW |
| P_m | - Mechanic power | MW |
| P_t | - Turbine power | MW |
| Q | - Volume flow rate | m^3/s |

| | | |
|----------------|---|------------------------|
| Q_0 | - Nominal volume flow rate | m^3/s |
| Q_{leak} | - Leakage volume flow rate | m^3/s |
| Q_p | - Probe volume flow rate | m^3/s |
| $R_{specific}$ | - Specific gas constant | J/kgK |
| Re_D | - Reynolds number | - |
| S | - Sutherland temperature | K |
| Sr_d | - Strouhal number | - |
| T | - Temperature | K |
| V_0 | - Initial volume | m^3 |
| V_b | - Volume bucket | m^3 |
| X | - Measurement | - |
| Z | - Number of blades/vanes | - |
| Z_r | - Number of runner blades | - |
| Z_s | - Number of guide vanes | - |
| a | - Isothermal constant | m^3/kg |
| a | - Speed of sound | m/s |
| c | - Velocity | m/s |
| c_p | - Specific heat capacity | J/kgK |
| d | - Orifice diameter | m |
| dF | - Change in force | N |
| dp | - Change in pressure | Pa |
| dx | - Change in distance | m |
| dV | - Change in volume | m^3 |
| e | - Absolute error | - |
| f | - Frequency | Hz |
| f | - Relative uncertainty | - |
| f_c | - Characteristic frequency | Hz |
| f_e | - Eigenfrequency | Hz |
| f_n | - Runner frequency | Hz |
| f_r | - RSI, rotating domain | Hz |
| f_{res} | - Frequency resolution | Hz |
| f_S | - Sampling frequency | Hz |
| f_s | - RSI, stationary domain | Hz |
| f_t | - Waterway frequency | Hz |
| $f_{t,DT}$ | - Draft tube frequency | Hz |
| $f_{t,O}$ | - Outlet tunnel frequency | Hz |
| $f_{t,PS}$ | - Penstock frequency | Hz |
| g | - Gravitational constant | m/s^2 |
| h | - Height from free surface to measuring point | m |
| j | - Harmonic number | - |

| | | |
|-------|--------------------------|-------------------|
| k | - Spring constant | N/m |
| l_c | - Length scale | m |
| m | - Mass | kg |
| n | - Number of measurements | - |
| n | - Rotational frequency | rpm |
| p | - Pressure | kPa |
| q_V | - Air flow rate | m ³ /s |
| q_m | - Air mass rate | kg/s |
| s | - Standard deviation | - |
| t | - Student-t factor | - |
| t_b | - Time to fill up bucket | s |
| x | - Measured value | - |
| z | - Reference height | m |

Greek letters

| | | |
|------------|---------------------------|-------------------|
| α | - Confidence interval | - |
| β | - Orifice diameter ratio | - |
| γ | - Ratio of specific heats | - |
| Δ | - Difference | - |
| ϵ | - Expansibility factor | - |
| η | - Efficiency | - |
| κ | - Adiabatic constant | - |
| μ | - Dynamic viscosity | Pa s |
| π | - Mathematical constant | - |
| ρ | - Density | kg/m ³ |
| ω | - Period | 1/s |

Subscripts

| | | |
|---------|---|-------------------------------------|
| 0 | - | Initial value |
| 0 / n | - | Nominal value |
| 1 | - | Turbine inlet centre |
| 1 | - | Air pipe upstream tapping |
| 1-1 | - | Probe measuring point turbine inlet |
| 1-2 | - | Air pipe pressure drop |
| 2 | - | Draft tube outlet centre |
| 2 | - | Air pipe downstream tapping |
| 2-1 | - | Measuring point draft tube outlet |
| g/gen | - | Generator |
| h | - | Hydraulic |
| l/leak | - | Labyrinth leakage water |
| m | - | Mechanic |
| ref | - | Reference |
| t | - | Turbine |

Abbreviations

| | | |
|-------------------|---|--|
| amb | - | Ambient |
| atm | - | Atmosphere |
| BEP | - | Best efficiency point |
| DAQ | - | Data acquisition |
| DFT | - | Discrete Fourier transformation |
| DT | - | Draft tube |
| FFT | - | Fast Fourier transformation |
| IEC | - | International Electrotechnical Commission |
| ISO | - | (International Organization for Standardization) |
| mas | - | Meters above sea-level |
| mH ₂ O | - | Meter water column |
| Δp | - | Peak to peak |
| Δp_{1-2} | - | Pressure drop |
| PDS | - | Power Density Spectrum |
| RSI | - | Rotor-stator interaction |
| RVR | - | Rotating vortex rope |
| SC | - | Spiral casing |
| LP | - | Leakage pipe |

CHAPTER 1

INTRODUCTION AND BACKGROUND



Figure 1.1: From left: Vegard Ulvan, Johannes Kverno, Rune Åsland, Bjørge Fossdal, Roger Thorsland, Job Willem De Vos, Reidar Åsland, Willy Åsland, Aanen Breilid (partially hidden) and Ole Thorsland. (Ole Gunnar Dahlhaug, 2018)

The main subject of this master thesis will be measurements completed at Smeland power plant in Vest-Agder, spring semester 2018, on behalf of Agder Energi. It will consist of a theory part, methodology, a presentation of results, discussion of said results, a conclusion, suggestions for further

work, and lastly, references. Also, there are three attachments in the appendix that is additional work done, which is not directly relevant to the main work. In the appendix are also example calculations, additional results, and miscellaneous.

Figures and tables not referenced are the work of the authors.

1.1 Background

A hydro power plant in Vest-Agder, Smeland power plant, is experiencing pressure pulsations in their turbine at full load. The owners of the power plant, Agder Energi, deemed the pressure pulsation matter great enough to seek help from the Waterpower Laboratory at NTNU. They were interested to find out what is causing this phenomenon, and what can be done to avoid it. Pressure pulsations in Francis runners at full load are a rare occurrence, and not something there is a lot of literature about, at the present time.

1.2 Problem and significance

The pulsations, registered on an excursion October 2017 with a dial indicator, was of a low frequency variety in the 3 Hz order of magnitude. The operator is worried that they might have a turbine breakdown if these pulsations ensues, and is today avoiding the region at full load where the problem occurs. Geographically, the power plant experiences a lot of inflow in the spring and summer, due to melting snow. It is in the interest of Agder Energi to be able to run the turbine flexibly at full load when there is an abundance of water, in order to maximise profit.

1.3 Response

To get to the bottom of the problem, measurements of the hydraulic efficiency, pressure pulsations, and the effect of air injection has been carried out at Smeland power plant. This allowed for an in-depth understanding of the pressure pulsations, possible causes, and what can be done in order to solve the problem, with what consequences.

1.4 About Smeland Power Plant

| Smeland power plant | |
|---------------------|--------------------|
| Turbine | Francis |
| Head | 95 m |
| Installed power | 24 MW |
| BEP | ~ 20 MW |
| Annual production | 119 GWh |
| Owner | Agder Energi |
| Built | 1985 |
| River system | Mandalsvassdraget |
| Water sources | Lognavatn and Monn |

Table 1.1: General information about the power plant (Agder-Energi, 2015)



Figure 1.2: Map showing the power plant location (Agder-Energi, 2015)



Figure 1.3: Entrance to Smeland power plant

2.1 Hydraulic efficiency

IEC-60041 (1991) defines the efficiency of a hydraulic turbine as

$$\eta = \frac{P}{P_h} \quad [-] \quad (2.1)$$

where P is the power delivered from the turbine shaft to the generator, and P_h is the available hydraulic power. The efficiency can be also be expressed as two other efficiencies, the mechanical and hydraulic efficiency

$$\eta = \eta_m \eta_h \quad [-] \quad (2.2)$$

that is furthermore defined as

$$\eta_m = \frac{P}{P_m} \quad [-] \quad (2.3)$$

$$\eta_h = \frac{P_m}{P_h} \quad [-] \quad (2.4)$$

where P_m is the power delivered from the runner to the turbine shaft. The hydraulic efficiency can be further written out by defining power as a function of specific energy

$$P = \rho Q E \quad [\text{W}] \quad (2.5)$$

$$\eta_h = \frac{P_m}{P_h} = \frac{\rho Q E_m}{\rho Q E_h} = \frac{E_m}{E_h} \quad [-] \quad (2.6)$$

2.2 Thermodynamic method for measuring efficiency

The thermodynamic method is a technique for measuring hydraulic efficiency in pumps and turbines. It relies on the first law of thermodynamics, which states that energy is never lost, but turns into other forms of energy. (Kjølle, 2003)

In a hydro power plant, hydraulic energy in front of the turbine is converted into mechanical energy. However, not all of the hydraulic energy is converted into mechanical energy, i.e. there are losses through the system. These energy losses are not gone, but have turned into thermal energy in the water itself. This means that the losses in a turbine can be accounted for by the change of temperature in the water running through it, or more accurately the change in enthalpy. This is the essence of the thermodynamic method, and it is a well-known method for measuring turbine efficiency.

The general equation for calculating the hydraulic efficiency is found by dividing the mechanical by the hydraulic energy as seen in equation 2.6.

$$\eta_h = \frac{E_m}{E_h} \quad [-] \quad (2.7)$$

The specific mechanical and hydraulic energy are found by exploring the energy in the inlet and outlet, in regards to pressure, velocity, height, and for the mechanical energy, temperature.

$$E_h = \frac{1}{\rho}(p_1 - p_2) + g(z_1 - z_2) + \frac{1}{2}(c_1^2 - c_2^2) \quad [\text{J/kg}] \quad (2.8)$$

$$E_m = \bar{a}(p_{1-1} - p_{2-1}) + g(z_{1-1} - z_{2-1}) + \frac{1}{2}(c_{1-1}^2 - c_{2-1}^2) + \bar{c}_p(T_{1-1} - T_{2-1}) + E_{m,leak} \quad [\text{J/kg}] \quad (2.9)$$

The term $E_{m,leak}$ needs to be included in Francis turbines, as part of the flow is lost as leakage over the labyrinth seals, and is expressed as

$$E_{m,leak} = \frac{Q_{leak}}{Q} \left(\bar{a}_l \left(\frac{\bar{\rho}gh_{2-1}}{1000} + p_{atm} \right) - \bar{c}_p(T_{leak} - T_{2-1}) - g(z_{leak} - z_{2-1}) \right) \text{ [J/kg]} \quad (2.10)$$

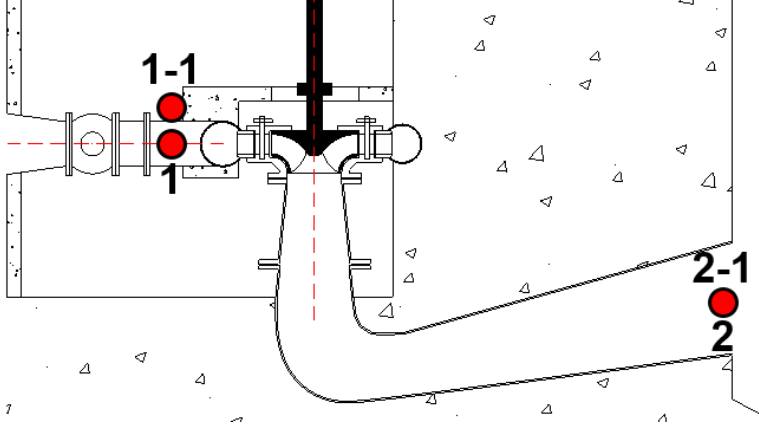


Figure 2.1: Different places of measurement

The subscripts denote places of review, and can be seen in figure 2.1. In a Pelton hydro power plant, point 2 will vary with discharge, as the outlet is not submerged.

By using this method, the need to measure discharge is completely eliminated, as the specific mechanical energy is a function of discharge itself

$$E_m = \frac{P_t}{\rho Q} \text{ [J/kg]} \quad (2.11)$$

Turbine power, P_t , can be found by measuring the generator power, and dividing with the generator efficiency.

2.2.1 Restrictions

The IEC sets the limit for the thermodynamic method at heads only larger than 100 m due to accuracy (IEC-60041, 1991). The lower the head, the lower the change in temperature is going to be, making it more difficult to measure accurately (Kverno and Ulvan, 2017). Only if the conditions are highly favourable are lower heads acceptable. This would be if one has

- Stable inlet temperatures
- Accurate temperature measurements
- Measured the energy distribution in the turbine outlet

If this is true then the conditions are quite favourable, and is in reality easily achieved. During winter in Norway, the upper reservoirs are covered by ice, making the inlet water temperatures very stable. Since the last edition of IEC 41 from 1991, thermistors with higher accuracy and superb stability have become available, allowing for much better measurements. Lastly, with several thermistors in the outlet and smart frames collecting water from several points, it is possible to measure the temperature distribution in the turbine outlet. (Hulaas and Vinnogg, 2010)

Furthermore, IEC says that the temperature gradient in the inflowing water should not exceed 5 mK/min for accurate measurements. IEC also sets the total systematic uncertainty for thermistors at 0,001 K regardless of calibration. In addition, two extra uncertainties must be added to E_m , $e_{E_{10}}$ and $e_{E_{20}}$, if there are no velocity measurements in inlet and outlet, respectively. (IEC-60041, 1991)

2.3 Affinity laws

In order to analyse and portray data from efficiency measurements in 2D-plots, the volume flow and turbine power have to be adjusted for head. This is because the head is not constant from operating point to operating point, and will vary with both head loss and change in upper reservoir level. As the turbine is designed for the nominal head H_0 , it is reasonable to choose this as reference head. The affinity laws are as follows (Brekke, 1999)

$$Q_0 = Q \left(\frac{H_0}{H} \right)^{1/2} \quad [\text{m}^3/\text{s}] \quad (2.12)$$

$$P_0 = P \left(\frac{H_0}{H} \right)^{3/2} \quad [\text{MW}] \quad (2.13)$$

2.4 Pressure pulsations

Most of the theory described in chapter 2.4.1 and 2.4.2 is taken straight out of «Efficiency and pressure pulsations at Smeland Power Plant» (Kverno and Ulvan, 2017), albeit with rephrasing and alterations in some places.

2.4.1 Runner influence and draft tube flows

One characteristic of hydraulic turbines and pipe flow is pressure pulsations, as the system is dynamic and the flow is often unstable to some extent. However, these instabilities do tend to reach a point of equilibrium with the dampening effects of friction as the oscillation amplitude is increased (Dörfler et al., 2013). When a Francis turbine with a fixed rotational velocity operates outside of its design point, the flow leaving the Francis turbine will have a rotating component due to the fixed runner blade outlet angle and off-design flow rate. The direction and magnitude of the rotating velocity component will depend on whether the turbine is operating at part- or full load, and how far off the design point it is, respectively. As a swirling flow moves through a cylinder, the bulk of the fluid transport will be along the walls, while a more stagnant region is found at the centre. If the swirl is severe enough, this stagnant flow might stop or move upstream (fig. 2.2), and a vortex breakdown occurs.

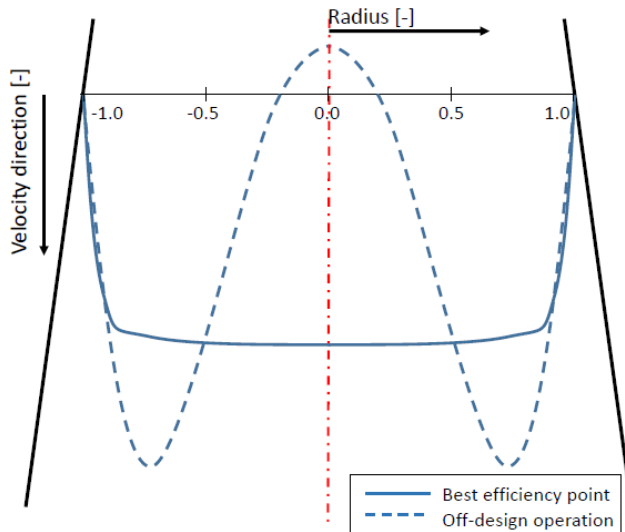


Figure 2.2: Flow profile in the draft tube at best efficiency, and off design. (Gogstad and Dahlhaug, 2016)

At part load, a helix shaped vortex filament can appear in the draft tube at the interface between the downwards moving water at the outer rim of the cross section, and the stagnated zone in the centre (Dörfler et al., 2013). This filament is typically called a “rotating vortex rope” (RVR). The rotational frequency of the RVR is typically $\sim 1/3$ of the runner speed, and can be found in both Francis and Kaplan units, and is referred to as the Rheingans frequency. Due to the shape of this vortex, the pressure pulsation in the draft tube will be asymmetrical, as a pressure gradient is rotating around the cross section.

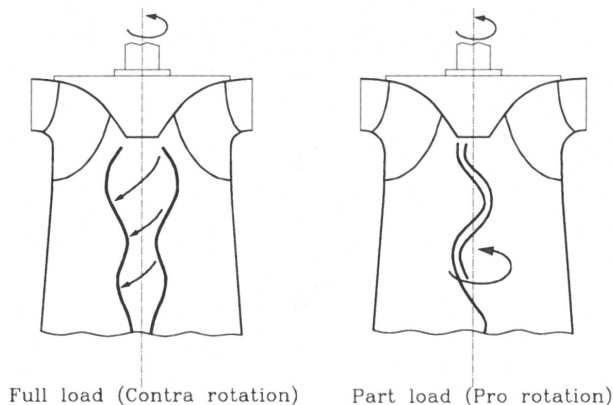


Figure 2.3: Illustration of the vortex filament typically found at full load (left) and part load (right) (Brekke, 1999).

When a Francis runner is operating at full load, i.e. above BEP, a symmetrical vortex appears. Due to the rotation of the flow, the bulk mass flow will occur along the walls of the draft tube, which severely increases the downwards velocity of the water while reducing the pressure (Dörfler et al., 2013). This vortex filament has a tendency to pulsate, and if the frequency of this pulsation resonates with some other part of the system, large pressure pulses can occur. The exact frequency of this vortex pulsation is difficult to pinpoint but it will change depending on the volume of the trapped gas and draft tube pressure, as both are parameters that dictates the natural oscillation frequency of a gas bubble suspended in a liquid.

Another source for pressure pulsations are the blades of the runner passing the stationary guide vanes in the spiral casing, this is typically referred to as “rotor-stator interaction” (RSI). Spikes in the local pressure between the guide vane trailing edge and the passing blade tip occurs each time

they pass each other. The frequency of the RSI pulsations have a direct relationship between the number of runner blades, guide vanes, and runner rotational speed (Dörfler et al., 2013). The severity of these pulsations are also dependent on the distance between the guide vanes and runner blades, and are usually more pronounced at full load as the guide vane opening angle is at its largest. Unless the number of runner blades and guide vanes are the same, the frequency experienced by the turbine and guide vanes will be different.

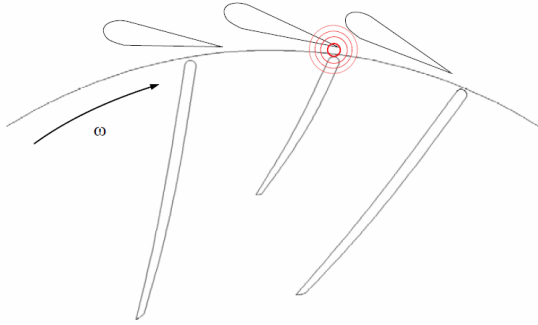


Figure 2.4: Illustration of RSI (Kobro, 2010)

The frequency experienced by the runner (rotating domain) can be expressed as

$$f_{r,j} = f_n Z_s j \quad (j = 1, 2, 3, \dots) \text{ [Hz]} \quad (2.14)$$

f_n is the rotational frequency of the runner, Z_s is the number of guide vanes and j is the harmonic number. The pressure pulse is also influenced by the wake trailing behind the guide vanes (Bue, 2013), especially at off-design conditions as the water is not entering the turbine at the same angle as the blade angle. Similarly, for a guide vane (stationary domain), the frequency is

$$f_{s,j} = f_n Z_r j \quad (j = 1, 2, 3, \dots) \text{ [Hz]} \quad (2.15)$$

where Z_r denotes the number of runner blades.

2.4.2 Waterway and pressure waves

When regulating a turbine, and thus changing the flow rate, the momentum of the water in the water way must be changed, and this change will result in a change in pressure (Nielsen, 1990). If a valve at the end of a long tunnel suddenly closes, the pressure at the valve will rapidly increase, as

the water upstream has momentum that is converted to pressure energy. A pressure wave will travel upstream until it reaches the first open water surface. At this point all the water has stopped, but the pressure at the valve is higher than the ambient pressure at the open water surface. The water will start to move back upstream, gaining some momentum, which causes an under-pressure at the valve, leading to water moving back down again. The frequency of this pressure wave travelling up and down the water way can be expressed as

$$f = \frac{a}{4L} \text{ [Hz]} \quad (2.16)$$

where a is the speed of sound in the water way and L is the length of the tunnel. The speed of sound in water depends on the stiffness of the tunnel walls, and the air content of the water. For infinitely stiff tunnel walls, $a = 1450$ m/s. However, for most practical applications, $a \sim 1200$ m/s. If the valve closing happens at a slower rate than the period of a pressure pulse, or a pressure pulse travels between two open water surfaces, the frequency is closer to

$$f = \frac{a}{2L} \text{ [Hz]} \quad (2.17)$$

For pulses moving between two free surfaces, the pressure at either end is determined by the ambient pressure, so the characteristics are not the same as in equation 2.16 (Nielsen, 1990).

2.4.3 Characteristic frequency of a suspended gas bubble

During the work associated with the specialisation project «*Efficiency and pressure pulsations at Smeland Power Plant*» (Kverno and Ulvan, 2017), Professor Nielsen came up with a conjecture regarding the eigenfrequency of a gas bubble, such as air or water vapour, suspended in water (memo in appendix I). The equation states that

$$f_e = \frac{1}{2\pi} \sqrt{\frac{\kappa p_0}{V_0 I}} \text{ [Hz]} \quad (2.18)$$

where p_0 is the initial pressure, V_0 the initial volume, and κ the adiabatic gas constant for the gas bubble. I is the inertia of the surrounding water. The equation is derived from the equation of state for the gas, and the momentum equation. I has the dimensions M L^{-4} , and Nielsen suggests that it might be the density of the water divided by some length scale such as the initial bubble diameter D_0

$$I = \frac{\rho}{D_0} \text{ [kg/m}^4\text{]} \quad (2.19)$$

With an assumption that an elongated gas bubble has roughly the same eigenfrequency as an ideal, spherical bubble of the same volume, the diameter D_0 could be set to be the same as that of the ideal bubble.

2.4.4 Signal processing and frequency analysis

When doing measurements of something physical, a device, such as a sensor or a probe, must be placed in or at the object or phenomena that is to be measured. The sensor will then typically give an output dependent on the input which can be communicated to and understood by some electronic device or a human, e.g. the filament in a thermometer expanding or contracting as the temperature changes. For the measurement of pressure, a sensor, such as the GE Druck UNIK-5000 used for this thesis, will output a current proportional to the pressure exerted on the piezoresistive silicon chip. Through calibration, this current can be translated to a pressure value.

Data acquisition

When logging physical measurements with a computer, a continuous input is typically stored as a series of discrete digital values, taken at some time interval. The interval between each sample, or more precisely, the sampling rate, given in Hz, is set depending both on the response time of the sensor and the requirements for the measurement themselves. Given a fast enough response time, the minimum limit must be at least high enough to satisfy the Nyquist theorem (Wheeler and Ganji, 2010), which states that

$$f_S = 2f_c \text{ [Hz]} \quad (2.20)$$

where f_S is the sampling rate, and f_c is the highest expected frequency of interest in the signal. If this criterion is not met when taking discrete samples of some continuous signal, e.g. a sine wave, the series of points can be interpreted as two or more sine waves of different frequencies, which is called aliasing (fig. 2.5). As the sampling frequency is increased, the likelihood of aliasing of the signal is greatly decreased. When sampling more complex signals, made up of many different frequencies, a higher sampling rate is preferable in order to ensure that all the peaks and troughs are captured. Bergan (2013) suggested that a sampling rate of about 10 times the highest frequency of interest is sufficient. The minimum length of a sampling series is set by the lowest expected frequency of interest and should be 10 full periods.

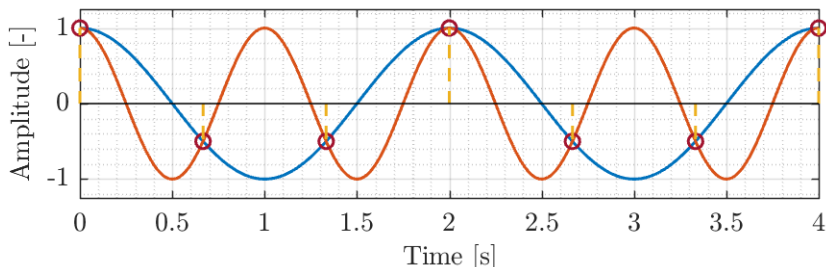


Figure 2.5: Illustration of signal aliasing when $f_S = 1,5f_c$

Recording and analysing audio

Another way to gather valuable data is through sound recording. Especially if the phenomena of interest can be easily heard, a sound recording will be a quick and easy way to gather some data when no other equipment is available. However, if the phenomena of interest does not appear directly as a specific sound frequency, but rather as varying amplitudes, i.e. an amplitude modulated signal, a direct frequency transformation of the sound might not reveal much. In that case, an envelope can be extracted from a Hilbert transformation. The envelope is just the magnitude part of the Hilbert transformation, and contains the amplitude modulation frequency of the signal.

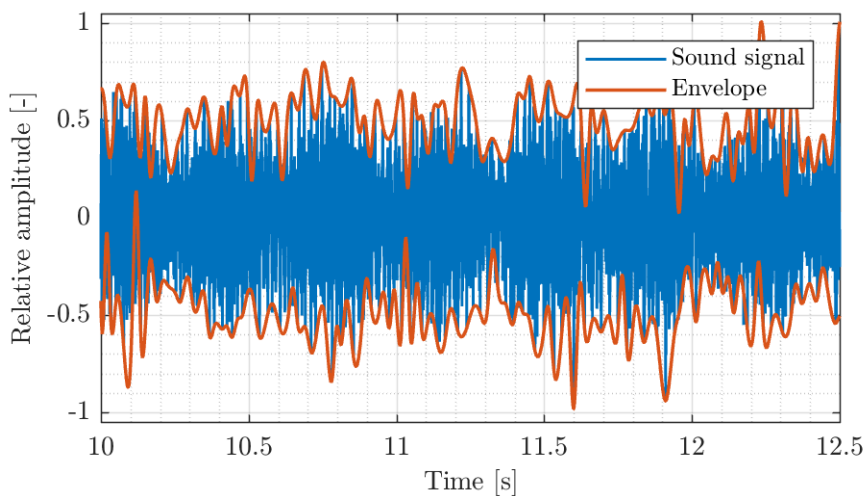


Figure 2.6: Hilbert peak envelope superimposed over a recorded sound signal

Frequency analysis

A commonly used, and very powerful tool when trying to make sense of seemingly messy and noisy signals, is Fourier transformation, or in the case of numerical computations, discrete Fourier transformation (DFT). DFT takes a time-domain signal and transforms it into the frequency-domain, separating the components of the signal and returns the constituent frequencies and their amplitudes from the signal (Heinzel et al., 2002). The base idea behind Fourier transformation is that an infinite series of sine waves of increasing frequency and different amplitude can generate any kind of output signal. The transformation assumes that the constituent parts of the signal are all based on perfect sine waves, meaning that some “false” frequencies or harmonics may appear if a non-sinusoidal signal is transformed, e.g. a square wave.

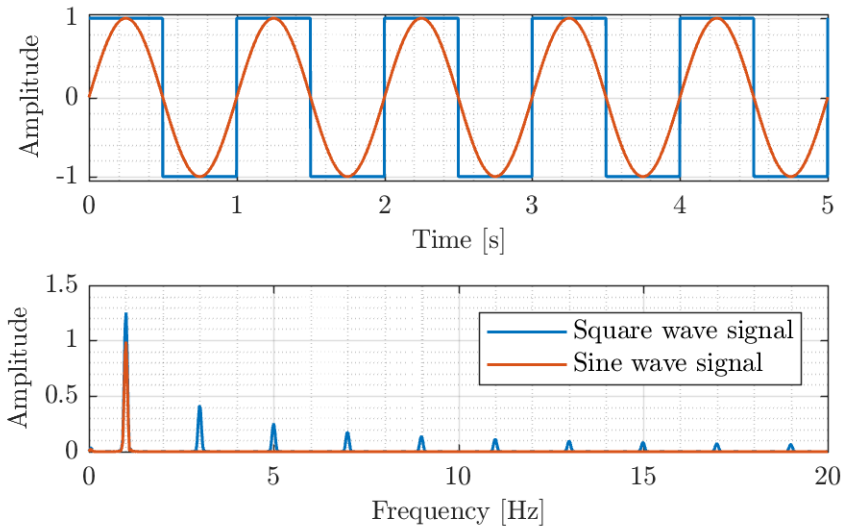


Figure 2.7: FFT results from both a regular sine wave, and a square wave with the same amplitude and frequency

In figure 2.7, two signals, both of the same frequency and amplitude are analysed. The perfect sine wave results in a near perfect result, one peak at 1 Hz with an amplitude of ~ 1 . The square wave however returns an exaggerated amplitude at the base frequency, and a set of $2n - 1$ harmonics of decreasing amplitudes from $n = 1$ to, in theory, $n \rightarrow \infty$. Because of this the amplitude values returned from a FFT analysis of a non-sinusoidal

signal, which many measurement signals often are, can not be regarded as the “true” amplitude, such as a pressure, experienced physically. Similarly, some harmonics may appear that is not actually present.

Even though there are several types of DFT’s, the one used during the work on this thesis is based on the fast Fourier transformation (FFT). One drawback of FFT is that it is fairly sensitive to noise, and it does not cope well when there are gaps in the measurement series. By using the power Welch method, these shortcomings can be overcome. In Welch’s method, the series is split into smaller segments, or windows, where the power of the frequencies are calculated for all of the windows, and then an average is calculated of all of the segments. Noise reduction and accuracy is further improved by multiplying each window, before the transformation, with a window function. The main drawback of Welch’s method is a reduction in spectral resolution, however the length of each window is what actually dictates the resolution. In theory, the frequency resolution $f_{res} = f_s/N$, where N is the number of samples. The actual resolution, i.e. the change in frequency per increment along the x -axis, is also affected by the window function used (Heinzel et al., 2002), so the resolution may deviate slightly from the calculated f_{res} . When using windows, the total length of the measurement series should be sufficiently long, e.g. 8 to 10 full wave lengths of the lowest expected frequency, to ensure that a wave length or two is within each window.

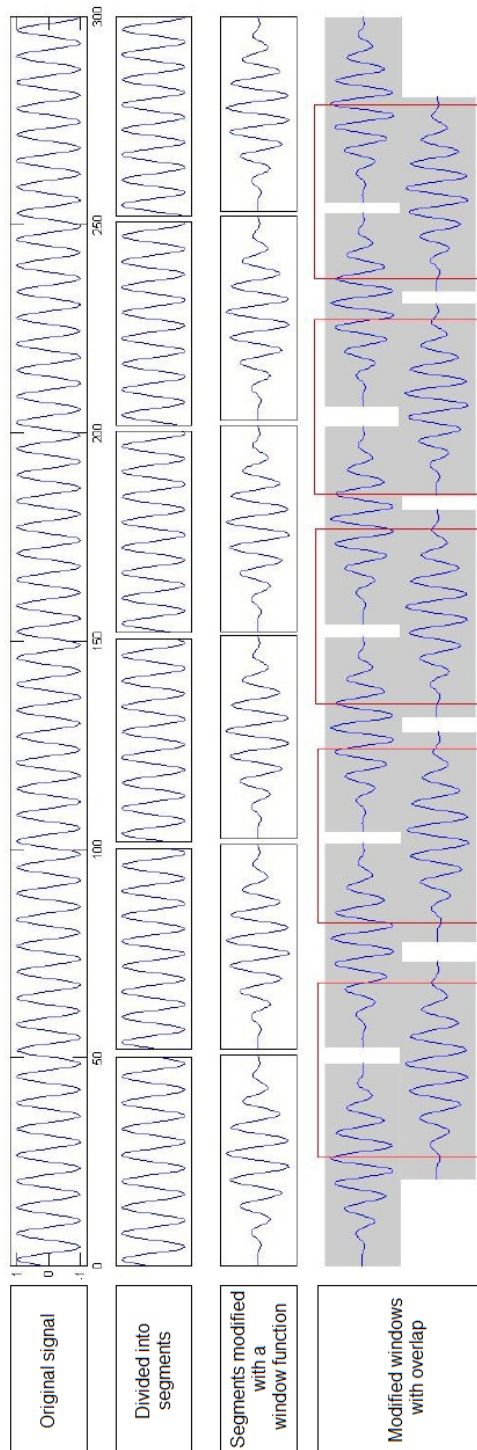


Figure 2.8: Example of windowing with overlap on a signal (Bergan, 2013)

Peak-to-peak

When discussing pressure pulsations it is often necessary to have some measure of the amplitude of the pulsation. Typically, the RMS or a peak-to-peak of the signal is used to represent the pressure fluctuations (Dörfler et al., 2013). As there are not any clearly defined rules or standards on how it should be done, different investigations will typically not do it the same way, and comparisons between them will be next to impossible. If the data is normally distributed, the standard deviation could be used as a measure, but for highly skewed distributions, this is not a good approach. Another method, occasionally referred to as the histogram method, is to use a 97 % confidence interval of the measured pressure values, and discard the remaining extremes, which in many cases can be non physical spikes in the data (International Electrotechnical Commission, 1999). Some care must be taken however, as the 97 % interval is just a suggestion from IEC 60193, and the actual limit must often be tweaked through trial and error, typically depending on the amount of non physical spikes.

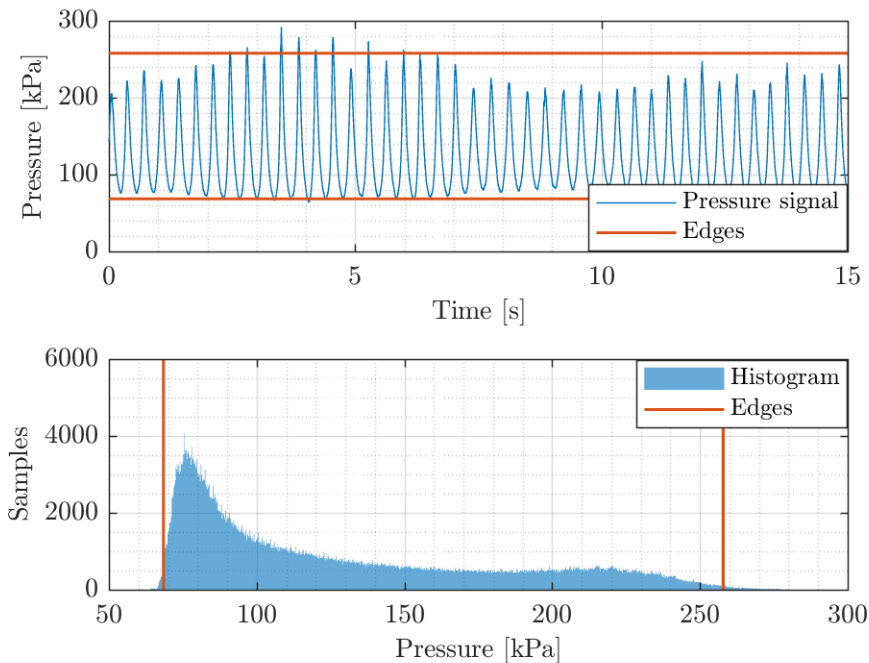


Figure 2.9: Example of a signal with a highly skewed distribution and histogram with a 99% confidence interval

2.5 Air injection

One common way of stabilising pulsations in hydro turbines is by injecting air into the draft tube (Dörfler et al., 2013). Without any instrument specifically designed to measure the flow of air in closed conduits, figuring out the flow rate to a sufficiently accurate degree can be challenging. The challenge is mostly due to the highly compressible nature of air. One possible way to measure air flow is by the means of putting an obstruction in the conduit as explained in ISO 5167 (International Organization for Standardization, 2003a), i.e. a nozzle or an orifice plate. The pressure difference between a point upstream, and another just downstream of the obstruction is measured, and the flow rate can be calculated. For the required measurements at Smeland power plant, and time constrains considering the melting snow in the region, an orifice plate was chosen (ISO 5167-2:2003) as it was much simpler to manufacture compared to a venturi nozzle. With the orifice plate in place, the mass flow rate of air can be calculated by

$$q_m = \frac{C}{\sqrt{1-\beta^4}} \varepsilon \frac{\pi}{4} d^2 \sqrt{2\Delta p \rho_1} \text{ [kg/s]} \quad (2.21)$$

and by dividing by the density of air at some stated temperature and pressure, the volume flow rate can be calculated from

$$q_V = \frac{q_m}{\rho} \text{ [m}^3\text{/s]} \quad (2.22)$$

In equation 2.21, β is the relationship between the orifice diameter and pipe diameter, d/D , while C and ε are coefficients provided by the standard. ε is an empirical factor, called the *expansibility factor*, and it is related to the compressibility of the fluid, being equal to unity for incompressible liquids, and less than unity for gases. For a venturi nozzle, ε comes from the theory, however the factor used in measurements with orifice plates are purely empirical, and only valid within the constraints presented in the standard. For measurements with an orifice plate, it is calculated from

$$\varepsilon = 1 - \left(0,351 + 0,256\beta^4 + 0,93\beta^8\right) \left[1 - \left(\frac{p_2}{p_1}\right)^{1/\kappa}\right] \text{ [-]} \quad (2.23)$$

The *discharge coefficient*, C , is given by the Reader-Harris/Gallagher equation (International Organization for Standardization, 2003b), and is

$$\begin{aligned}
C = & 0,5961 + 0,0261\beta^2 - 0,216\beta^8 + 521 \cdot 10^{-6} \left(\frac{10^6 \beta}{Re_D} \right)^{0,7} \\
& + (18,8 + 6,3A') 10^{-3} \beta^{3,5} \left(\frac{10^6}{Re_D} \right)^{0,3} \\
& + \left(0,043 + 0,080e^{-10L_1} - 0,123e^{-7L_1} \right) (1 - 0,11A') \frac{\beta^4}{1 - \beta^4} \\
& - 0,031 \left(M'_2 - 0,8M'_2{}^{1,1} \right) \beta^{1,3} + 0,011 (0,75 - \beta) \left(2,8 - \frac{D}{25,4} \right) \quad [-]
\end{aligned} \tag{2.24}$$

with the last term being included to compensate for a pipe diameter smaller than 71,12 mm. A' and M'_2 is

$$\begin{aligned}
A' &= \left(\frac{19000\beta}{Re_D} \right)^{0,8} \quad [-] \\
M'_2 &= \frac{2L'_2}{1 - \beta} \quad [-]
\end{aligned}$$

L_1 and L'_2 are the distances between the faces of the plate to the pressure tappings, relative to the pipe diameter. One thing which becomes apparent is that while equation 2.21 gives the mass flow rate, the discharge coefficient C is dependent on the Reynolds number, meaning that the calculations must be done through an iterative process, where an initial Reynolds number is set to infinity, giving a guess for $C = C_\infty$. ISO 5167-2 also specifies a set of restrictions and limits of use. Most importantly,

- $50\text{mm} \leq D \leq 1000\text{mm}$
- $d \geq 12,5\text{mm}$
- $0,1 \leq \beta \leq 0,75$
- $Re_D \geq 5000$, for $0,1 \leq \beta \leq 0,56$
- $Re_D \geq 16000\beta^2$, for $\beta > 0,56$
- $0,75 \leq \frac{p_2}{p_1} \leq 0,98$
- $\frac{\Delta p'_{1-2,rms}}{\Delta p_{1-2}} \leq 0,10$

$\overline{\Delta p_{1-2}}$ is the mean air pressure drop, and $\Delta p'_{1-2,rms}$ is the root mean square value of the fluctuating pressure component $\Delta p'_{1-2}$ in the pipe flow. If the fluctuation/mean pressure ratio is greater than 10 %, ISO/TR 3313 must be followed as well in order to compensate for the higher uncertainty of the measurements and calculated results.

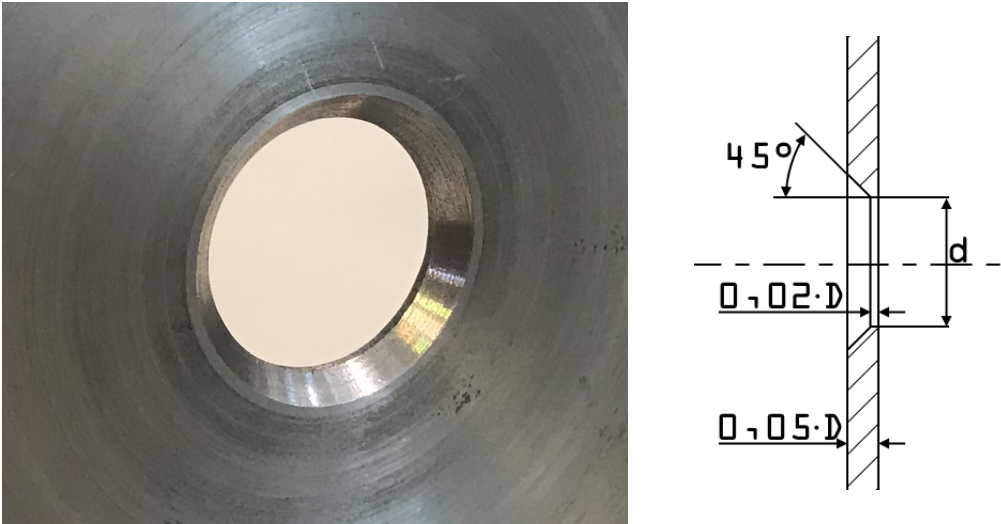


Figure 2.10: Picture of an orifice plate (left), and a cross section sketch with dimensions (right)

Pulsating air flows

Even though turbulent pipe flow is not stable, if the turbulence is the only source of fluctuations it can be said to be stable over time. If the pressure measurements of the airflow in the pipe are pulsating more than what ISO 5167-1 accepts, an additional error must be added to the calculated total uncertainty of the air mass flow rate. The estimate of the total error, f_T , is

$$f_T = \left(\frac{1}{2} \left\{ 1 + \left[1 - \left(\frac{\Delta p'_{1-2,rms}}{\overline{\Delta p_{1-2}}} \right)^2 \right]^{\frac{1}{2}} \right\} \right)^{-\frac{1}{2}} - 1 \quad [-] \quad (2.25)$$

By multiplying the discharge coefficient with $(1 - f_T)$, the systematic error that can be compensated for (International Organization for Standardiza-

tion, 2018), however there are still some uncertainty regarding the discharge coefficient due to the pulsating pressure measurements. At higher Strouhal numbers, $Sr_d > 0,02$, there will be an additional uncertainty due to inertial effects. In the end, ISO/TR 3313 states that the additional relative uncertainty is equal to f_T , or $\frac{1}{2}f_T$ if $Sr_d < 0,02$. The error calculated with equation 2.25 is only applicable if the flow can be regarded as incompressible, meaning that $\varepsilon \geq 0,99$.

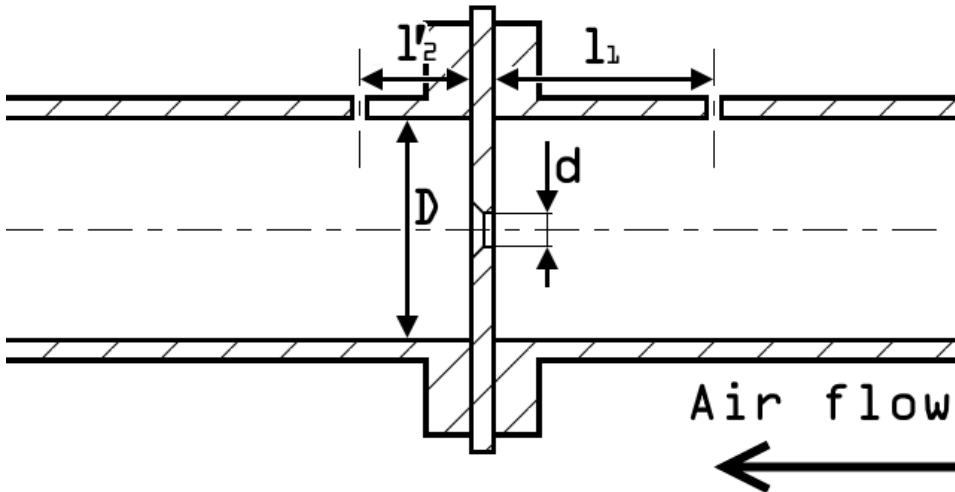


Figure 2.11: Example sketch of an orifice plate mounted in a pipe with flanges

2.6 Uncertainty analysis

Say we have a known function N dependent on several variables

$$N = f(u_1, \dots, u_n) \quad (2.26)$$

all the variables have uncertainty, so a change in N would be

$$N \pm \Delta N = f(u_1 \pm \Delta u_1, \dots, u_n \pm \Delta u_n) \quad (2.27)$$

The right-hand-side can be made into a Taylor-series and simplifications can be made

$$N \pm \Delta N = f(u_1, \dots, u_n) + \frac{\partial f}{\partial u_1} \Delta u_1 + \dots + \frac{\partial f}{\partial u_n} \Delta u_n \quad (2.28)$$

$$\Delta N = \left| \frac{\partial f}{\partial u_1} \Delta u_1 \right| + \dots + \left| \frac{\partial f}{\partial u_n} \Delta u_n \right| \quad (2.29)$$

If we assume the Δu_i 's to be confidence intervals, then the probable error in N will be

$$\Delta N = \pm \sqrt{\left(\frac{\partial f}{\partial u_1} \Delta u_1 \right)^2 + \dots + \left(\frac{\partial f}{\partial u_n} \Delta u_n \right)^2} \quad (2.30)$$

This is called Gauss' propagation of uncertainty. Here the root sum squared (RSS) method is used to combine uncertainties. The RSS-method is statistical tolerance analysis method that assumes a normal distribution. (Storli, 2007)

2.6.1 Useful rules

When

$$N = u_1 \pm u_2 \quad (2.31)$$

then

$$(\Delta N)^2 = (\Delta u_1)^2 + (\Delta u_2)^2 \quad (2.32)$$

When

$$N = u_1 u_2 \quad (2.33)$$

then

$$\left(\frac{\Delta N}{N} \right)^2 = \left(\frac{\Delta u_1}{u_1} \right)^2 + \left(\frac{\Delta u_2}{u_2} \right)^2 \quad (2.34)$$

When

$$N = u^b \quad (2.35)$$

then

$$\left(\frac{\Delta N}{N}\right) = b \left(\frac{\Delta u}{u}\right) \quad (2.36)$$

2.7 Uncertainty in measurements

This section is based on Solemslie (2010). The instruments used for measurements, their calibrations, and the calibration instruments have error components. This have to be taken into account when finding the uncertainty of a measurement. In table 2.1 one can see the errors to consider when finding the maximum total relative uncertainty of a calibration, $f_{X_{cal}}$. It can be found using the RSS-method

$$f_{X_{cal}} = \pm \sqrt{\sum (f_{X_i})^2} \quad (2.37)$$

where “i” denotes the different components in table 2.1.

| Error | Description |
|---------------|--|
| $\pm f_{X_a}$ | Systematic error of the primary calibration method |
| $\pm f_{X_b}$ | Random error of the primary calibration method |
| $\pm f_{X_c}$ | Systematic error of the secondary instrument |
| $\pm f_{X_d}$ | Random error of the secondary instrument |
| $\pm f_{X_e}$ | Physical phenomena and external influences |
| $\pm f_{X_f}$ | Error in physical properties |

Table 2.1: Component errors in the calibration of an instrument

| Error | Description |
|-------------------|---|
| $\pm f_{X_{cal}}$ | Systematic error in calibration |
| $\pm f_{X_h}$ | Additional systematic error in the instrument |
| $\pm f_{X_j}$ | Error in physical properties |
| $\pm f_{X_{ks}}$ | Systematic errors due to physical phenomena and external influences |
| $\pm f_{X_{kr}}$ | Random errors due to physical phenomena and external influences |
| $\pm f_{X_l}$ | Random error in repeatability of secondary instrument |

Table 2.2: Component errors in measurement with an instrument

In table 2.2 one can see all the errors to consider when finding the total maximum uncertainty of a measurement. Once again the RSS-method can be used to find the measurement’s total relative uncertainty

$$f_{X_{tot}} = \pm \sqrt{\sum (f_{X_j})^2} \quad (2.38)$$

where “j” denotes the different components in table 2.2.

2.7.1 Random error in repeatability of secondary instrument

Random error e_{X_l} is found by using the standard deviation and student-t confidence interval for the logged values from the measurements

$$e_{X_l} = \frac{t_{\alpha/2} s}{\sqrt{n}} \quad (2.39)$$

where n is the number of measurements, $t_{\alpha/2}$ is the student’s t-factor based on chosen confidence interval α and n , and s is the standard deviation. The standard deviation is defined as

$$s = \left(\frac{\sum_{i=1}^n (x_i - \bar{x})^2}{n - 1} \right)^{1/2} \quad (2.40)$$

where x_i is the measured value and \bar{x} is the mean. One important aspect to take from equation 2.39 and 2.40 is that they both get smaller as the number of measurements increases. Meaning a lot of measurements will make the random error minuscule. (Storli, 2007)

2.8 Uncertainty in the thermodynamic method

Following the IEC guidelines, the uncertainty for the efficiency found using the the thermodynamic method is

$$f_{\eta} = \pm \sqrt{f_{E_m}^2 + f_{E_h}^2} \quad (2.41)$$

In-built in E_m and E_h are physical properties, measurements, and constants that all have uncertainty. Some are imposed by IEC-60041 (1991), some are from calibration and measuring, and others are assumed. A complete list of all uncertainties, and an extensive step-by-step calculation of efficiency uncertainty can be found in appendix E.

3.1 Programs and measuring equipment

At the beginning of the semester, a lot of time was spent on making the required programs for the acquisition and storing of measurement data at Smeland power plant. For all measurements National Instruments LabVIEW software was used. For the efficiency measurements, the program had to read pressure data from the transducer on a probe, send requests to all five temperature sensors, read the temperature data as they sent it back, and display all the data. Due to the temperature sensors slow response time, it takes approximately 1,4 seconds for each cycle of logging. An additional program was made to read and store pressure data from a transducer on the inlet right after the main valve, and a sensor measuring the local atmospheric pressure. The reason for not including the last two pressure sensors to the first program was that the transducer mounted on the inlet pipe was also used for the pressure pulsation measurements, and as the two sets of measurements were done with two different computers. It was considered easier to have two separate programs run in parallel than switching cables around. For the pressure pulsation measurements, the program had to read pressure data from five transducers, display the data, do a quick FFT analysis on the signal from a user specified sensor and display it, and upon request store a time series to a file for a set amount of time.

3.1.1 Equipment

| Measuring Equipment | Quantity | Usage |
|-----------------------------|----------|------------------|
| SBE 38 Digital Thermometer | 5 | Temperature |
| Custom suitcase PC | 1 | ADC & Logging |
| GE Druck UNIK-5000 50 bar a | 1 | Pressure |
| GE Druck UNIK-5000 15 bar a | 2 | Pressure |
| GE Druck UNIK-5000 5 bar a | 3 | Pressure |
| GE Druck UNIK-5000 3 bar a | 1 | Pressure |
| Lenovo ThinkPad | 1 | Logging |
| NI-USB 6211 I/O device | 1 | ADC |
| PT-100 sensor | 1 | Air temperature |
| NI-USB 9217 I/O device | 1 | ADC |
| Leica DISTO Laser | 1 | Distance measure |
| Measuring rope | 1 | Distance measure |
| Custom kWh-counter | 1 | Counting flashes |

Table 3.1: Key components used for the measurements at Smeland power plant

| Other Equipment | Usage |
|-----------------|---|
| Probe | Extracting water from the inlet |
| Isotherm bucket | Measuring labyrinth water temperature |
| 10 litre bucket | Measuring flow rate in probe |
| Isolation foam | Isolating |
| Orifice plates | Placed in air pipe to obstruct the flow |

Table 3.2: Other components used for the measurements at Smeland power plant



Figure 3.1: Unloading the equipment at Smeland power plant

3.2 Measurements on Smeland power plant

The measurements at Smeland power plant took place in late February, 2018. As previously mentioned, the preparations leading up to the measurements started back in August 2017. These preparations were based on an inspection done in October 2017, and several conversations with the staff involved with the power plant. A more detailed description about the planning process and the choices that were made can be found in the specialisation project report, «*Efficiency and pressure pulsations at Smeland Power Plant*», by Kverno and Ulvan (2017).

The planned operation points for the measurements were chosen according to the seven points Kværner had in their report (Brede, 1985), plus an additional three above BEP, as that is the region where the pulsations occur. There were also two repetition points which is used to validate the results. These two points were set at the two operation points of interest for the measurements, namely the BEP for the efficiency measurements, and the point of most vibrations for the pulsation measurements. The repetition point for the efficiency measurements was changed on site, as the temperature was unstable at $M-I$.

| $M- \#$ | Indicated P_{gen} [MW] |
|---------|-----------------------------|
| I | 19,6 |
| II | 21 |
| III | 22,2 |
| IV | 23 |
| V | 24 |
| VI | 6,2 |
| VII | 9,8 |
| VIII | 13,25 |
| IX | 15,0 |
| X | 16,9 |
| XI | 19,6 |
| XII | 23 |

Table 3.3: Chosen points of operation during the measurement

The indicated generator power on $M-XIII$ and onward to $M-XXIV$ was not decided beforehand, but rather found on site as the points of most pulsation.

| $M- \#$ | Indicated P_{gen} [MW] | Note |
|---------|-----------------------------|--------------------------------|
| XIII | 22,7 | Air injected, full compressor |
| XIV | 22,7 | Air injected, empty compressor |
| XV | 22,7 | Water injected |
| XVI | 22,7 | Check-valve off |

Table 3.4: Additional measurement points in February 2018

| $M- \#$ | Indicated P_{gen} [MW] | Note |
|---------|-----------------------------|-------------------------------|
| XVII | 23,6 | No air injection |
| XVIII | 23,6 | Air injection, lowest opening |
| XIX | 23,6 | Air injection, mid opening |
| XX | 23,6 | Air injection, mid opening |
| XXI | 23,6 | Air injection, full opening |
| XXII | 23,4 | No air injection |
| XXIII | 23,4 | Air injection, mid opening |
| XXIV | 23,4 | Air injection, full opening |

Table 3.5: Measurement points from the air injection test in April 2018. Note that M -XVII to M -XXI is with the intake at Monn open, while M -XXII to M -XXIV is with the intake closed.

3.2.1 Thermodynamic method

Although there are a lot of parameters that can be measured directly in regard to equation 2.8, 2.9, and 2.10, it is often difficult and not necessary. The pressures in the outlet can be estimated by knowing the water column height and atmospheric pressure

$$p_2 = \frac{\bar{\rho}gh_2}{1000} + p_{atm} \text{ [kPa]} \quad (3.1)$$

$$p_{2-1} = \frac{\bar{\rho}gh_{2-1}}{1000} + p_{atm} \text{ [kPa]} \quad (3.2)$$

The velocities in the probe, inlet, and outlet can be estimated with volume flow and area

$$c_{1-1} = \frac{Q_p}{A_p} = \frac{4V_b}{t_b\pi D_p^2} \text{ [m/s]} \quad (3.3)$$

$$c_1 = \frac{Q}{A_1} = \frac{4P_g}{\eta_g \bar{\rho} E_m \pi D_1^2} \text{ [m/s]} \quad (3.4)$$

$$c_2 = c_{2-1} = \frac{Q}{A_2} = \frac{P_g}{\eta_g \bar{\rho} E_m A_2} \text{ [m/s]} \quad (3.5)$$

Therefore, what was measured directly at Smeland power plant was p_1 , p_{1-1} , p_{atm} , T_{1-1} , T_{2-1} , h , P_g , t_b and T_{leak} . The placement of the pressure and temperature sensors can be seen in figure 3.2.

In order to calculate the kinetic energy in the mechanical energy from equation 2.9, c_{2-1} is needed. However, as one can see in equation 3.5, the volume flow is used. So an assumption is made

$$Q_{assumed} = \frac{P_t}{p_1 - p_{atm}} \text{ [m}^3\text{/s]} \quad (3.6)$$

This yields a slightly erroneous mechanical energy, however it can be used to calculate a more correct Q

$$Q = \frac{P_t}{\bar{\rho} E_m} \text{ [m}^3\text{/s]} \quad (3.7)$$

By using the new volume flow and iterating, both the volume flow and mechanical energy will converge towards their correct values.

Generator power

The regulator at Smeland Power Plant had, as most hydro power plants, a display that showed the generator power. However, these numbers are known to be somewhat unreliable, and a precision measurement of the generator power was done. In the control room was an indicator light that flashed for every 1,4 kWh that was produced. By counting the number of flashes with the kWh-counter, and taking the time with a stopwatch, the generator power, P_g , could be calculated with precision.

Probe and inlet

In order to measure the inlet temperature T_{1-1} and p_{1-1} , water was extracted from the inlet before the spiral casing using a measuring probe. The probe was mounted on the inlet in place of the bleed valve. Then the temperature and pressure sensor was placed on the probe for measurements as seen in figure 3.4 (left). To ensure a temperature that was not affected by the ambient temperature, the probe wrapped in an isolating material.

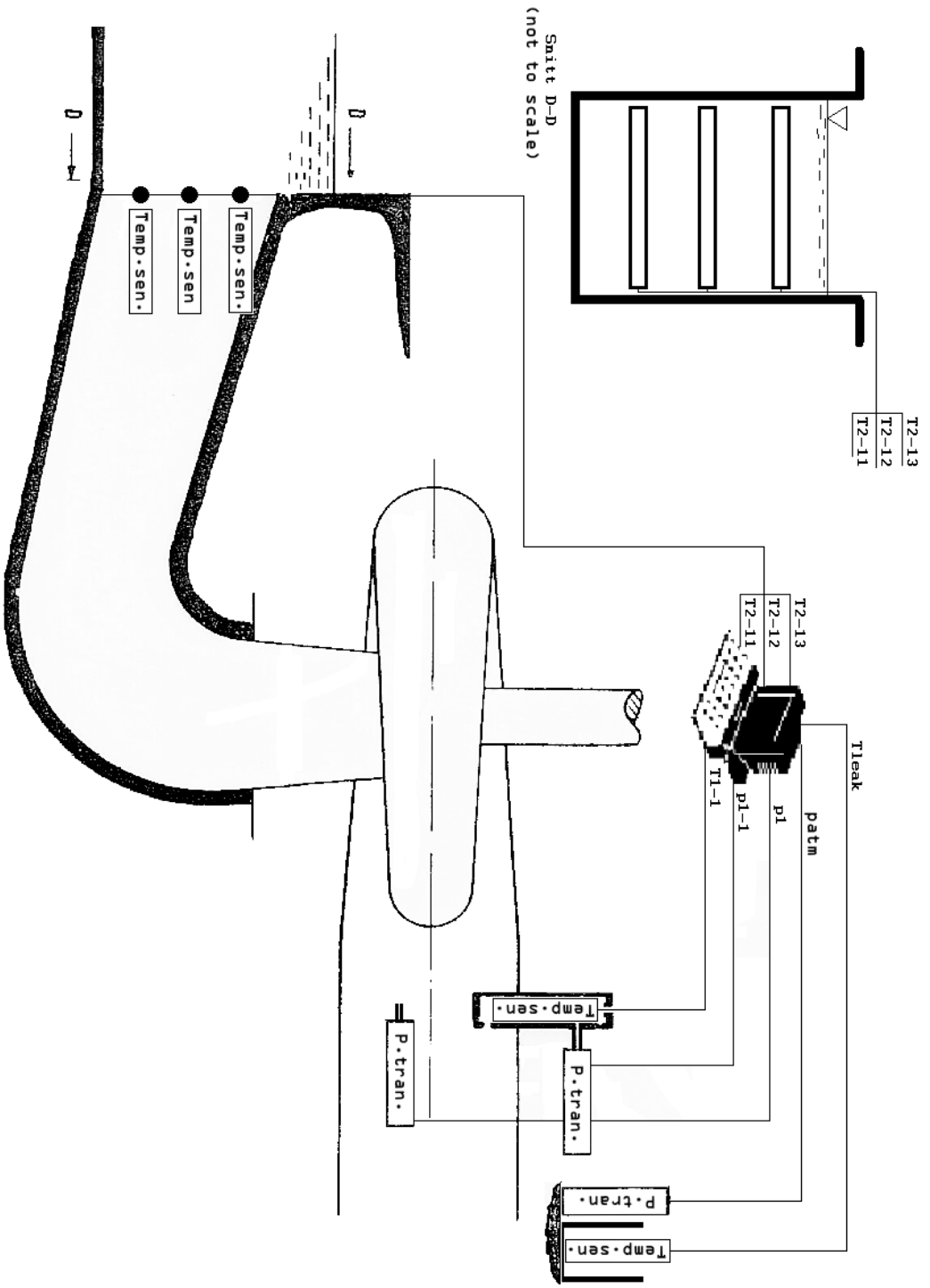


Figure 3.2: Setup for the thermodynamic method (Brede, 1985)

From the probe lead a hose that went to a bucket. Under different points of operation, the time it took to fill up the bucket was measured.

To measure p_1 , a pressure sensor was connected to the outer wall of the inlet, bottom side, on a tap with a valve, as seen in figure 3.2. This was not at the same height as the centre-line of the inlet, point 1, so the height-difference was measured and used in the calculations of the correct p_1 .

On the same floor p_{atm} was measured continuously for each point of operation, the sensors placement can be seen in figure 3.2.

Outlet

To measure the temperature in the draft tube outlet, T_{2-1} , 3 sensors were used. They were placed in a frame that consisted of three modified, rectangular, hollow beams, that had holders for one sensor each. These were mounted at 3 different heights to the sidewalls. All three beams had 4 holes spread evenly, directed upstream, that collected water. The water was then mixed and guided toward the temperature sensors. The use of several sensors at different heights, and several holes in the beams was to get a full picture of the temperature in the whole cross-section. A sketch and a real-life picture of the frame can be seen in figure 3.3 and 3.5, respectively.

Above the draft tube outlet, a piece of string was lowered to measure the relative height to the water free surface for each point of operation. These relative heights h , together with different known heights in the power plant, were used to find the different pressures in the draft tube outlet.

Labyrinth water

As Smeland power plant has a Francis turbine, there is energy loss in the labyrinth water that never makes it through the turbine. To be able to find this loss, the temperature of the water, T_{leak} , was measured with a temperature sensor in an isolated bucket. The amount of flow, Q_{leak} , was measured by a pre-installed “Annubar Flow Meter Station”, and read off a meter on the wall. The exact way of measurement the flow station uses is not known.

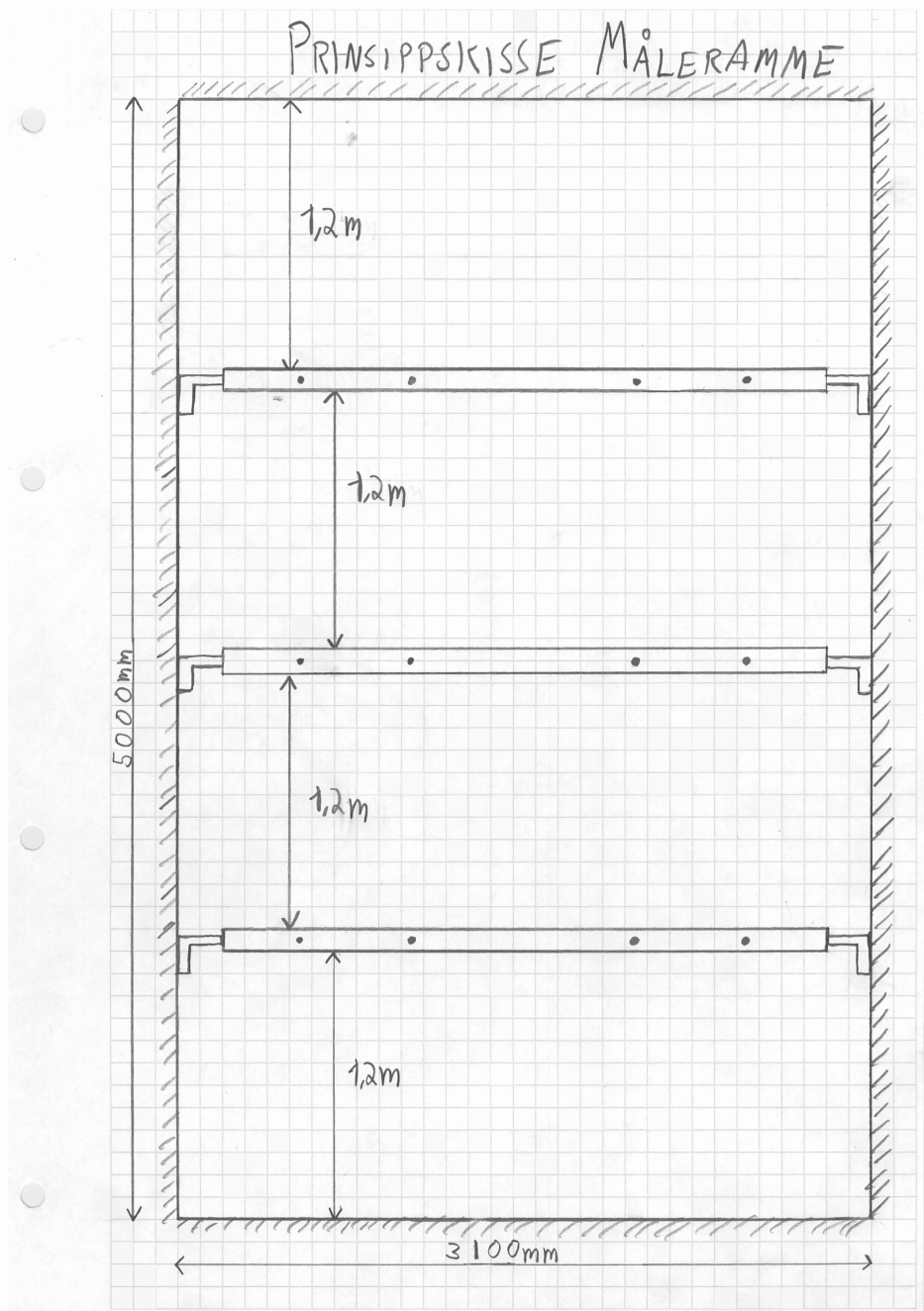


Figure 3.3: Sketch of frame

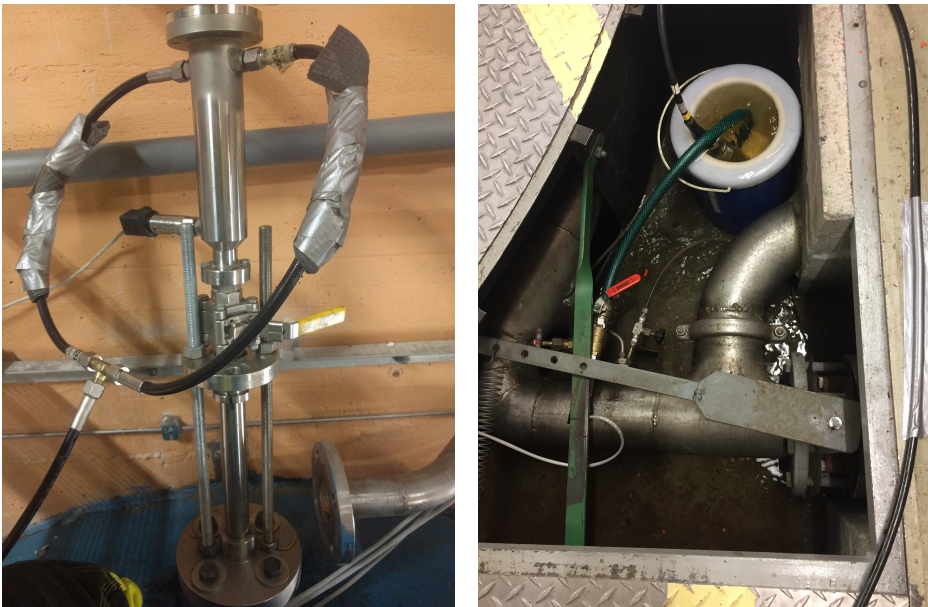


Figure 3.4: Probe on inlet (left), labyrinth water temperature measurement (right)



Figure 3.5: Frame used in outlet, 3 individual beams

3.2.2 Pressure pulsations

For the pressure pulsation measurements, five pressure transducers were placed on various locations on the turbine. At the bare minimum, two sensors should be placed on the draft tube wall, as close as possible to the tapping hole in order to avoid the introduction of new system frequencies stemming from the extra lines and pipes. The draft tube sensors should be spaced 180° apart, so that symmetrical and asymmetrical pulsations can be identified and separated during the analysis, and be mounted as close to the runner outlet as possible. For the measurements at Smeland power plant, two sensors were placed on preexisting taps for a pressure gauge mounted on the wall of the draft tube accordingly.

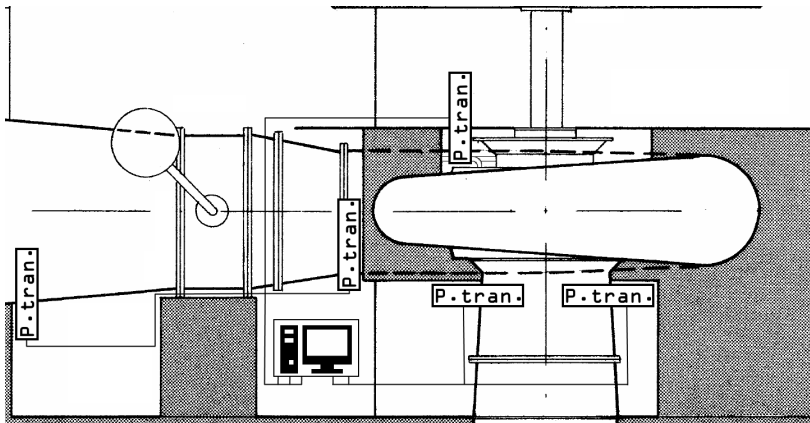


Figure 3.6: Pressure sensor placements

Two sensors were placed on the inlet, one upstream of the main inlet valve, and another close to the spiral casing inlet. Part of the intention with the sensor at the spiral casing inlet was that it would be better suited at picking up the RSI pulsations, which also can be used to validate the frequency analysis. With the sensor upstream of the main inlet valve, the head loss across the main valve could be measured. The fifth and final sensor was placed on the leakage water pipe coming from the upper turbine cover. This sensor was included after professor Nielsen suggested that the pump vane arrangement typically found on Kværner turbines might be the culprit and worth looking into. Four of the sensors were mounted on preexisting taps with globe valves connected to pressure gauges mounted on the wall. The final one, mounted on the labyrinth leakage water pipe, was connected to a T-joint right after another globe valve which were not in use. The other part of the T-joint went to the efficiency measurement arrangement,

explained in chapter 3.2.1.

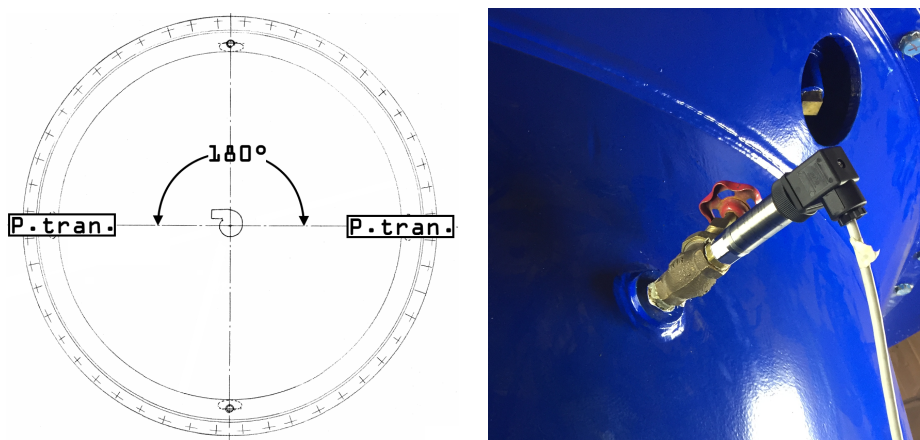


Figure 3.7: Draft tube sensor placement

When the measurements were done, there were taken 3 – 4 independent measurement series, in part due to the long time between changing operation points, at about 90 seconds per series. This was to ensure that everything of interest was captured, and if some of the series turned out to be unusable, it could be discarded, while still having enough measurements left to do the analysis. Before starting the first measurement series at an operation point, the live readouts of the measured values were checked to ensure that the system had stabilised. After a measurement series were done, it was copied over to a different laptop with an analysis script which would import, analyse and display the results. This was done to ensure that the data had been logged and saved correctly. By comparing the analysis with the live readout from the logging program, the risk of discovering some major errors after returning to Trondheim was avoided.

Sound recording

Sound recordings of the noise coming from the draft tube at the operation point of most vibrations was taken during the visit in October 2017, February 2018, and in April 2018. The intention was to have something to compare what was observed in October 2017, with what was measured with pressure transducers in February and April 2018, and if possible, validate the results from the pressure signal analysis with a secondary and independent “measurement”.

3.2.3 Air injection

Preliminary air- and water injection tests in February 2018

When air injection was attempted, it was done through a check valve on the upper turbine cover, as this check valve led to an air vent in the centre of the runner (fig. 3.8). The check valve and air vent is there to let air into the turbine and draft tube if something were to happen and the pressure in the turbine drops below ambient pressure. Through this valve, air could be injected directly into the suspected origin of the pulsations, and thus maybe increase the effect it would have compared to injecting it along the draft tube wall.



Figure 3.8: Check valve at the turbine cover (left), air vent in the runner centre (right).

While doing the tests in February 2018, the check valve was first taken off, and a standard air tool connector was mounted on with a simple ball valve. There was no possibility at the time to neither measure the air flow rate, nor properly control it. The only thing that could be done was to let the compressor fill up the tank and pipes leading to the valve, and open it when it was full and wait until the compressor was drained, all while taking measurements.

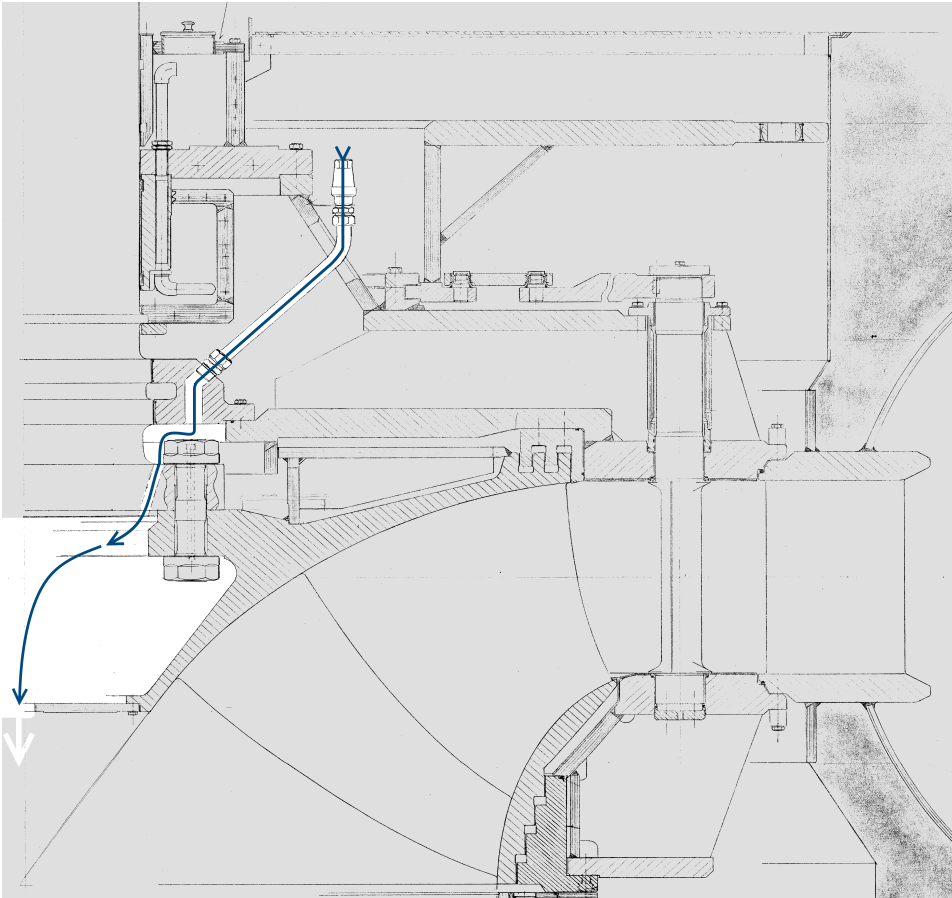


Figure 3.9: Sketch showing where the air goes in the turbine (Andresen & Grøner AS, 1984b)



Figure 3.10: Air hose and valve mounted in place of the check valve

Air flow measurements in April 2018

When the air flow measurements were done, the turbine had two pressure transducers mounted on the draft tube cone, in the same arrangement as explained in chapter 3.2.2, separated by 180° . Two sensors were mounted on the air pipe, as specified in ISO 5167-2, in the D and $D/2$ pressure tapping arrangement (fig. 3.11). This and other key dimensions for the pipe are listed in table 3.6.

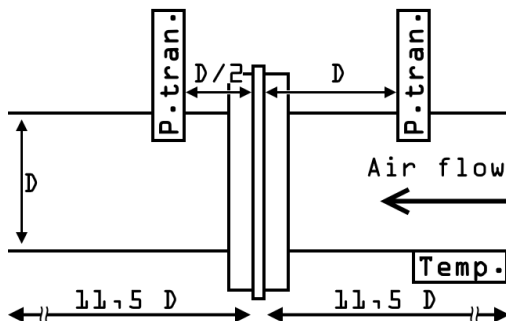


Figure 3.11: Sketch of the sensor placements on the air pipe

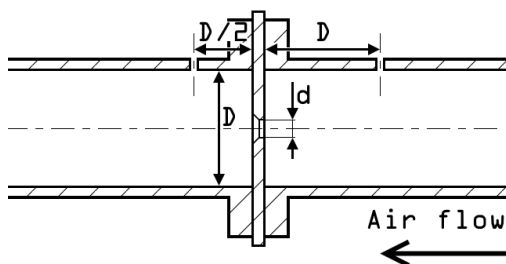


Figure 3.12: Cross section sketch of the air pipe and orifice plate arrangement

| | | |
|----------------------------|----------|----------|
| Pipe inner diameter | D | 52 mm |
| Upstream pipe length | L_{p1} | $11,5D$ |
| Downstream pipe length | L_{p2} | $11,5D$ |
| Upstream sensor position | L_1 | D |
| Downstream sensor position | L_2 | $D/2$ |
| Orifice hole diameter | d | $0,254D$ |

Table 3.6: Key dimensions for the measurement pipe and orifice plate

A fifth sensor was used to get a reading of the atmospheric pressure on the site as well. In addition, a PT100 temperature probe was mounted on the pipe wall, and the whole arrangement was thoroughly isolated with foam in order to get a more accurate reading of the air temperature. It was done this way mainly because of the challenge of mounting something in the air pipe that would be both able to withstand the pressure and not leak, as well as not protrude into the pipe, introducing disturbances in the flow. The temperature readout would only come in to play when estimating the density of the air, and it was found that within the pressure and temperature range that was expected, an error of ± 1 °C would not change the results significantly.

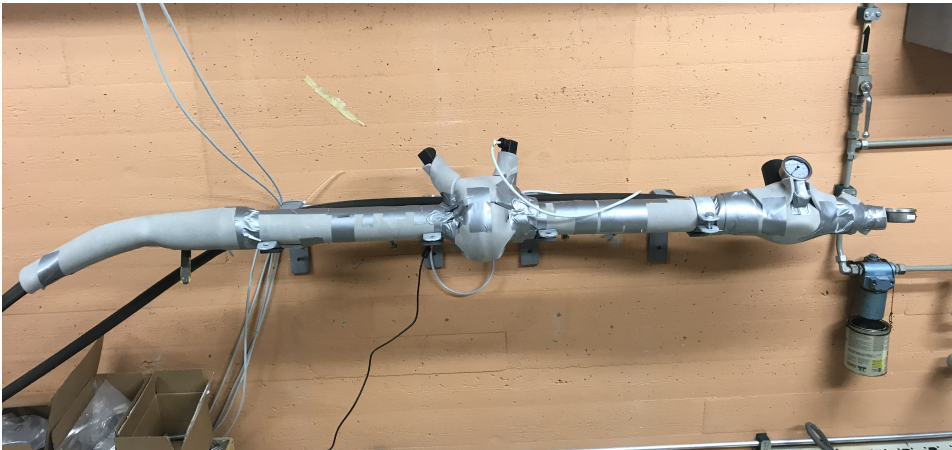


Figure 3.13: Arrangement used for air flow measurements

During the measurements, the turbine was first put in to the operation point at which the pulsations were most severe. Then a benchmark measurement was taken with no air injected, before moving on to doing measurements at varying air flow rates. Since one orifice plate has a somewhat restricted range of operation, $0,75 < p_2/p_1 < 0,98$, several plates were fabricated to increase the possible measuring range. If necessary, the orifice plate would be taken out and replaced with a plate with a larger orifice diameter. This was to be done until the pulsations ceased.

3.3 Data handling

3.3.1 Efficiency

A spreadsheet was used for calculating both the efficiency and its uncertainty, using numerous, serial calculations in regard to the thermodynamic method and uncertainty analysis. A numerical computing program, like MATLAB, could also have been used, but as there are no heavy calculations done and a spreadsheet can give a better overview, Excel was used for this purpose. MATLAB was, however, used to import the data from the measurement files, and to calculate the mean values and random error. From there the measured data and basic data were used to calculate the efficiency, its uncertainty, and other relevant values. This was done by breaking down equation 2.8, 2.9 and 2.10 into pressure, temperature, potential and kinetic terms. Example calculations can be found in appendix D and E.

3.3.2 Pressure pulsations

For the analysis of the pressure pulsation data, MATLAB was used extensively throughout the process, from importing and sorting the vast amounts of data to analysing and presenting the results. One key advantage of MATLAB is its large library of built in functions, such as the power Welch method. Similarly, when the calculation of the air flow rate was done, an iterative calculation was required, and as the number of necessary iterations is not really known beforehand, a spreadsheet would not really be practical.

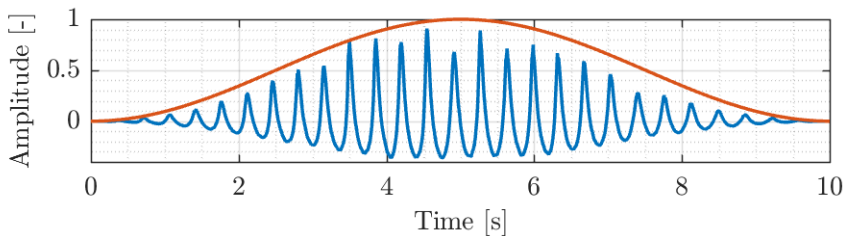


Figure 3.14: Window modified signal with Hann window function superimposed. Signal amplitude reduced to scale with window amplitude.

Welch windowing

For the power Welch analysis, a Hann window was chosen, as recommended in IEC 60193. The length of each window, and thus the number of windows, was chosen on the basis of the desired frequency resolution, which was set to

$f_{res} = 0,1$ Hz, resulting in windows of ~ 10 seconds in length. The window overlap was set to 45 % of the window length.

Histogram method

When calculating the peak-to-peak (Δp) values of the pressure signals, a 99 % confidence interval of the measured pressure values was used to find the Δp pressure, as the raw signals contained next to no spikes, and any lower settings were considered to exclude too much of the extremities of the measurements.

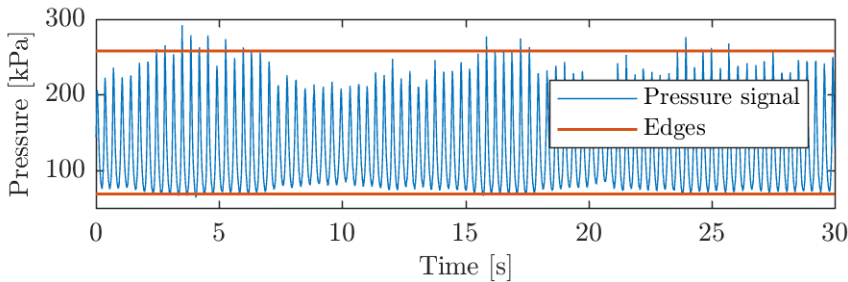


Figure 3.15: Pressure signal with the peak-to-peak edges superimposed.

Hilbert envelope

The Hilbert envelope was used to extract the amplitude modulation frequency of the sound recordings using a “peak” type envelope with windows of 720 samples in length. The window length was found through trial and error. As the sampling frequency of the sound recording was 48 kHz, this meant that each window was 0,015 seconds long. The resulting envelopes were then put through the same power Welch analysis with a Hann window function as described earlier.

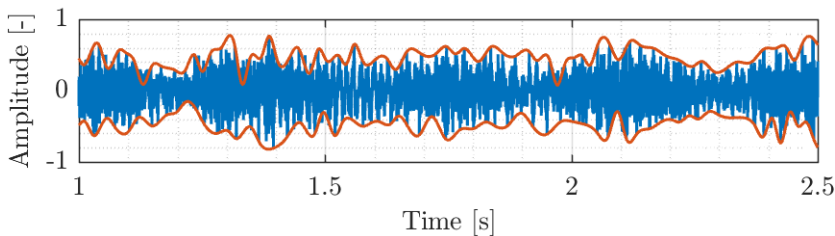


Figure 3.16: Sound signal with the Hilbert envelope superimposed.

3.3.3 Assumptions made for the air mass flow rate calculations

To calculate the mass flow rate of the air, q_m , μ_1 , ρ_1 , D , d , κ and Δp_{1-2} is needed. Δp_{1-2} is the measured pressure drop over the orifice plate, D is the pipe diameter and d is the orifice diameter. The adiabatic exponent, κ , is assumed to be 1,4, while μ_1 and ρ_1 is calculated using the pressure before the orifice plate p_1 , and the measured air temperature T_1 . To calculate the dynamic viscosity μ_1 , Sutherland's viscosity law is used

$$\mu_1 = \mu_{ref} \left(\frac{T_1}{T_{ref}} \right)^{\frac{3}{2}} \left(\frac{T_{ref} + S}{T_1 + S} \right) \text{ [Pa s]} \quad (3.8)$$

where μ_{ref} is some reference viscosity, T_{ref} is the temperature at that reference point and S is the Sutherland temperature ($S = 110,4 \text{ K}$). All the temperatures are given in Kelvin. The air density, ρ_1 was calculated using the ideal gas law

$$\rho_1 = \frac{p_1}{T_1 R_{specific}} \text{ [kg/m}^3\text{]} \quad (3.9)$$

where $R_{specific}$ is the specific gas constant for the air.

4.1 Hydraulic efficiency at Smeland

Following IEC guidelines, the spiral casing, stay vanes, and guide vanes were inspected. Irregularities like cavitation, and accumulation of waste in the end of the spiral casing, were not found.

| M # | η_h [-] | e_{η_h} [-] | Q [m^3/s] | e_Q [m^3/s] | P_t [MW] |
|------|--------------|------------------|---------------|-------------------|------------|
| I | 0,947 | 0,0083 | 23,6 | 0,2612 | 19,96 |
| II | 0,941 | 0,0083 | 25,6 | 0,2834 | 21,56 |
| III | 0,935 | 0,0084 | 27,8 | 0,3067 | 23,21 |
| IV | 0,932 | 0,0084 | 29,1 | 0,3212 | 24,22 |
| V | 0,925 | 0,0084 | 30,5 | 0,3372 | 25,26 |
| VI | 0,798 | 0,0077 | 8,5 | 0,1026 | 6,08 |
| VII | 0,884 | 0,0080 | 12,2 | 0,1401 | 9,65 |
| VIII | 0,921 | 0,0081 | 15,9 | 0,1793 | 13,11 |
| IX | 0,932 | 0,0082 | 18,1 | 0,2019 | 15,06 |
| X | 0,941 | 0,0083 | 20,3 | 0,2250 | 17,05 |
| XI | 0,944 | 0,0083 | 23,8 | 0,2631 | 20,07 |
| XII | 0,932 | 0,0084 | 29,1 | 0,3211 | 24,21 |
| XIII | 0,932 | 0,0084 | 29,2 | 0,3221 | 24,31 |

Table 4.1: Main results in tabular form, adjusted for nominal head and flow

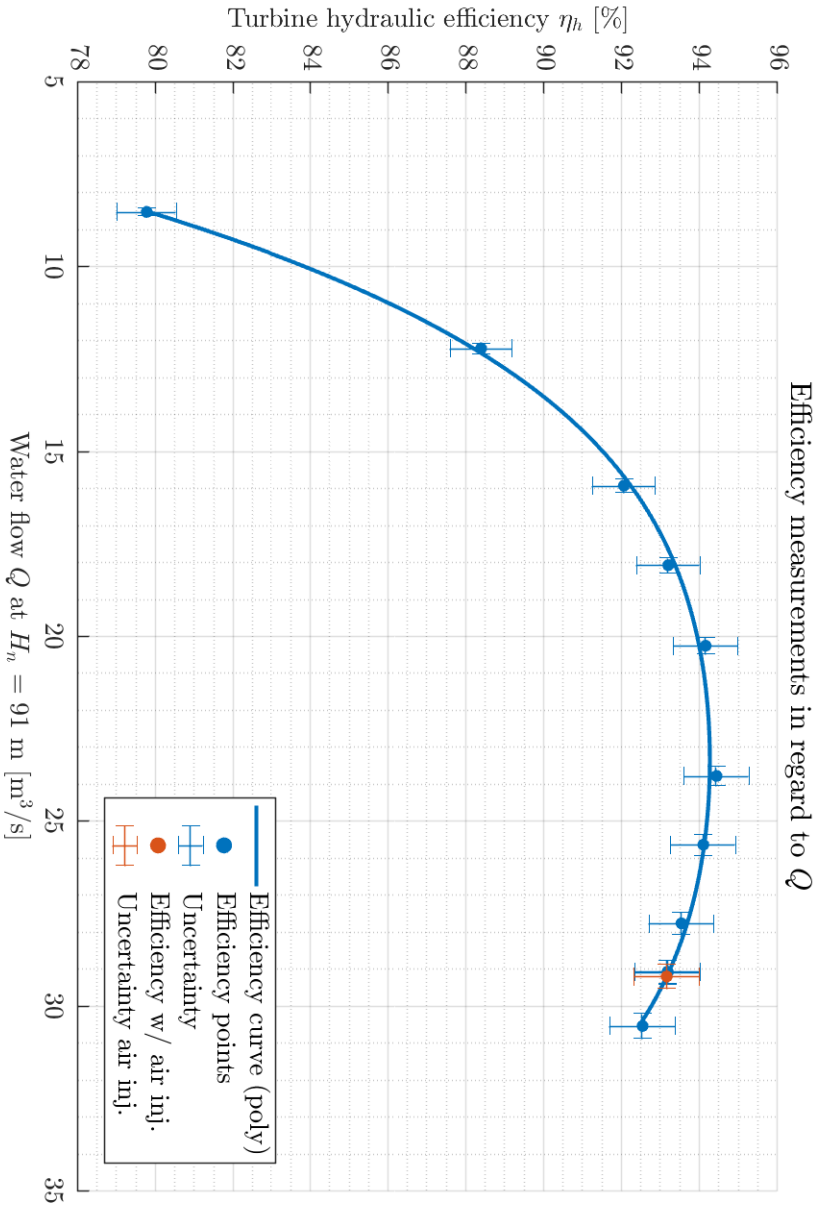


Figure 4.1: $\eta - Q$ plot with the air injection point superimposed at $H_n = 91$ m

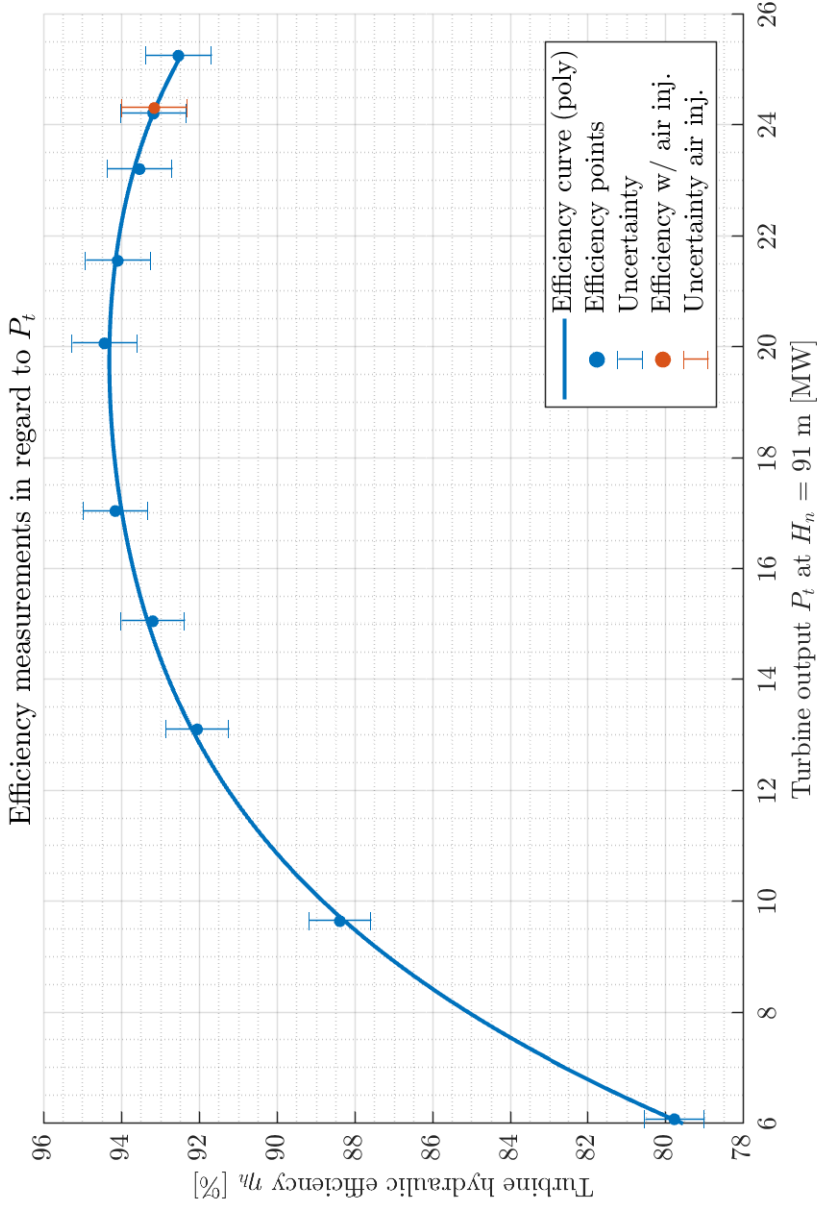


Figure 4.2: $\eta - P_t$ plot with the air injection point superimposed at $H_n = 91$ m

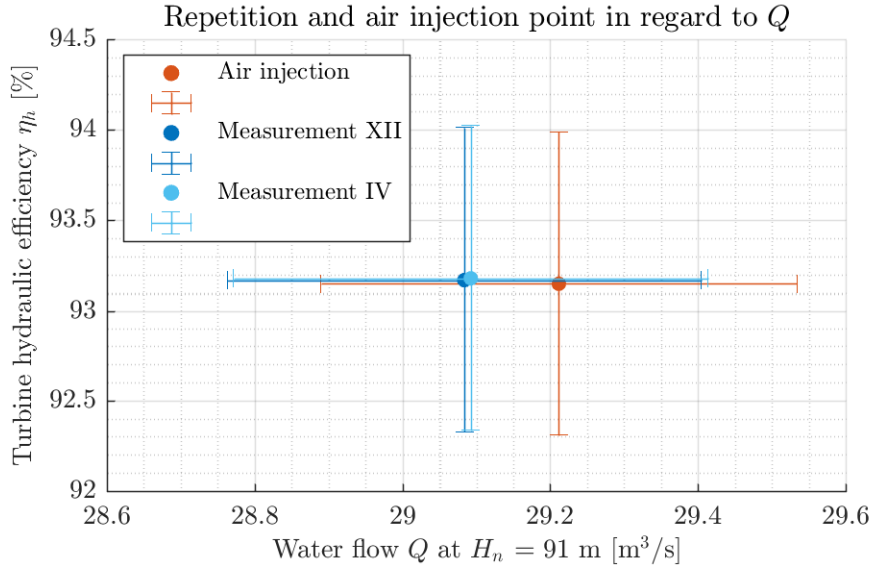


Figure 4.3: Closeup of the repetition point in the $\eta - Q$ plot, at $H_n = 91$ m

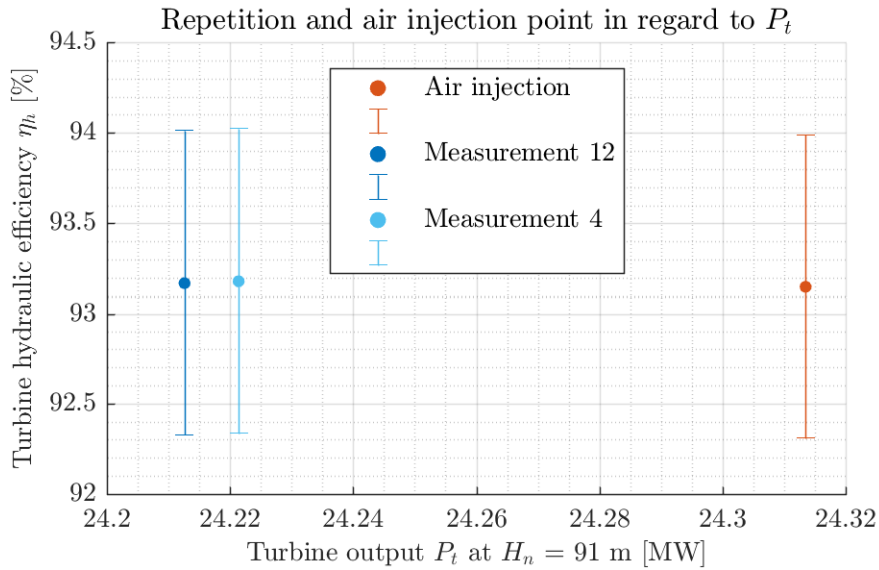


Figure 4.4: Closeup of the repetition point in the $\eta - P_t$ plot, at $H_n = 91$ m

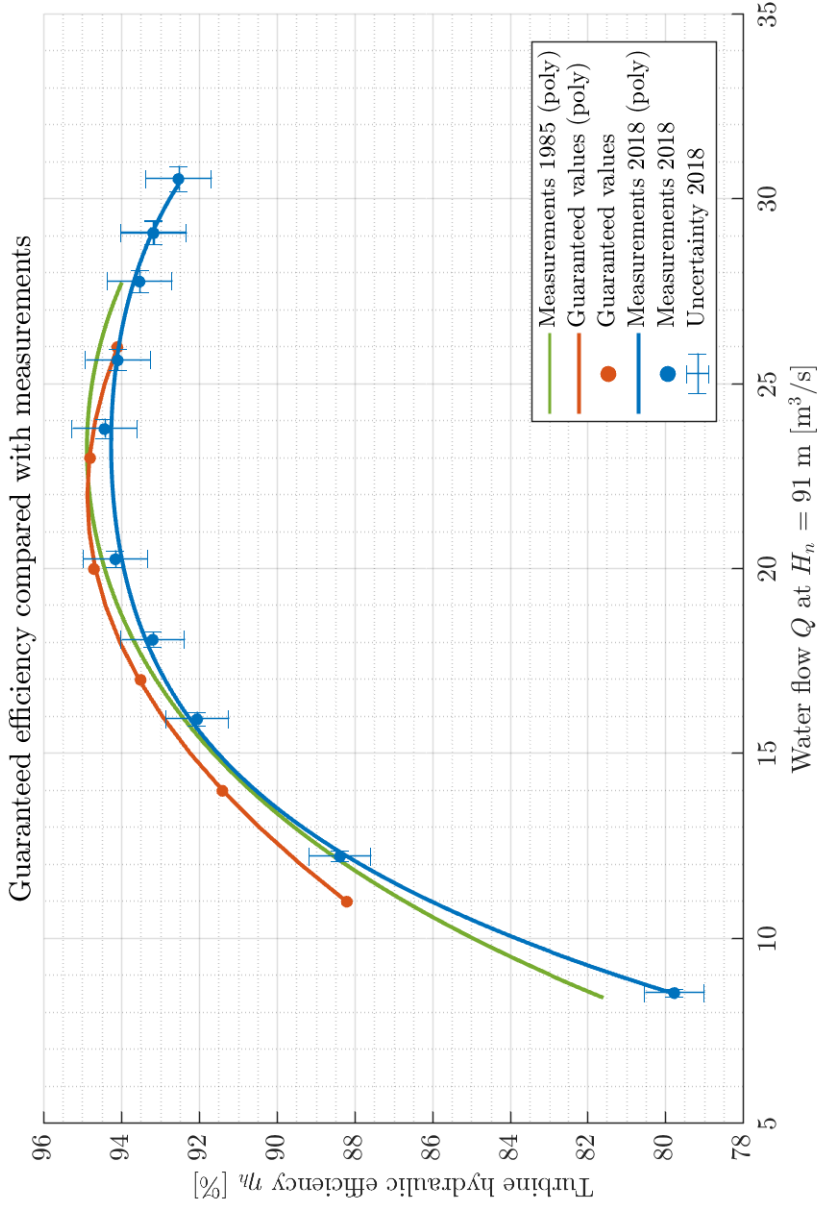


Figure 4.5: Comparison between the guaranteed efficiency, results from the Kværner report, and the calculated efficiency, at $H_n = 91$ m

4.2 Pressure pulsations

4.2.1 Observed frequencies

All the frequencies presented here are normalised with the runner rotational frequency, which is $n = 250 \text{ rpm} \Rightarrow f_n = 4,1667 \text{ Hz}$. Similarly, most of the presented pressures are normalised with the design head of Smeland power plant, $H_0 = 91 \text{ m} \Rightarrow p_0 \approx 994,7 \text{ kPa}$. The turbine has $Z_s = 24$ guide vanes, and $Z_r = 28$ runner blades in a 14/14 arrangement of half- and full length blades. The pressure amplitude presented in the FFT results are given in kPa, as the analysed signals were given in kPa.

| | | |
|----------------|---|--|
| M # | = | Measurement number |
| $P_{gen,i}$ | = | Indicated power as read from regulator display |
| SC | = | Spiral casing inlet |
| DT 0° | = | Draft tube sensor at 0° |
| LP | = | Leakage water pipe from upper cover |
| f/f_n | = | Frequency divided by runner frequency |
| $\Delta p/H_0$ | = | Peak to peak pressure divided by design head |

Table 4.2: Nomenclature used in table 4.4

| $M- \#$ | Note | $M- \#$ | Note |
|---------|--------------------------------|---------|-------------------------------|
| XIII | Air injected, full compressor | XVII | No air injection |
| XIV | Air injected, empty compressor | XVIII | Air injection, lowest opening |
| XV | Water injected | XIX | Air injection, mid opening |
| XVI | Check-valve off | XX | Air injection, mid opening |
| | | XXI | Air injection, full opening |
| | | XXII | No air injection |
| | | XXIII | Air injection, mid opening |
| | | XXIV | Air injection, full opening |

Table 4.3: Additional measurement points in February 2018 (left) and April 2018 (right). Note that $M-XVII$ to $M-XXI$ is with the intake at Monn open, while $M-XXII$ to $M-XXIV$ is with the intake closed.

| M # | $P_{gen,i}$ | | SC | DT 0° | LP | |
|------|-------------|----------------|-------|-------|-------------------|-----|
| I | 19,6 MW | f/f_n | 28,01 | 1,95 | 17,01 | [-] |
| | | $\Delta p/H_0$ | 0,89 | 0,43 | 4,04 | [%] |
| II | 20,8 MW | f/f_n | 28,00 | 1,15 | 17,00 | [-] |
| | | $\Delta p/H_0$ | 1,07 | 0,78 | 3,85 | [%] |
| III | 22,0 MW | f/f_n | 1,06 | 1,06 | 1,06 [†] | [-] |
| | | $\Delta p/H_0$ | 8,62 | 9,01 | - [†] | [%] |
| IV | 22,8 MW | f/f_n | 0,67 | 0,67 | 0,67 [†] | [-] |
| | | $\Delta p/H_0$ | 16,65 | 18,52 | - [†] | [%] |
| V | 23,5 MW | f/f_n | 0,51 | 0,51 | 0,51 [†] | [-] |
| | | $\Delta p/H_0$ | 9,50 | 12,74 | - [†] | [%] |
| VI | 6,1 MW | f/f_n | 0,22 | 0,22 | 17,00 | [-] |
| | | $\Delta p/H_0$ | 0,98 | 3,04 | 4,45 | [%] |
| VII | 9,8 MW | f/f_n | 0,25 | 0,26 | 17,01 | [-] |
| | | $\Delta p/H_0$ | 1,02 | 2,56 | 3,19 | [%] |
| VIII | 13,2 MW | f/f_n | 0,23 | 0,23 | 17,01 | [-] |
| | | $\Delta p/H_0$ | 0,93 | 1,68 | 3,28 | [%] |
| IX | 14,9 MW | f/f_n | 0,21 | 0,28 | 17,01 | [-] |
| | | $\Delta p/H_0$ | 0,85 | 1,24 | 3,32 | [%] |
| X | 16,7 MW | f/f_n | 1,00 | 1,00 | 16,99 | [-] |
| | | $\Delta p/H_0$ | 0,91 | 0,76 | 3,48 | [%] |
| XI | 19,5 MW | f/f_n | 1,00 | 2,78 | 16,99 | [-] |
| | | $\Delta p/H_0$ | 0,75 | 0,43 | 4,03 | [%] |
| XII | 22,7 MW | f/f_n | 0,67 | 0,67 | 0,67 [†] | [-] |
| | | $\Delta p/H_0$ | 16,76 | 18,98 | - [†] | [%] |

Table 4.4: Normalised measured frequencies and peak to peak pressures

[†]Pressure exceeded maximum range of sensor, and clipping occurred

| M # | | SC | DT 0° | LP | |
|------|----------------|-------|-------|--------|-----|
| XIII | f/f_n | 0,48 | 0,48 | 17,02 | [-] |
| | $\Delta p/H_0$ | 1,17 | 1,26 | 4,27 | [%] |
| XIV | f/f_n | 0,60 | 0,60 | 0,60 | [-] |
| | $\Delta p/H_0$ | 4,85 | 6,41 | 4,92 | [%] |
| XV | f/f_n | 0,64 | 0,64 | 0,64 † | [-] |
| | $\Delta p/H_0$ | 18,02 | 20,04 | - † | [%] |
| XVI | f/f_n | 0,67 | 0,67 | 0,67 † | [-] |
| | $\Delta p/H_0$ | 15,76 | 18,06 | - † | [%] |

Table 4.5: Normalised measured frequencies and peak to peak pressures during the various tests done in February 2018 at the same load as M –XII

| M # | | DT 0° | |
|-------|----------------|-------|-----|
| XVII | f/f_n | 0,73 | [-] |
| | $\Delta p/H_0$ | 21,46 | [%] |
| XVIII | f/f_n | 0,54 | [-] |
| | $\Delta p/H_0$ | 2,22 | [%] |
| XIX | f/f_n | 0,54 | [-] |
| | $\Delta p/H_0$ | 1,62 | [%] |
| XX | f/f_n | 0,53 | [-] |
| | $\Delta p/H_0$ | 1,28 | [%] |
| XXI | f/f_n | 0,44 | [-] |
| | $\Delta p/H_0$ | 0,62 | [%] |
| XXII | f/f_n | 0,69 | [-] |
| | $\Delta p/H_0$ | 19,09 | [%] |
| XXIII | f/f_n | 0,44 | [-] |
| | $\Delta p/H_0$ | 0,82 | [%] |
| XXIV | f/f_n | 0,45 | [-] |
| | $\Delta p/H_0$ | 0,87 | [%] |

Table 4.6: Normalised measured frequencies and peak to peak pressures in the draft tube in April 2018

4.2.2 Draft tube pressure

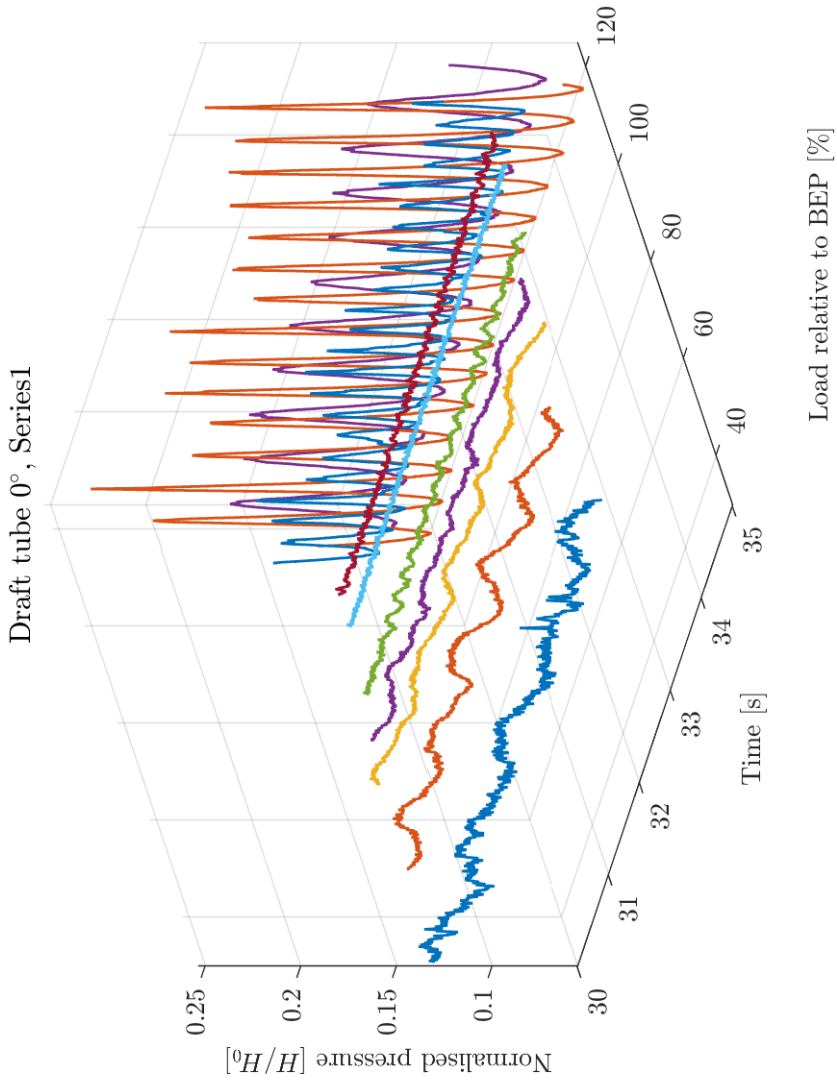


Figure 4.6: 5 second samples of the measured pressure in the draft tube (DT 0°) at all the measured loads

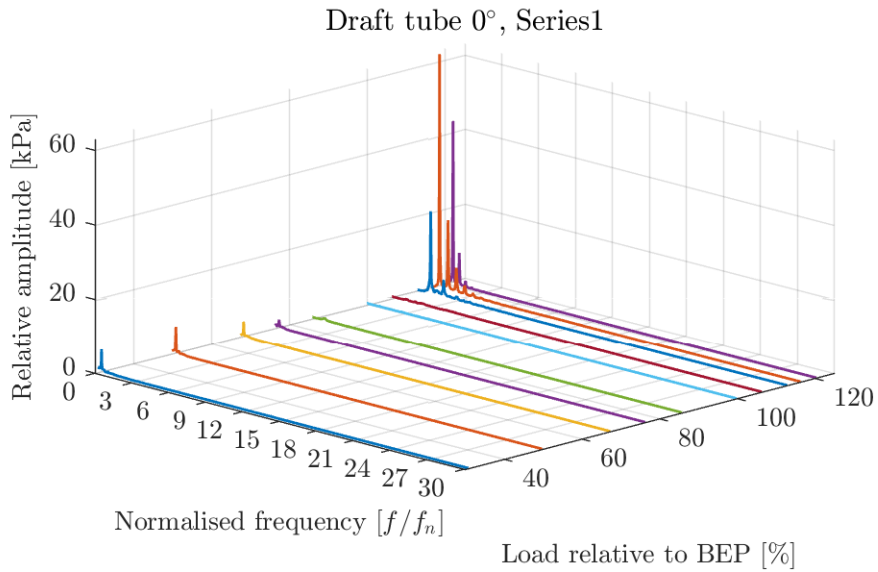


Figure 4.7: Frequencies for the measurements in the draft tube (DT 0°) at all the measured loads

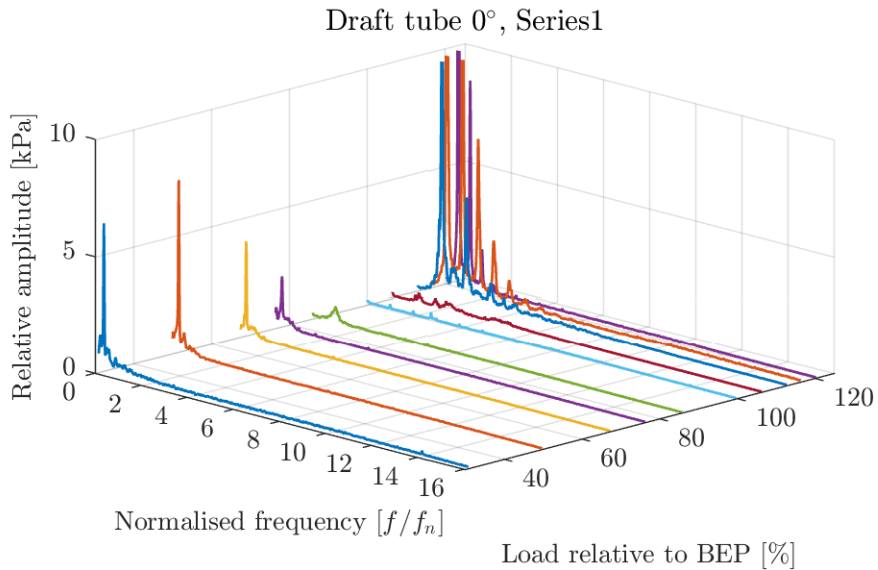


Figure 4.8: Frequencies for the measurements in the draft tube (DT 0°) at all the measured loads, with the x -axis limited to 0 – 16, and the z -axis limited to 0 – 10kPa.

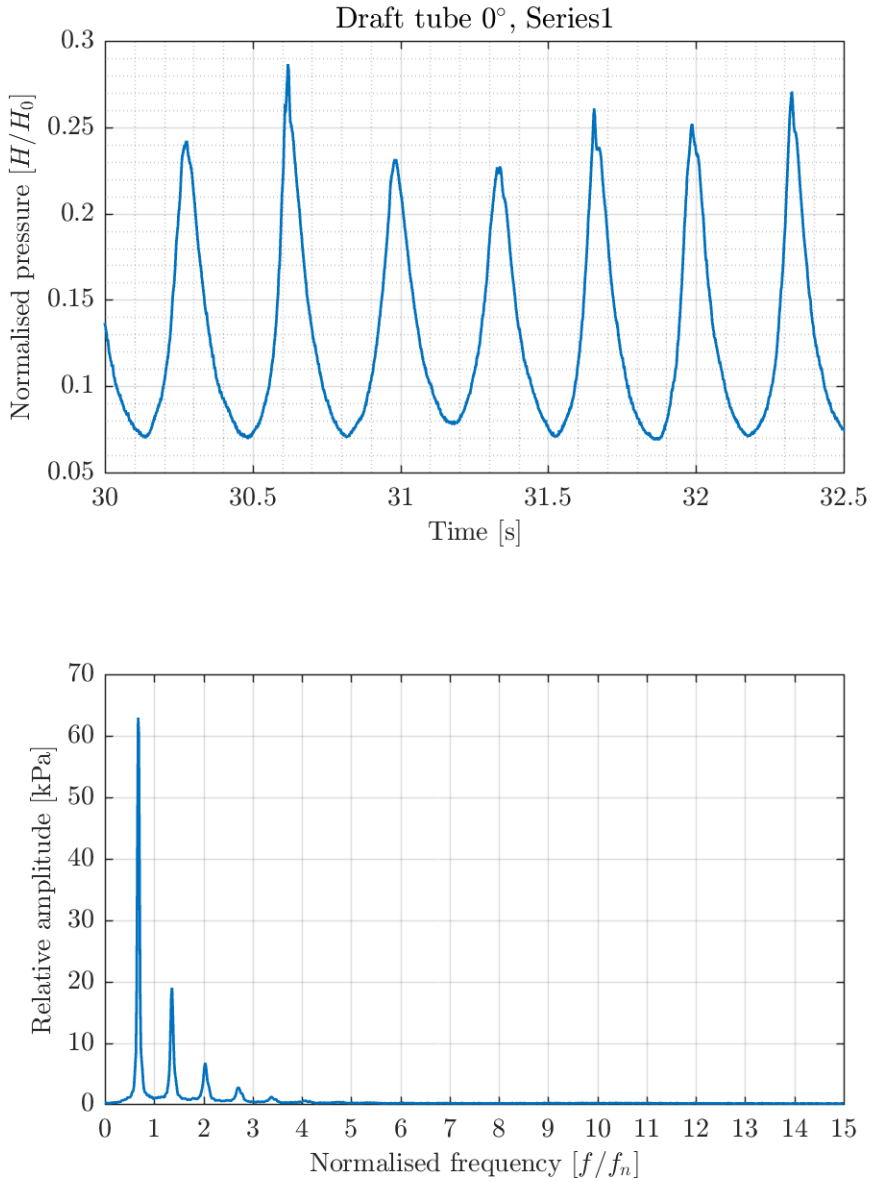


Figure 4.9: Pressure signal and frequencies from the draft tube (DT 0°) at $M-XII$

4.2.3 Spiral casing inlet

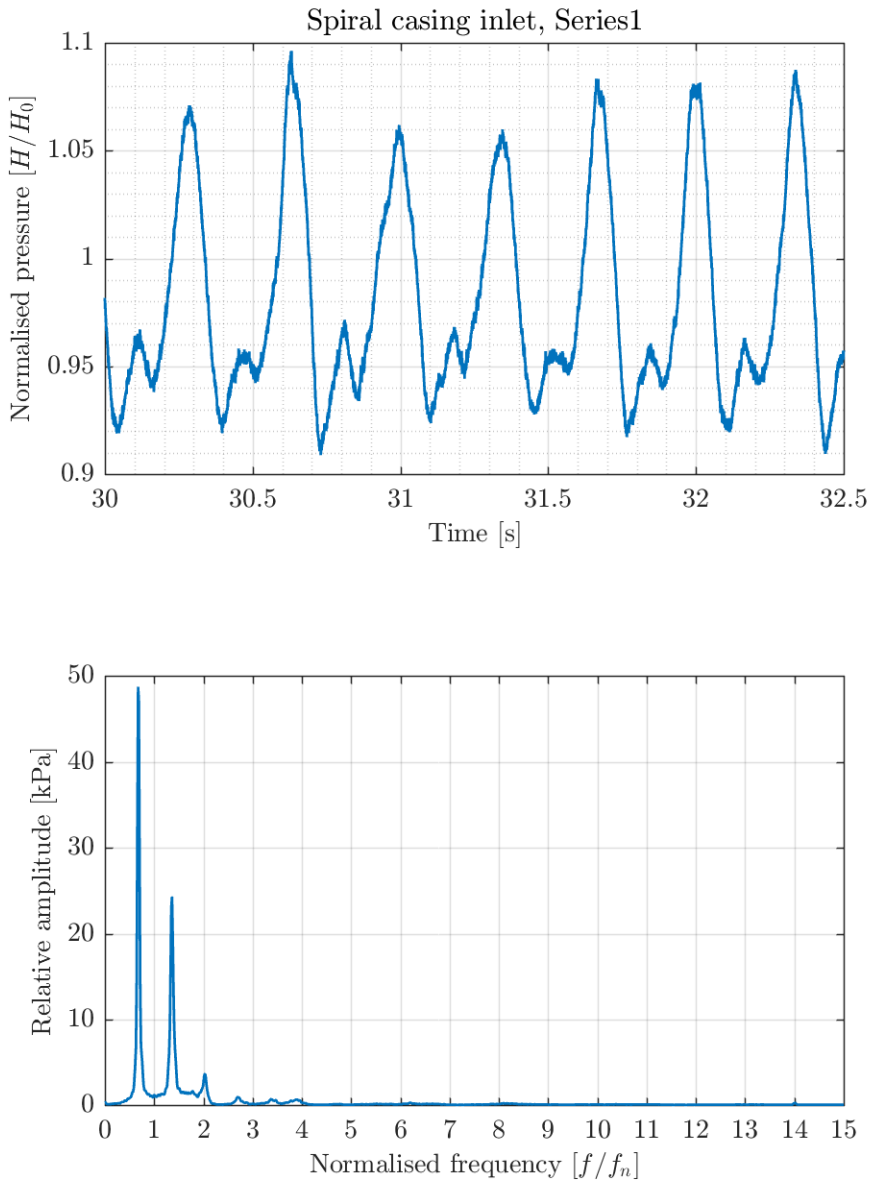


Figure 4.10: Pressure signal and frequencies from the spiral casing inlet (SC) at $M-XII$

4.2.4 Leakage pipe

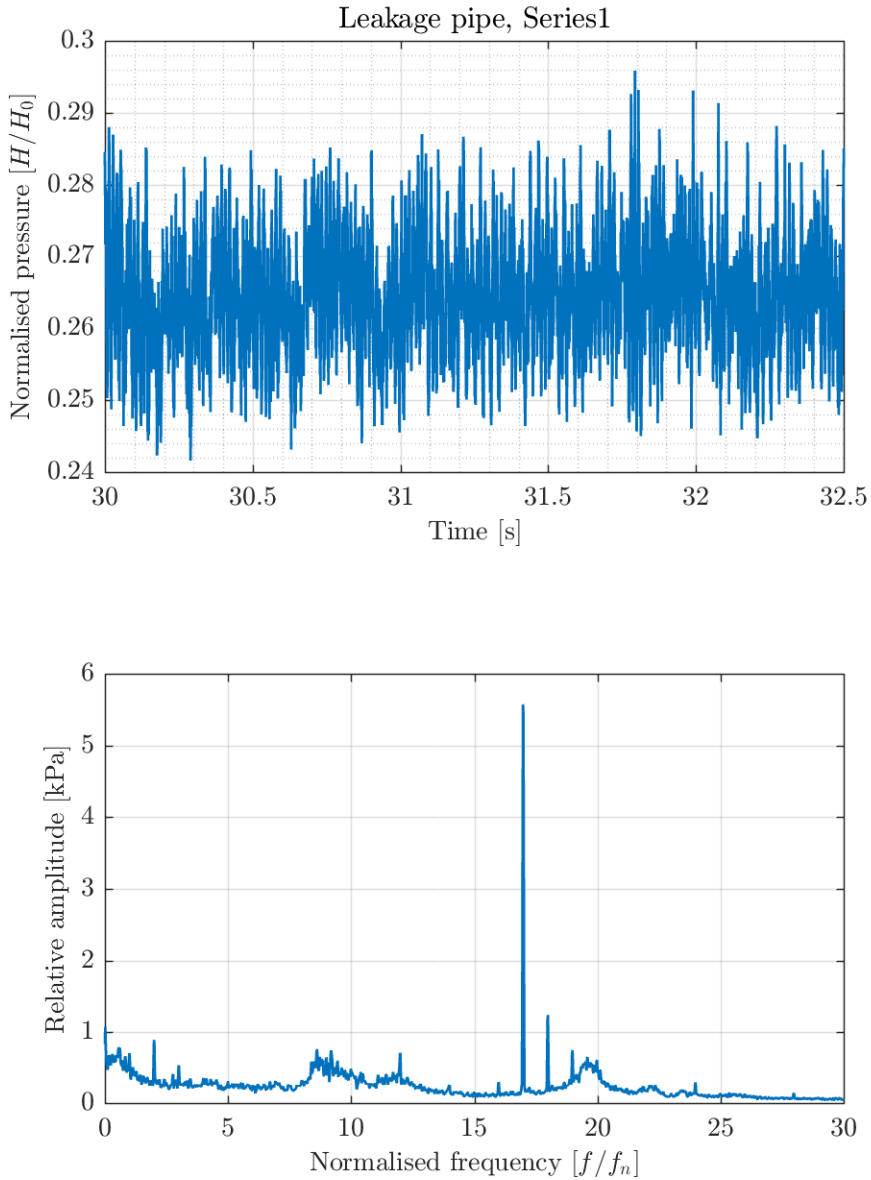
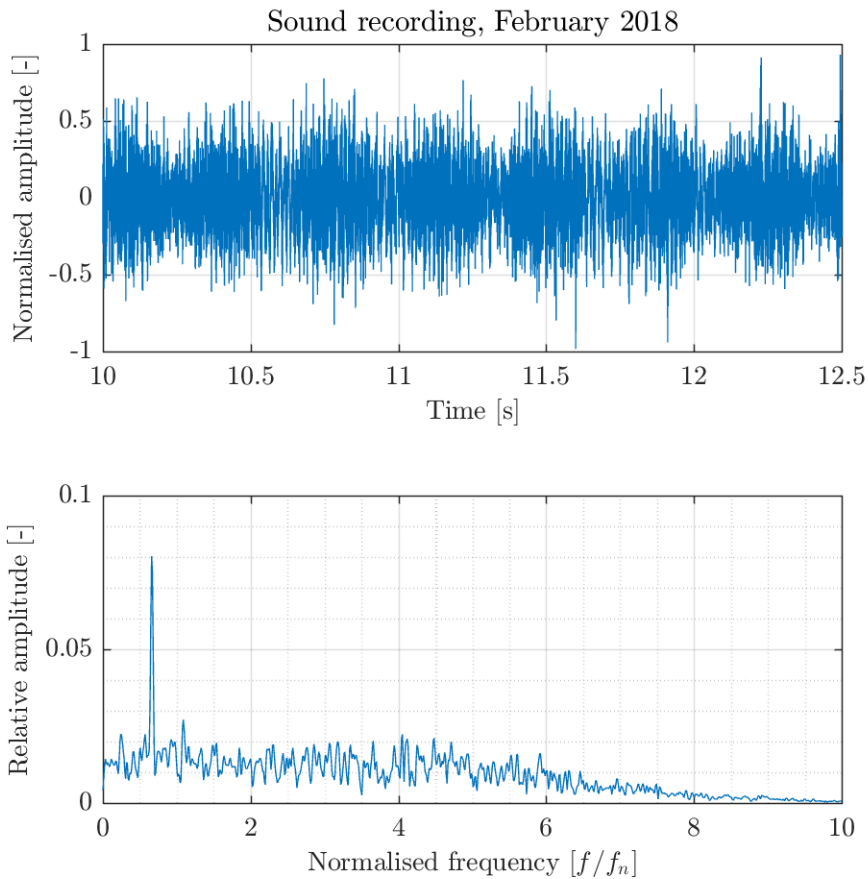


Figure 4.11: Pressure signal and frequencies from the leakage pipe (LP) at $M-XI$ (BEP)

4.2.5 Sound recordings

| Time of recording | f/f_n [-] |
|-------------------|-------------|
| October 2017 | 0,93 |
| February 2018 | 0,66 |
| April 2018 | 0,74 |

Table 4.7: Dominating frequencies obtained from the sound recordings**Figure 4.12:** Sound signal and frequencies of the envelope

4.2.6 RSI

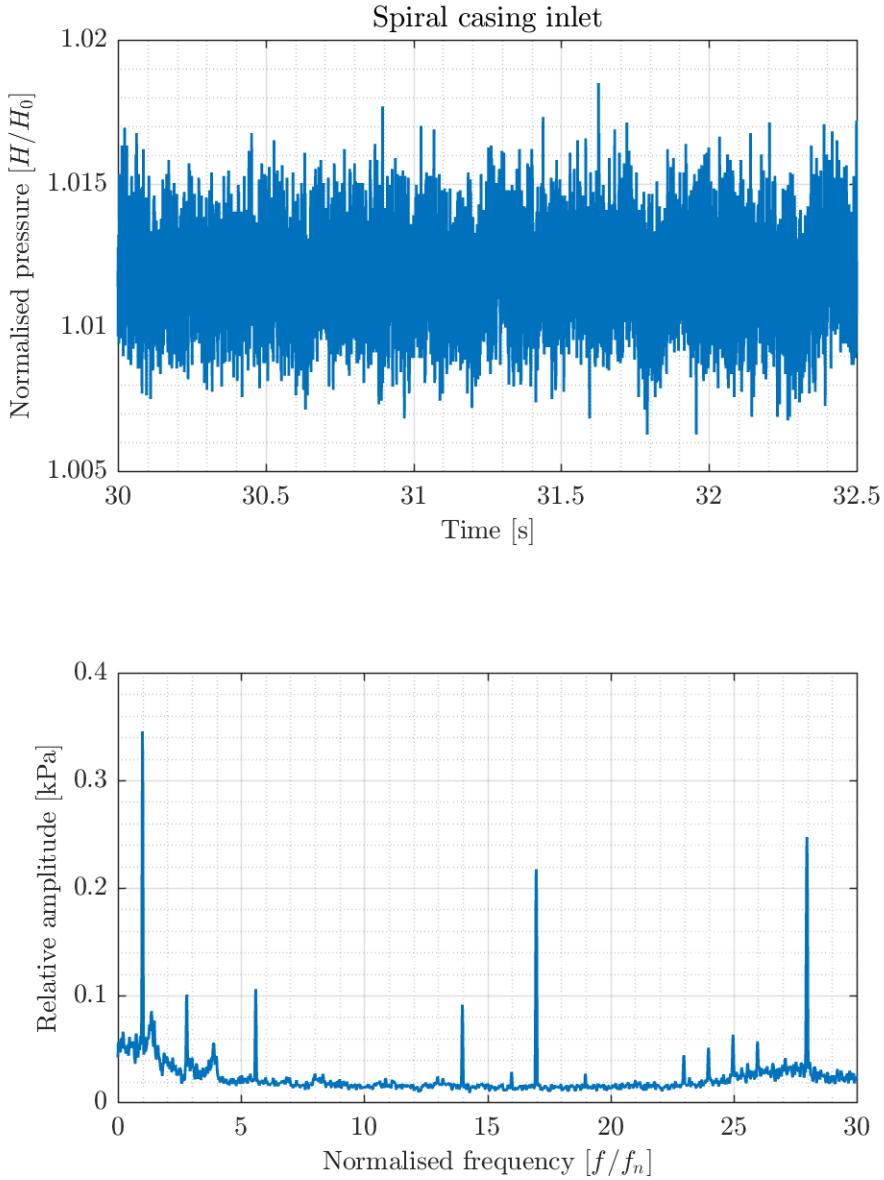


Figure 4.13: Spiral casing inlet during operation at BEP, clearly showing the runner frequency, pump vane frequency (as in figure 4.11), and the RSI.

4.3 Calculated system frequencies

When calculating the pressure wave frequencies in the waterway, a range of both lengths and speed of sound in the water were used, as neither can be pinpointed exactly. For the lower end, a slower speed of sound and higher water levels in the surge chambers was used, and conversely for the higher end, a faster speed of sound and lower water levels was used. The lengths for $f'_{penstock}$ and $f'_{drafttube}$ were set to be from the turbine and to the first abrupt change in cross sectional area, such as the draft tube ending into the large surge chamber, or the penstock starting at the sand trap. The speed of sound was assumed to be in the range of 800 m/s – 1300 m/s.

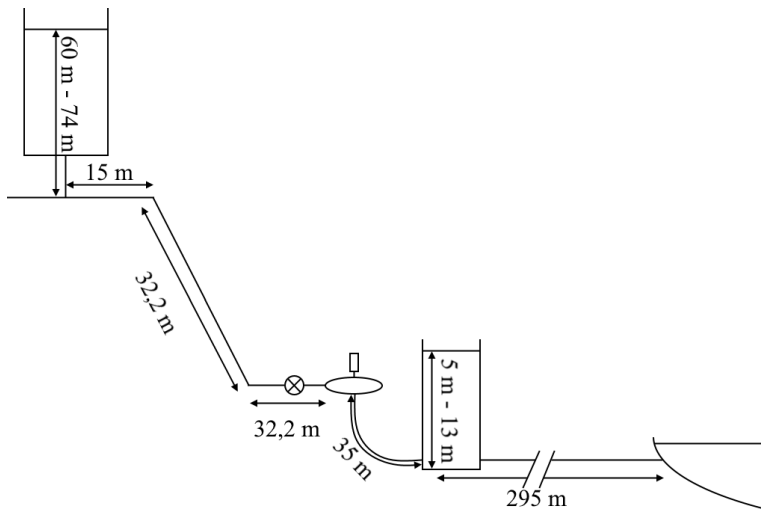


Figure 4.14: Schematic of the water way with lengths, not to scale

| | Lower end | Higher end | |
|----------------------|-----------|------------|-----|
| f_n/f_n | 1 | 1 | [-] |
| f_s/f_n | 28 | 28 | [-] |
| f_r/f_n | 24 | 24 | [-] |
| $f_{penstock}/f_n$ | 0.30 | 0.54 | [-] |
| $f'_{penstock}/f_n$ | 0.73 | 1.21 | [-] |
| $f_{drafttube}/f_n$ | 1.02 | 1.95 | [-] |
| $f'_{drafttube}/f_n$ | 1.39 | 2.25 | [-] |
| f_{outlet}/f_n | 0.31 | 0.52 | [-] |

Table 4.8: Calculated system frequencies for Smeland normalised with the runner frequency

4.4 Calculated suspended bubble volume

Using Nielsen's conjecture (eqn. 2.18), the volume of the suspected draft tube vortex bubble was calculated, ranging from 1.8 – 4 Hz or 0,43 – 0,96 in normalised values. The assumptions made for this was that $\kappa \approx 1,4$, and that D_0 is equal to the idealised case of a spherical bubble of the same volume V_0 .

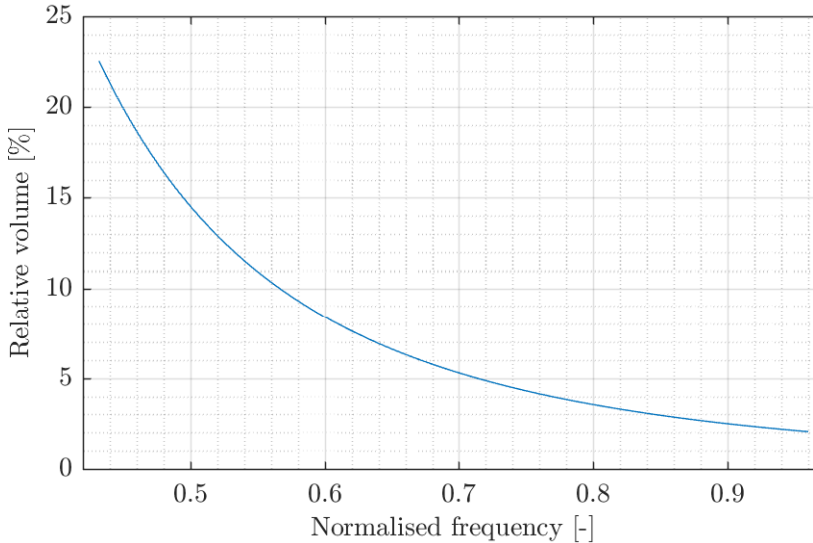


Figure 4.15: Calculated volume to frequency. Normalised with the draft tube cone volume (10.17 m³)

4.5 Air injection

4.5.1 Preliminary test

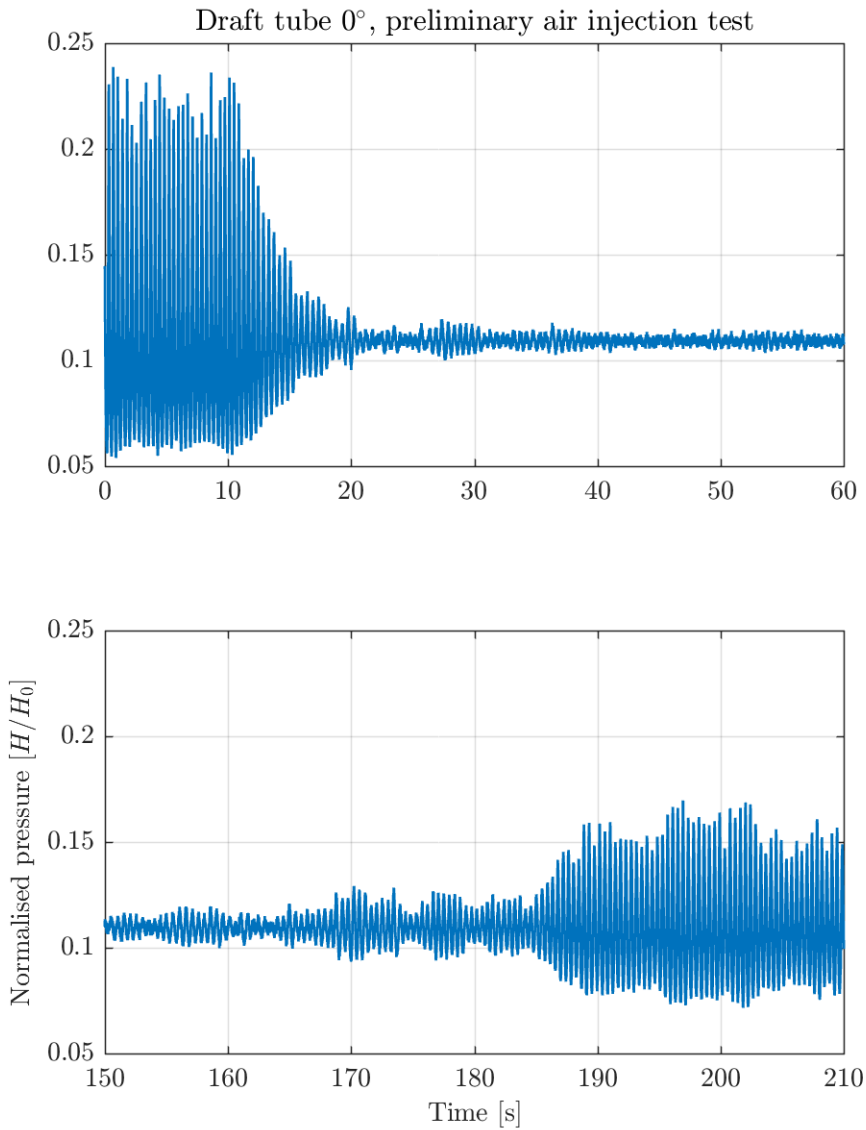


Figure 4.16: Measured pressure in the draft tube during the air injection, both at the opening of the valve (top) and when the compressor was drained (bottom)

4.5.2 Orifice plate

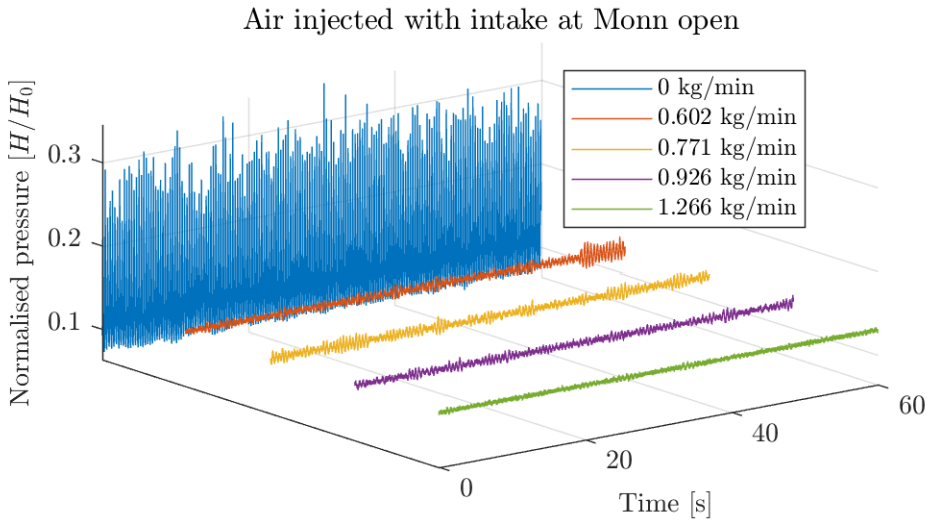


Figure 4.17: Measured draft tube pressure (DT 0°) normalised with design head, at various calculated air mass flow rates, intake gate at Monn open.

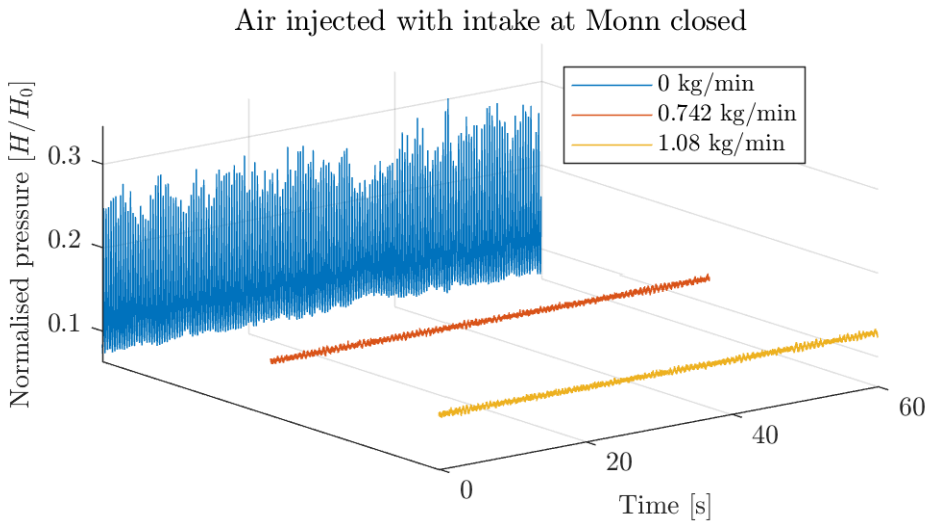


Figure 4.18: Measured draft tube pressure (DT 0°) normalised with design head, at various calculated air mass flow rates, intake gate at Monn closed.

| \bar{p}_1 [kPa] | \bar{p}_{DT} [kPa] | $\Delta p/H_0$ [%] | q_m [kg/min] | f_{q_m} [%] | q_V [l/min] [‡] | f_{q_V} [%] |
|----------------------|-------------------------|-----------------------|-------------------|------------------|-------------------------------|------------------|
| - | 129,423 | 21,46 | 0 | 0 | 0 | 0 |
| 163,831 | 128,646 | 2,22 | 0,602 | 1,781 | 499,862 | 1,792 |
| 164,181 | 128,686 | 1,62 | 0,771 | 1,070 | 640,237 | 1,089 |
| 163,650 | 128,649 | 1,28 | 0,926 | 0,911 | 769,352 | 0,933 |
| 165,218 | 128,253 | 0,62 | 1,266 | 0,892 | 1051,61 | 0,914 |
| - | 129,194 | 19,09 | 0 | 0 | 0 | 0 |
| 162,584 | 127,340 | 0,82 | 0,742 | 1,096 | 616,121 | 1,114 |
| 163,115 | 127,392 | 0,87 | 1,080 | 0,914 | 896,609 | 0,935 |

Table 4.9: Results from the air injection measurements, both with the intake at Monn open (top), and closed (bottom)

| M # | V_0 [m ³] | ΔV_0 [m ³] | $\Delta V_0/V_0$ [%] |
|-------|----------------------------|-----------------------------------|-------------------------|
| XVII | 0,476 | - | - |
| XVIII | 1,173 | 0,698 | 147 |
| XIX | 1,173 | 0,698 | 147 |
| XX | 1,238 | 0,763 | 160 |
| XXI | 2,181 | 1,705 | 358 |
| XXII | 0,565 | - | - |
| XXIII | 2,181 | 1,615 | 286 |
| XXIV | 2,011 | 1,446 | 256 |

Table 4.10: Calculated air bubble volume change for each of the measurement points in April 2018

[‡]Calculated at 20 °C and 1 atm

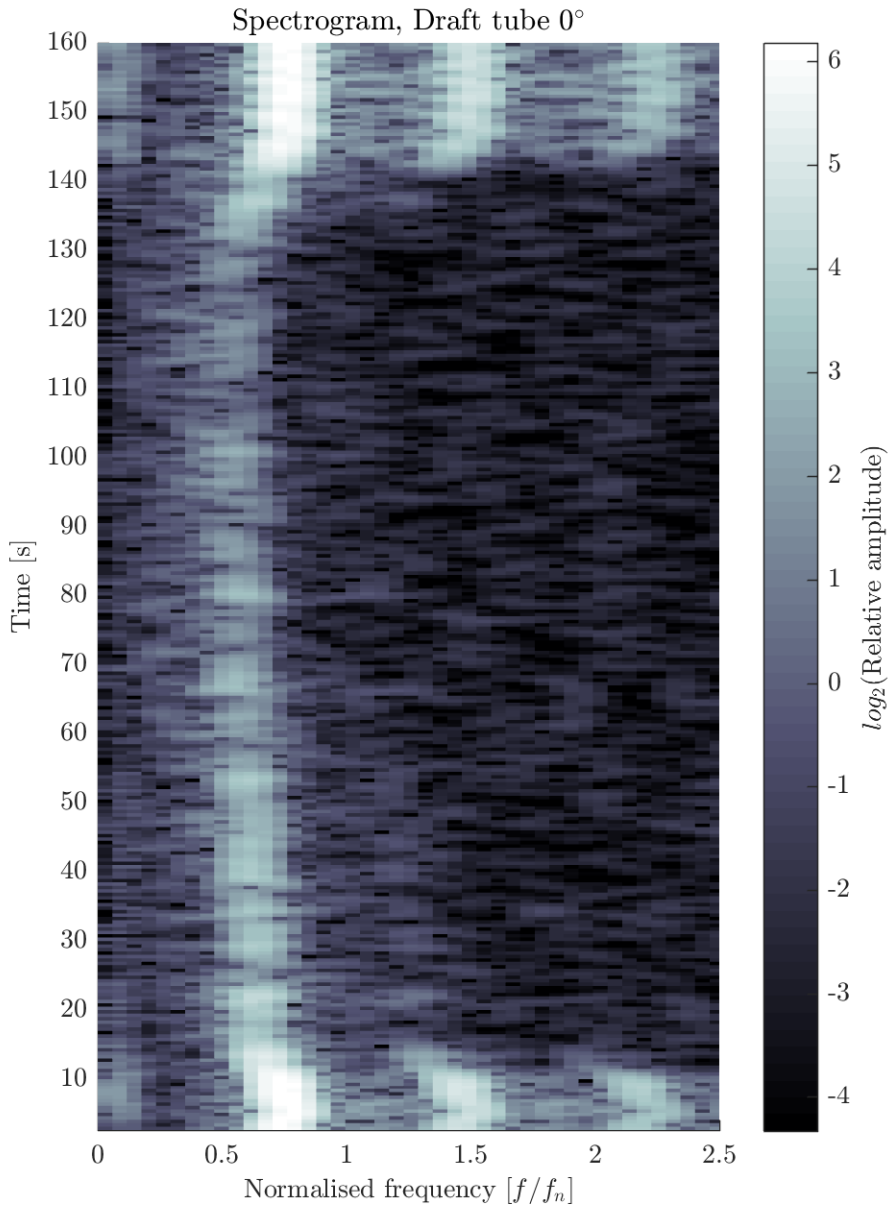


Figure 4.19: Spectrogram of the pressure measurement in the draft tube, starting and ending with no air injection, illustrating the reduction in pulsation frequency as air is injected

5.1 Hydraulic efficiency

5.1.1 Measuring conditions

The conditions when measuring were quite good. Inlet temperatures were stable throughout the whole day, except in measurement point I ($M-I$). The instability was probably due to the closing of the Monn intake, where it was underestimated how long it would take for the remaining water from Monn to run through the turbine. $M-I$ is not included in the efficiency plots in the results due to aforementioned temperature instability.

5.1.2 Uncertainty

Following IEC-60041 (1991) guidelines, and doing an extensive statistical analysis using Gauss' law of propagation and a student-t distribution (95 %), the uncertainty for each point of operation was found. The uncertainty of the efficiency η_h is of the order 0,9 %, and 1,1 % for the volume flow rate Q .

5.1.3 State of the Francis runner

As seen in figure 4.5, both the guaranteed values (but one) and the previous measurements overlap with the current measurements, when including uncertainty. Due to the uncertainty, nothing can be said for sure, other than that the trend line matches very well with both the previous measurement and guaranteed values. This measurements trend line is however a little

lower. Even so, the state of the runner seems not to have changed much since commissioning in 1985. This could point to two cases. The pressure pulsations have been present from the start in 1985 and their influence have always been, inadvertently, taken into account when measuring efficiency. Or, the pressure pulsations occurred later, but have no observable effect in the measurements.



Figure 5.1: Runner as seen from under

5.1.4 Repetition points

In figure 4.3 and 4.4 it can be observed that $M-IV$ and $M-XII$ (the repetition point), lie very close to each other, and in figure 4.3 their uncertainties

overlap. Hence, the measurements pass the repetition test.

5.1.5 Efficiency with air injection

Air injection was tested on the same point of operation as $M-IV$ and $M-XII$, and is included in figure 4.1, 4.2, 4.3, and 4.4. It is clearly seen that the efficiency point when air injection is present, follows the polynomial trend lines nicely and lies very close to $M-IV$ and $M-XII$. Because of the uncertainty, it is difficult to come to a conclusion whether air injection has an impact on efficiency or not. It is also important to note that the air injection measurement, $M-XIII$, took 10 minutes, and the air compressor ran out of air after 2-3 minutes and was only providing a fraction of the initial air flow for the remaining time, suppressing only two thirds of the pressure pulsation amplitude.

5.1.6 Sources of error

The labyrinth water flow rate was not measured directly, but read off a meter connected to an “Annubar Flow Meter Station”. This set up has, presumably, not been calibrated since installation in 1985. A 10 % uncertainty was therefore added to this value to compensate.

A clear weakness in the method used at Smeland power plant is that no velocity measurements were done in the inlet and outlet. It is assumed a uniform velocity based on flow rate and area, which is not the case in reality. Especially in the outlet can the velocity vary in the same cross-section (Solemslie, 2016). As mentioned in chapter 2, IEC imposes additional uncertainties because of this.

The hose that was supposed to lead the generator cooling water further downstream from the draft tube outlet, had a leakage in its connection. As a result, water with far higher temperature than the outlet water, spilled into the water exiting the draft tube. However, this was not detected in the temperature measurements.

Air injection

It is reasonable to assume that the expanded air after the compressor in $M-XIII$ had a temperature of the same magnitude as the expanded air in the measurements done in April 2018, which had a different compressor.

This means that a medium of far higher temperature than the flow itself was injected before the temperature sensors in the outlet, in *M*–XIII. The temperature difference between the air and the water would have approximately been around 20 degrees Celsius. If the warmer air, or heated up parts of water, came in direct contact with the sensors, the measured temperature would have been higher than it really was. However, the amount of air injected was just a tiny fraction, $\sim 0,5 \text{ ‰}$, of the total volume flow, so it is difficult to see how it would have had an impact. Also, with waters very high specific heat capacity, it would have taken a lot of energy to heat it up. The efficiency point for *M*–XIII show no signs of being affected by the air itself.

5.2 Pressure pulsations

5.2.1 History and Agder Energi's observations

After speaking with several employees at Agder Energi who have been involved with Smeland power plant in some way or another throughout the years, it became apparent that the vibration problems might not have started between 1998 and 2007 as Norconsult suggests (Brevig, 2007). It is not known if it has been a problem since the power plant was commissioned in 1985, or started some time after. All that is known is that it has been a problem for many years, and from their experiences, it seems to be worse during periods of flood. Whether the cause is the higher water levels in the reservoirs or in the tail water is also unknown. What was observed at Smeland power plant in April 2018 however, was that with the intake gate open at Monn, which lies ~ 50 m higher than the intake at Logna, the pressure pulsation Δp values were higher than with the intake gate closed. This comparison was also done with the turbine running and regulating according to a power setpoint, due to some issues with running it in manual mode. The frequency was also altered slightly with a $\sim 0,25$ Hz, or $\sim 6\%$ increase in frequency when the Monn intake gate was open compared to when it was closed.

5.2.2 General observations

The pressure pulsation problem at Smeland power plant seems quite severe, and when present they dominated the pressure measurements done on all places, even upstream of the main inlet valve. During the measurements in February 2018, they appeared somewhere between 21 and 22 MW (as indicated on the regulator), and persisted all the way to full load, which at the time was at about 23,5 MW. The Δp reached a maximum at $\sim 22,7$ MW. The highest measured Δp in February was about 19% of the nominal design head ($\Delta p/H_0$). In April 2018, the intake gate at Monn was open during some of the measurements, and when it was, the Δp reached a value of 21,5% of $\Delta p/H_0$. The frequency of the pulsations started at about 4,42 Hz which is 1,06 times the runner frequency ($f_n = 4,167$ Hz). As the load was increased, the frequency decreased, reaching 2,79 Hz or $0,67f_n$ at the point of most pulsations, and at full load it went down to $0,51f_n$. During the measurements in February, some preliminary tests to mitigate the problem was done, and while the air injection showed great promise, the water injection test showed no conclusive change in the behaviour of the pulsations.

5.2.3 Possible causes

When trying to identify the cause of the severe pulsations experienced at Smeland power plant, all the common and relevant system frequencies were calculated, and is listed in table 4.8. One thing to note here is that the apparent overlap of $f_{penstock}/f_n$ and f_{outlet}/f_n , and furthermore, that f/f_n falls within the 2nd harmonic of these.

| | Lower end | Higher end |
|---|-----------|---------------|
| f/f_n | 0,67 | 0,73 (0,93) * |
| $f_{penstock}/f_n$ 2 nd harmonic | 0,60 | 1,08 |
| f_{outlet}/f_n 2 nd harmonic | 0,62 | 1,04 |

Table 5.1: Comparison of observed frequencies and calculated waterway pressure wave frequency

The changes in f/f_n could possibly be explained by different temperatures and varying amounts of air in the water, both of which will change the speed of sound in the water way. Additionally, different levels of water in both the reservoir and tail water will alter the total length for the propagating pressure wave. Also, different water levels will change the pressure in the draft tube, moving the power load at which the pulsations occur.

Sound recordings

As mentioned, sound recordings were taken near the draft tube both in October 2017, as well as February and April of 2018. The calculated pulsation frequency from the measurements in February and April can be further validated from the sound recordings, as it shows the same. The recording done in October 2017 is clearly and audibly of a higher pulsation frequency, and the analysis confirms this. The generated power, as indicated by the control room monitor was 22,95 MW, which is about the same as the indicated power was when the pulsations were at their highest in February, provided that the offset on the monitor is constant over time. The different frequency may be because of different water levels and air content, none of which was measured or documented in any way at the time. It is still interesting to see that the frequency of the pulsations seems to change by a significant amount.

*The higher end limit not in parentheses are from the pressure measurements in April 2018, the value in parentheses was obtained from the sound recording done back in October 2017.

Pressure spikes

In figure 4.9, a 2,5 seconds sample of the measured pressure in the draft tube can be seen, and it seems to have fairly high pressure spike. Why the pressure have these large spikes is not known. Earlier during the post processing, it was speculated that it might have been a collapsing vapour bubble followed by a water hammer pulse. For this to be the case, the pressure in the centre of the draft tube cone must be low enough for the water to vaporise. As the lowest measured pressure along the draft tube wall was about 60 kPa, a fairly large pressure gradient must be present for this to be the case.

Labyrinth water pipe

During the pressure measurements, a distinct pulsation was observed in the leakage pipe (fig. 4.11) with a frequency of $17f_n$ at all the measurements. The Δp of this pulsation also seemed to be significant enough to look into its origin, which is suspected to be the pump vanes on the top of the runner. The thinking is that a pulse is sent through the pipe each time a vane passes by the inlet to the pipe. The frequency can be observed in other parts of the turbine as well when there are not any major vibrations, but the amplitude there is very low, and it is also far away from the frequencies of the severe pulsations experienced above BEP.

5.2.4 Air injection

One interesting thing that was observed during the preliminary air tests was that when the compressor ran out of accumulated air and could no longer feed enough into the turbine to fully stabilise the system, the peak-to-peak value of the pressure pulsations were $\sim 1/3$ of the Δp when no air was injected. Additionally, the frequency of the pulsations themselves were lowered. This might indicate some correlation between the pulsation frequency and the eigenfrequency of the entrapped air/vapour filament in the draft tube. The pressure signal itself also has a more typical sine wave shape during the insufficient air injection, and not the sharp spikes seen when no air was injected at all. During the air injection measurements in April, the frequency of the pulsation also seems to decrease as air is injected into the stream, as seen in figure 4.19. This reduction in the pulsation frequency, and the fact that the necessary air flow rate is as low as it is ($< 0,5\%$ of the water flow rate), suggests that the only function that the air has is to move the eigenfrequency of the bubble away from what ever

it is resonating with. This would also explain why the water injection did nothing to mitigate the pulsations, as the water will not do much to the volume of the bubble.

Calculated air bubble volume change

In table 4.10, the change in air bubble volume with respect to measured pulsation frequency is listed, and calculated using equation 2.16. There does not seem to be any correlation between the calculated volume change and injected air volume flow rate. Even with the lowest possible air amount, ~ 210 l/min, which stabilised the system within about 10 seconds, the calculated volume change is about 3 times of that. It is, however, believed that one key issue here is the assumptions made regarding the shape of the bubble. The inertia, I , is a function of some length scale, assumed to be a diameter. The behaviour of this diameter will probably not be equal for various bubble shapes of equal volumes, as the ratio of volume to surface area is not the same. One possibility is that the length scale actually is the ratio of volume to surface area, as this is more correctly related to the interface between the bubble (spring/force) and the water (mass/inertia). This is, however, only speculation at this point, and should be verified.

5.2.5 Error sources

Uncooperative regulator

When the measurements were done in April 2018, there were some difficulties in running the turbine in fully manual mode with direct control of the guide vanes, as the generator fell off the grid when the regulator was switched over to manual mode. As a result, the only way to control the turbine was to change the power setpoint locally, meaning that the guide vanes might have been regulated ever so slightly during the measurements. It was however deemed not to be too critical, as the main goal at that point was to figure out how much air that needed to be injected to stabilise the turbine.

Pulsations in the air flow

When the air flow measurements were done, there were some pulsations or fluctuations in the measured air pressure at the lower flow rates, necessitating the use of ISO/TR-3313 as well when calculating the uncertainty of the results. The additional error was however very low, and combined with the low flow rate, the end result was almost negligible compared with the total calculated error. The probable cause of the pulsations is most likely the abrupt change in pipe cross section and the lack of a flow straightener. A longer pipe section upstream would probably have helped as well. There was however also a contribution in the pulsations from the turbine itself, as the pulsations could be felt when squeezing the hose leading from the pipe and to the check valve on the turbine. How this could have been dealt with is not known at this point. In the end though, the authors still feel that the calculated results can be trusted to a reasonable degree.

The hydraulic efficiency of the Francis runner at Smeland power plant seems to be nearly unchanged since the last measurement in 1985. The trend line is somewhat lower around BEP, however, nothing can be said conclusively because of uncertainty. Taking into account uncertainty, both the previous measurement and the runners guaranteed values, but one, overlap the present measurement. This could either mean that the pressure pulsations have always been present and is included in both efficiency measurements, or they occurred later but have no observable effect on the efficiency. The repetition point overlaps the original point which help to validate the measurements. Air injection seem to have no effect on the hydraulic efficiency, though it is important to note that the compressor was not running on max throughout the whole measurement, and there is the uncertainty to consider. The uncertainty of the efficiency η_h is of the order 0,9 %, and 1,1 % for the volume flow Q . Circumstances that might have an impact on the measurements are the lack of energy distribution exploration in the outlet, a leaking hose with cooling water in the outlet, and air (or water heated up by the air) coming in contact with the temperature sensors.

The standing hypothesis is that the pressure pulsation problem at Smeland stems from a full load vortex bubble oscillating and resonating with the penstock and/or outlet tunnel. The observed frequency matches the 2nd harmony of the calculated water way pressure wave- and u-tube frequencies of said conduits. The amount of necessary air to stabilise the whole system seems to be too small to have any significant dampening effect in and by itself. It might rather be that the injected air changes the volume of the bubble enough to push the eigenfrequency out of resonance, and thus decreasing the severity of the pulsations drastically. When the compressor used in February 2018 had ran out of air, and was just supplying with what little it could, the frequency of the pulsations changed by $\sim 10\%$ and the peak to peak, Δp , in the draft tube was reduced to $\sim 1/3$ of its original value. The lowest air flow rate measured in April 2018 reduced the vibrations by $\sim 90\%$, and was about 0,602 kg/min, which is $\sim 0,12\%$ of the total discharge. Injecting 1,266 kg/min of air reduced the Δp by about 97%. The frequency and operation point where the pressure pulsations are at their worst does not seem to be fixed either, but change, probably because of varying water levels and air content through the different seasons.

CHAPTER 7

FURTHER WORK

Firstly, Agder Energi should implement an air injection system that starts when the pulsations exceeds a set limit. A fixed power setpoint could be used, but it is the authors advice that this must be checked over time, as the load at which the worst pulsations happen seems to move around. How much the point moves around should then be recorded. If it actually is a bubble eigenfrequency resonance problem, pulsations might occur closer to BEP with air injected, so care must be taken when setting the system up, to ensure that the problem does not start at a different point.

Secondly, if Agder Energi wants to confirm the hypothesis that there is a resonating full load vortex in the draft tube cone causing the pressure pulsations, it is recommended that they install a “window” in the draft tube cone with appropriate lighting. Then they can check visually if there is in fact a full load vortex, and that it is pulsating with the frequency of the pressure pulsations. Next they could inject air and see what happens with the full load vortex, if it stops pulsating the hypothesis that air changes the bubbles eigenfrequency is strengthened.

Finally, some measurements could also be done in the laboratory at NTNU where a suspended gas bubble would be excited by some external source to test the frequency to volume relationship. If the relationship seems to hold, the appropriate length scale could be found, and the correctly calculated volume to frequency relationship could be checked against the observed frequency changes with air injection at Smeland power plant.

BIBLIOGRAPHY

- Agder-Energi, 2015. Smeland kraftstasjon agder energi. Accessed: 2017-09-12.
URL <https://www.ae.no/virksomhet/vannkraft/kraftstasjoner/smeland-kraftstasjon/>
- Andresen & Grøner AS, 1984a. Ae108495, blueprint.
- Andresen & Grøner AS, 1984b. Ae109006, blueprint.
- Bergan, C., 2013. Trykkpulsasjoner i francisturbiner. Specialization project, Norges teknisk- naturvitenskapelige universitet.
- Brede, F., 1985. Virkningsgradsmålinger smeland kraftverk. Tech. rep., Kværner Brug A/S.
- Brekke, H., 1999. Pumper & turbiner.
- Brevig, L., 2007. Smeland kraftverk vibrasjonsmålinger. Tech. rep., Norconsult.
- Bue, I. L., 2013. Pressure pulsations and stress in a high head turbine ? comparison between model and geometrically similar prototype. Master's thesis, Norges teknisk- naturvitenskapelige universitet.
- Dörfler, P., Sick, M., Coutu, A., 2013. Flow-Induced Pulsation and Vibration in Hydroelectric Machinery. Springer-Verlag, London.
- Gogstad, P. J., Dahlhaug, O. G., 2016. Evaluation of runner cone extension to dampen pressure pulsations in a francis model turbine. IOP Conference Series: Earth and Environmental Science.

-
- Heinzel, G., Rüdiger, A., Schilling, R., 2002. Spectrum and spectral density estimation by the discrete fourier transform (dft), including a comprehensive list of window functions and some new flat-top windows. Tech. rep., Max-Planck-Institut für Gravitationsphysik, Teilinstitut Hannover.
- Hulaas, H., Vinnogg, L., 2010. Iec 60041–1991, “field acceptance tests to determine the hydraulic performance of hydraulic turbines, storage pumps and pumpturbines”. clause 14 “thermodynamic method for measuring efficiency” comments. In: Proceeding from the 8th IGHEM conference, Roorkee, India.
- IEC-60041, 1991. Field acceptance tests to determine the hydraulic performance of hydraulic turbines, storage pumps and pump-turbines. 60041 3.
- International Electrotechnical Commission, 1999. IEC 60193:1999 - hydraulic turbines, storage pumps and pump-turbines : model acceptance tests.
- International Organization for Standardization, 2003a. ISO 5167-1:2003 - Measurement of fluid flow by means of pressure differential devices inserted in circular cross-section conduits running full, pt 1. General principles and requirements. Standard Norge.
- International Organization for Standardization, 2003b. ISO 5167-2:2003 - Measurement of fluid flow by means of pressure differential devices inserted in circular cross-section conduits running full, pt 2. Orifice plates. Standard Norge.
- International Organization for Standardization, 2018. ISO/TR 3313 - measurement of fluid flow in closed conduits - guidelines on the effects of flow pulsations on flow-measurement instruments. Tech. rep., Standard Norge.
- Kjølle, A., 2003. Hydraulisk måleteknikk. Grunnleggende prinsipper og målemetoder 2.
- Kobro, E., 2010. Measurement of pressure pulsations in francis turbines. Phd thesis, Norges teknisk- naturvitenskapelige universitet.
- Kverno, J., Ulvan, V., 2017. Efficiency and pressure pulsations at smeland power plant. Specialisation project, Norges teknisk- naturvitenskapelige universitet.
- Nielsen, T. K., 1990. Dynamisk dimensjonering av vannkraftverk. SINTEF.

Solemslie, B. W., 2010. Compendium in instrumentation, calibration and uncertainty analysis. Vannkraftlaboratoriet NTNU.

Solemslie, B. W., 2016. Experimental methods and design of a pelton bucket.

Storli, P.-T. S., 2007. Usikkerhetsanalyse. Lecture material, NTNU.

Wheeler, A. J., Ganji, A. R., 2010. Introduction to Engineering Experimentation. Pearson.

APPENDIX A

MEASURED VALUES, EFFICIENCY

MEASUREMENTS

| Measurement number | 1 | 2 | 3 |
|---|----------------------|----------|----------|
| Date | - | | |
| Time at the start | watch | | |
| Height difference draft tube upper floor to water level | watch | | |
| Water level at the intake during the measurement | laser/rope (h) | 4,57 | 4,513 |
| Servo | control room | | |
| Blinks per second | control room | | |
| Power precision | counter/stopwatch | 3,900 | 4,167 |
| Power from generator given in the control room | blink counter | 19,500 | 20,833 |
| Pressure at p11-transducer | control room | 19,600 | 20,770 |
| Pressure at p1-transducer | measured | 1009,588 | 1003,329 |
| Inlet pressure (meeter close to the turbine) | measured | 1007,186 | 996,229 |
| Atmospheric pressure | present on site | | |
| Temperature at the inlet | measured | 99,537 | 99,498 |
| Temperature at the outlet (avg ABC) | measured | 0,859 | 0,866 |
| Temp diff adjusted for time | measured | 0,871 | 0,879 |
| Temperature for the leakage water | measured | 0,012 | 0,013 |
| Time for filling bucket from the temperature probe | measured | 1,536 | 1,562 |
| Load factor (Cos θ) | stopwatch | 43,35 | 42,56 |
| Leakage water Flow Rate | might not need | | |
| Time when finish | meeter turbine floor | 59,5 | 58 |
| | watch | | |
| | - | | |
| | l/s | | 60 |
| | - | | |

APPENDIX B _____
_____ MEASURED VALUES, PRESSURE PULSATIONS

| M # | $P_{gen,i}$ | | PS | SC | DT _{0°} | DT _{180°} | LP | |
|------|-------------|------------|--------|--------|------------------|--------------------|-------------------|-------|
| I | 19,6MW | f | 4,15 | 116,70 | 8,12 | 8,12 | 70,86 | [Hz] |
| | | Δp | 7,08 | 8,83 | 4,31 | 4,21 | 40,14 | [kPa] |
| II | 20,8MW | f | 4,15 | 116,66 | 4,79 | 4,76 | 70,82 | [Hz] |
| | | Δp | 8,65 | 10,62 | 7,74 | 7,81 | 38,32 | [kPa] |
| III | 22,0MW | f | 4,44 | 4,44 | 4,44 | 4,44 | 4,44 [†] | [Hz] |
| | | Δp | 98,92 | 85,72 | 89,59 | 87,40 | - [†] | [kPa] |
| IV | 22,8MW | f | 2,78 | 2,78 | 2,78 | 2,78 | 2,78 [†] | [Hz] |
| | | Δp | 182,90 | 165,62 | 184,25 | 185,77 | - [†] | [kPa] |
| V | 23,5MW | f | 2,12 | 2,12 | 2,12 | 2,12 | 2,12 [†] | [Hz] |
| | | Δp | 89,22 | 94,49 | 126,74 | 127,74 | - [†] | [kPa] |
| VI | 6,1MW | f | 0,92 | 0,92 | 0,92 | 0,87 | 70,83 | [Hz] |
| | | Δp | 9,79 | 9,76 | 30,26 | 23,64 | 44,26 | [kPa] |
| VII | 9,8MW | f | 1,05 | 1,05 | 1,10 | 1,10 | 70,89 | [Hz] |
| | | Δp | 9,70 | 10,18 | 25,47 | 27,30 | 31,71 | [kPa] |
| VIII | 13,2MW | f | 0,98 | 0,98 | 0,98 | 0,98 | 70,89 | [Hz] |
| | | Δp | 9,02 | 9,28 | 16,70 | 15,80 | 32,63 | [kPa] |
| IX | 14,9MW | f | 0,85 | 0,85 | 1,13 | 1,16 | 70,86 | [Hz] |
| | | Δp | 8,18 | 8,46 | 12,36 | 11,68 | 33,04 | [kPa] |
| X | 16,7MW | f | 4,24 | 4,23 | 4,23 | 4,32 | 70,79 | [Hz] |
| | | Δp | 9,51 | 9,09 | 7,57 | 7,72 | 34,60 | [kPa] |
| XI | 19,5MW | f | 4,15 | 4,15 | 11,58 | 11,54 | 70,79 | [Hz] |
| | | Δp | 6,92 | 7,44 | 4,29 | 4,29 | 40,08 | [kPa] |
| XII | 22,7MW | f | 2,81 | 2,81 | 2,81 | 2,81 | 2,81 [†] | [Hz] |
| | | Δp | 191,53 | 166,68 | 188,84 | 189,57 | - [†] | [kPa] |
| XIII | 22,7MW | f | 2,01 | 2,01 | 2,01 | 2,01 | 70,92 | [Hz] |
| | | Δp | 10,25 | 11,62 | 12,55 | 12,43 | 42,43 | [kPa] |
| XIV | 22,7MW | f | 2,50 | 2,50 | 2,50 | 2,50 | 2,50 | [Hz] |
| | | Δp | 44,30 | 48,23 | 63,79 | 63,52 | 48,90 | [kPa] |
| XV | 22,7MW | f | 2,69 | 2,69 | 2,69 | 2,69 | 2,69 [†] | [Hz] |
| | | Δp | 212,07 | 179,29 | 199,32 | 199,90 | - [†] | [kPa] |
| XVI | 22,7MW | f | 2,81 | 2,81 | 2,81 | 2,81 | 2,81 [†] | [Hz] |
| | | Δp | 178,29 | 156,73 | 179,67 | 180,44 | - [†] | [kPa] |

Table B.1: Measured peak to peak pressure and dominating frequencies on all sensors

[†]Pressure exceeded maximum range of sensor, and clipping occurred

| M # | $P_{gen,i}$ | $q_{m,air}$ | | DT _{0°} | DT _{180°} | |
|-------|-------------|----------------|------------|------------------|--------------------|-------|
| XVII | 23,6MW | 0 [kg/min] | f | 3,05 | 3,05 | [Hz] |
| | | | Δp | 213,48 | 213,79 | [kPa] |
| XVIII | 23,6MW | 0,602 [kg/min] | f | 2,26 | 2,26 | [Hz] |
| | | | Δp | 22,10 | 21,94 | [kPa] |
| XIX | 23,6MW | 0,771 [kg/min] | f | 2,26 | 2,26 | [Hz] |
| | | | Δp | 16,12 | 16,09 | [kPa] |
| XX | 23,6MW | 0,926 [kg/min] | f | 2,20 | 2,20 | [Hz] |
| | | | Δp | 12,77 | 12,67 | [kPa] |
| XXI | 23,6MW | 1,266 [kg/min] | f | 1,83 | 1,83 | [Hz] |
| | | | Δp | 6,14 | 6,01 | [kPa] |
| XXII | 23,4MW | 0 [kg/min] | f | 2,87 | 2,87 | [Hz] |
| | | | Δp | 189,93 | 189,97 | [kPa] |
| XXIII | 23,4MW | 0,742 [kg/min] | f | 1,83 | 1,83 | [Hz] |
| | | | Δp | 8,20 | 7,76 | [kPa] |
| XXIV | 23,4MW | 1,080 [kg/min] | f | 1,89 | 1,89 | [Hz] |
| | | | Δp | 8,62 | 8,21 | [kPa] |

Table B.2: Measured peak to peak pressure and dominating frequencies in the draft tube during the measurements in April 2018, both with and without air, and the intake gate at Monn open and closed.

APPENDIX C



GRAPHS FROM PRESSURE PULSATION
MEASUREMENTS IN FEBRUARY 2018

Results from measurements on the draft tube, 0°

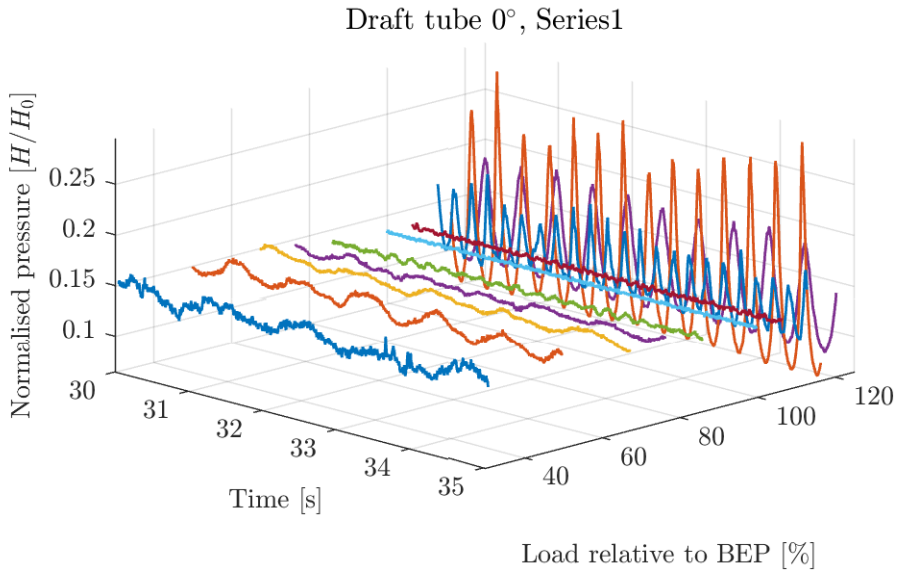


Figure C.1: Measured pressure on the draft tube, 0°, series 1

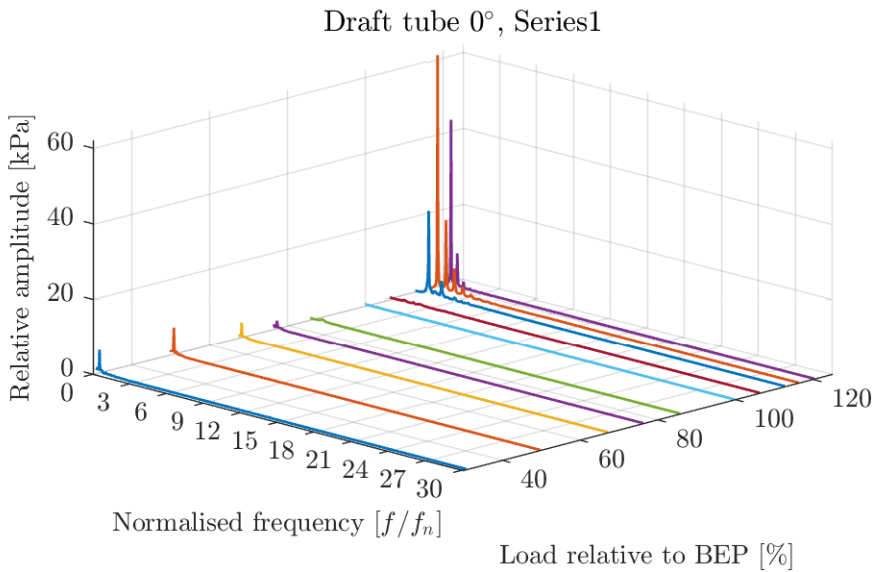


Figure C.2: Frequency analysis of measurement on the draft tube, 0°, series 1

Results from measurements on the draft tube, 180°

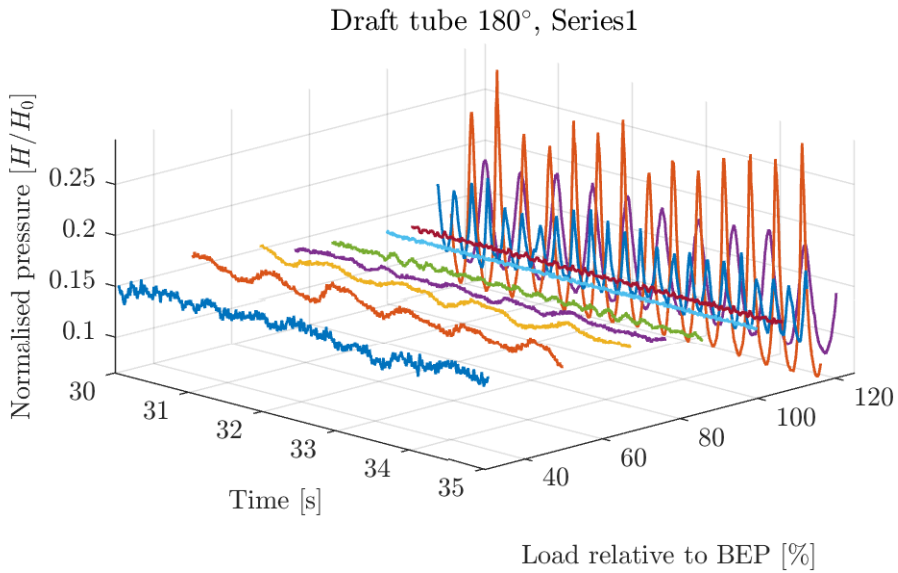


Figure C.3: Measured pressure on the draft tube, 180°, series 1

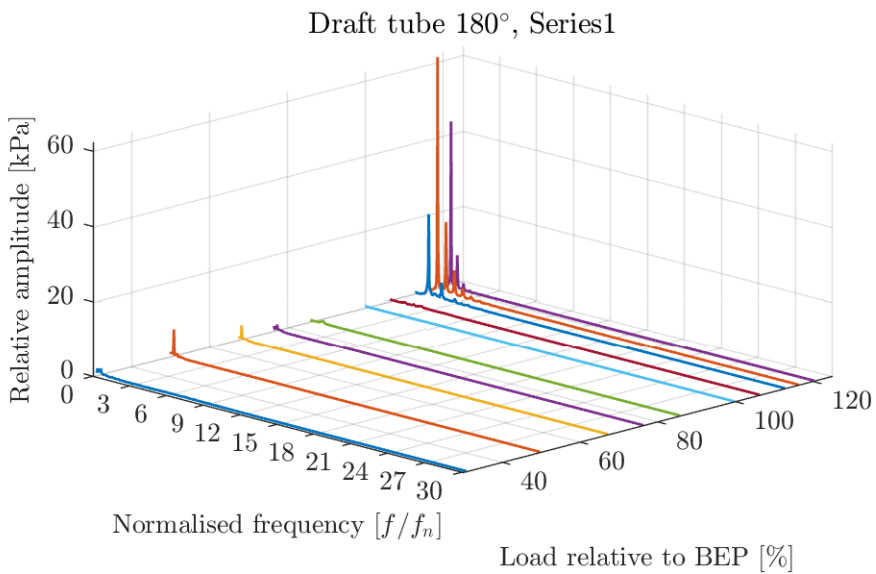


Figure C.4: Frequency analysis of measurement on the draft tube, 180°, series 1

Results from measurements, asymmetric component

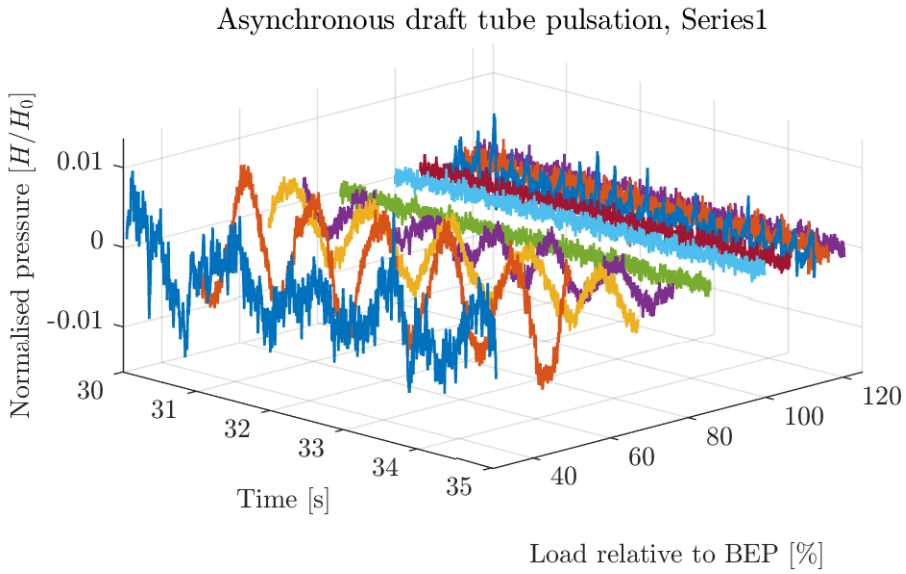


Figure C.5: Measured pressure, asymmetric component, series 1

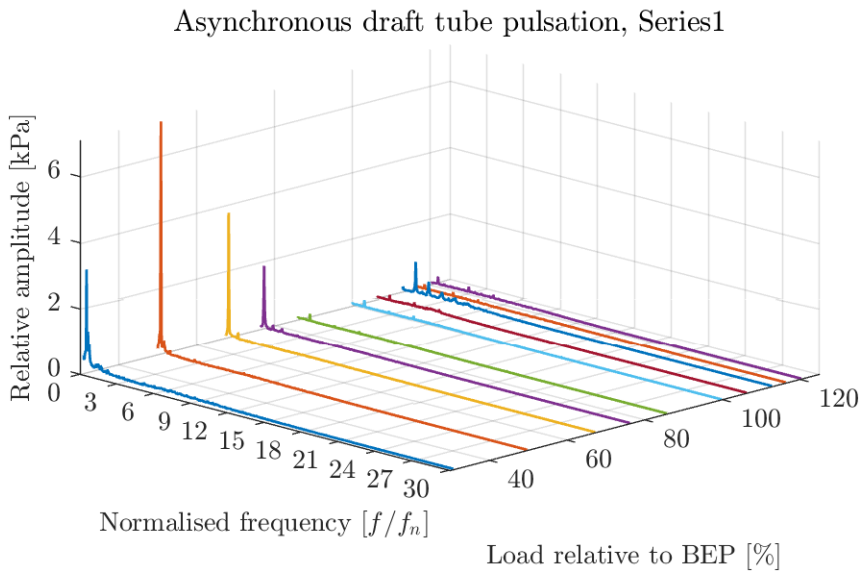


Figure C.6: Frequency analysis of the asymmetric component, series 1

Results from measurements, symmetric component

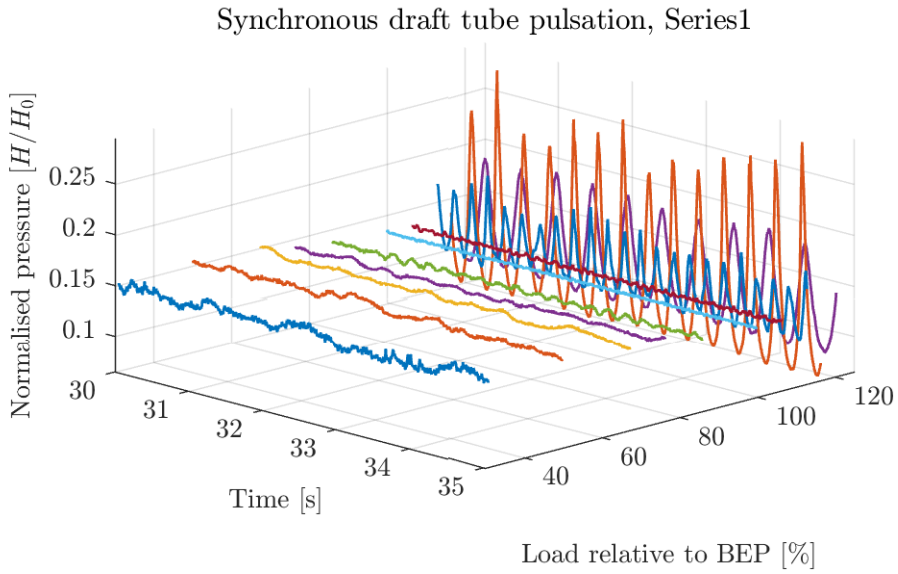


Figure C.7: Measured pressure, symmetric component, series 1

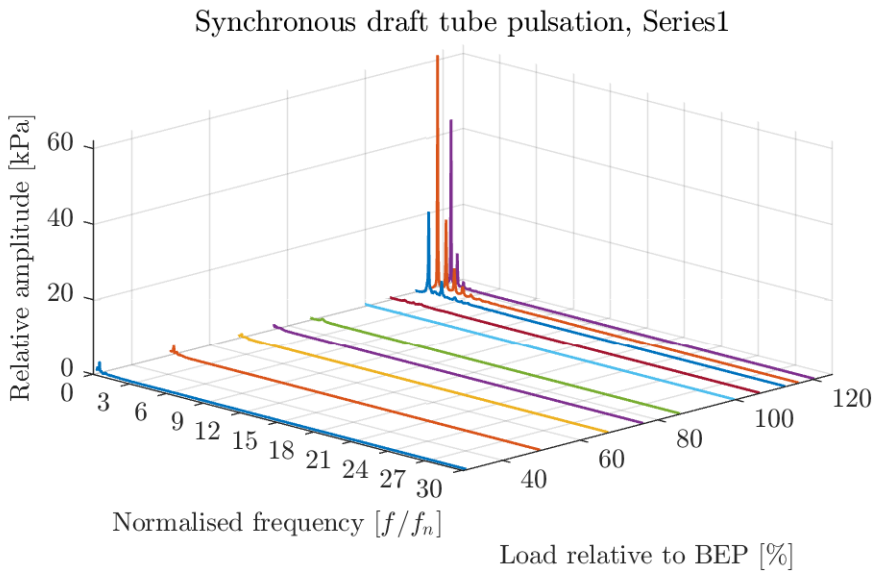


Figure C.8: Frequency analysis of the symmetric component, series 1

Results from measurements at the outlet of the penstock

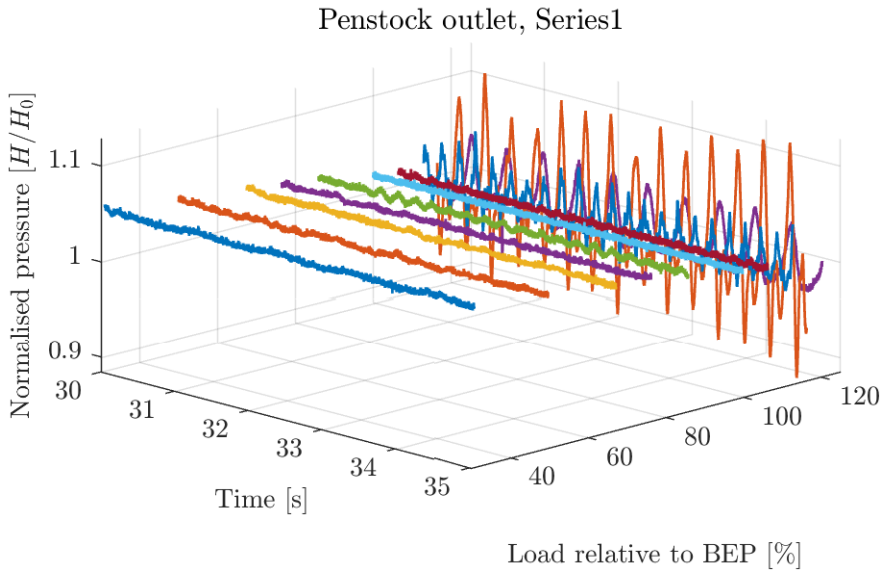


Figure C.9: Measured pressure at penstock outlet series 1

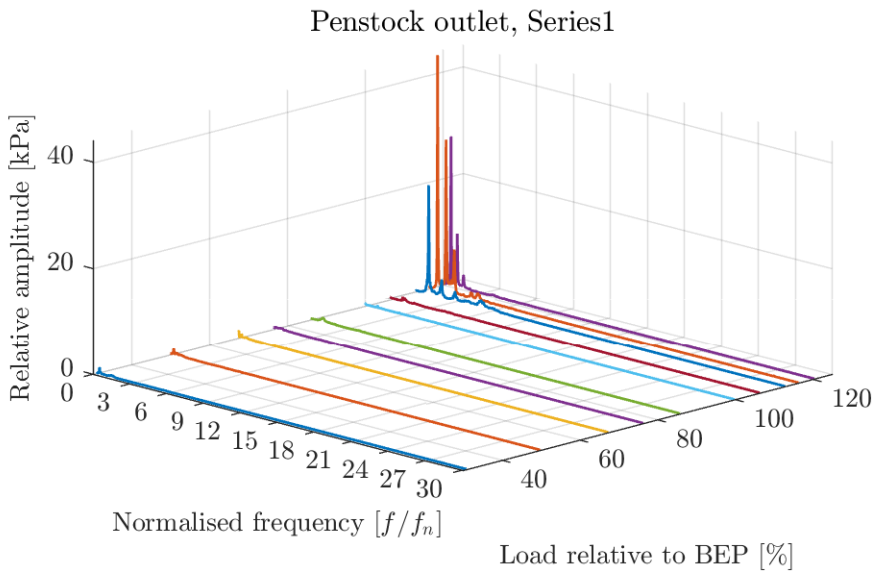


Figure C.10: Frequency analysis of measurement at penstock outlet series 1

Results from measurements at the inlet of the spiral casing

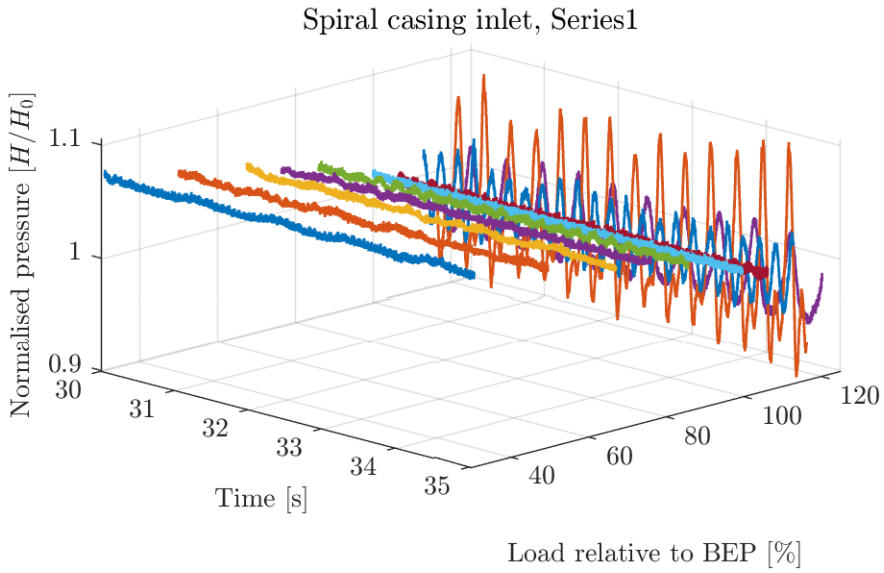


Figure C.11: Measured pressure at the spiral casing inlet series 1

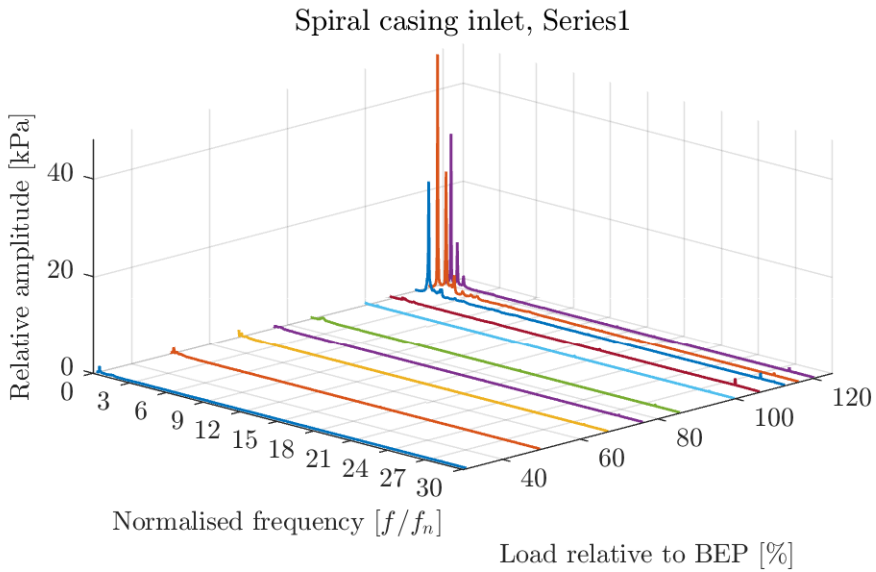


Figure C.12: Frequency analysis of measurement at the spiral casing inlet series 1

Results from measurements on the leakage pipe

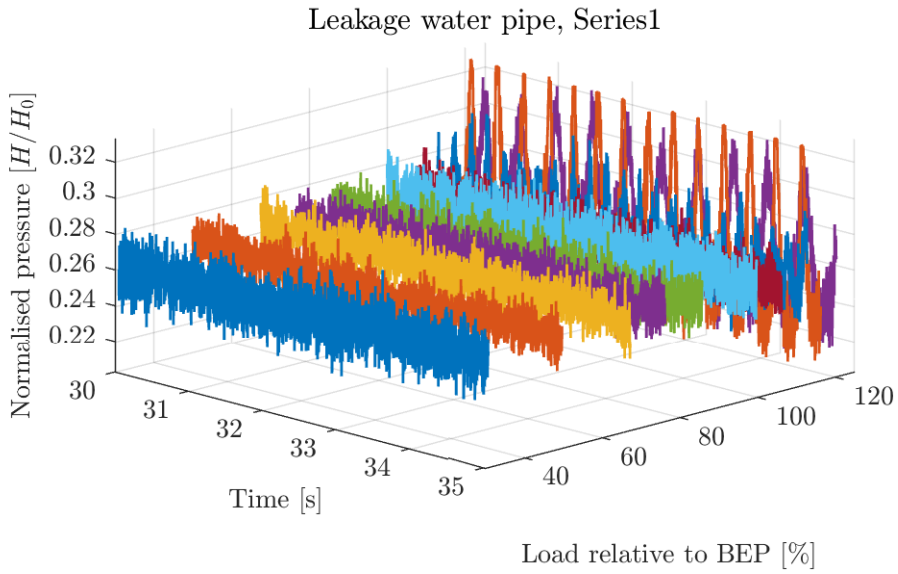


Figure C.13: Measured pressure on the leakage pipe series 1

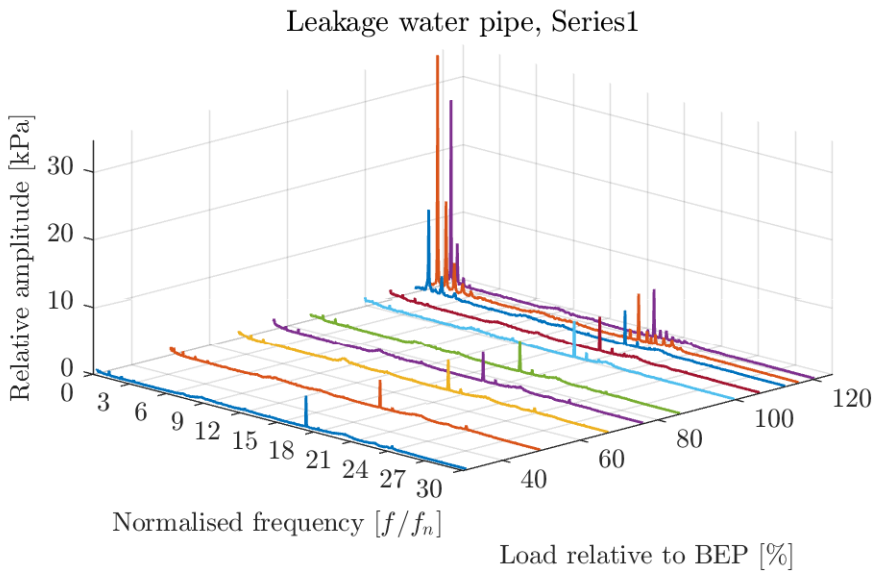


Figure C.14: Frequency analysis of measurement on the leakage pipe series 1

APPENDIX D

HYDRAULIC EFFICIENCY EXAMPLE CALCULATION, $M-I$

| Data | Smeland |
|---------------------------|----------|
| z_1 [mas] | 259,45 |
| z_2 [mas] | 257,3 |
| z_{1-1} [mas] | 261,0 |
| z_{2-1} [mas] | 257,19 |
| Δz_1 [m] | -0,777 |
| Δz_{1-1} [m] | 0,0 |
| z_{uf} [mas] | 267,8 |
| z_{lf} [mas] | 254,8 |
| z_{leak} [mas] | 260,37 |
| D_1 [m] | 2,00 |
| D_p [m] | 0,0175 |
| A_2 [m^2] | 15,5 |
| g [m/s^2] | 9,81734 |
| V_b [m^3] | 0,01 |
| k_{blink} [MW(s/blink)] | 5 |
| ϕ [°] | 58,66757 |

Table D.1: Basic data

$$P_g = \frac{blink}{s} k_{blink} = 19,5 \text{ [MW]} \quad (\text{D.1})$$

| | |
|--------------------------|---------|
| Measurement 1 | Smeland |
| ΔT [C°] | -0,0118 |
| T_{leak} [C°] | 1,5363 |
| p'_1 [kPa] | 1007,2 |
| p'_{1-1} [kPa] | 1009,6 |
| p_{atm} [kPa] | 99,5 |
| blink/s | 3,9 |
| t_b [s] | 43,35 |
| Q_{leak} [m^3/s] | 59,5 |
| h [m] | 4,57 |

Table D.2: $M-I$

| | |
|---|-------------|
| Property | Smeland |
| \bar{a} [m^3/kg] | 0,001013574 |
| \bar{c}_p [$\frac{J}{kg K}$] | 4203,854918 |
| $\bar{\rho}$ [kg/m^3] | 1000,135910 |
| $\bar{c}_{p,leak}$ [$\frac{J}{kg K}$] | 4203,710866 |
| \bar{a}_{leak} [m^3/kg] | 0,001012085 |
| g [m/s^2] | 9,817341 |

Table D.3: Physical properties based on tables and equations in IEC-60041 (1991)

$$Q_{assumed} = \frac{P_g/\eta_g}{p_1 - p_{atm}} = 21,85 \text{ [m}^3/s\text{]} \quad (D.2)$$

$$h_{2-1} = z_{uf} - z_{2-1} - h = 6,04 \text{ [m]} \quad (D.3)$$

$$p'_{1-1} = p_{1-1} + \frac{\bar{\rho}g\Delta z_{1-1}}{1000} = 1009,6 \text{ [kPa]} \quad (D.4)$$

$$p_{2-1} = \frac{\bar{\rho}gh_{2-1}}{1000} + p_{atm} = 158,8 \text{ [kPa]} \quad (D.5)$$

$$E_{m,p} = \bar{a}(p'_{1-1} - p_{2-1}) = 862,3 \text{ [J/kg]} \quad (D.6)$$

$$E_{m,T} = \bar{c}_p(T_{1-1} - T_{2-1}) = -49,7 \text{ [J/kg]} \quad (D.7)$$

$$E_{m,pot} = g(z_{1-1} - z_{2-1}) = 37,4 \text{ [J/kg]} \quad (D.8)$$

$$c_{1-1} = Q_p/A_p = \frac{4V_b}{t_b\pi D_p^2} = 0,96 \text{ [m/s]} \quad (\text{D.9})$$

$$c_{2-1} = Q_{assumed}/A_2 = \frac{P_g}{\eta_g \bar{\rho} E_m A_2} = 1,52 \text{ [m/s]} \quad (\text{D.10})$$

$$E_{m,kin} = \frac{1}{2}(c_{1-1}^2 - c_{2-1}^2) = -0,7 \text{ [J/kg]} \quad (\text{D.11})$$

$$E'_m = E_{m,p} + E_{m,T} + E_{m,pot} + E_{m,kin} = 849,4 \text{ [J/kg]} \quad (\text{D.12})$$

$$Q_{corr1} = \frac{P_g/\eta_g}{\bar{\rho} E'_m} = 23,35 \text{ [m}^3\text{/s]} \quad (\text{D.13})$$

$$E_{m,leak} = \frac{Q_{leak}}{Q_{corr1}} \left(\bar{a}_l \left(\frac{\bar{\rho} g h_{2-1}}{1000} + p_{atm} \right) - \bar{c}_p (T_{leak} - T_{2-1}) - g(z_{leak} - z_{2-1}) \right) = -7,0 \text{ [J/kg]} \quad (\text{D.14})$$

$$E_m = E'_m + E_{m,leak} = 842,4 \text{ [J/kg]} \quad (\text{D.15})$$

$$Q_{corr2} = \frac{P_g/\eta_g}{\bar{\rho} E_m} = 23,54 \text{ [m}^3\text{/s]} \quad (\text{D.16})$$

By iterating these calculations, using the results from D.16, the factors become more accurate and converges.

$$h_2 = z_{uf} - z_2 - h = 5,93 \text{ [m]} \quad (\text{D.17})$$

$$p'_1 = p_1 + \frac{\bar{\rho} g \Delta z_1}{1000} = 999,6 \text{ [kPa]} \quad (\text{D.18})$$

$$p_2 = \frac{\bar{\rho} g h_2}{1000} + p_{atm} = 157,8 \text{ [kPa]} \quad (\text{D.19})$$

$$E_{h,p} = \bar{a}(p'_1 - p_2) = 841,7 \text{ [J/kg]} \quad (\text{D.20})$$

$$E_{h,pot} = g(z_1 - z_2) = 21,1 \text{ [J/kg]} \quad (\text{D.21})$$

$$c_1 = Q/A_1 = \frac{4Q}{\pi D_1^2} = 7,49 \text{ [m/s]} \quad (\text{D.22})$$

$$c_2 = Q/A_2 = 1,52 \text{ [m/s]} \quad (\text{D.23})$$

$$E_{h,kin} = \frac{1}{2}(c_1^2 - c_2^2) = 26,9 \text{ [J/kg]} \quad (\text{D.24})$$

$$E_h = E_{h,p} + E_{h,pot} + E_{h,kin} = 889,7 \text{ [J/kg]} \quad (\text{D.25})$$

$$\eta_h = \frac{E_m}{E_h} = 0,9468 \text{ [-]} \quad (\text{D.26})$$

APPENDIX E

HYDRAULIC EFFICIENCY UNCERTAINTY EXAMPLE CALCULATION, $M-I$

The hydraulic efficiency is found by dividing the specific mechanical energy by the specific hydraulic energy. To find its total uncertainty, it is easiest to split the equation into smaller and smaller parts, find their uncertainty, and make use of the RSS-method.

$$\eta_h = \frac{E_m}{E_h} \quad [-] \quad (\text{E.1})$$

$$f_{\eta_h} = \frac{e_{\eta_h}}{\eta_h} = \pm \sqrt{f_{E_m}^2 + f_{E_h}^2} = \pm \sqrt{\left(\frac{e_{E_m}}{E_m}\right)^2 + \left(\frac{e_{E_h}}{E_h}\right)^2} \quad [-] \quad (\text{E.2})$$

First, some errors are found to be used in the uncertainty calculations.

$$e_{h_2} = e_{h_{21}} = \sqrt{2e_z^2 + e_{h_s}^2} \quad [\text{m}] \quad (\text{E.3})$$

$$e_{\Delta z} = \sqrt{2e_z^2} \quad [\text{m}] \quad (\text{E.4})$$

$$e_{A_1} = \sqrt{\left(\frac{\partial A_1}{\partial D_1} e_{D_1}\right)^2} = \frac{\pi}{2} D_1 e_{D_1} \quad [\text{m}^2] \quad (\text{E.5})$$

$$e_{A_2} = A_2 \sqrt{\left(\frac{e_w}{w}\right)^2 + \left(\frac{e_l}{l}\right)^2} \quad [\text{m}^2] \quad (\text{E.6})$$

| Factor | e |
|----------------------|--------------------------|
| $e_{h_2}/e_{h_{21}}$ | 0,1500 [m] |
| $e_{\Delta z}$ | 0,1414 [m] |
| e_{A_1} | 0,0314 [m ²] |
| e_{A_2} | 0,5883 [m ²] |

Table E.1: Other errors calculated

| Factor | e | f | Comment |
|-----------------|----------------------------|--------|--------------------|
| ρ_{table} | - | 0,1 % | IEC |
| a_{table} | - | 0,2 % | IEC |
| $c_{p_{table}}$ | - | 0,5 % | IEC |
| P_{gen} | - | 0,7 % | IEC |
| E_{10} | - | 0,2 % | IEC |
| E_{20} | - | 0,6 % | IEC |
| Q_{leak} | - | 10,0 % | assumed |
| z | 0,1 [m] | - | assumed |
| Δz | 0,01 [m] | - | mm-ruler |
| ΔT | 0,001 [C°] | - | IEC |
| h | 0,05 [m] | - | assumed |
| V_b | 0,0001 [m ³ /s] | - | assumed |
| t_b | 0,1 [s] | - | assumed |
| D_{probe} | 0,001 [m] | - | mm-ruler |
| D_1 | 0,01 [m] | - | assumed |
| w | 0,1 [m] | - | assumed |
| l | 0,1 [m] | - | assumed |
| ρ_{temp} | 0 | - | low variation in T |
| a_{temp} | 0 | - | low variation in T |
| $c_{p,temp}$ | 0 | - | low variation in T |
| g | 0 | - | IEC |
| η_{gen} | 0 | - | assumed |

Table E.2: Basic data errors

| | SBE38 [C°] | 15bar [kPa] | 50 bar [kPa] | 5bar a [kPa] |
|---------------|------------|-------------|--------------|--------------|
| $e_{X_{ab}}$ | - | 0,140 | 0,140 | 0,000123 |
| $e_{X_{cd}}$ | - | 0,206 | 0,196 | 0,008353 |
| e_{X_f} | - | - | - | - |
| $e_{X_{cal}}$ | 0,00100 | 0,249 | 0,241 | 0,008354 |
| e_{X_h} | - | - | - | - |
| e_{X_j} | - | - | - | - |
| $e_{X_{ks}}$ | - | - | - | - |
| $e_{X_{kr}}$ | - | - | - | - |
| e_{X_l} | 0,00016 | 0,009 | 0,065 | 0,000380 |
| $e_{X_{tot}}$ | 0,00101 | 0,249 | 0,250 | 0,008363 |

Table E.3: Total uncertainty from calibration and $M-1$

| Measurement 1 | Smeland |
|---------------------|----------|
| e_{p1} [kPa] | 0,249 |
| e_{p11} [kPa] | 0,250 |
| e_{patm} [kPa] | 0,008363 |
| $e_{\Delta T}$ [C°] | 0,00101 |

Table E.4: Measurement 1 errors

Specific mechanical energy

All the following factors starting with "E" and "e" have the unit [J/kg].

$$E_m = E_{m,p} + E_{m,T} + E_{m,pot} + E_{m,kin} + E_{m,leak} \quad (\text{E.7})$$

$$e_{E_m}^2 = e_{E_{m,p}}^2 + e_{E_{m,T}}^2 + e_{E_{m,pot}}^2 + e_{E_{m,kin}}^2 + e_{E_{m,leak}}^2 \quad (\text{E.8})$$

Pressure term

$$E_{m,p} = \bar{a}(p'_{1-1} - p_{2-1}) = \bar{a} \left(p_{1-1} + \frac{\bar{\rho}g\Delta z_{1-1}}{1000} - \frac{\bar{\rho}gh_{2-1}}{1000} - p_{atm} \right) \quad (\text{E.9})$$

$$E_{m,p} = f(\bar{a}, p_{1-1}, \bar{\rho}, \Delta z_{1-1}, h_{2-1}, p_{atm}) \quad (\text{E.10})$$

$$e_{E_{m,p,\bar{a}}}^2 = \left(\left(p_{1-1} + \frac{\bar{\rho}g\Delta z_{1-1}}{1000} - \frac{\bar{\rho}gh_{2-1}}{1000} - p_{atm} \right) e_{\bar{a}} \right)^2 \quad (\text{E.11})$$

$$e_{E_{m,p,p_{1-1}}}^2 = (\bar{a}e_{p_{1-1}})^2 \quad (\text{E.12})$$

$$e_{E_{m,p,\bar{p}}}^2 = \left(\frac{g(\Delta z_{1-1} - h_{2-1})}{1000} e_{\bar{p}} \right)^2 \quad (\text{E.13})$$

$$e_{E_{m,p,\Delta z_{1-1}}}^2 = \left(\frac{\bar{\rho}g}{1000} e_{\Delta z_{1-1}} \right)^2 \quad (\text{E.14})$$

$$e_{E_{m,p,h_{2-1}}}^2 = \left(\frac{\bar{\rho}g}{1000} e_{h_{2-1}} \right)^2 \quad (\text{E.15})$$

$$e_{E_{m,p,p_{atm}}}^2 = (\bar{a}e_{p_{atm}})^2 \quad (\text{E.16})$$

$$e_{E_{m,p}}^2 = e_{E_{m,p,\bar{a}}}^2 + e_{E_{m,p,p_{1-1}}}^2 + e_{E_{m,p,\bar{p}}}^2 + e_{E_{m,p,\Delta z_{1-1}}}^2 + e_{E_{m,p,h_{2-1}}}^2 + e_{E_{m,p,p_{atm}}}^2 \quad (\text{E.17})$$

Thermal term

$$E_{m,T} = \bar{c}_p(T_{1-1} - T_{2-1}) \quad (\text{E.18})$$

$$E_{m,T} = f(\bar{c}_p, T_{1-1} - T_{2-1}) \quad (\text{E.19})$$

$$e_{E_{m,T,c_p}}^2 = (T_{1-1} - T_{2-1})e_{\bar{c}_p} \quad (\text{E.20})$$

$$e_{E_{m,T,\Delta T}}^2 = \bar{c}_p e_{\Delta T} \quad (\text{E.21})$$

$$e_{E_{m,T}}^2 = e_{E_{m,T,c_p}}^2 + e_{E_{m,T,\Delta T}}^2 + e_{E_{10}}^2 + e_{E_{20}}^2 \quad (\text{E.22})$$

Potential term

$$E_{m,pot} = g(z_{1-1} - z_{2-1}) \quad (\text{E.23})$$

$$E_{m,pot} = f(z_{1-1} - z_{2-1}) \quad (\text{E.24})$$

$$e_{E_{m,pot}}^2 = e_{E_{m,pot,\Delta z}}^2 = g e_{\Delta z} \quad (\text{E.25})$$

Kinetic term

$$E_{m,kin} = \frac{1}{2}(c_{1-1}^2 - c_{2-1}^2) \quad (\text{E.26})$$

$$E_{m,kin} = f(c_{1-1}, c_{2-1}) \quad (\text{E.27})$$

$$c_{1-1} = Q_p/A_p = \frac{4V_b}{t_b\pi D_p^2} = f(V_b, t_b, D_p) \text{ [m/s]} \quad (\text{E.28})$$

$$e_{c_{1-1}}^2 = \left(\frac{4eV_b}{t_b\pi D_p^2}\right)^2 + \left(\frac{4V_b e t_b}{t_b^2\pi D_p^2}\right)^2 + \left(\frac{8V_b e D_p}{t_b\pi D_p^3}\right)^2 \quad (\text{E.29})$$

$$c_{2-1} = Q/A_2 = \frac{P_g}{\eta_g \bar{\rho} E_m A_2} = f(P_g, \bar{\rho}, E_m, A_2) \text{ [m/s]} \quad (\text{E.30})$$

$$e_{c_{2-1}}^2 = \left(\frac{eP_g}{\eta_g \bar{\rho} E_m A_2}\right)^2 + \left(\frac{P_g e \bar{\rho}}{\eta_g \bar{\rho}^2 E_m A_2}\right)^2 + \left(\frac{P_g e E_m}{\eta_g \bar{\rho} E_m^2 A_2}\right)^2 + \left(\frac{P_g e A_2}{\eta_g \bar{\rho} E_m A_2^2}\right)^2 \quad (\text{E.31})$$

$$e_{E_{m,kin}}^2 = (c_{1-1} e_{c_{1-1}})^2 + (c_{2-1} e_{c_{2-1}})^2 \quad (\text{E.32})$$

Leakage loss term

$$E_{m,leak} = \frac{Q_{leak}}{Q} \left(\bar{a}_l \left(\frac{\bar{\rho} g h_{2-1}}{1000} + p_{atm} \right) + \bar{c}_p (T_{leak} - T_{2-1}) + g(z_{leak} - z_{2-1}) \right) \quad (\text{E.33})$$

$$E_{m,leak} = f(Q_{leak}, P_g, E_m, \bar{a}_l, \bar{\rho}, p_{atm}, \bar{c}_p, T_{leak} - T_{2-1}, z_{leak} - z_{2-1}, h_{2-1}) \quad (\text{E.34})$$

$$e_{E_{m,leak}, Q_{leak}}^2 = \left(\frac{e_{Q_{leak}}}{Q} \left(\bar{a}_l \left(\frac{\bar{\rho} g h_{2-1}}{1000} + p_{atm} \right) + \bar{c}_p (T_{leak} - T_{2-1}) + g(z_{leak} - z_{2-1}) \right) \right)^2 \quad (\text{E.35})$$

$$e_{E_m, leak, P_g}^2 = \left(\frac{Q_{leak} e_{P_g} \eta_g E_m \bar{\rho}}{P_g^2} (\bar{a}_l \left(\frac{\bar{\rho} g h_{2-1}}{1000} + p_{atm} \right) + \bar{c}_p (T_{leak} - T_{2-1}) + g(z_{leak} - z_{2-1})) \right)^2 \quad (\text{E.36})$$

$$e_{E_m, leak, E_m}^2 = \left(\frac{Q_{leak} \eta_g \bar{\rho} e_{E_m}}{P_g} (\bar{a}_l \left(\frac{\bar{\rho} g h_{2-1}}{1000} + p_{atm} \right) + \bar{c}_p (T_{leak} - T_{2-1}) + g(z_{leak} - z_{2-1})) \right)^2 \quad (\text{E.37})$$

$$e_{E_m, leak, \bar{a}}^2 = \left(\frac{Q_{leak}}{Q} \left(\frac{\bar{\rho} g h_{2-1}}{1000} + p_{atm} \right) e_{\bar{a}} \right)^2 \quad (\text{E.38})$$

$$e_{E_m, leak, \bar{\rho}}^2 = \left(\frac{Q_{leak}}{Q \bar{\rho}} \left(\bar{a}_l \left(\frac{2 \bar{\rho} g h_{2-1}}{1000} + p_{atm} \right) + \bar{c}_p (T_{leak} - T_{2-1}) + g(z_{leak} - z_{2-1}) \right) e_{\bar{\rho}} \right)^2 \quad (\text{E.39})$$

$$e_{E_m, leak, p_{atm}}^2 = \left(\frac{Q_{leak}}{Q} (\bar{a}_l e_{p_{atm}}) \right)^2 \quad (\text{E.40})$$

$$e_{E_m, leak, \bar{c}_p}^2 = \left(\frac{Q_{leak}}{Q} (e_{\bar{c}_p} (T_{leak} - T_{2-1})) \right)^2 \quad (\text{E.41})$$

$$e_{E_m, leak, \Delta T}^2 = \left(\frac{Q_{leak}}{Q} (\bar{c}_p e_{\Delta T}) \right)^2 \quad (\text{E.42})$$

$$e_{E_m, leak, \Delta z}^2 = \left(\frac{Q_{leak}}{Q} (g e_{\Delta z}) \right)^2 \quad (\text{E.43})$$

$$e_{E_m, leak, h_{2-1}}^2 = \left(\frac{Q_{leak}}{Q} (\bar{a}_l \bar{\rho} g e_{h_{2-1}}) \right)^2 \quad (\text{E.44})$$

$$e_{E_m, leak}^2 = e_{E_m, leak, Q_{leak}}^2 + e_{E_m, leak, P_g}^2 + e_{E_m, leak, E_m}^2 + e_{E_m, leak, \bar{a}}^2 + e_{E_m, leak, \bar{\rho}}^2 + e_{E_m, leak, p_{atm}}^2 + e_{E_m, leak, \bar{c}_p}^2 + e_{E_m, leak, \Delta T}^2 + e_{E_m, leak, \Delta z}^2 \quad (\text{E.45})$$

Specific hydraulic energy

All the following factors starting with "E" and "e" have the unit [J/kg].

$$E_h = E_{h,p} + E_{h,pot} + E_{h,kin} \quad (\text{E.46})$$

$$e_{E_h}^2 = e_{E_{h,p}}^2 + e_{E_{h,pot}}^2 + e_{E_{h,kin}}^2 \quad (\text{E.47})$$

Pressure term

$$E_{h,p} = \frac{p_1' - p_2}{\bar{\rho}} = \frac{1}{\bar{\rho}} \left(p_1 + \frac{\bar{\rho}g\Delta z_1}{1000} - \frac{\bar{\rho}gh_2}{1000} - p_{atm} \right) \quad (\text{E.48})$$

$$E_{h,p} = f(\bar{\rho}, p_1, \Delta z_1, h_2, p_{atm}) \quad (\text{E.49})$$

$$e_{E_{h,p,p_1}}^2 = \left(\frac{e_{p_1}}{\bar{\rho}} \right)^2 \quad (\text{E.50})$$

$$e_{E_{h,p,\bar{\rho}}}^2 = \left(\frac{p_1 - p_{atm}}{\bar{\rho}^2} e_{\bar{\rho}} \right)^2 \quad (\text{E.51})$$

$$e_{E_{h,p,\Delta z_1}}^2 = \left(\frac{\bar{\rho}g}{1000} e_{\Delta z_1} \right)^2 \quad (\text{E.52})$$

$$e_{E_{h,p,h_2}}^2 = \left(\frac{\bar{\rho}g}{1000} e_{h_2} \right)^2 \quad (\text{E.53})$$

$$e_{E_{h,p,p_{atm}}}^2 = \left(\frac{e_{p_{atm}}}{\bar{\rho}} \right)^2 \quad (\text{E.54})$$

$$e_{E_{h,p}}^2 = e_{E_{h,p,p_1}}^2 + e_{E_{h,p,\bar{\rho}}}^2 + e_{E_{h,p,\Delta z_1}}^2 + e_{E_{h,p,h_2}}^2 + e_{E_{h,p,p_{atm}}}^2 \quad (\text{E.55})$$

Potential term

$$E_{h,pot} = g(z_1 - z_2) \quad (\text{E.56})$$

$$E_{h,pot} = f(z_1 - z_2) \quad (\text{E.57})$$

$$e_{E_{h,pot}}^2 = e_{E_{h,pot,\Delta z}}^2 = ge_{\Delta z} \quad (\text{E.58})$$

Kinetic term

$$E_{h,kin} = \frac{1}{2}(c_1^2 - c_2^2) \quad (\text{E.59})$$

$$E_{h,kin} = f(c_1, c_2) \quad (\text{E.60})$$

$$c_1 = \frac{Q}{A_1} = \frac{4P_g}{\eta_g \bar{\rho} E_m \pi D_1^2} = f(P_g, \bar{\rho}, E_m, D_1) \text{ [m/s]} \quad (\text{E.61})$$

$$e_{c_1}^2 = \left(\frac{4eP_g}{\eta_g \bar{\rho} E_m \pi D_1^2} \right)^2 + \left(\frac{4P_g e_{\bar{\rho}}}{\eta_g \bar{\rho}^2 E_m \pi D_1^2} \right)^2 + \left(\frac{4P_g e_{E_m}}{\eta_g \bar{\rho} E_m^2 \pi D_1^2} \right)^2 + \left(\frac{8P_g e_{D_1}}{\eta_g \bar{\rho} E_m \pi D_1^3} \right)^2 \quad (\text{E.62})$$

$$c_2 = c_{2-1} = Q/A_2 \text{ [m/s]} \quad (\text{E.63})$$

$$e_{c_2}^2 = e_{c_{2-1}}^2 \quad (\text{E.64})$$

$$e_{E_{h,kin}}^2 = (c_1 e_{c_1})^2 + (c_2 e_{c_2})^2 \quad (\text{E.65})$$

Uncertainties in numbers

| | |
|------------------------------|----------|
| e | Smeland |
| $e_{E_{m,p,\bar{a}}}$ | 1,72459 |
| $e_{E_{m,p,p_{1-1}}}$ | 0,25246 |
| $e_{E_{m,p,\bar{\rho}}}$ | -0,00006 |
| $e_{E_{m,p,\Delta z_{1-1}}}$ | 0,00010 |
| $e_{E_{m,p,h_{2-1}}}$ | 0,00071 |
| $e_{E_{m,p,p_{atm}}}$ | 0,00848 |
| $e_{E_{m,p}}$ | 1,74297 |
| $e_{E_{m,T,cp}}$ | -0,24827 |
| $e_{E_{m,T,\Delta T}}$ | 4,23192 |
| e_{E10} | 1,68470 |
| e_{E20} | 5,05411 |
| $e_{E_{m,T}}$ | 6,80831 |

| | |
|-----------------------------------|----------|
| $e_{E_m, pot}$ | 1,38838 |
| $e_{c_{1-1}}$ | 0,11023 |
| $e_{c_{2-1}}$ | 0,06004 |
| $e_{E_m, kin}$ | 0,12510 |
| $e_{E_m, leak, Q_{leak}}$ | 0,00595 |
| $e_{E_m, leak, P_g}$ | 0,13650 |
| $e_{E_m, leak, E_m}$ | 0,06057 |
| $e_{E_m, leak, \bar{a}}$ | 0,00202 |
| $e_{E_m, leak, \bar{\rho}}$ | 1,00014 |
| $e_{E_m, leak, p_{atm}}$ | 0,00000 |
| $e_{E_m, leak, \bar{\epsilon}_p}$ | 0,03536 |
| $e_{E_m, leak, \Delta T}$ | 0,01069 |
| $e_{E_m, leak, \Delta z}$ | 0,00175 |
| $e_{E_m, leak, h_{2-1}}^2$ | -0,00018 |
| $e_{E_m, leak}$ | 0,71888 |
| e_{E_m} | 7,09990 |
| e_{E_h, p, p_1} | 0,24931 |
| $e_{E_h, p, \bar{\rho}}$ | -0,90753 |
| $e_{E_h, p, \Delta z_1}$ | -0,00010 |
| e_{E_h, p, h_2} | -0,00070 |
| $e_{E_h, p, p_{atm}}$ | -0,00836 |
| $e_{E_h, p}$ | 0,94119 |
| $e_{E_h, pot}$ | 1,38838 |
| e_{c_1} | 0,87417 |
| e_{c_2} | 0,06004 |
| $e_{E_h, kin}$ | 0,65270 |
| e_{E_h} | 1,44160 |
| e_{η_h} | 0,00834 |
| f_{η_h} | 0,88058 |

Table E.5: All part uncertainties

APPENDIX F

AIR MASS FLOW RATE EXAMPLE CALCULATION, M-XXI

Example calculation of the flow rate of air in a closed conduit through an orifice plate.

ISO 5167-1:2003 states that the mass flow rate, q_m is

$$q_m = \frac{C}{\sqrt{1 - \beta^4}} \varepsilon \frac{\pi}{4} d^2 \sqrt{2\Delta p \rho_1} \text{ [kg/s]} \quad (\text{F.1})$$

and the volume flow rate q_V

$$q_V = \frac{q_m}{\rho} \text{ [m}^3\text{/s]} \quad (\text{F.2})$$

for the pressure and temperature for which ρ is stated. Additionally, a series of empirical coefficients is required. C is the *discharge coefficient*, and is

$$\begin{aligned} C = & 0,5961 + 0,0261\beta^2 - 0,216\beta^8 + 521 \cdot 10^{-6} \left(\frac{10^6 \beta}{Re_D} \right)^{0,7} \\ & + (18,8 + 6,3A) 10^{-3} \beta^{3,5} \left(\frac{10^6}{Re_D} \right)^{0,3} \\ & + \left(0,043 + 0,080e^{-10L_1} - 0,123e^{-7L_1} \right) (1 - 0,11A) \frac{\beta^4}{1 - \beta^4} \\ & - 0,031 \left(M_2' - 0,8M_2'^{1,1} \right) \beta^{1,3} + 0,011 (0,75 - \beta) \left(2,8 - \frac{D}{25,4} \right) \text{ [-]} \end{aligned} \quad (\text{F.3})$$

ε is the *expansibility factor*, and is

$$\varepsilon = 1 - \left(0,351 + 0,256\beta^4 + 0,93\beta^8\right) \left[1 - \left(\frac{p_2}{p_1}\right)^{1/\kappa}\right] \quad [-] \quad (\text{F.4})$$

$$Re_D = \frac{uD}{\nu_1} = \frac{4q_m}{\pi\mu_1 D} \quad [-] \quad (\text{F.5})$$

The orifice diameter ratio, β is simply

$$\beta = \frac{d}{D} \quad [-] \quad (\text{F.6})$$

Finally, there are two coefficients used in the calculation of C which are

$$A' = \left(\frac{19000\beta}{Re_D}\right)^{0,8} \quad [-] \quad (\text{F.7})$$

$$M'_2 = \frac{2L'_2}{1 - \beta} \quad [-] \quad (\text{F.8})$$

L_1 and L'_2 are the distances between the faces of the plate to the pressure tappings, relative to the pipe diameter.

$$L_1 = \frac{l_1}{D} = 1 \quad (\text{F.9})$$

$$L'_2 = \frac{l'_2}{D} = 0,47 \quad (\text{F.10})$$

The objective is to find q_m . The necessary inputs are μ_1 , ρ_1 , D , d and Δp .

| | Data |
|------------------|-----------------------|
| p_1 [kPa] | 165,219 |
| p_2 [kPa] | 148,384 |
| Δp [kPa] | 16,835 |
| T [C°] | 21,5 |
| D [m] | $52 \cdot 10^{-3}$ |
| d [m] | $13,21 \cdot 10^{-3}$ |

Table F.1: Measured values

Checking pulsations regarding the flow

$$\frac{\Delta p'_{rms}}{(p_1 - p_2)} = \frac{1,325 \text{ kPa}}{(165,219 - 148,384) \text{ kPa}} = 0,0787 \quad (\text{F.11})$$

| | Data | Method of calculation |
|-------------------------------|------------------------|------------------------------|
| $\Delta p'_{rms}$ [kPa] | 1,325 | As stated in ISO 5167-1:2003 |
| μ_1 [Pa s] | $18,205 \cdot 10^{-6}$ | Sutherlands viscosity law |
| ρ_1 [kg/m ³] | 1,953 | Ideal gas law |
| β [-] | 0,254 | As stated in ISO 5167-2:2003 |

Table F.2: Calculated values

No excess pulsation in the air flow.

Next up an iterative method is required to calculate the mass flow rate, as the coefficients used are also a product of the Reynolds number, and thus the air velocity.

For the iterative method, an invariant A_1 is calculated

$$A_1 = \frac{\varepsilon d^2 \sqrt{2\Delta p \rho_1}}{\mu_1 D \sqrt{1 - \beta^4}} \quad (\text{F.12})$$

First, set $Re_d = \infty$ and calculate ε and the invariant A_1

$$\varepsilon = 1 - \left(0,351 + 0,256 \cdot 0,254^4 + 0,93 \cdot 0,254^8 \right) \left[1 - \left(\frac{148,384 \text{ kPa}}{165,219 \text{ kPa}} \right)^{1/1,4} \right] = 1 \quad (\text{F.13})$$

$$A_1 = \frac{1 \cdot (13,21 \cdot 10^{-3} \text{ m})^2 \sqrt{2 \cdot 16,835 \text{ kPa} \cdot 1,953 \text{ kg/m}^3}}{18,205 \cdot 10^{-6} \text{ Pa s} \cdot 52 \cdot 10^{-3} \text{ m} \cdot \sqrt{1 - 0,254^4}} = 47\,368,54 \quad (\text{F.14})$$

Then calculate C_∞

$$\begin{aligned} C_\infty &= 0,5961 + 0,0261 \cdot 0,254^2 - 0,216 \cdot 0,254^8 + 521 \cdot 10^{-6} \cdot 0 \\ &\quad + (18,8 + 0) 10^{-3} \cdot 0,254^{3,5} \cdot 0 \\ &\quad + \left(0,043 + 0,080e^{-10} - 0,123e^{-7} \right) (1 - 0) \frac{0,254^4}{1 - 0,254^4} \\ &\quad - 0,031 \left(1,26 - 0,8 \cdot 1,26^{1,1} \right) 0,254^{1,3} \\ &\quad + 0,011 (0,75 - 0,254) \left(2,8 - \frac{52}{25,4} \right) = 0,600874 \end{aligned} \quad (\text{F.15})$$

Then compare Re_D with CA_1 , as they should be nearly equal with the precision criterion

$$\left| \frac{A_1 - \frac{Re_D}{C}}{A_1} \right| = \left| \frac{47\,368,54 - \frac{\infty}{0,6009}}{47\,368,54} \right| = \infty \quad (\text{F.16})$$

The precision criterion should be lower than 10^{-n} , where n is set by the user and is 6 in this example. As the criterion is not met, set Re_D to be CA_1 and calculate C again with the new $Re_D = 28\,462,52$

$$A' = \left(\frac{19000 \cdot 0,254}{28\,462,52} \right)^{0,8} = 0,241797 \quad (\text{F.17})$$

$$\begin{aligned} C = & 0,5961 + 0,0261 \cdot 0,254^2 - 0,216 \cdot 0,254^8 + 521 \cdot 10^{-6} \left(\frac{10^6 \cdot 0,254}{28\,462,52} \right)^{0,7} \\ & + (18,8 + 6,3 \cdot 0,241797) 10^{-3} \cdot 0,254^{3,5} \left(\frac{10^6}{28\,462,52} \right)^{0,3} \\ & + \left(0,043 + 0,080e^{-10} - 0,123e^{-7} \right) (1 - 0,11 \cdot 0,241797) \frac{0,254^4}{1 - 0,254^4} \\ & - 0,031 \left(1,26 - 0,8 \cdot 1,26^{1,1} \right) 0,254^{1,3} \\ & + 0,011 (0,75 - 0,254) \left(2,8 - \frac{52}{25,4} \right) = 0,603911 \end{aligned} \quad (\text{F.18})$$

Check the precision again

$$\left| \frac{47\,368,54 - \frac{28\,462,52}{0,60391}}{47\,368,54} \right| = 5,03 \cdot 10^{-3} \quad (\text{F.19})$$

Recalculate $Re_D = 28\,606,38 \rightarrow C = 0,60390$

$$\left| \frac{47\,368,54 - \frac{28\,606,38}{0,60390}}{47\,368,54} \right| = 1,82 \cdot 10^{-5} \quad (\text{F.20})$$

Recalculate $Re_D = 28\,605,86 \rightarrow C = 0,60390$

$$\left| \frac{47\,368,54 - \frac{28\,605,86}{0,60390}}{47\,368,54} \right| = 4,57 \cdot 10^{-8} \quad (\text{F.21})$$

The precision criterion is now met, so q_m can be calculated

$$q_m = Re_D \frac{\pi}{4} \mu_1 D = 21,27 \cdot 10^{-3} \text{ kg/s} \quad (\text{F.22})$$

APPENDIX G

CRHT VIII PAPER

Paper presented at CRHT VIII in Kathmandu University, Nepal, to be published in IOP conference series. Written in march 2018, and is thus not up to date on later observations, analysis, and discussion. For a complete take on the problems at Smeland, it is recommended to look at the main work rather than this paper. NOTE: the hydraulic efficiency when air injection was tested has been adjusted since this paper.

Pressure pulsations and hydraulic efficiency at Smeland power plant

V S Ulvan*, J O Kverno and O G Dahlhaug

Department of Energy and Process Engineering Norwegian University of Technology and Science, Trondheim, Norway

* Corresponding author (vegarsul@stud.ntnu.no)

Abstract. Smeland power plant in Norway is experiencing pressure pulsations in their Francis turbine when running above best efficiency point. By measuring both the pressure pulsations and runner efficiency, the cause and effect of the pulsations are to be investigated thoroughly, which is this work's main purpose. To find the Francis runner's efficiency the thermodynamic method has been used, which builds on the principle that all of the hydraulic losses turn into heat in the flow itself. By measuring the change of temperature before and after the turbine one can, with little other data, calculate the hydraulic efficiency. To identify the pressure pulsations, pressure transducers were placed on the inlet to the spiral casing, draft tube, and upper labyrinth. While doing measurements, air-injection through the runner was tested on full load, which nearly eradicated the pressure pulsations. This might be due to an increase of volume in a pulsating full load vortex that changed its eigenfrequency, and therefore stopped resonating.

1. Introduction

Table 1. Smeland power plant characteristics [4]

| Characteristic | Data |
|-------------------|-------------------|
| Runner | Low head Francis |
| Head | 95 m |
| Installed power | 24 MW |
| BEP | 20 MW |
| Annual production | 119 GWh |
| Owner | Agder Energi |
| Built | 1985 |
| River system | Mandalsvassdraget |

A hydro power plant in Vest-Agder County, Smeland power plant, is experiencing pressure pulsations in their turbine. The pulsations they have registered were of a low frequency variety, 2.8 Hz, which indicated that the the problem may be in the draft tube. The turbine is equipped

with a check valve which lets air into the draft tube at sub-atmospheric pressures, however this proved to be blocked. The owners of the power plant, Agder Energi, deemed the pressure pulsation matter great enough to seek help from the Waterpower Laboratory at NTNU in order to find out what is causing this phenomenon. By taking measurements of both the hydraulic efficiency and the pressure pulsations one might be able to discern and find the cause of the pressure pulsations.

2. Hydraulic efficiency and the thermodynamic method

In a water turbine, energy is converted from hydraulic energy to mechanical energy which in turn drives an electric generator. However, not all of the energy is converted into mechanical energy, i.e. there are losses through the system. The turbine efficiency says how much of the available hydraulic energy that is turned into mechanic energy. The thermodynamic method builds on the principle that all of the losses in the flow going through the turbine turns into heat in the flow itself. Then the hydraulic losses in a water turbine can be accounted for by the change of temperature in the water running through it, or more accurately the change in enthalpy. By mainly measuring the temperature and pressure at the inlet and outlet, the turbine hydraulic efficiency can be found. The thermodynamic method is a method for measuring efficiency which does not require a direct measurement of the volumetric flow, which can be a very difficult parameter to measure in existing power plants. [1]

The general equation for calculating the hydraulic efficiency is found by dividing the mechanic power by the hydraulic power [3]. The subscripts denotes place of measurement in figure 1.

$$\eta_h = \frac{P_m}{P_h} = \frac{(\rho Q g) E_m}{(\rho Q g) E_h} = \frac{E_m}{E_h} \quad (1)$$

$$\eta_h = \frac{E_m}{E_h} = \frac{\bar{a}(p_{1-1} - p_{2-1}) + g(z_{1-1} - z_{2-1}) + \frac{1}{2}(c_{1-1}^2 - c_{2-1}^2) + \bar{c}_p(T_{1-1} - T_{2-1})}{\frac{1}{\rho}(p_1 - p_2) + g(z_1 - z_2) + \frac{1}{2}(c_1^2 - c_2^2)} \quad (2)$$

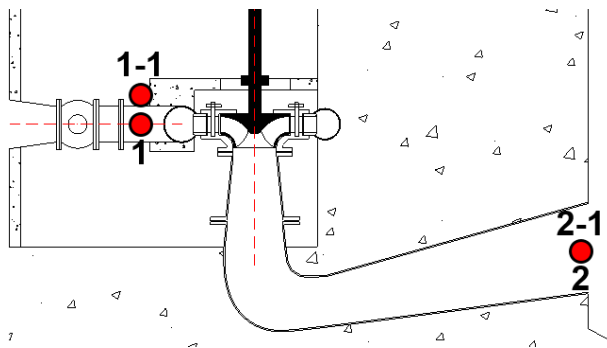


Figure 1. Different places of measurement

3. Pressure pulsations and full load vortex

One characteristic of hydraulic turbines and pipe flow is pressure pulsations, as the system is dynamic and the flow is often unstable to some extent. These instabilities do however tend to reach a point of equilibrium with the dampening effects of friction as the oscillation amplitude is increased. When a Francis turbine with a fixed rotational frequency operates outside of its design point, the flow leaving the Francis runner will have a rotating component. The direction and magnitude of the rotating velocity component will depend on whether the turbine is operating at part or full load, and how far off the design point it is, respectively. As a swirling flow moves through a cylinder, the bulk of the fluid transport will be along the walls, while a more stagnant region is found at the centre. If the swirl is severe enough, this stagnant flow might stop or move upstream, and a vortex breakdown occurs. [2]

When a Francis runner is operating at full load, i.e. above BEP, a symmetrical vortex appears. Due to the rotation of the flow, the bulk mass flow will occur along the walls of the draft tube, which severely increases the downwards velocity of the water. This vortex can pulsate if the frequency of this pulsation resonates with an exciting frequency from the system. This is when resonance can occur. The exact frequency of this vortex pulsation is difficult to pinpoint but it will change depending on the volume and pressure, as both are parameters that dictates the natural frequency of a gas bubble suspended in a liquid. [2]

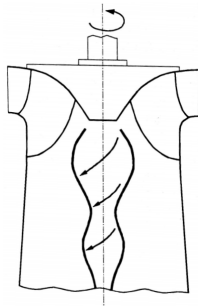


Figure 2. Full load vortex [5]

We can simplify the full load vortex to be a bubble. To find the natural frequency of such a bubble, the problem was simplified and regarded as an analogy to a mass spring system

$$\omega = \sqrt{\frac{k}{m}} \rightarrow f = \frac{1}{2\pi} \sqrt{\frac{k}{m}} \quad (3)$$

where k is the spring constant and m is the mass attached to the spring. k is defined to be

$$k = \frac{dF}{dx} \quad (4)$$

and could, when dealing with changing volumes and pressure, be defined as

$$k = \frac{dp}{dV} \quad (5)$$

$$\Rightarrow dp = \frac{-\gamma p_0}{V_0} dV \quad (6)$$

where γ is the ratio of specific heats for the gas, p_0 is the pressure, and V_0 is the volume of the gas. Equation 6 stems from the derivative of the equation of state. Professor Nielsen at the Waterpower Laboratory suggested that this, combined with the momentum equation could be used to find the natural frequency of the vortex. He derived the following expression

$$f_e = \frac{1}{2\pi} \sqrt{\frac{\gamma p_0}{V_0 I}} \quad (7)$$

where f_e is the eigenfrequency of the vortex filament and I is an inertial factor related to the mass and inertia of the surrounding water. It has the unit kg/m^4 , which Nielsen suggested could be something like ρ/l_c , where ρ is the density of the water, and l_c is some length scale related to the filament. The natural frequencies for various vortex volumes were calculated, with l_c being set to both the circumference, diameter and radius of the vortex cross section, and compared with the frequencies observed at Smeland power plant. Out of all of these, the diameter seems to make most sense in terms of what type of length scale that would affect the flow.

4. Measurement set-up

In order to calculate the efficiency seven sensors were used, five temperature sensors and two pressure transducers. Using a probe on the inlet bleed valve, one temperature and pressure sensor were used to find inlet temperature with corresponding pressure. One temperature sensor measured the leakage water, and the last three measured the temperature in the outlet of the draft tube. The last pressure sensor was placed directly on the inlet pipe in order to calculate the hydraulic specific energy. To find the pressure in the outlet, water column calculations were utilized using the measured height from upper draft tube floor to the water surface.

Pressure pulsation measurement were done with five pressure sensors; one upstream and downstream the main inlet valve, two on the draft tube cone 180° apart, and lastly, one on the upper labyrinth.

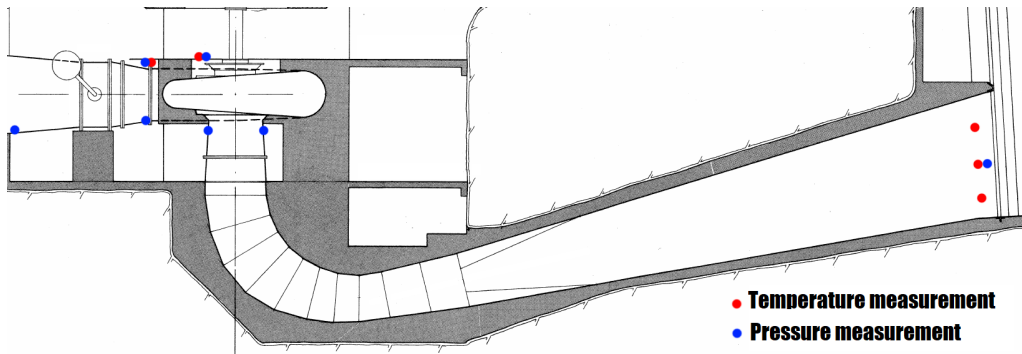


Figure 3. Measurement of temperature and pressure

5. Measurement procedure

Thirteen measurements were made with ten different points of operation. BEP was measured twice due to unstable temperature in the first measurement, 23 MW was done thrice to check repeatability and to test air injection.

Table 2. Sensors

| Name | Type | Systematic accuracy |
|----------------------------|-------------|---------------------|
| Oceanographic SeaBird 38 | Temperature | 0.0001°C |
| GE Druck UNIK-5000 3bar a | Pressure | 0.01% |
| GE Druck UNIK-5000 5bar a | Pressure | 0.01% |
| GE Druck UNIK-5000 15bar a | Pressure | 0.01% |
| GE Druck UNIK-5000 50bar a | Pressure | 0.04% |

Table 3. Points of operation

| Measurement # | P_{gen} [MW] |
|-------------------|----------------|
| 1 | 19.6 |
| 2 | 21 |
| 3 | 22.2 |
| 4 | 23 |
| 5 | 24 |
| 6 | 6.2 |
| 7 | 9.8 |
| 8 | 13.25 |
| 9 | 15.0 |
| 10 | 16.9 |
| 11 | 19.6 |
| 12 | 23 |
| 13 (w/air injec.) | 23 |

6. Results

The pressure pulsations started right after BEP and were present toward maximum effect. The pulsations varied in amplitude and frequency, where both peaked around 23 MW. The results presented here will mainly concern the pulsations at its worst, namely at 23 MW. In the figures, H is the measured head and H0 is net head.

As seen in figure 4, the pulsations have a peak to peak value of 18 % of the head and are dominating the measurements. The pulsations were of a low frequency, about 2.8 Hz.

In discussion with the staff at Smeland power plant it was revealed that the runner had a check valve designed to let air through its center, and it was decided to test air injection through the valve. Upon inspection it was found that the the valve was blocked, not allowing the draft tube to "breathe". The valve was removed and a standard compressor for tools was connected and turned on with a pressure of 8-10 bar. This nearly eradicated the pulsations as can be seen in figure 5.

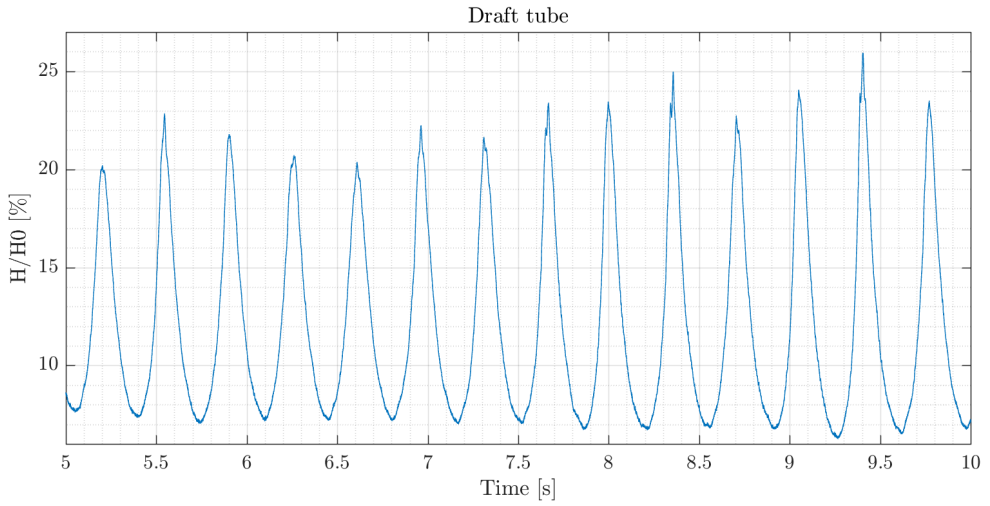


Figure 4. Pressure in draft tube, measurement no. 12

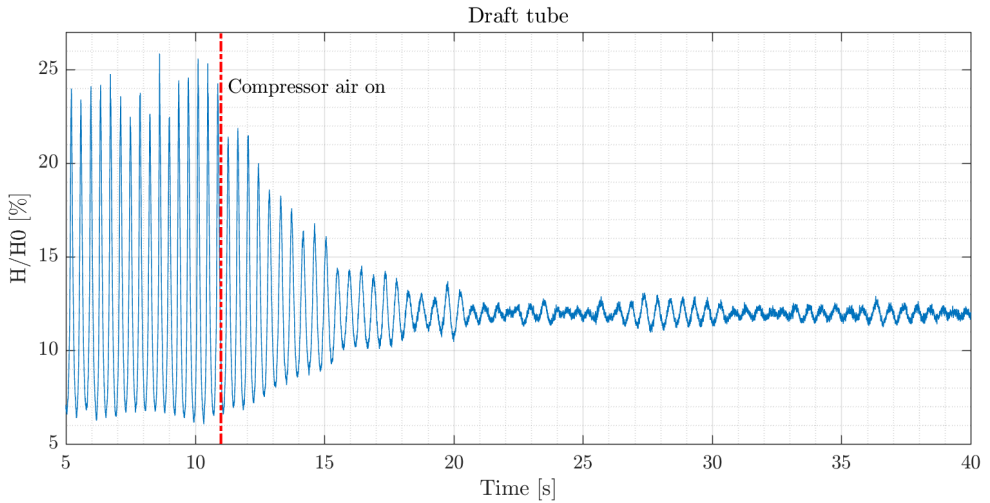


Figure 5. Air injection through the runner, measurement no. 13

As the compressor ran out of air, its pressure dropped to about 2 bar. Still, the air injection nearly halved the initial pulsations as can be seen in figure 6. It was under these circumstances an additional point for hydraulic efficiency were measured. The efficiency curve can be seen in figure 7, and it is the circle that represent the additional point.

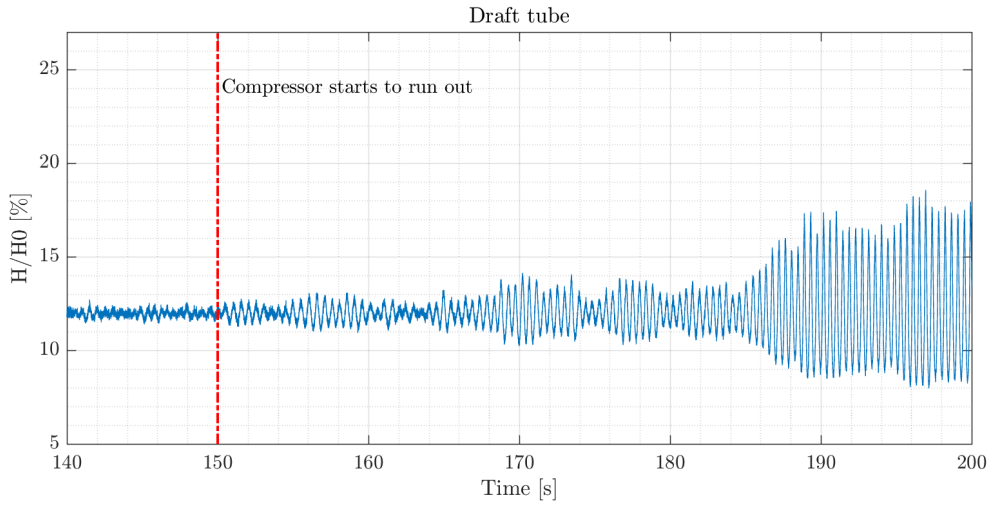


Figure 6. Compressor runs out of air, measurement no. 13

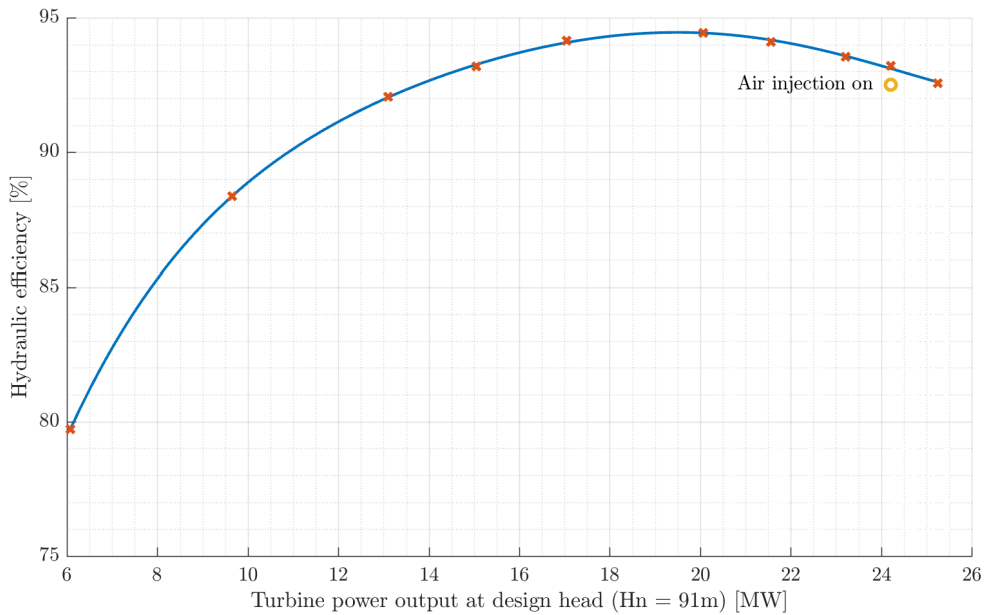


Figure 7. Hydraulic efficiency

An injection of water was also tried, however, as can be seen in figure 8, this had no perceivable effect.

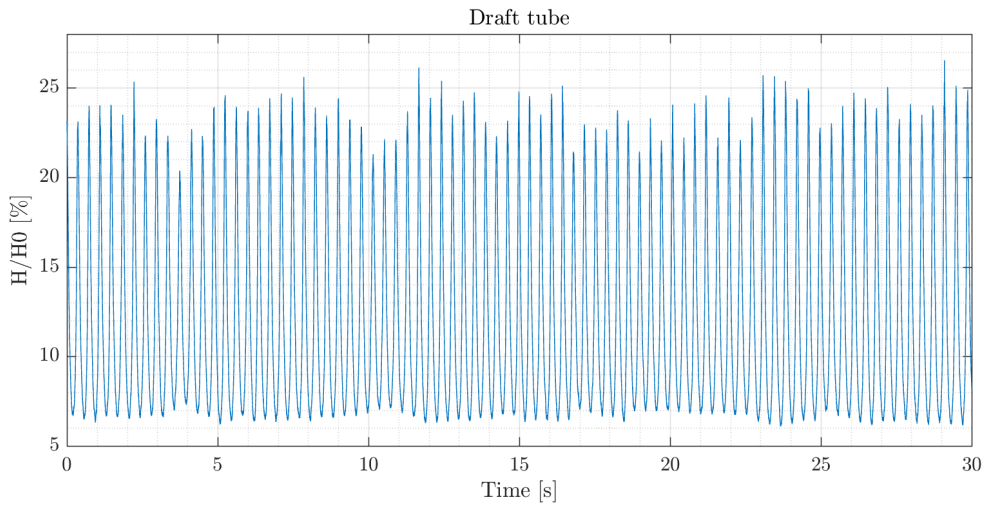


Figure 8. Water injection, measurement no. 13



Figure 9. Staff at Smeland checking valve



Figure 10. Compressor connection

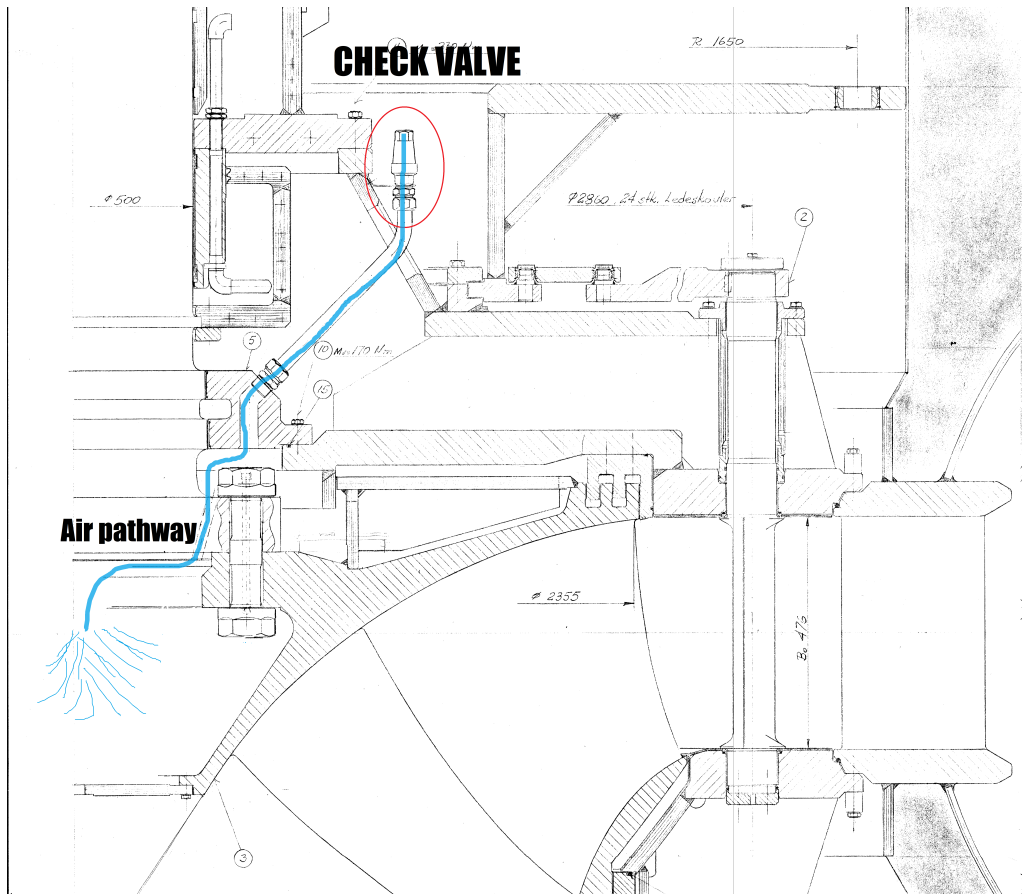


Figure 11. Vertical cross-section of turbine showing check valve and air pathway

7. Discussion

The pressure pulsations at Smeland power plant occur at full load, and the frequency is seemingly dependent on the load. This implies that there is a full load vortex happening in the draft tube, which has its own eigenfrequency. If this eigenfrequency were to match any other pressure pulsations happening in the power plant, resonance would present itself. This other frequency could be a number of many things; pressure wave propagation in the water, von Karman vortices, natural frequency in construction elements, pole passing frequency, RSI, the list goes on.

When injecting air through the runner vertically, with no rotational element, mass in form of gas is essentially added. This would change the volume of the bubble in the draft tube cone, which in turn changes the bubbles eigenfrequency, as the eigenfrequency is a function of volume. Moving the eigenfrequency means leaving the range in which resonance would occur, as all other frequencies would stay the same.

Looking at figure 4, it looks like the pressure pulsations collapse reaching maximum value. If there really is a full load vortex present, and it collapses, then added air could function as a dampener. This dampening effect might be another reason why air injection worked against the pressure pulsations.

When it comes to the hydraulic efficiency it would seem like the pressure pulsations had no effect at all, as the efficiency is quite close to the measurements done in 1985 by the turbine supplier. One could argue that the pressure pulsations were present from day 1, and therefore the pulsations were included during the very first efficiency measurement.

The drop in efficiency during air injection is difficult to say anything certain about. When the uncertainty analysis is done the three points at 23 MW will surely overlap, and one could not conclude that air injection reduced the hydraulic efficiency. However, the uncertainty is highly determined by IECs strict standards [3], and the fact that the repeatability of the measurement without air injection gave nearly exact results several hours between is cause for concern. On the other hand the temperature of the air can influence the temperature measurement at the outlet. A more thorough look at the data is needed.

8. Further work

There is a lot of measurement data that still need to be addressed and analysed. An uncertainty analysis on the efficiency measurements are essential, and a harder look at the efficiency with air injection is needed. A spectral analysis of the pressure pulsations must be done, and will give a more clear view of all the present frequencies and their peak to peak values. Furthermore, the theory of a full load vortex pulsating with another pulsation needs to be fully investigated.

If possible a real-life simulation of a full load vortex with air injection will be done in the Waterpower Laboratory NTNU. This might give more insight into the effects of air injection, as the draft tube cone is see-through.

References

- [1] Kjoelle, A. 2003. Hydraulisk maaleteknikk. Grunnleggende prinsipper og maalemetoder, 2.
- [2] Dorfler, P., Sick, M., Coutu, A., 2013. Flow-Induced Pulsation and Vibration in Hydro-electric Machinery. Springer-Verlag, London
- [3] International Electrotechnical Commission. 1991. Field Acceptance Tests to Determine the Hydraulic Performance of Hydraulic Turbines, Storage Pumps and Pump-turbines. International Electrotechnical Commission.
- [4] Agder Energi, 'Smeland kraftstasjon', 2015. [Online]. Available: <https://www.ae.no/virksomhet/vannkraft/kraftstasjoner/smeland-kraftstasjon/>. [Accessed: 12- Sep- 2017].
- [5] Brekke, H. 2003. Pumper og turbiner. Vannkraftlaboratoriet NTNU.

APPENDIX H

INLET AND OUTLET, ADDITIONAL DRAWINGS

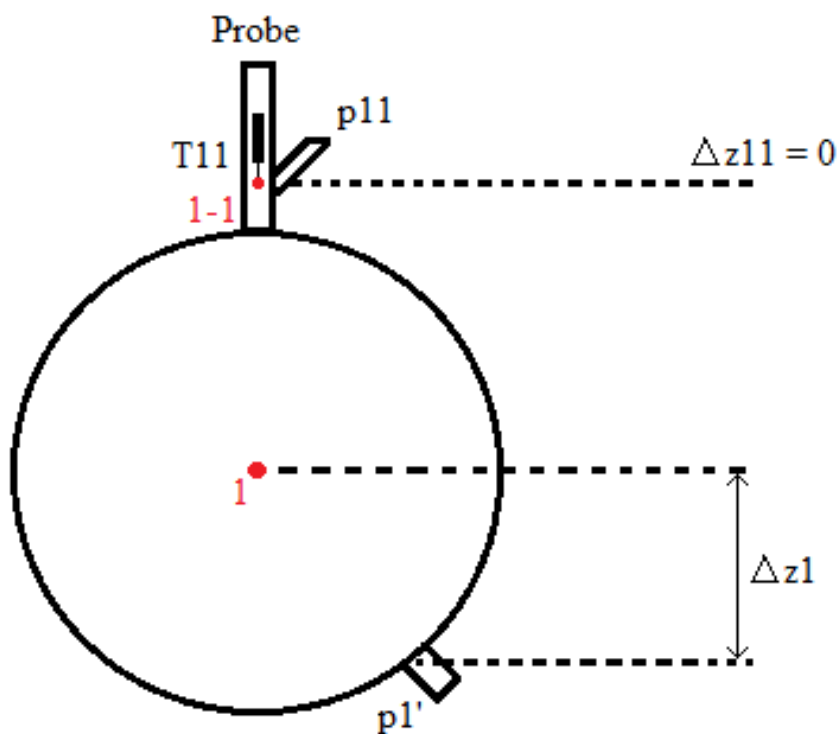


Figure H.1: Drawing of inlet cross-section with measuring points and setup

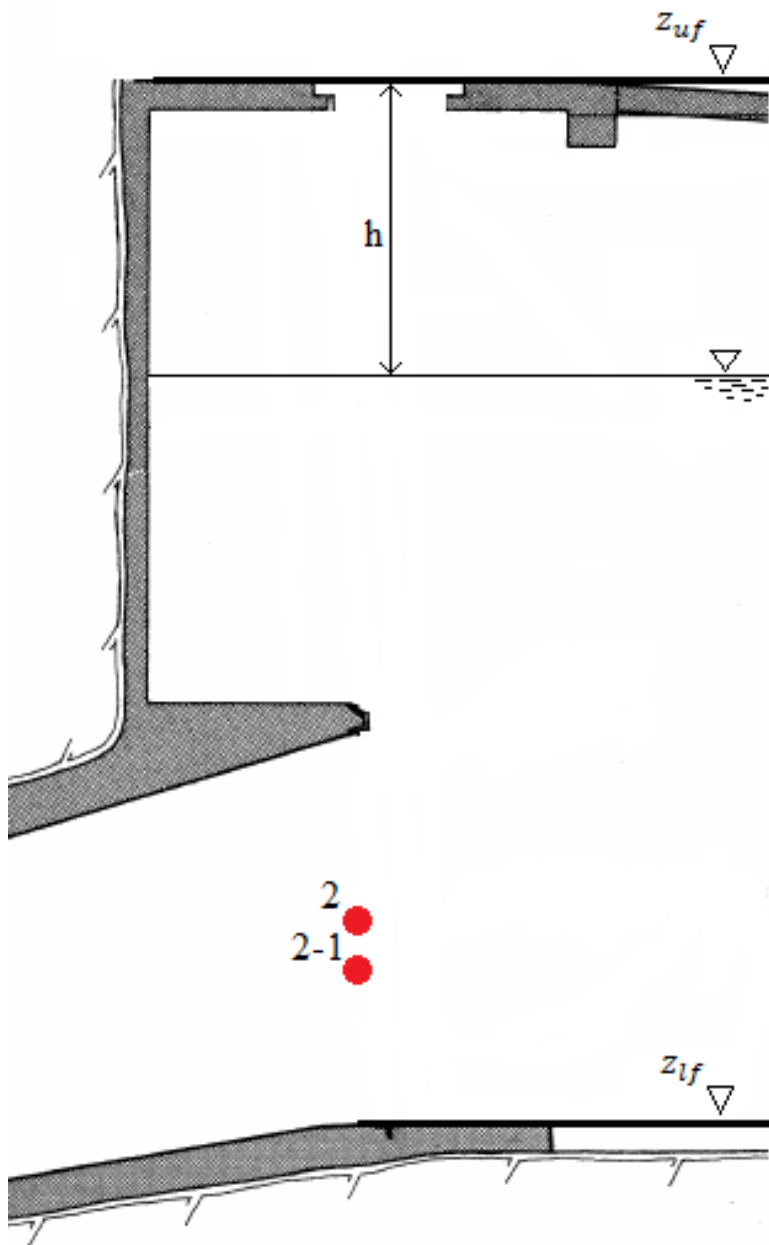


Figure H.2: Outlet measuring points, with relative measured height h (Andresen & Grøner AS, 1984a)

APPENDIX I

CHARACTERISTIC FREQUENCY OF AN AIR
BUBBLE IN WATER

MEMO

Torbjørn K. Nielsen

07.12.2017

The Waterpower Laboratory, NTNU

Characteristic frequency of an air bubble in water

Introduction

An air bubble submerged in water will have a dynamic behavior, i.e. causing a pressure oscillation with a given characteristic frequency. The air bubble has a flexibility dependent on volume and pressure according to the equation of state. The surrounding water masses has an inertia equivalent to a mass in a mechanical system.

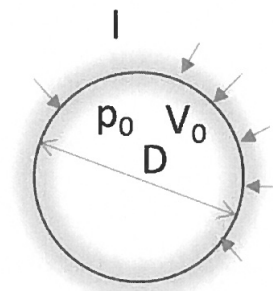


Figure 1 Air bubble surrounded by water

In hydro power turbines, the cavity in the draft tube cone just beneath the turbine runner is an example of such a bubble. The volume of this particular bubble depends on the operational point of the turbine, as well as of the pressure in the draft tube.

As shown below, the characteristic frequency of the submerged air bubble is:

$$\omega = \sqrt{\frac{\kappa p_0}{V_0 I}} \quad (1)$$

Nomenclature:

p – pressure [N/m²]

V – Volume of the air bubble [m³]

Q – flow [m³/s]

κ – Adiabatic constant (1.4 for one atomic gas)

I – Inertia (dimension, see below)

Subscript 0 initial initial state

Equations

To find the characteristic frequency, two central equations defines the physics:

The equation of state: $pV^\kappa = p_0V_0^\kappa$ (2)

The momentum equation: $I \frac{dQ}{dt} = \Delta p$ (3)

Taking the derivative of equation (2) gives:

$$\frac{dp}{dV} = -\frac{\kappa p_0}{V_0} \quad (4)$$

By writing the equation:

$$dp = -\frac{\kappa p_0}{V_0} dV \quad (5)$$

The spring constant can be identified as:

$$C_b = \frac{\kappa p_0}{V_0} \quad (6)$$

The time derivative of the pressure p (eq. 5), is:

$$\frac{dp}{dt} = -C_b \frac{dV}{dt} = -C_b \Delta Q \quad (7)$$

or:

$$\Delta Q = -C_b \frac{dp}{dt} \quad (8)$$

Taking the time derivative again:

$$\frac{dQ}{dt} = -C_b \frac{d^2 p}{dt^2} \quad (9)$$

and inserted in the momentum equation $I \frac{dQ}{dt} = \Delta p$ gives:

$$-C_b I \frac{d^2 p}{dt^2} - \Delta p = 0 \quad (10)$$

Rearranging:

$$I \frac{d^2 p}{dt^2} + \frac{1}{C_b} \Delta p = 0 \quad (11)$$

The eigen value of this equation is a complex figure:

$$\lambda = i\sqrt{\frac{C_b}{I}} = i\sqrt{\frac{\kappa P_0}{V_0 I}} \quad (12)$$

Which gives a steady oscillation with a characteristic frequency of:

$$\omega = \sqrt{\frac{\kappa P_0}{V_0 I}} \quad (13)$$

Comments

The spring constant is well defined by equation (3) as long as the bubble geometry and the surrounding pressure is known.

The inertia of the water masses is not that well defined. However, using the momentum equation, (2), the dimension of I can be found and might give a clearer picture:

$$[I] = \left[\frac{kg}{m^4} \right] \text{ or } [I] = \left[\frac{kg}{m^3 m} \right]$$

The dimension of the density $[\rho] = \left[\frac{kg}{m^3} \right]$ so the dimension of the inertia, I, is density per length. A suggestion is to use the bubble diameter as the length dimension.

Sample calculations

In model scale, the cavity in the draft tube has a typically diameter of 0.1m

The volume of a spherical bubble is $V_0 = \frac{4}{3} R^3 = 0.0005$, the water density is 1000 kg/m^3 and the pressure in the draft tube is $1 \text{ bar} = 10^5 \text{ N/m}^2$.

Inserted in equation (13):

$$\omega = \sqrt{\frac{1.4 \cdot 10^5}{0.0005 \cdot \frac{1000}{0.1}}} = 167.3 \text{ rad / sec}$$

The frequency in Hz: $f = 26.6 \text{ Hz}$

In prototype scale the bubble diameter is more like 1m, hence the spherical volume is 1.33 m^3 .

$$\omega = \sqrt{\frac{1.4 \cdot 10^5}{1.33 \cdot \frac{1000}{1}}} = 10.3 \text{ rad / sec}$$

The frequency in Hz: $f = 1.6 \text{ Hz}$.

Santa Rosa power plant

This chapter is taken straight out of the introduction in «Efficiency and pressure pulsations at Smeland Power Plant» (Kverno and Ulvan, 2017).

At some point during the semester (fall 2017), professor Dahlhaug was contacted by Santa Rosa II, a small hydro power plant in Brazil (Statkraft, 2017). They were struggling with pressure pulsations in their Francis turbines, and wanted to test a forced air injection system they were installing. Initially they wanted to inject the air in to the centre close to the runner cone. However during the initial testing one of the tubes were ripped off by the flow (see figure J.2), so the measuring was conducted with air injected along the draft tube walls. They did six different runs, one with no air injection, one with natural air injection, where the low pressure in the draft tube drives the injection, and four where the air was forced in. The test runs were however done a little too late for a full assessment, but some preliminary analyses were done on the data in order to verify the MATLAB code, and see if the expected frequencies can be identified. The turbine in question is one of three horizontal Francis turbines, with a power rating of about 10 MW, 125 m head, and 10 m³/s flow rate each.



Figure J.1: Santa Rosa II plant (Statkraft, 2017).



Figure J.2: The broken air injection tube (Statkraft International, 2017)

Evaluation of the measurement data

The frequency analysis utilised to gather the frequencies listed in table J.2 and J.3 was Welch's power spectral density method, with Hann windows. The frequencies presented are normalised with respect to the runner frequency, $f_n = 10$ Hz.

| | | |
|---------|---|---------------------------|
| No air | - | 0 l/s |
| N/A air | - | 25 – 103 l/s [†] |
| Air 1 | - | ~ 134 l/s |
| Air 2 | - | ~ 183 l/s |
| Air 3 | - | ~ 235 l/s |
| Air 4 | - | ~ 277 l/s |

Table J.1: Amount of injected air in each test run

| Draft tube 0° Relative load | No air | N/A air | Air 1 | Air 2 | Air 3 | Air 4 | |
|--------------------------------|--------|---------|----------------|----------------|----------------|----------------|-----------|
| 10 % | 16,00 | 16,01 | 16,00 | 16,00 | 16,00 | 16,00 | $[f/f_n]$ |
| 20 % | 16,00 | 16,00 | 15,99 | 16,01 | 16,01 | 16,01 | $[f/f_n]$ |
| 30 % | 1,425 | 1,294 | 0,141 | 0,116 | 17,99 | 1,002 | $[f/f_n]$ |
| 40 % | 0,010 | 0,443 | 0,131 | 0,393 | 0,403 | 15,98 | $[f/f_n]$ |
| 50 % | 0,277 | 0,287 | 0,287 | 0,297 | 0,297 | 0,302 | $[f/f_n]$ |
| 60 % | 0,257 | 0,282 | 0,287 | 0,297 | 0,101 | 0,086 | $[f/f_n]$ |
| 70 % | 0,247 | 0,272 | 0,020 | 0,106 | 16,00 | 16,00 | $[f/f_n]$ |
| 80 % | 0,262 | 0,272 | - [‡] | - [‡] | - [‡] | - [‡] | $[f/f_n]$ |
| 90 % | 0,272 | 0,262 | - [‡] | - [‡] | - [‡] | - [‡] | $[f/f_n]$ |
| 100 % | 0,529 | 13,00 | - [‡] | - [‡] | - [‡] | - [‡] | $[f/f_n]$ |

Table J.2: Dominating frequencies in the draft tube, 0°

[†]The turbine was naturally aspirated during this test.

| Draft tube 180° Relative load | No air | N/A air | Air 1 | Air 2 | Air 3 | Air 4 | |
|----------------------------------|--------|---------|-------|-------|-------|-------|-----------|
| 10 % | 0,065 | 0,111 | 0,071 | 16,00 | 16,00 | 16,00 | $[f/f_n]$ |
| 20 % | 2,382 | 1,355 | 1,642 | 0,096 | 16,01 | 16,01 | $[f/f_n]$ |
| 30 % | 1,445 | 2,020 | 0,141 | 0,111 | 0,076 | 16,00 | $[f/f_n]$ |
| 40 % | 0,292 | 0,388 | 0,398 | 0,388 | 0,428 | 0,111 | $[f/f_n]$ |
| 50 % | 0,277 | 0,287 | 0,287 | 0,297 | 0,277 | 0,353 | $[f/f_n]$ |
| 60 % | 0,257 | 0,277 | 0,287 | 0,297 | 0,307 | 0,086 | $[f/f_n]$ |
| 70 % | 0,247 | 0,272 | 0,272 | 0,287 | 0,307 | 0,091 | $[f/f_n]$ |
| 80 % | 0,262 | 0,272 | -‡ | -‡ | -‡ | -‡ | $[f/f_n]$ |
| 90 % | 0,272 | 0,262 | -‡ | -‡ | -‡ | -‡ | $[f/f_n]$ |
| 100 % | 0,529 | 0,212 | -‡ | -‡ | -‡ | -‡ | $[f/f_n]$ |

Table J.3: Dominating frequencies in the draft tube, 180°

When looking at the effect of injecting air, calculating a Δp was done through the Histogram method, where a 99% confidence interval was used for all the pressure values to find the upper and lower limits.

In the end, injecting ~ 277 l/s reduced the Δp by about 30% looking at the pressure measured at 0°. Looking at the measurement at 180°, the Δp was reduced by nearly 57%. The exact cause of this discrepancy is not known, as the measurements were done by the operator of the power plant by themselves. All that can be concluded is that the reduction lies somewhere in the region between 30% and 57%. The relative drop in measured Δp was fairly linear, and the test with a naturally aspirating turbine showed nearly no reduction in pulsations. This indicates that the necessary air flow rate probably is at least $\sim 2,5\%$ of the design discharge of the turbine. The probable cause of the pulsations is the Rheingan's frequency, as the dominating frequency tables indicates. The other prominent frequency, $16f_n$, that appears in several cases is probably the wake of the runner blades, as the runner at Santa Rosa has 16 blades.

‡No measurements were done at this point.

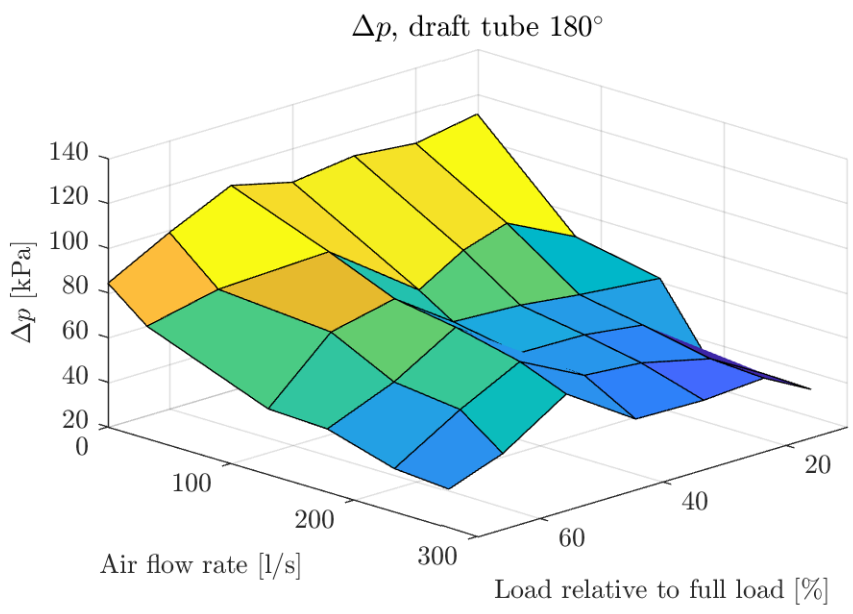
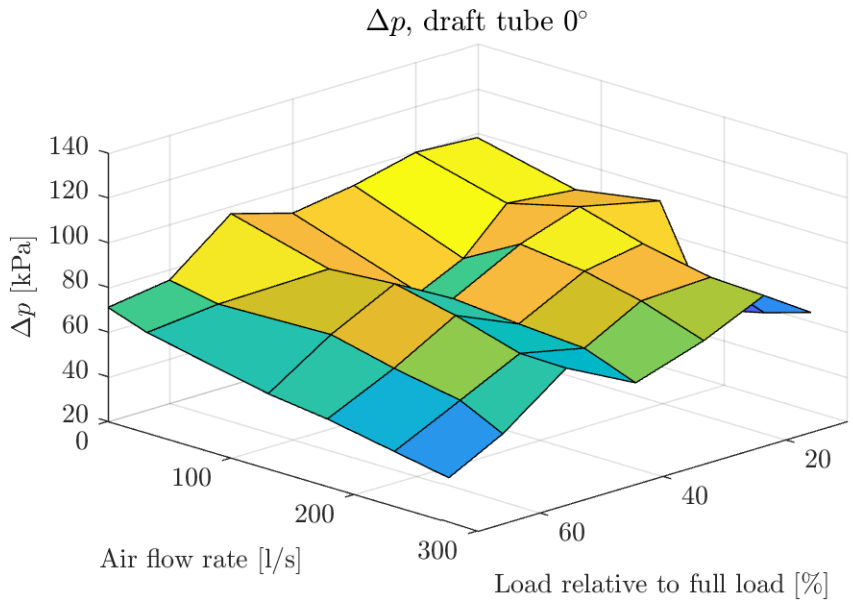


Figure J.3: Calculated Δp in the draft tube

Conclusion

The turbine at Santa Rosa II seems to struggle with pressure pulsations at part load stemming from the swirling flow in the draft tube, oscillating at $\sim 1/3$ of the runner frequency. Injecting air shows promising results, as the pressure amplitude is reduced by 30% to 57%.

Further work at this point could consist of trying to identify the cause of the discrepancy between the two draft tube sensors and the measured pulsation reduction. This could be as simple as the placement of the sensors on the draft tube relative to the 90° bend on the pipe, to some unidentified flow phenomena. Additionally, more tests with more air could be done until an acceptable level of Δp reduction is achieved.

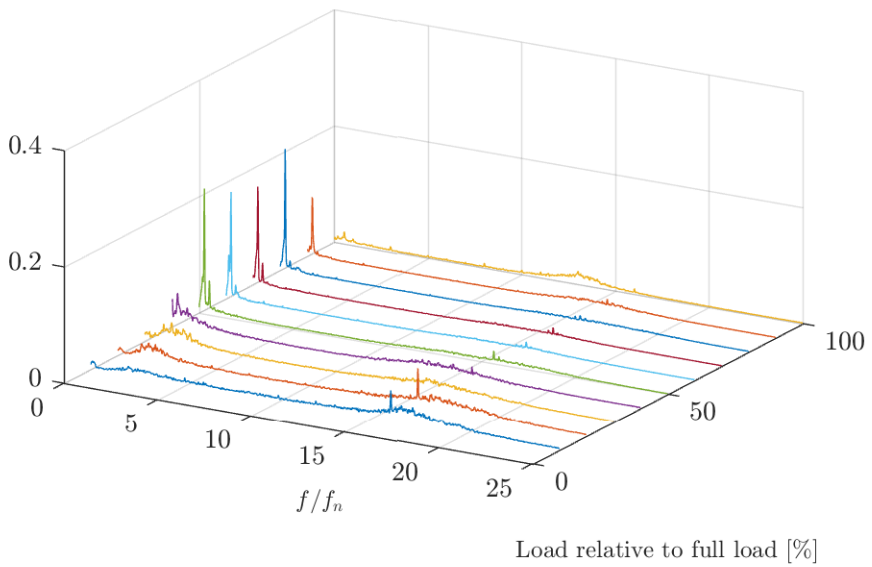
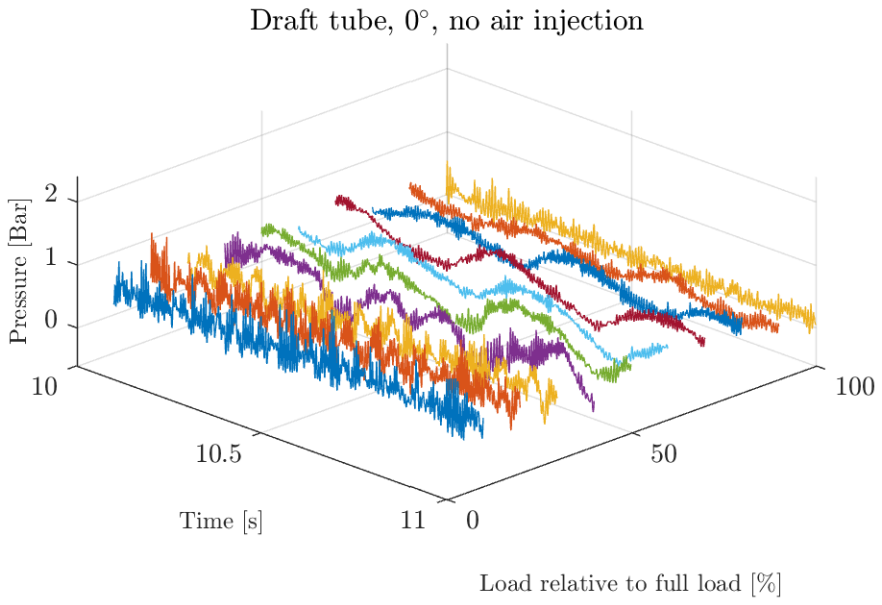


Figure J.4: Measured pressure and FFT analysis, no air injection

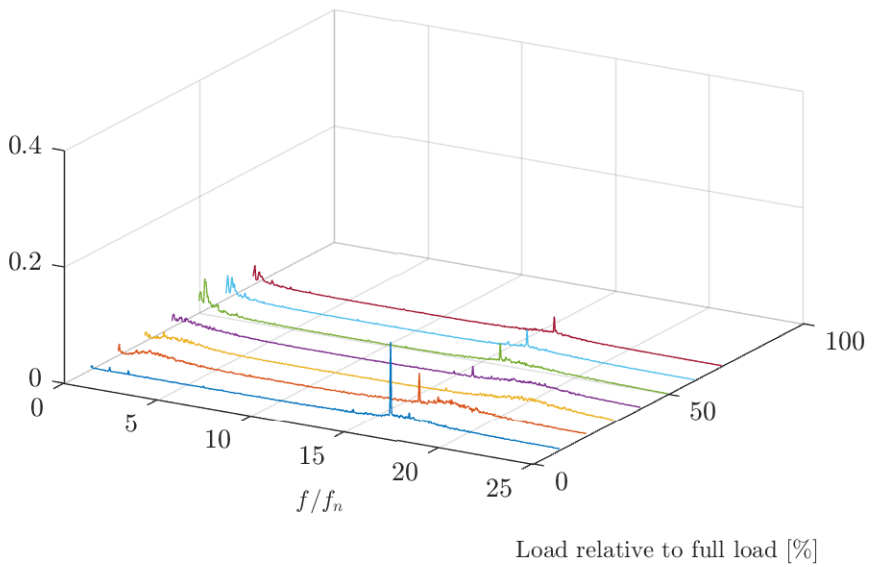
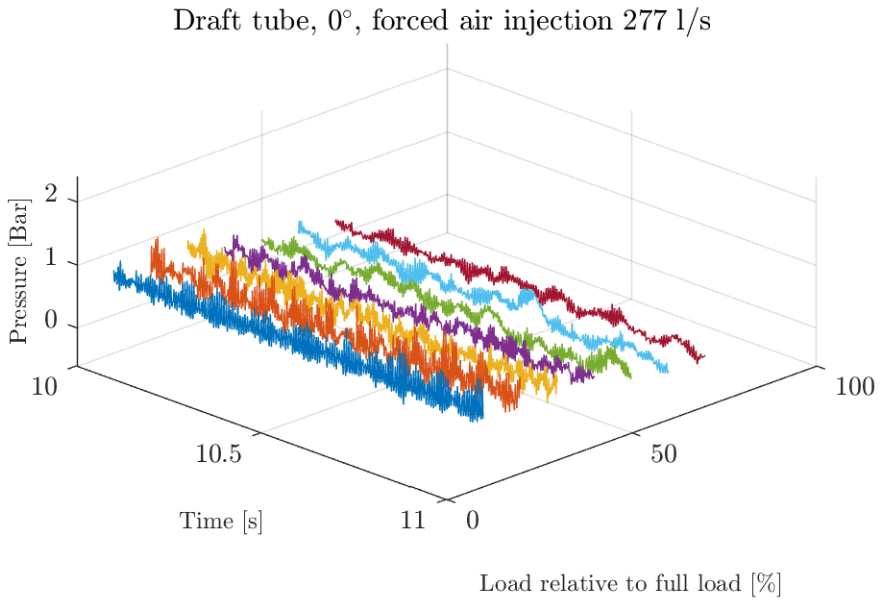


Figure J.5: Measured pressure and FFT analysis, ~ 277 l/s of air injection

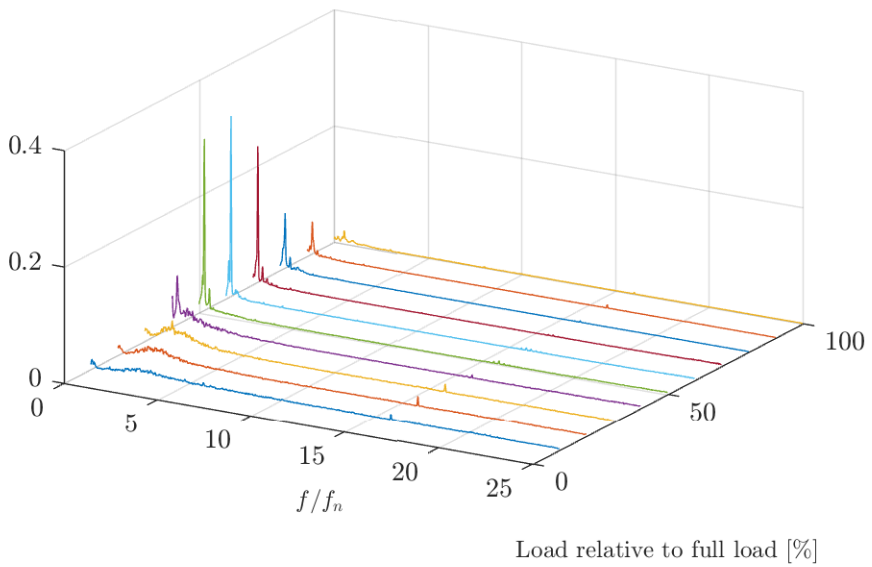
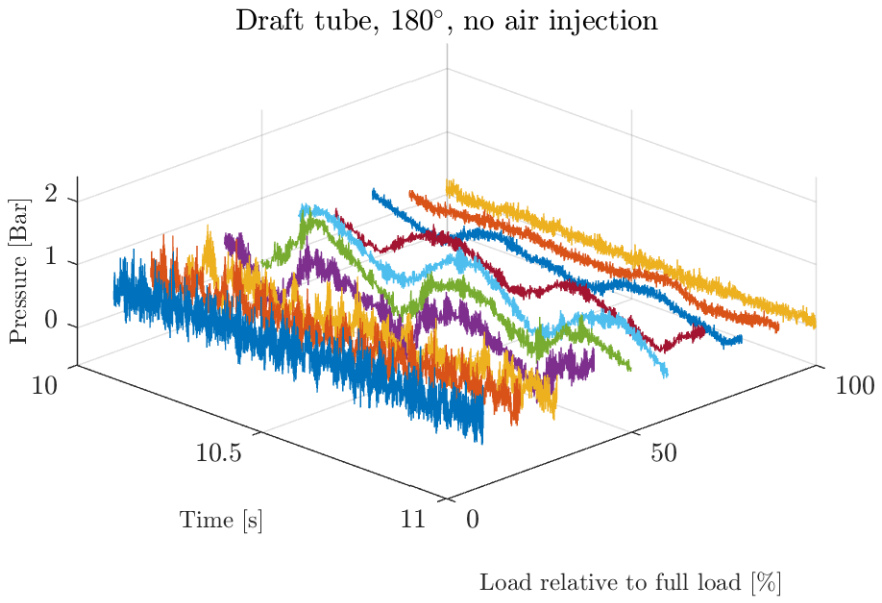


Figure J.6: Measured pressure and FFT analysis, no air injection

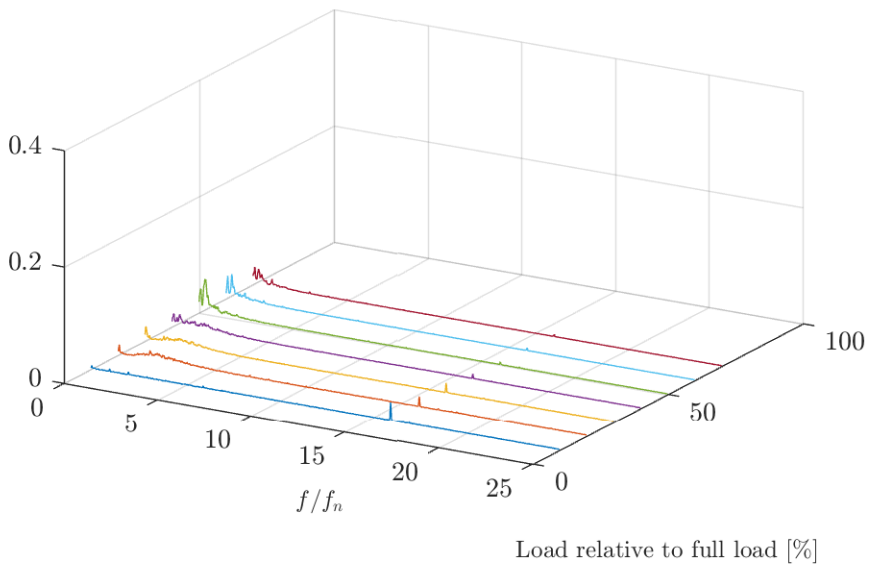
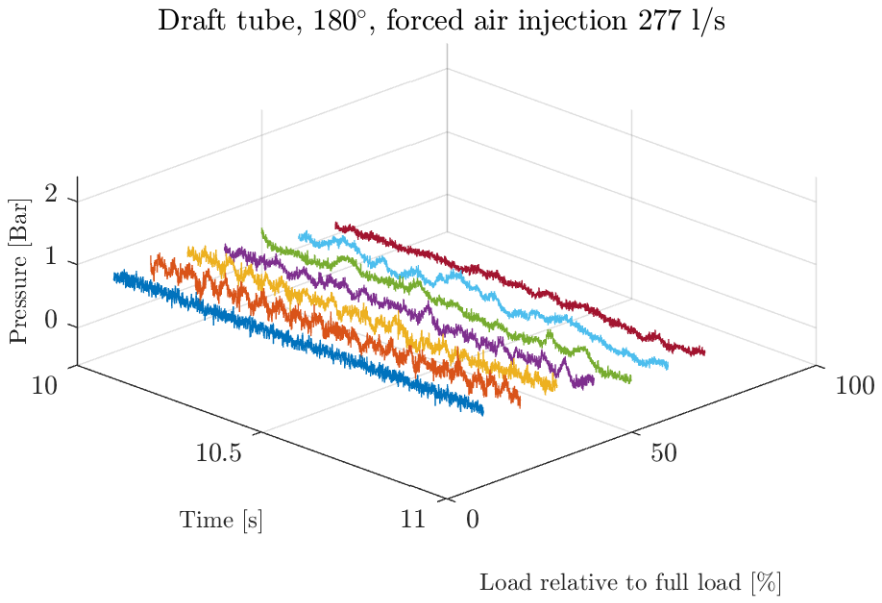


Figure J.7: Measured pressure and FFT analysis, ~ 277 l/s of air injection

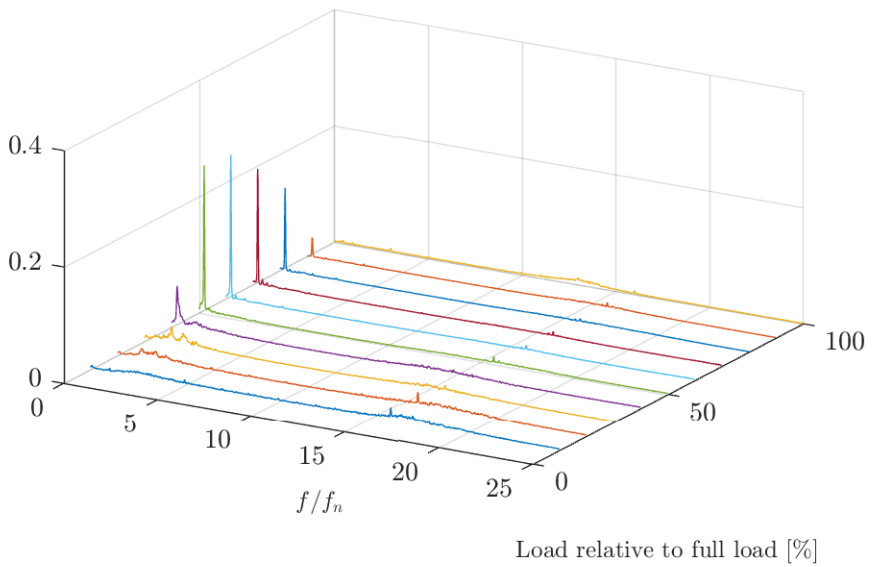
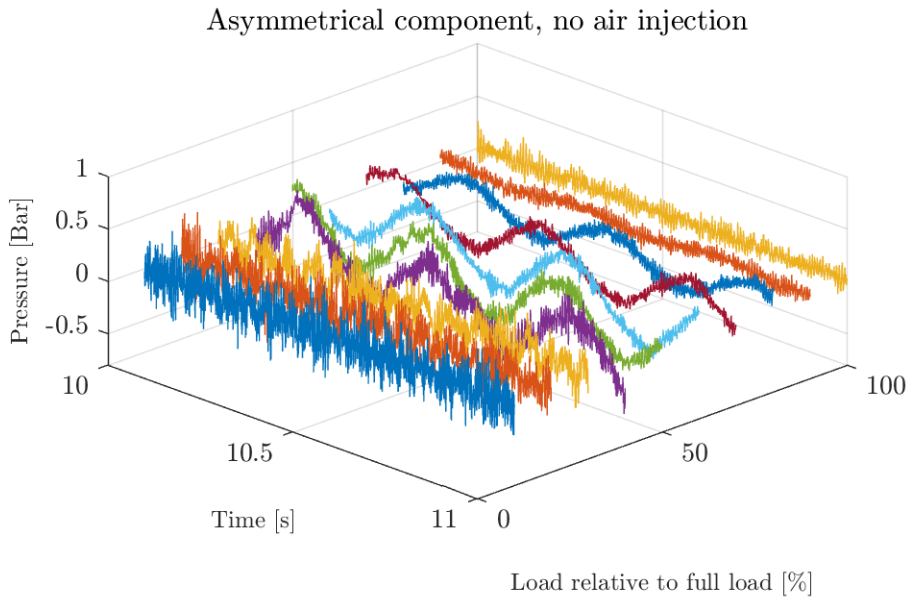


Figure J.8: Asymmetrical component of the draft tube pulsation

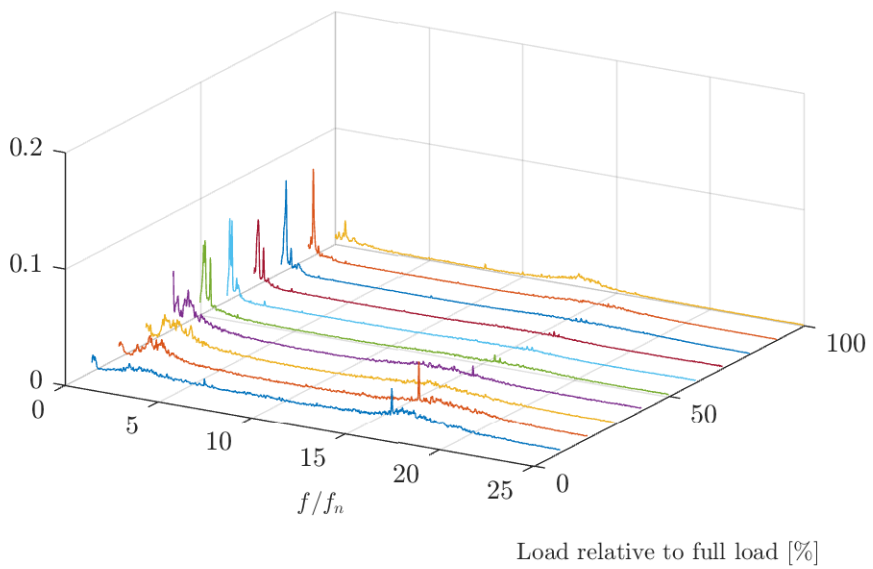
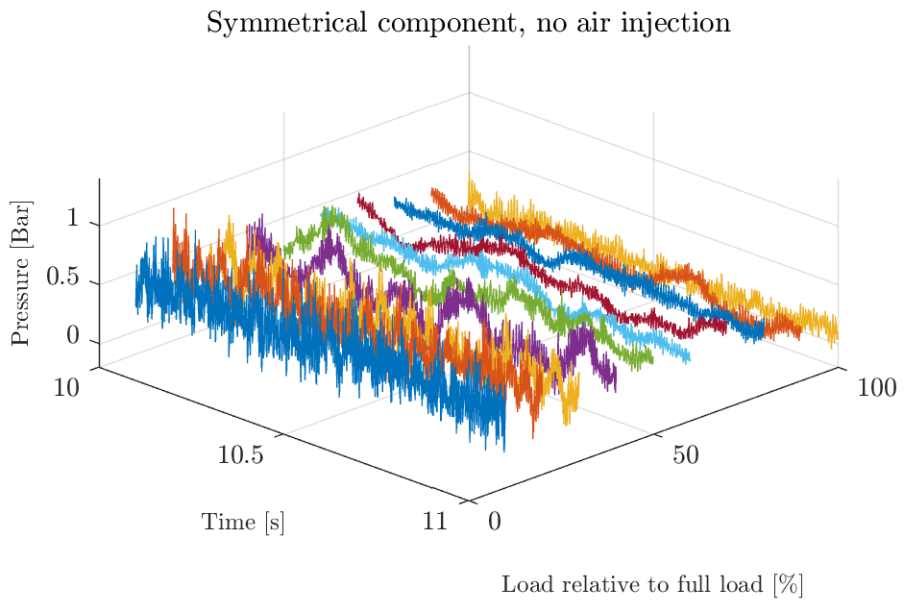


Figure J.9: Symmetrical component of the draft tube pulsation

APPENDIX **K** _____
_____ TECHNICAL REPORT YLJA

Technical report of hydraulic efficiency measurements at Ylja power plant.

Technical report

NTNU
Norwegian University of
Science and Technology
Faculty of Engineering
Department of Energy and Process Engineering

Vegard Ulvan

Hydraulic measurements

Ylja Power Plant

Trondheim, 06 2018



NTNU – Trondheim
Norwegian University of
Science and Technology

Summary

In early April 2018, hydraulic efficiency measurements were done at Ylja power plant. The power plant is owned by Oppland Energi and operated by Eidsiva Energi. This report is written as a part of the master thesis work done by Vegard Ulvan, Johannes Kverno, and Trine Brath, master students at the NTNU Waterpower Laboratory.

To find the hydraulic efficiency of the runner, the thermodynamic method was used. In the calculations both the power and flow are adjusted to nominal head ($H_n = 670$). The physical conditions at Ylja power plant were quite good as the temperatures were stable under all measurements. It was not possible to log the generator power from the regulator, which had to be read off the display, and could fluctuate at times. The measurements were done in accordance with the guidelines of IEC-60041 (1991).

In hindsight, an additional measurement should have been made with 1 needle to get a defined curve. Also, the other efficiency curves should have been measured so that they would overlap more.

While the report from 2008 concludes that there has been a significant decrease in efficiency with 6 needles, this report will suggest that there is no basis for this claim.

Table of Contents

| | |
|---|-----------|
| Summary | 2 |
| List of Tables | 5 |
| List of Figures | 6 |
| 1 Introduction | 7 |
| 1.1 Parties involved | 7 |
| 1.2 Measuring period | 7 |
| 1.3 Basic data about Ylja power plant | 7 |
| 2 Thermodynamic method theory | 8 |
| 3 Measuring equipment | 9 |
| 4 Method | 10 |
| 4.1 Data handling | 10 |
| 4.2 Thermodynamic method | 10 |
| 5 Results | 15 |
| 6 Discussion | 19 |
| 6.1 Efficiency | 19 |
| 6.2 Uncertainty | 20 |
| 6.3 Sources of error | 20 |
| 6.3.1 Distance from runner | 20 |
| 6.3.2 Temperature distribution | 20 |
| 6.3.3 Generator power | 20 |
| 6.3.4 Relative height outlet | 20 |
| 6.3.5 Regulator restraints | 20 |
| 6.4 Other conditions | 20 |
| Bibliography | 20 |
| Appendix | 21 |
| A Example calculation efficiency | A1 |

| | | |
|----------|--|-----------|
| B | Basis for uncertainty calculations | B1 |
| B.1 | Specific mechanical energy | B2 |
| B.1.1 | Pressure term | B2 |
| B.1.2 | Thermal term | B3 |
| B.2 | Specific hydraulic energy | B3 |
| B.2.1 | Pressure term | B3 |
| B.2.2 | Potential term | B4 |
| B.2.3 | Kinetic term | B4 |
| B.3 | Uncertainty calculated for measurement 1 | B5 |
| C | Calculation spreadsheet | C1 |
| D | Calibration reports | D1 |

List of Tables

| | | |
|-----|--|----|
| 1.1 | Basic data | 7 |
| 3.1 | Equipment used at Ylja power plant | 9 |
| 5.1 | Main results in tabular form | 15 |
| A.1 | Measurement 1 values | A1 |
| B.1 | Uncertainties of different factors | B1 |
| B.2 | Values uncertainty measurement 1 | B5 |

List of Figures

| | | |
|-----|---|----|
| 3.1 | Setup for measuring pressure | 9 |
| 4.1 | Setup for the thermodynamic method at Ylja | 12 |
| 4.2 | Probe on inlet, SBE38 black wire, Digiquartz white wire | 13 |
| 4.3 | Digiquartz for p_1 | 14 |
| 4.4 | Three measuring pipes in outlet | 14 |
| 5.1 | Efficiency measurement, all needle combinations | 16 |
| 5.2 | Efficiency measurement, 6 needles | 17 |
| 5.3 | Efficiency measurements comparison | 18 |

Chapter 1

Introduction

1.1 Parties involved

This report is written for Eidsiva Energi, who operates Ylja power plant on behalf of the owner, Oppland Energi. On site, Nils Olav Dalåker represented Eidsiva Energi, and from NTNU were master students Vegard UIvan and Trine Brath. Bjørnar Svingen from Rainpower/NTNU was also present for the measurements.

1.2 Measuring period

The equipment for the measurements were set up on Tuesday 10.04.2018, and the measurements were executed Wednesdays 11.04.2018 and Thursday 12.04.2018.

1.3 Basic data about Ylja power plant

| | |
|----------------------|---------|
| Turbine | Pelton |
| Manufacturer | Kværner |
| Installed power [MW] | 65 |
| Head [m] | 670 |
| Flow [m^3/s] | 12 |
| RPM [rev/min] | 600 |
| Commisioned | 1973 |
| z_1 [mas] | 517,5 |
| z_{1-1} [mas] | 518,475 |
| z_{2-1} [mas] | 513,4 |
| Δz_1 [m] | 0,695 |
| Δz_{1-1} [m] | 0 |
| z_{uf} [mas] | 519,4 |
| z_{lf} [mas] | 512,0 |
| D_1 [m] | 1,07 |
| g [m/s^2] | 9,81855 |
| w [m] | 3,25 |

Table 1.1: Basic data

Chapter 2

Thermodynamic method theory

The thermodynamic method is a technique for measuring hydraulic efficiency in pumps and turbines. It relies on the first law of thermodynamics, which states that energy is never lost, but turns into other forms of energy. (Kjølle, 2003)

In a hydro power plant, hydraulic energy in front of the turbine is converted into mechanical energy. However, not all of the hydraulic energy is converted into mechanical energy, i.e. there are losses through the system. These energy losses are not gone, but have turned into thermal energy in the water itself. This means that the losses in a turbine can be accounted for by the change of temperature in the water running through it, or more accurately the change in enthalpy. This is the essence of the thermodynamic method, and is a well-known method for measuring turbine efficiency.

The general equation for calculating the hydraulic efficiency is found by dividing the specific mechanic by the specific hydraulic energy

$$\eta_h = \frac{E_m}{E_h} [-] \quad (2.1)$$

The mechanic and hydraulic energy are found by exploring the energy in the inlet and outlet, in regards to pressure, velocity, height, and, for the mechanic energy, temperature.

$$E_h = \frac{1}{\rho}(p_1 - p_2) + g(z_1 - z_2) + \frac{1}{2}(c_1^2 - c_2^2) \text{ [J/kg]} \quad (2.2)$$

$$E_m = \bar{a}(p_{1-1} - p_{2-1}) + g(z_{1-1} - z_{2-1}) + \frac{1}{2}(c_{1-1}^2 - c_{2-1}^2) + \bar{c}_p(T_{1-1} - T_{2-1}) \text{ [J/kg]} \quad (2.3)$$

By using this method, the need to measure discharge is completely eliminated, as the mechanic energy is a function of discharge itself

$$E_m = \frac{P_t}{\rho Q} \text{ [J/kg]} \quad (2.4)$$

P_t can be found by measuring the generator power, and dividing with the generator efficiency. (Kjølle, 2003)

Chapter 3

Measuring equipment

| Measuring Equipment | Quantity | Usage |
|----------------------------|----------|---------------------------|
| SBE 38 Digital Thermometer | 4 | Temperature inlet/outlet |
| Custom suitcase PC | 1 | ADC & logging temperature |
| Paroscientific Digiquartz | 2 | Pressure inlet/probe |
| Custom ADC suitcase | 1 | ADC pressure |
| GE Druck UNIK-5000 5 bar a | 1 | Atmospheric pressure |
| NI-USB 6211 I/O device | 1 | ADC |
| Leica DISTO Laser | 1 | Underwater height |
| Measuring rope | 1 | Underwater height |

Table 3.1: Equipment used at Ylja power plant



Figure 3.1: Setup for measuring pressure

Chapter 4

Method

4.1 Data handling

NTNUs standard measurement software was used to acquire, visualise, and log data on site. The logged data was used in a spreadsheet that automatically calculated the hydraulic efficiency, its uncertainty, and more.

4.2 Thermodynamic method

Although there are a lot of parameters that can be measured directly in regards to eq. 2.2 and 2.3, it is often difficult and not necessary. The pressures in the outlet were estimated by measuring the water column height and atmospheric pressure

$$p_2 = \frac{\bar{\rho}gh_2}{1000} + p_{atm} \text{ [kPa]} \quad (4.1)$$

$$p_{2-1} = \frac{\bar{\rho}gh_{2-1}}{1000} + p_{atm} \text{ [kPa]} \quad (4.2)$$

The velocity in the probe, c_{1-1} , is included in the measured pressure on the probe, p_{1-1} , as the probe stagnates the flow before the pressure transducer.

The kinetic energy due to the velocity before the temperature sensors in the outlet, c_{2-1} , is assumed included in 4.2.

The overall velocity in the inlet and outlet can be found by using continuity, as we know the volume flow Q and the areas A_1 and A_2

$$c_1 = \frac{Q}{A_1} \text{ [m/s]} \quad (4.3)$$

$$c_2 = Q/A_2 \text{ [m/s]} \quad (4.4)$$

What was measured directly at Ylja power plant was p_1 , p_{1-1} , p_{atm} , T_{1-1} , T_{2-1} , and h .

Generator power

Then regulator at Ylja Power Plant had a regulator that showed the generator power on a display, real-time. However, as this value fluctuated, a logging of the generator power was planned. It turned out that the signal from the regulator was not as expected, and the brought equipment could not be used. The values were therefore written down manually.

Probe and inlet

In order to measure the inlet temperature and corresponding pressure, T_{1-1} and p_{1-1} , water was extracted from the inlet before the spiral casing using a measuring probe. The probe was mounted on the inlet where a lid was prior. Then the temperature and pressure sensor was placed on the probe for measurements. To ensure a temperature that was not affected by the ambient temperature, the probe wrapped in an isolating material. From the probe lead a hose that went to a drain.

To measure the inlet pressure p_1 , a pressure sensor was connected to the outer wall of the inlet, on the top, on a tap with a valve. This was not at the same height as the center-line of the inlet, point 1, so the height-difference was measured and used in the calculations of the correct p_1 .

On the same floor p_{atm} was measured continuously for each point of operation.

Outlet

To measure the temperature in the draft tube outlet, T_{2-1} , 3 sensors were used. These were slid down three vertical pipes that were mounted in the outlet, 1,4 m from the bottom. The pipes were installed $\sim 2,5$ turbine runner lengths from the runner itself. The pipes are the same ones used in 1982 and 2008. The pipes had holes drilled in them, that allowed water to enter, be mixed, and led to the temperature sensors. The sensors heights were not adjusted for the thermodynamic measurements.

Above the draft tube outlet, a laser was used to measure the relative height to the water free surface for each point of operation. These relative heights h , together with different known heights in the power plant, were used to find the different pressures in the outlet.

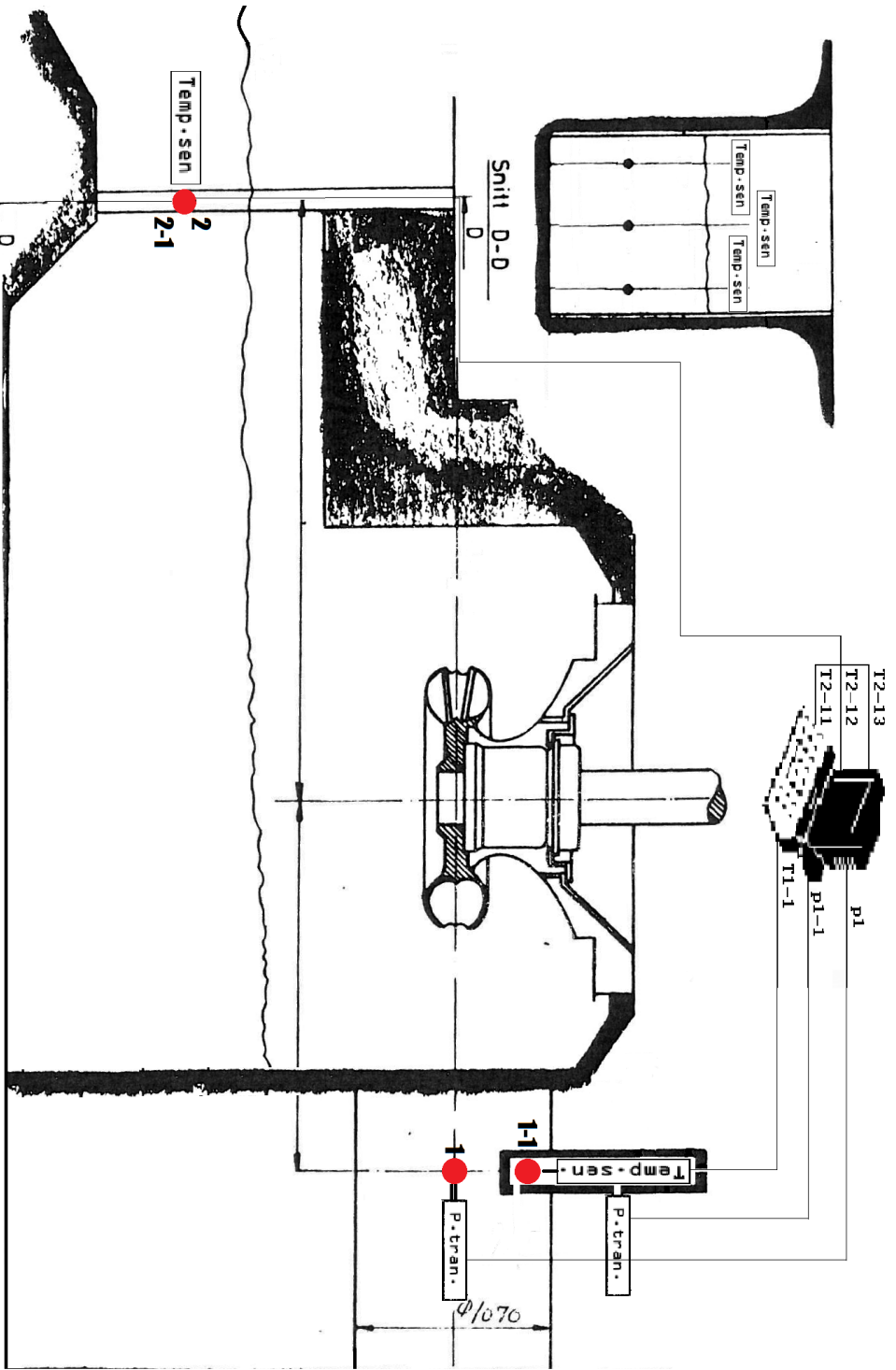


Figure 4.1: Setup for the thermodynamic method at Ylja



Figure 4.2: Probe on inlet, SBE38 black wire, Digiquartz white wire



Figure 4.3: Digiquartz for p_1



Figure 4.4: Three measuring pipes in outlet

Chapter 5

Results

| Needles # | η_h [-] | e_{η_h} [-] | P_t [MW] | Q [m^3/s] | e_Q [m^3/s] |
|-----------|--------------|------------------|------------|---------------|-------------------|
| 1 | 0,852 | 0,0059 | 4,42 | 0,79 | 0,008 |
| 1 | 0,875 | 0,0061 | 8,12 | 1,41 | 0,014 |
| 1 | 0,899 | 0,0062 | 10,59 | 1,78 | 0,018 |
| 2 | 0,898 | 0,0062 | 14,59 | 2,46 | 0,024 |
| 2 | 0,901 | 0,0062 | 16,75 | 2,82 | 0,028 |
| 2 | 0,898 | 0,0062 | 20,78 | 3,50 | 0,034 |
| 3 | 0,903 | 0,0062 | 18,55 | 3,11 | 0,030 |
| 3 | 0,907 | 0,0062 | 23,10 | 3,86 | 0,038 |
| 3 | 0,907 | 0,0062 | 29,74 | 4,97 | 0,049 |
| 4 | 0,901 | 0,0062 | 24,71 | 4,15 | 0,041 |
| 4 | 0,903 | 0,0062 | 28,88 | 4,85 | 0,047 |
| 4 | 0,904 | 0,0062 | 33,57 | 5,62 | 0,055 |
| 4 | 0,901 | 0,0062 | 38,00 | 6,39 | 0,062 |
| 6 | 0,900 | 0,0062 | 35,18 | 5,92 | 0,058 |
| 6 | 0,900 | 0,0062 | 40,92 | 6,88 | 0,067 |
| 6 | 0,901 | 0,0062 | 41,46 | 6,97 | 0,068 |
| 6 | 0,900 | 0,0062 | 47,72 | 8,03 | 0,078 |
| 6 | 0,897 | 0,0062 | 52,39 | 8,85 | 0,086 |
| 6 | 0,892 | 0,0062 | 58,29 | 9,89 | 0,096 |
| 6 | 0,887 | 0,0061 | 63,27 | 10,80 | 0,105 |
| 6 | 0,882 | 0,0061 | 67,66 | 11,62 | 0,112 |

Table 5.1: Main results in tabular form

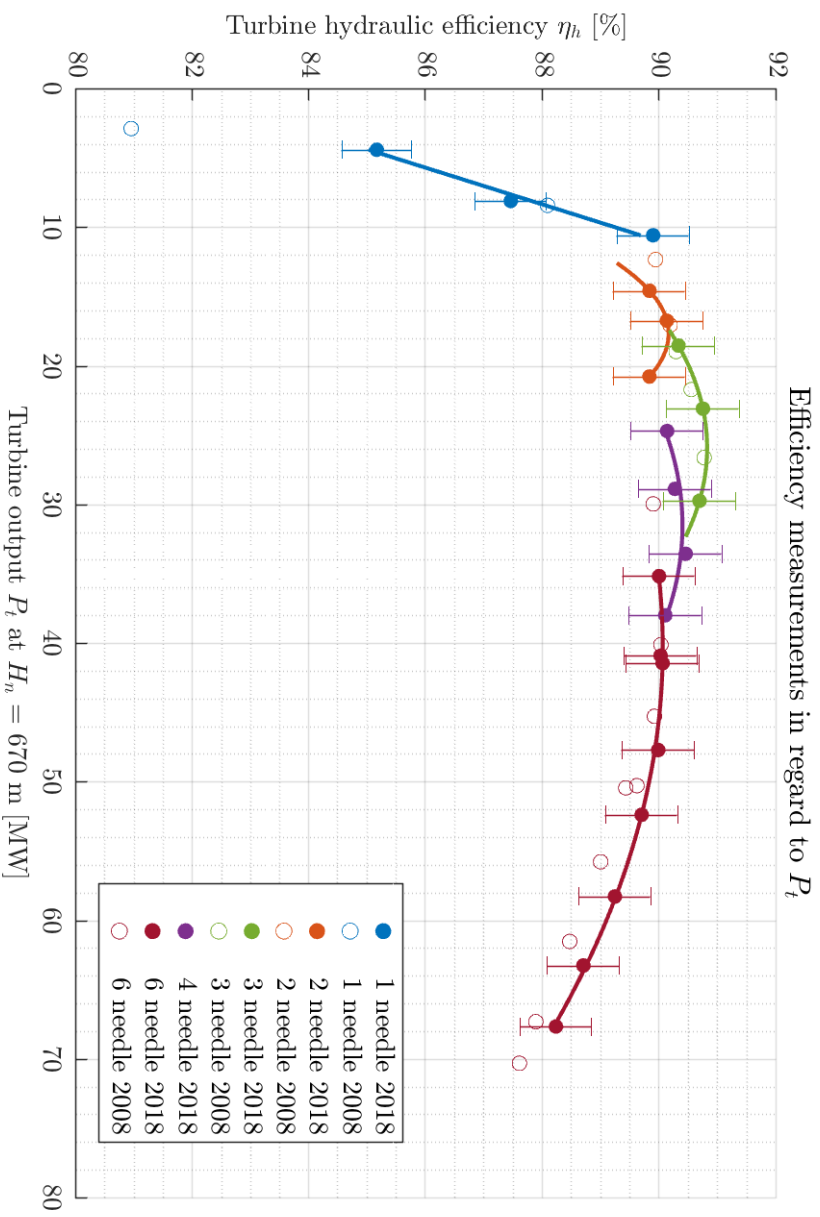


Figure 5.1: Efficiency measurement, all needle combinations

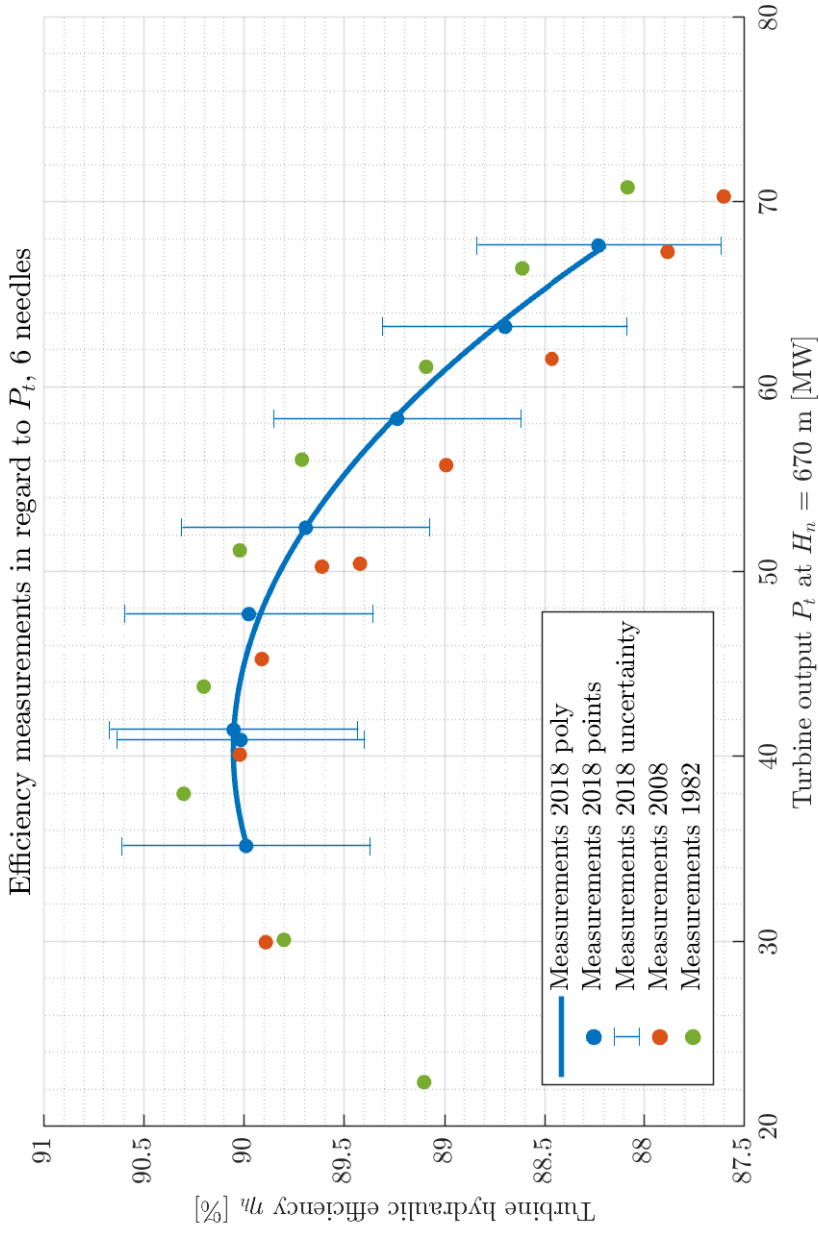


Figure 5.2: Efficiency measurement, 6 needles

Earlier efficiency measurements in regard to P_t , 6 needles

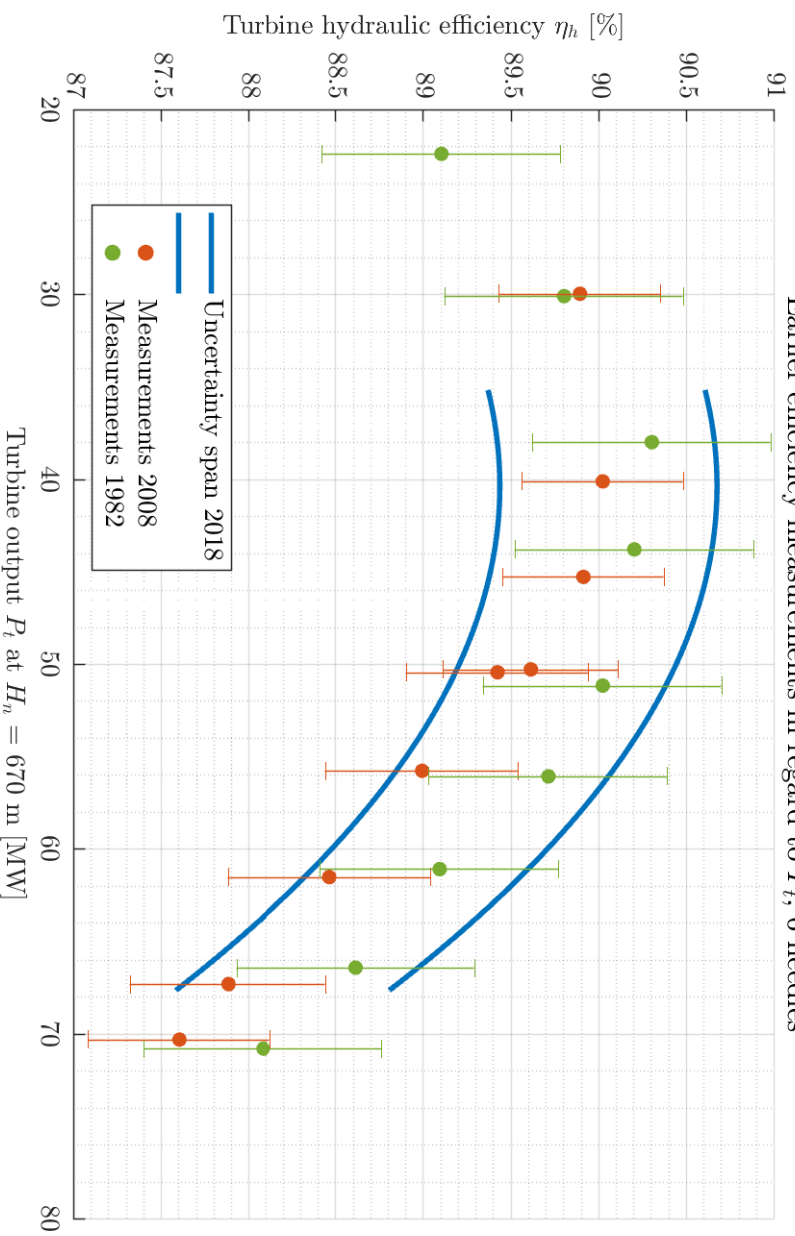


Figure 5.3: Efficiency measurements comparison

Chapter 6

Discussion

6.1 Efficiency

In the previous efficiency measurement, E-CO claimed a drop in efficiency with 6 needles (Lundekvam, 2008). When comparing their measurements with Kværners measurements from 1985 (Bøkkø, 1982), their uncertainties overlap, which can be seen in 5.3. This means one can't say anything for sure about a drop in efficiency.

Measurements in this report show a trend line with 6 needles that matches more with Kværners measurements than E-COs, as seen in 5.2. By the looks of it, E-COs trendline seems to "change course" after the repetition point, making it go lower. Plotting the outer uncertainty lines from the measurements, in fig. 5.3, show how all the measurements previously made is well within this boundary. This measurements repetition point, with 6 needles, overlap nicely. This helps to validate the measurements done.

If one takes a look at the raw data for the temperature in E-COs report from 2008, one can see that they have registered 9 different temperature differences in the outlet, however they are not explicit in how they handle these numbers. According to page 66. in E-COs report they use the mean of the values to find the hydraulic efficiency, which means the 9 temperatures are weighted equally. In a Pelton turbine, the water exiting the buckets goes on top of the exiting flow, and does not immediately interact with the bottom of the flow. As the measurements takes place only 2,5 runner diameters downstream from the runner, there might not have be enough interaction in the flow to get a sensible temperature at the bottom. So an equal weighting of all the temperature might give a misrepresented picture of the temperature in total. This might be the reason for E-COs "skewed" hydraulic efficiency with 6 needles. Their repetition point also drops significantly, for what it is worth.

For the first time, efficiency measurements were done on 4 needles. A rough read-off shows that between 33 to 38 MW turbine output, 4 needles would be to prefer over 3 and 6 needles, as this gives a higher efficiency. Calculations should be made if upgrading the system to run on 4 needles would be profitable.

6.2 Uncertainty

To find the uncertainty, a comprehensive statistical analysis was made for each point of operation. Additional uncertainties were added in compliance with IEC. The uncertainties for the efficiencies were of the magnitude $\pm 0,6 \%$. Example calculations can be found in app. A.

6.3 Sources of error

6.3.1 Distance from runner

The measurements in the outlet were done $\sim 2,5$ turbine runner lengths from the runner itself. The guidelines (IEC-60041, 1991) insists that the length should be somewhere between 4 - 10 runner lengths. This is to achieve adequate mixing.

6.3.2 Temperature distribution

For more accurate results, temperature at the bottom and top should have been included. But as the equipment for measuring velocity in the outlet broke down, the velocity profile is not known, making it difficult to know how to weight the different temperatures. The fact that the measurements in the outlet were done too close to the runner itself, only worsens the dilemma.

6.3.3 Generator power

The generator power could not be logged and could at times fluctuate a lot. It had to be written down by hand several times, and the mean was calculated. This makes the value less accurate than it could be.

6.3.4 Relative height outlet

A lot of foam when running 4 and 6 needles made it difficult to accurately measure the distance down to the free surface.

6.3.5 Regulator restraints

Eidsiva did not allow for a turning off of the frequency regulator, but only an increase in the static to 20 %. This might have had an effect on the preferred steady-state operation.

6.4 Other conditions

No faults were found when inspecting the runner and needles. It is assumed that there are little to no loss in the bearings.

Bibliography

Bøkko, E., 1982. Virkningsgradsmaalinger. Tech. rep., Kvaerner Brug as.

IEC-60041, 1991. Field acceptance tests to determine the hydraulic performance of hydraulic turbines, storage pumps and pump-turbines. 60041 3.

Kjølle, A., 2003. Hydraulisk måleteknikk. Grunnleggende prinsipper og målemetoder 2.

Lundekvam, A., 2008. Hydrauliske målinger ylja kraftverk. Tech. rep., E-CO Vannkraft as.

Appendix A

Example calculation efficiency

| Measurement 1 | Ylja |
|--------------------------|---------|
| $\Delta T [C^\circ]$ | -0,1647 |
| $p'_1 [\text{kPa}]$ | 6628,9 |
| $p'_{1-1} [\text{kPa}]$ | 6653,6 |
| $p_{atm} [\text{kPa}]$ | 96,3 |
| $P_g [\text{MW}]$ | 28,8 |
| $h [\text{m}]$ | 4,36 |
| $e_{p1} [\text{kPa}]$ | 1,26 |
| $e_{p11} [\text{kPa}]$ | 1,92 |
| $e_{patm} [\text{kPa}]$ | 0,01 |
| $e_{\Delta T} [C^\circ]$ | 0,001 |

Table A.1: Measurement 1 values

$$h_{2-1} = z_{uf} - z_{2-1} - h = 1,6410 [m] \quad (\text{A.1})$$

$$p'_{1-1} = p_{1-1} + \frac{\bar{\rho}g\Delta z_{1-1}}{1000} = 6653,6 [kPa] \quad (\text{A.2})$$

$$p_{2-1} = \frac{\bar{\rho}gh_{2-1}}{1000} + p_{atm} = 112,4 [kPa] \quad (\text{A.3})$$

$$E_{m,p} = \bar{a}(p'_{1-1} - p_{2-1}) = 6596,8 [J/kg] \quad (\text{A.4})$$

$$E_{m,T} = \bar{c}_p(T_{1-1} - T_{2-1}) = -690,1 [J/kg] \quad (\text{A.5})$$

$$E_{m,pot} = g(z_{1-1} - z_{2-1}) = 49,8 [J/kg] \quad (\text{A.6})$$

$$E_{m,kin} = \frac{1}{2}(c_{1-1}^2 - c_{2-1}^2) = 0 [J/kg] \quad (\text{A.7})$$

$$E_m = E_{m,p} + E_{m,T} + E_{m,pot} + E_{m,kin} = 5956,4 [J/kg] \quad (\text{A.8})$$

$$Q = \frac{P_g/\eta_g}{\bar{\rho}E_m} = 4,96 [m^3/s] \quad (\text{A.9})$$

$$h_2 = z_{uf} - z_{lf} - \frac{3}{2}h = 1,5205 [m] \quad (\text{A.10})$$

$$p'_1 = p_1 + \frac{\bar{\rho}g\Delta z_1}{1000} = 6635,7 [kPa] \quad (\text{A.11})$$

$$p_2 = \frac{\bar{\rho}gh_2}{1000} + p_{atm} = 111,2 [kPa] \quad (\text{A.12})$$

$$E_{h,p} = \bar{a}(p'_1 - p_2) = 6514,4 [J/kg] \quad (\text{A.13})$$

$$E_{h,pot} = g(z_1 - z_2) = 39,1 [J/kg] \quad (\text{A.14})$$

$$l_y = z_{uf} - z_{lf} - h = 3,04 [m] \quad (\text{A.15})$$

$$A_2 = l_y w = 10,64 [m^2] \quad (\text{A.16})$$

$$c_1 = Q/A_1 = \frac{4Q}{\pi D_1^2} = 5,51 [m/s] \quad (\text{A.17})$$

$$c_2 = Q/A_2 = 0,50 [m/s] \quad (\text{A.18})$$

$$E_{h,kin} = \frac{1}{2}(c_1^2 - c_2^2) = 15,1 [J/kg] \quad (\text{A.19})$$

$$E_h = E_{h,p} + E_{h,pot} + E_{h,kin} = 6568,6 [J/kg] \quad (\text{A.20})$$

$$\eta_h = \frac{E_m}{E_h} = 0,9068 \quad (\text{A.21})$$

Appendix B

Basis for uncertainty calculations

The hydraulic efficiency is found by dividing the specific mechanical energy by the specific hydraulic energy. To find its total uncertainty, it is easiest to split the equation into smaller and smaller parts, find their uncertainty, and make use of the RSS-method.

$$\eta_h = \frac{E_m}{E_h} \quad (\text{B.1})$$

$$f_{\eta_h} = \frac{e_{\eta_h}}{\eta_h} = \pm \sqrt{f_{E_m}^2 + f_{E_h}^2} = \pm \sqrt{\left(\frac{e_{E_m}}{E_m}\right)^2 + \left(\frac{e_{E_h}}{E_h}\right)^2} \quad (\text{B.2})$$

| Factor | e | f | Comment |
|----------------------|--------------------------|-------|----------------------|
| ρ_{table} | - | 0,1 % | IEC |
| a_{table} | - | 0,2 % | IEC |
| $c_{p_{table}}$ | - | 0,5 % | IEC |
| P_{gen} | - | 0,7 % | IEC |
| E_{10} | - | 0,2 % | IEC |
| E_{20} | - | 0,6 % | IEC |
| z | 0,1 [m] | - | assumed |
| Δz | 0,01 [m] | - | mm-ruler |
| ΔT | 0,001 [C°] | - | IEC |
| h | 0,1 [m] | - | assumed, lot of foam |
| D_{probe} | 0,001 [m] | - | mm-ruler |
| D_1 | 0,01 [m] | - | assumed |
| w | 0,1 [m] | - | assumed |
| ρ_{temp} | 0 | - | low variation in T |
| a_{temp} | 0 | - | low variation in T |
| $c_{p_{temp}}$ | 0 | - | low variation in T |
| g | 0 | - | IEC |
| η_{gen} | 0 | - | assumed |
| $e_{h_2}/e_{h_{21}}$ | 0,1732 [m] | - | eq. B.3 |
| e_l | 0,1732 [m] | - | eq. B.4 |
| $e_{\Delta z}$ [m] | 0,1414 | - | eq. B.5 |
| e_{A_1} | 0,0168 [m ²] | - | eq. B.6 |
| e_{A_2} | (varies w/ h) | - | eq. B.7 |

Table B.1: Uncertainties of different factors

$$e_{h_2} = e_{h_{21}} = \sqrt{2 e_z^2 + e_h^2} \quad (\text{B.3})$$

$$e_l = \sqrt{2 e_z^2 + e_h^2} \quad (\text{B.4})$$

$$e_{zdiff} = \sqrt{2 e_z^2} \quad (\text{B.5})$$

$$e_{A_1} = \sqrt{\left(\frac{\partial A_1}{\partial D_1} e_{D_1}\right)^2} = \frac{\pi}{2} D_1 e_{D_1} \quad (\text{B.6})$$

$$e_{A_2} = A_2 \sqrt{\left(\frac{e_w}{w}\right)^2 + \left(\frac{e_l}{l}\right)^2} \quad (\text{B.7})$$

B.1 Specific mechanical energy

$$E_m = E_{m,p} + E_{m,T} + E_{m,pot} + E_{m,kin} \quad (\text{B.8})$$

$$e_{E_m}^2 = e_{E_{m,p}}^2 + e_{E_{m,T}}^2 + e_{E_{m,pot}}^2 + e_{E_{m,kin}}^2 \quad (\text{B.9})$$

B.1.1 Pressure term

$$E_{m,p} = \bar{a}(p'_{1-1} - p_{2-1}) = \bar{a} \left(p_{1-1} + \frac{\bar{\rho}g\Delta z_{1-1}}{1000} - \frac{\bar{\rho}gh_{2-1}}{1000} - p_{atm} \right) \quad (\text{B.10})$$

$$E_{m,p} = f(\bar{a}, p_{1-1}, \bar{\rho}, \Delta z_{1-1}, h_{2-1}, p_{atm}) \quad (\text{B.11})$$

$$e_{E_{m,p},\bar{a}}^2 = \left(\left(p_{1-1} + \frac{\bar{\rho}g\Delta z_{1-1}}{1000} - \frac{\bar{\rho}gh_{2-1}}{1000} - p_{atm} \right) e_{\bar{a}} \right)^2 \quad (\text{B.12})$$

$$e_{E_{m,p},p_{1-1}}^2 = (\bar{a} e_{p_{1-1}})^2 \quad (\text{B.13})$$

$$e_{E_{m,p},\bar{\rho}}^2 = \left(\frac{g(\Delta z_{1-1} - h_{2-1})}{1000} e_{\bar{\rho}} \right)^2 \quad (\text{B.14})$$

$$e_{E_{m,p},\Delta z_{1-1}}^2 = \left(\frac{\bar{\rho}g}{1000} e_{\Delta z_{1-1}} \right)^2 \quad (\text{B.15})$$

$$e_{E_{m,p},h_{2-1}}^2 = \left(\frac{\bar{\rho}g}{1000} e_{h_{2-1}} \right)^2 \quad (\text{B.16})$$

$$e_{E_{m,p},p_{atm}}^2 = (\bar{a} e_{p_{atm}})^2 \quad (\text{B.17})$$

$$e_{E_{m,p}}^2 = e_{E_{m,p,\bar{a}}}^2 + e_{E_{m,p,p_{1-1}}}^2 + e_{E_{m,p,\bar{\rho}}}^2 + e_{E_{m,p,\Delta z_{1-1}}}^2 + e_{E_{m,p,h_{2-1}}}^2 + e_{E_{m,p,p_{atm}}}^2 \quad (\text{B.18})$$

B.1.2 Thermal term

$$E_{m,T} = \bar{c}_p (T_{1-1} - T_{2-1}) \quad (\text{B.19})$$

$$E_{m,T} = f(\bar{c}_p, T_{1-1} - T_{2-1}) \quad (\text{B.20})$$

$$e_{E_{m,T,c_p}}^2 = (T_{1-1} - T_{2-1}) e_{\bar{c}_p} \quad (\text{B.21})$$

$$e_{E_{m,T,\Delta T}}^2 = \bar{c}_p e_{\Delta T} \quad (\text{B.22})$$

$$e_{E_{m,T}}^2 = e_{E_{m,T,c_p}}^2 + e_{E_{m,T,\Delta T}}^2 + e_{E_{10}}^2 + e_{E_{20}}^2 \quad (\text{B.23})$$

Potential term

$$E_{m,pot} = g(z_{1-1} - z_{2-1}) \quad (\text{B.24})$$

$$E_{m,pot} = f(z_{1-1} - z_{2-1}) \quad (\text{B.25})$$

$$e_{E_{m,pot}}^2 = e_{E_{m,pot,\Delta z}}^2 = g e_{\Delta z} \quad (\text{B.26})$$

B.2 Specific hydraulic energy

$$E_h = E_{h,p} + E_{h,pot} + E_{h,kin} \quad (\text{B.27})$$

$$e_{E_h}^2 = e_{E_{h,p}}^2 + e_{E_{h,pot}}^2 + e_{E_{h,kin}}^2 \quad (\text{B.28})$$

B.2.1 Pressure term

$$E_{h,p} = \frac{p'_1 - p_2}{\bar{\rho}} = \frac{1}{\bar{\rho}} \left(p_1 + \frac{\bar{\rho}g\Delta z_1}{1000} - \frac{\bar{\rho}gh_2}{1000} - p_{atm} \right) \quad (\text{B.29})$$

$$E_{h,p} = f(\bar{\rho}, p_1, \Delta z_1, h_2, p_{atm}) \quad (\text{B.30})$$

$$e_{E_{h,p,p_1}}^2 = \left(\frac{e_{p_1}}{\bar{\rho}} \right)^2 \quad (\text{B.31})$$

$$e_{E_{h,p,\bar{\rho}}}^2 = \left(\frac{p_1 - p_{atm}}{\bar{\rho}^2} e_{\bar{\rho}} \right)^2 \quad (\text{B.32})$$

$$e_{E_{h,p,\Delta z_1}}^2 = \left(\frac{\bar{\rho}g}{1000} e_{\Delta z_1} \right)^2 \quad (\text{B.33})$$

$$e_{E_{h,p,h_2}}^2 = \left(\frac{\bar{\rho}g}{1000} e_{h_2} \right)^2 \quad (\text{B.34})$$

$$e_{E_{h,p,p_{atm}}}^2 = \left(\frac{e_{p_{atm}}}{\bar{\rho}} \right)^2 \quad (\text{B.35})$$

$$e_{E_{h,p}}^2 = e_{E_{h,p,p_1}}^2 + e_{E_{m,p,\bar{\rho}}}^2 + e_{E_{h,p,\Delta z_1}}^2 + e_{E_{h,p,h_2}}^2 + e_{E_{h,p,p_{atm}}}^2 \quad (\text{B.36})$$

B.2.2 Potential term

$$E_{h,pot} = g(z_1 - z_2) \quad (\text{B.37})$$

$$E_{h,pot} = f(z_1 - z_2) \quad (\text{B.38})$$

$$e_{E_{h,pot}}^2 = e_{E_{h,pot,\Delta z}}^2 = g e_{\Delta z} \quad (\text{B.39})$$

B.2.3 Kinetic term

$$E_{h,kin} = \frac{1}{2}(c_1^2 - c_2^2) \quad (\text{B.40})$$

$$E_{h,kin} = f(c_1, c_2) \quad (\text{B.41})$$

$$c_1 = \frac{Q}{A_1} = \frac{4P_g}{\eta_g \bar{\rho} E_m \pi D_1^2} = f(P_g, \bar{\rho}, E_m, D_1) \quad (\text{B.42})$$

$$e_{c_1}^2 = \left(\frac{4e_{P_g}}{\eta_g \bar{\rho} E_m \pi D_1^2} \right)^2 + \left(\frac{4P_g e_{\bar{\rho}}}{\eta_g \bar{\rho}^2 E_m \pi D_1^2} \right)^2 + \left(\frac{4P_g e_{E_m}}{\eta_g \bar{\rho} E_m^2 \pi D_1^2} \right)^2 + \left(\frac{8P_g e_{D_1}}{\eta_g \bar{\rho} E_m \pi D_1^3} \right)^2 \quad (\text{B.43})$$

$$c_2 = c_{2-1} = Q/A_2 \quad (\text{B.44})$$

$$e_{c_2}^2 = e_{c_{2-1}}^2 \quad (\text{B.45})$$

$$e_{E_{h,kin}}^2 = (c_1 e_{c_1})^2 + (c_2 e_{c_2})^2 \quad (\text{B.46})$$

B.3 Uncertainty calculated for measurement 1

| e | Ylja |
|------------------------------|----------|
| $e_{E_{m,p,\bar{a}}}$ | 13,19350 |
| $e_{E_{m,p,p_{1-1}}}$ | 1,91944 |
| $e_{E_{m,p,\bar{p}}}$ | -0,00002 |
| $e_{E_{m,p,\Delta z_{1-1}}}$ | 0,00010 |
| $e_{E_{m,p,h_{2-1}}}$ | 0,00071 |
| $e_{E_{m,p,p_{atm}}}$ | 0,01147 |
| $e_{E_{m,p}}$ | 13,33240 |
| $e_{E_{m,T,c_p}}$ | -3,45069 |
| $e_{E_{m,T,\Delta T}}$ | 4,20047 |
| $e_{E_{10}}$ | 11,91289 |
| $e_{E_{20}}$ | 35,73866 |
| $e_{E_{m,T}}$ | 38,06206 |
| $e_{E_{m,pot}}$ | 1,38855 |
| $e_{E_{m,kin}}$ | 0,00000 |
| e_{E_m} | 40,33553 |
| $e_{E_{h,p,p_1}}$ | 1,26060 |
| $e_{E_{h,p,\bar{p}}}$ | -6,52249 |
| $e_{E_{h,p,\Delta z_1}}$ | -0,00010 |
| $e_{E_{h,p,h_2}}$ | -0,00070 |
| $e_{E_{h,p,p_{atm}}}$ | -0,01136 |
| $e_{E_{h,p}}$ | 6,64320 |
| $e_{E_{h,pot}}$ | 1,38855 |
| e_{c_1} | 0,11750 |
| e_{c_2} | 0,36510 |
| $e_{E_{h,kin}}$ | 0,67330 |
| e_{E_h} | 6,71310 |
| e_{η_h} | 0,00622 |
| f_{η_h} | 0,68488 |

Table B.2: Values uncertainty measurement 1

Appendix C

Calculation spreadsheet

Here are all the measured values and calculations done to find the efficiency and its uncertainty.

| Measurement # | | 1 | 2 | 3 | 4 | 5 |
|--------------------------------------|---------------------|--------------------|--------------------|--------------------|--------------------|--------------------|
| Temperature inlet | T11 | 0,934231116 | 0,932063441 | 0,94472087 | 0,952167804 | 0,9542862 |
| Temperature outlet | T21 | 1,098901216 | 1,096058136 | 1,114932101 | 1,128746127 | 1,13073949 |
| Temperature difference | Tdiff | -0,1646701 | -0,163994695 | -0,170211232 | -0,176578323 | -0,176453291 |
| Temperatuaure leakage water | nåler | 3 | 3 | 3 | 2 | 2 |
| Pressure @p1-sensor | p1 | 6628,884352 | 6652,803229 | 6665,244218 | 6659,466109 | 6674,095364 |
| Pressure @p11-sensor | p11 | 6653,602949 | 6671,193525 | 6678,550678 | 6668,059462 | 6677,3001 |
| Atmospheric pressure | pamb | 96,28767543 | 96,28695004 | 96,27592102 | 96,28274915 | 96,34893804 |
| | h2 | 1,5205 | 1,745 | 1,75 | 1,32 | 1,3155 |
| Water depth @T21-sensors | h21 | 1,641 | 2,09 | 2,1 | 1,24 | 1,231 |
| Generator power | P_g | 28,8 | 22,4 | 18 | 20,2 | 14,2 |
| Generator efficiency | eta_g | 0,973573616 | 0,971936368 | 0,97081076 | 0,971373564 | 0,969838644 |
| Turbine power | P_t | 29,58173838 | 23,04677625 | 18,54120364 | 20,79529519 | 14,64161084 |
| Assumption for Q | Q_assumed | 4,528327684 | 3,515094795 | 2,822544242 | 3,168476949 | 2,225931176 |
| Water depth center draft tube | h2 | 1,5205 | 1,745 | 1,75 | 1,32 | 1,3155 |
| Water density | rho11 | 1001,549771 | 1001,554638 | 1001,557068 | 1001,553771 | 1001,556166 |
| Water density | rho21 | 1001,549771 | 1001,554638 | 1001,557068 | 1001,553771 | 1001,556166 |
| Pressure @T11-sensor | p11 abs | 6653,602949 | 6671,193525 | 6678,550678 | 6668,059462 | 6677,3001 |
| Pressure @T21-sensor | p21 abs | 112,4248876 | 116,8396237 | 116,9269829 | 108,4766694 | 108,4543829 |
| Isothermal factor | a-empr | 1,00849601 | 1,00849188 | 1,008415803 | 1,008379741 | 1,00836341 |
| Mechanical pressure energy | Empr | 6596,751977 | 6610,012686 | 6616,845024 | 6614,550396 | 6623,783664 |
| Specific heat capacity | Cp-th | 4191,028591 | 4190,985956 | 4190,959756 | 4190,986018 | 4190,964089 |
| Mechanical thermal energy | Emth | -690,1370978 | -687,299465 | -713,3484229 | -740,0372814 | -739,5094054 |
| Mechanical potential energy | Empot | 49,82914552 | 49,82914552 | 49,82914552 | 49,82914552 | 49,82914552 |
| Water velocity in probe | c11 | 0 | 0 | 0 | 0 | 0 |
| Water velocity in draft tube | c21 | 0 | 0 | 0 | 0 | 0 |
| Mechanical kinetic energy | Emkin | 0 | 0 | 0 | 0 | 0 |
| Mechanical energy w/o leakage energy | Em' | 5956,444025 | 5972,542367 | 5953,325747 | 5924,342261 | 5934,103404 |
| Mechanical energy | Em | 5956,444025 | 5972,542367 | 5953,325747 | 5924,342261 | 5934,103404 |
| Water density | rho-corr | 1001,549771 | 1001,554638 | 1001,557068 | 1001,553771 | 1001,556166 |
| Iteration 2 for volume flow Q | Q_corr2 | 4,95865726 | 3,852798533 | 3,109586036 | 3,504698628 | 2,463533321 |
| Water density | rho1 | 1001,549771 | 1001,554638 | 1001,557068 | 1001,553771 | 1001,556166 |
| Pressure @ center of inlet | p1' | 6635,71882 | 6659,63773 | 6672,078736 | 6666,300604 | 6680,929876 |
| Pressure @ center of outlet | p2 | 111,2399187 | 113,4469575 | 113,4851393 | 109,2633739 | 109,2853416 |
| Hydraulic pressure energy | Ehp | 6514,383102 | 6536,029612 | 6548,397297 | 6546,864903 | 6561,433855 |
| Hydraulic potential energy | Ehpot | 39,07292308 | 36,86865841 | 36,81956566 | 41,04154252 | 41,085726 |
| Water velocity inlet | c1 | 5,514506518 | 4,284684645 | 3,458160458 | 3,897563879 | 2,739687347 |
| Water velocity draft tube | c2 | 0,465885964 | 0,315415353 | 0,253843758 | 0,379296388 | 0,267528188 |
| Hydraulic kinetic energy | Ehkin | 15,0963662 | 9,12951783 | 5,947218551 | 7,52356922 | 3,717157714 |
| Hydraulic energy | Eh | 6568,552391 | 6582,027789 | 6591,164081 | 6595,430014 | 6606,236739 |
| Turbine efficiency | eta | 0,906812288 | 0,907401573 | 0,903228273 | 0,898249583 | 0,898257758 |
| Mean pressure Em | Emp_avg | 3382,410612 | 3392,30778 | 3396,00539 | 3388,651997 | 3393,283317 |
| Mean pressure Eh | Ehp_avg | 3373,479369 | 3386,542344 | 3392,781938 | 3387,781989 | 3395,107609 |
| Mean temperature | temperature_avg | 1,016566166 | 1,014060789 | 1,029826486 | 1,040456965 | 1,042512845 |
| Mean pressure leak | Elmp_avg | 3374,945312 | 3383,740237 | 3387,413299 | 3382,171105 | 3386,824519 |
| Mean temp leak | TI_avg | 1,967115558 | 1,96603172 | 1,972360435 | 1,476083902 | 1,4771431 |
| 0 - 20 celsius | | | | | | |
| Isothermal factor | a | 1,00849601 | 1,00849188 | 1,008415803 | 1,008379741 | 1,00836341 |
| Specific heat capacity | cp | 4191,028591 | 4190,985956 | 4190,959756 | 4190,986018 | 4190,964089 |
| Density | rho | 1001,549771 | 1001,554638 | 1001,557068 | 1001,553771 | 1001,556166 |
| Specific heat capacity leakage | cpleak | 4190,454517 | 4190,416611 | 4190,396301 | 4190,741644 | 4190,72036 |
| Isothermal factor leakage | aleak | 1,00429861 | 1,004290191 | 1,004256899 | 1,006453242 | 1,006441462 |
| 20 - 40 celsius | | | | | | |
| Isothermal factor | a | 0,996684426 | 0,996679773 | 0,996623805 | 0,996598787 | 0,996586131 |
| Specific heat capacity | cp | 4166,5952 | 4166,561711 | 4166,560294 | 4166,590991 | 4166,577465 |
| Density | rho | 1001,817132 | 1001,822051 | 1001,823795 | 1001,822009 | 1001,822373 |
| Specific heat capacity leakage | cpleak | 4167,233493 | 4167,204659 | 4167,19688 | 4166,897216 | 4166,882971 |
| Isothermal factor leakage | aleak | 0,993614482 | 0,993606836 | 0,993581727 | 0,995194224 | 0,995184835 |
| | H | 668,9940804 | 670,366523 | 671,2970363 | 671,7315132 | 672,8321567 |
| | Correction | 1,002256293 | 0,999179987 | 0,997103198 | 0,996135963 | 0,993626889 |
| | Turbine output corr | 29,64848344 | 23,02787759 | 18,48749345 | 20,7149414 | 14,54926165 |
| | Correction Qt | 1,000751533 | 0,999726588 | 0,999033466 | 0,998710325 | 0,997893127 |
| | Qt | 4,962383853 | 3,85174513 | 3,106580514 | 3,500178706 | 2,45834297 |

Measurement

| | | | | | |
|-------------------------|--------------|--------------|--------------|--------------|--------------|
| | 1 | 2 | 3 | 4 | 5 |
| e_a *[10 ³] | 0,002016992 | 0,002016984 | 0,002016832 | 0,002016759 | 0,002016727 |
| e_p11 [kPa] | 1,903272801 | 1,901702324 | 1,900138424 | 1,905342141 | 1,910447112 |
| e_patm [kPa] | 0,011373769 | 0,011377422 | 0,011376405 | 0,011376194 | 0,011374785 |
| e_deltaz11 | 0,01 | 0,01 | 0,01 | 0,01 | 0,01 |
| e_h21 | 0,1732 | 0,1732 | 0,1732 | 0,1732 | 0,1732 |
| e_rho | 1,001549771 | 1,001554638 | 1,001557068 | 1,001553771 | 1,001556166 |
| e_Emp a | 13,19350395 | 13,22002537 | 13,23369005 | 13,22910079 | 13,24756733 |
| e_Emp p11 | 1,919443026 | 1,917851351 | 1,916129614 | 1,921308414 | 1,926424972 |
| e_Emp deltax | 9,91732E-05 | 9,91732E-05 | 9,9166E-05 | 9,91621E-05 | 9,91607E-05 |
| e_Emp patm | 0,011470401 | 0,011474037 | 0,011472147 | 0,011471524 | 0,011469917 |
| e_Emp h21 | 0,001717679 | 0,00171768 | 0,001717555 | 0,001717488 | 0,001717464 |
| e_Emp rho | -1,62743E-05 | -2,07272E-05 | -2,08249E-05 | -1,22961E-05 | -1,22067E-05 |
| e_Emp | 13,33240198 | 13,35841904 | 13,37169546 | 13,36789693 | 13,38690733 |
| e_cp | 20,96 | 20,95 | 20,95 | 20,95 | 20,95 |
| e_Tdiff | 0,001002253 | 0,001000021 | 0,001001688 | 0,001002413 | 0,001000053 |
| e_EmT cp | -3,450685489 | -3,436497325 | -3,566742114 | -3,700186407 | -3,697547027 |
| e_EmT Tdiff | 4,200469876 | 4,191867295 | 4,198035079 | 4,201096998 | 4,193185751 |
| e_E10 | 11,91288805 | 11,94508473 | 11,90665149 | 11,84868452 | 11,86820681 |
| e_E20 | 35,73866415 | 35,8352542 | 35,71995448 | 35,54605356 | 35,60462042 |
| e_EmT | 38,06205715 | 38,16060479 | 38,05297157 | 37,88474422 | 37,9446701 |
| e_(z11-z21) | 0,141421356 | 0,141421356 | 0,141421356 | 0,141421356 | 0,141421356 |
| e_Emz | 1,388552776 | 1,388552776 | 1,388552776 | 1,388552776 | 1,388552776 |
| e_Em | 40,35345358 | 40,45500212 | 40,35788602 | 40,19804213 | 40,26084147 |
| f_Em [%] | 0,677475578 | 0,677349772 | 0,677904884 | 0,678523292 | 0,678465452 |
| e_rho | 1,001549771 | 1,001554638 | 1,001557068 | 1,001553771 | 1,001556166 |
| e_p1 [kPa] | 1,262553862 | 1,258265165 | 1,257387292 | 1,265849308 | 1,273938147 |
| e_patm [kPa] | 0,011373769 | 0,011377422 | 0,011376405 | 0,011376194 | 0,011374785 |
| e_deltaz1 | 0,01 | 1,01 | 2,01 | 3,01 | 4,01 |
| e_h2 | 0,1732 | 0,1732 | 0,1732 | 0,1732 | 0,1732 |
| e_Ehp rho | -6,522488316 | -6,546339091 | -6,558755868 | -6,553001497 | -6,567526266 |
| e_Ehp p1 | 1,260600221 | 1,256312054 | 1,255432498 | 1,26388552 | 1,271958769 |
| e_Ehp patm | -0,01135617 | -0,011359761 | -0,011358719 | -0,011358546 | -0,011357112 |
| e_Ehp deltax1 | -9,81855E-05 | -0,009916736 | -0,019735287 | -0,029553838 | -0,039372389 |
| e_Ehp h2 | -0,001700573 | -0,001700573 | -0,001700573 | -0,001700573 | -0,001700573 |
| e_Ehp | 6,643199426 | 6,66581621 | 6,677867226 | 6,673847508 | 6,689690757 |
| e_z1-z2 | 0,141421356 | 0,141421356 | 0,141421356 | 0,141421356 | 0,141421356 |
| e_Ehz | 1,388552776 | 1,388552776 | 1,388552776 | 1,388552776 | 1,388552776 |
| e_Pgen [MW] | 0,2016 | 0,1568 | 0,126 | 0,1414 | 0,0994 |
| e_rho | 1,001549771 | 1,001554638 | 1,001557068 | 1,001553771 | 1,001556166 |
| e_Em | 40,35345358 | 40,45500212 | 40,35788602 | 40,19804213 | 40,26084147 |
| e_Di | 0,01 | 0,01 | 0,01 | 0,01 | 0,01 |
| e_A2 | 0,100498756 | 0,100498756 | 0,100498756 | 0,100498756 | 0,100498756 |
| Factor 1 | 12,97061578 | 7,856822437 | 5,129865715 | 6,508768146 | 3,226174959 |
| Factor 2 | 1,227931769 | 1,230057001 | 1,230095244 | 1,22504646 | 1,224966191 |
| e_Ehc Pgen | 0,211349127 | 0,12781325 | 0,08326106 | 0,105329969 | 0,052040208 |
| e_Ehc rho | -0,031854062 | -0,019328679 | -0,012620447 | -0,015947087 | -0,00790391 |
| e_Ehc Em | -0,215803493 | -0,130922762 | -0,085554626 | -0,108204698 | -0,053625302 |
| e_Ehc Di | -0,599683273 | -0,363252221 | -0,237174141 | -0,300926297 | -0,149158929 |
| e_Ehc A2 | 0,002049441 | 0,000818527 | 0,000528637 | 0,001564754 | 0,000781108 |
| e_Ehc | 0,672219094 | 0,407189686 | 0,265825368 | 0,337069805 | 0,167018934 |
| e_Eh | 6,819974775 | 6,821069418 | 6,825881088 | 6,825096001 | 6,834320409 |
| f_Eh [%] | 0,103827668 | 0,103631732 | 0,103561086 | 0,103482199 | 0,103452552 |
| e_eta | 0,00621516 | 0,006217802 | 0,006194065 | 0,006165307 | 0,006164809 |
| f_eta [%] | 0,685385544 | 0,68523153 | 0,68576959 | 0,686369014 | 0,686307365 |
| e_Pgen [MW] | 0,2016 | 0,1568 | 0,126 | 0,1414 | 0,0994 |
| e_rho | 1,001549771 | 1,001554638 | 1,001557068 | 1,001553771 | 1,001556166 |
| e_Em | 40,35345358 | 40,45500212 | 40,35788602 | 40,19804213 | 40,26084147 |
| e_Q Pgen | 0,034710601 | 0,02696959 | 0,021767102 | 0,02453289 | 0,017244733 |
| e_Q rho | -0,004958657 | -0,003852799 | -0,003109586 | -0,003504699 | -0,002463533 |
| e_Q Em | -0,033593692 | -0,026096922 | -0,021080036 | -0,023780167 | -0,016714222 |
| e_Q | 0,04855873 | 0,037726014 | 0,030460535 | 0,034345937 | 0,024141563 |
| f_Q [%] | 0,979271749 | 0,979184719 | 0,979568799 | 0,979996866 | 0,97995682 |

| | | | | | | | | | |
|--------------|--------------|--------------|--------------|--------------|--------------|--------------|--------------|-------------|--------------|
| 6 | 7 | 8 | 9 | 10 | 11 | 12 | 13 | 14 | 15 |
| 1,034438889 | 1,089561161 | 0,9346881 | 0,934589394 | 0,986881075 | 0,969700637 | 0,93653944 | 0,969890929 | 0,955986032 | 0,946856681 |
| 1,247844815 | 1,338772247 | 1,113921434 | 1,120425613 | 1,180244659 | 1,169183723 | 1,11080783 | 1,142507127 | 1,130770783 | 1,119638075 |
| -0,213405926 | -0,249211086 | -0,179233333 | -0,185836219 | -0,193363584 | -0,199483086 | -0,174268391 | -0,172661999 | -0,17478475 | -0,172781394 |
| 1 | 1 | 6 | 6 | 6 | 6 | 6 | 6 | 6 | 6 |
| 6684,142207 | 6687,827087 | 6511,446425 | 6468,518111 | 6423,89 | 6385,757544 | 6606,334688 | 6575,677397 | 6538,755062 | 6576,875605 |
| 6684,680995 | 6687,609117 | 6574,229072 | 6544,656664 | 6513,594 | 6484,490404 | 6633,795022 | 6612,196352 | 6591,526996 | 6610,01591 |
| 96,42302655 | 96,44493399 | 96,30763042 | 96,29582945 | 96,27883682 | 96,267826 | 96,42149986 | 96,43080095 | 96,34055061 | 96,25333791 |
| 1,276 | 1,284 | 1,6525 | 1,6525 | 1,721 | 1,709 | 1,415 | 1,5705 | 1,6105 | 1,4375 |
| 1,152 | 1,168 | 1,89 | 1,905 | 2,042 | 2,018 | 1,43 | 1,741 | 1,821 | 1,474 |
| 7,9 | 4,3 | 50 | 55,3 | 59,6 | 63,4 | 34 | 39,9 | 45,7 | 39,4 |
| 0,968226978 | 0,967306026 | 0,978997 | 0,980352846 | 0,981452872 | 0,982424988 | 0,97490388 | 0,976413218 | 0,977896974 | 0,976285308 |
| 8,159243834 | 4,445335689 | 51,07267949 | 56,40826181 | 60,72629843 | 64,53418915 | 34,87523303 | 40,86384664 | 46,73293937 | 40,35705513 |
| 1,23855368 | 0,674416319 | 7,961274279 | 8,852211884 | 9,597033835 | 10,2606399 | 5,357250094 | 6,306882449 | 7,253947924 | 6,227342602 |
| 1,276 | 1,284 | 1,645 | 1,6525 | 1,721 | 1,709 | 1,415 | 1,5705 | 1,6105 | 1,437 |
| 1001,561434 | 1001,564679 | 1001,530479 | 1001,523203 | 1001,517623 | 1001,509791 | 1001,544843 | 1001,541001 | 1001,535434 | 1001,539248 |
| 1001,561434 | 1001,564679 | 1001,530479 | 1001,523203 | 1001,517623 | 1001,509791 | 1001,544843 | 1001,541001 | 1001,535434 | 1001,539248 |
| 6684,680995 | 6687,609117 | 6574,229072 | 6544,656664 | 6513,594 | 6484,490404 | 6633,795022 | 6612,196352 | 6591,526996 | 6610,01591 |
| 107,7516585 | 107,9309452 | 114,8930927 | 115,0286593 | 116,3587452 | 116,1115764 | 110,483718 | 113,55124 | 114,2475846 | 110,7481587 |

| | | | | | | | | | |
|-------------|--------------|--------------|--------------|--------------|--------------|-------------|--------------|--------------|--------------|
| 1,007918332 | 1,007590991 | 1,008521907 | 1,008530436 | 1,00830371 | 1,008389316 | 1,008480305 | 1,008350662 | 1,008423616 | 1,008455925 |
| 6629,007649 | 6629,624447 | 6514,381839 | 6484,475535 | 6450,356044 | 6421,805167 | 6578,630973 | 6552,913103 | 6531,841528 | 6554,22507 |
| 4190,887343 | 4190,835158 | 4191,19822 | 4191,262123 | 4191,295107 | 4191,369159 | 4191,070432 | 4191,095096 | 4191,14848 | 4191,117484 |
| -894,360194 | -1044,402582 | -751,2024275 | -778,8883073 | -810,4438444 | -836,1072529 | -730,3711 | -723,4509039 | -732,5488406 | -724,1471199 |

| | | | | | | | | | |
|-------------|-------------|-------------|-------------|-------------|-------------|-------------|-------------|-------------|-------------|
| 49,82914552 | 49,82914552 | 49,82914552 | 49,82914552 | 49,82914552 | 49,82914552 | 49,82914552 | 49,82914552 | 49,82914552 | 49,82914552 |
| 0 | 0 | 0 | 0 | 0 | 0 | 0 | 0 | 0 | 0 |
| 0 | 0 | 0 | 0 | 0 | 0 | 0 | 0 | 0 | 0 |
| 0 | 0 | 0 | 0 | 0 | 0 | 0 | 0 | 0 | 0 |

| | | | | | | | | | |
|-------------|-------------|-------------|-------------|-------------|-------------|-------------|-------------|-------------|-------------|
| 5784,4766 | 5635,05101 | 5813,008557 | 5755,416373 | 5689,741345 | 5635,52706 | 5898,089018 | 5879,291344 | 5849,121833 | 5879,907096 |
| 5784,4766 | 5635,05101 | 5813,008557 | 5755,416373 | 5689,741345 | 5635,52706 | 5898,089018 | 5879,291344 | 5849,121833 | 5879,907096 |
| 1001,561434 | 1001,564679 | 1001,530479 | 1001,523203 | 1001,517623 | 1001,509791 | 1001,544843 | 1001,541001 | 1001,535434 | 1001,539248 |
| 1,408342386 | 0,787639903 | 8,772502703 | 9,785994204 | 10,65677239 | 11,43405083 | 5,903851108 | 6,939777245 | 7,977487111 | 6,853004723 |
| 1001,561434 | 1001,564679 | 1001,530479 | 1001,523203 | 1001,517623 | 1001,509791 | 1001,544843 | 1001,541001 | 1001,535434 | 1001,539248 |
| 6690,976754 | 6694,661657 | 6518,280762 | 6475,352398 | 6430,724249 | 6392,921429 | 6613,169122 | 6582,511806 | 6545,589433 | 6583,710002 |
| 108,9710598 | 109,0716792 | 112,4838661 | 112,5456989 | 113,2022072 | 113,0730635 | 110,3362122 | 111,8745973 | 112,1776062 | 110,3843131 |
| 6571,744351 | 6575,301741 | 6396,007941 | 6353,129595 | 6307,948956 | 6270,052205 | 6492,802552 | 6460,68129 | 6423,548891 | 6463,376951 |
| 41,47355876 | 41,39501035 | 37,8505135 | 37,77687436 | 37,10430363 | 37,22212624 | 40,10878019 | 38,58199553 | 38,1892535 | 39,89277207 |
| 1,56621296 | 0,87593176 | 9,755871559 | 10,88297214 | 11,85136172 | 12,71577053 | 6,565653505 | 7,717703572 | 8,871737319 | 7,621204135 |
| 0,1576738 | 0,087632388 | 0,761832627 | 0,845990422 | 0,884599642 | 0,955784572 | 0,596047563 | 0,631261859 | 0,707631801 | 0,681280915 |
| 1,214081005 | 0,379788506 | 47,29832046 | 58,86169142 | 69,83612985 | 80,38864798 | 21,37626662 | 29,58222845 | 39,10349015 | 28,80930439 |
| 6614,431991 | 6617,07654 | 6481,156775 | 6449,768161 | 6414,889389 | 6387,662979 | 6554,287598 | 6528,845514 | 6500,841634 | 6532,079028 |

| | | | | | | | | | |
|-------------|-------------|------------|------------|-------------|-------------|-------------|-------------|-------------|-------------|
| 0,874523558 | 0,851592237 | 0,89690911 | 0,89234469 | 0,886958605 | 0,882251784 | 0,899882547 | 0,900510103 | 0,899748396 | 0,900158597 |
|-------------|-------------|------------|------------|-------------|-------------|-------------|-------------|-------------|-------------|

| | | | | | | | | | |
|-------------|-------------|-------------|-------------|-------------|-------------|-------------|-------------|-------------|-------------|
| 3396,816873 | 3398,331165 | 3343,344917 | 3328,589635 | 3313,386126 | 3298,769905 | 3372,05558 | 3362,024364 | 3351,840952 | 3360,189958 |
| 3399,973907 | 3401,866668 | 3315,382314 | 3293,949048 | 3271,963228 | 3252,832401 | 3361,752667 | 3347,193202 | 3328,883519 | 3347,047157 |
| 1,141141852 | 1,214166704 | 1,024304767 | 1,027507504 | 1,083562867 | 1,06944218 | 1,023673635 | 1,056199028 | 1,043378408 | 1,033247378 |
| 3390,552011 | 3392,027025 | 3335,268351 | 3320,476247 | 3304,936418 | 3290,379115 | 3365,108261 | 3354,313576 | 3343,933773 | 3353,134624 |
| 1,017219444 | 1,04478058 | 3,46734405 | 3,467294697 | 3,493440538 | 3,484850318 | 3,46826972 | 3,484945464 | 3,477993016 | 3,473428341 |

| | | | | | | | | | |
|-------------|-------------|-------------|-------------|-------------|-------------|-------------|-------------|-------------|-------------|
| 1,007918332 | 1,007590991 | 1,008521907 | 1,008530436 | 1,00830371 | 1,008389316 | 1,008480305 | 1,008350662 | 1,008423616 | 1,008455925 |
| 4190,887343 | 4190,835158 | 4191,19822 | 4191,262123 | 4191,295107 | 4191,369159 | 4191,070432 | 4191,095096 | 4191,14848 | 4191,117484 |
| 1001,561434 | 1001,564679 | 1001,530479 | 1001,523203 | 1001,517623 | 1001,509791 | 1001,544843 | 1001,541001 | 1001,535434 | 1001,539248 |
| 4190,99185 | 4190,968296 | 4189,579118 | 4189,642438 | 4189,68965 | 4189,758269 | 4189,450811 | 4189,484744 | 4189,534233 | 4189,498235 |
| 1,008480498 | 1,008355235 | 0,99785329 | 0,99784575 | 0,997784855 | 0,997842332 | 0,997806828 | 0,997750893 | 0,997795401 | 0,997801812 |

| | | | | | | | | | |
|-------------|-------------|-------------|-------------|-------------|-------------|-------------|-------------|-------------|-------------|
| 0,996261439 | 0,996022569 | 0,996709769 | 0,996718431 | 0,996555978 | 0,996620717 | 0,996674724 | 0,996582056 | 0,996636842 | 0,996658961 |
| 4166,631361 | 4166,674575 | 4166,725973 | 4166,775939 | 4166,86156 | 4166,899243 | 4166,633218 | 4166,687043 | 4166,711295 | 4166,677728 |
| 1001,823489 | 1001,823695 | 1001,797729 | 1001,790398 | 1001,775284 | 1001,775383 | 1001,811961 | 1001,806804 | 1001,801832 | 1001,806027 |
| 4166,569455 | 4166,583009 | 4168,261013 | 4168,308003 | 4168,372357 | 4168,413725 | 4168,166711 | 4168,210567 | 4168,239572 | 4168,207717 |
| 0,996671785 | 0,996580391 | 0,988833249 | 0,988851597 | 0,988786818 | 0,988832276 | 0,988793589 | 0,988753376 | 0,988788435 | 0,988791765 |

| | | | | | | | | | |
|-------------|-------------|-------------|-------------|-------------|-------------|-------------|-------------|-------------|-------------|
| 673,6668269 | 673,936169 | 660,0930095 | 656,8961413 | 653,3438072 | 650,5708513 | 667,5412394 | 664,9500134 | 662,0978736 | 665,2793404 |
| 0,99184649 | 0,991251955 | 1,022596975 | 1,030070946 | 1,038483345 | 1,045129973 | 1,005530048 | 1,011413405 | 1,017955784 | 1,010662492 |
| 8,09271736 | 4,406447692 | 52,22676755 | 58,10451163 | 63,06324949 | 67,44661533 | 35,06809474 | 41,33024228 | 47,57206594 | 40,78736192 |
| 0,997274743 | 0,99707544 | 1,007476291 | 1,009924821 | 1,01266666 | 1,014822531 | 1,001839962 | 1,003790085 | 1,005949791 | 1,003541606 |
| 1,404504291 | 0,785336403 | 8,838088484 | 9,883118444 | 10,7917581 | 11,60353241 | 5,914713968 | 6,966079594 | 8,024951493 | 6,877275368 |

| | | | | | | | | | | |
|--------------|--------------|--------------|--------------|--------------|--------------|--------------|--------------|--------------|--------------|----|
| | 6 | 7 | 8 | 9 | 10 | 11 | 12 | 13 | 14 | 15 |
| 0,002015837 | 0,002015182 | 0,002017044 | 0,002017061 | 0,002016607 | 0,002016779 | 0,002016961 | 0,002016701 | 0,002016847 | 0,002016912 | |
| 1,924575738 | 1,911960271 | 1,905114217 | 1,928110321 | 1,914681311 | 1,911964955 | 1,906898903 | 1,90172905 | 1,902282215 | 1,905795806 | |
| 0,011384263 | 0,011382262 | 0,011374181 | 0,011376149 | 0,011378879 | 0,011371914 | 0,011380714 | 0,011380785 | 0,01138001 | 0,011375985 | |
| 0,01 | 0,01 | 0,01 | 0,01 | 0,01 | 0,01 | 0,01 | 0,01 | 0,01 | 0,01 | |
| 0,1732 | 0,1732 | 0,1732 | 0,1732 | 0,1732 | 0,1732 | 0,1732 | 0,1732 | 0,1732 | 0,1732 | |
| 1,001561434 | 1,001564679 | 1,001530479 | 1,001523203 | 1,001517623 | 1,001509791 | 1,001544843 | 1,001541001 | 1,001535434 | 1,001539248 | |
| 13,2580153 | 13,25924889 | 13,02876368 | 12,96895107 | 12,90071209 | 12,84361033 | 13,15726195 | 13,10582621 | 13,06368306 | 13,10845014 | |
| 1,939815168 | 1,926473944 | 1,921349423 | 1,944557943 | 1,930580271 | 1,928005032 | 1,923069987 | 1,917609747 | 1,91830631 | 1,921911072 | |
| 9,91175E-05 | 9,90856E-05 | 9,91738E-05 | 9,91739E-05 | 9,91511E-05 | 9,91587E-05 | 9,91711E-05 | 9,9158E-05 | 9,91646E-05 | 9,91682E-05 | |
| 0,011474407 | 0,011468665 | 0,011471111 | 0,011473192 | 0,011473366 | 0,011467316 | 0,011477226 | 0,011475822 | 0,011475871 | 0,01147218 | |
| 0,001716715 | 0,001716163 | 0,00171769 | 0,001717692 | 0,001717296 | 0,001717429 | 0,001717644 | 0,001717416 | 0,001717531 | 0,001717593 | |
| -1,14183E-05 | -1,15732E-05 | -1,87438E-05 | -1,88926E-05 | -2,02466E-05 | -2,00102E-05 | -1,41815E-05 | -1,72634E-05 | -1,80579E-05 | -1,46174E-05 | |
| 13,3991786 | 13,39847445 | 13,16967734 | 13,11392893 | 13,04437224 | 12,98751956 | 13,29706264 | 13,24537815 | 13,20378161 | 13,24859773 | |
| 20,95 | 20,95 | 20,96 | 20,96 | 20,96 | 20,96 | 20,96 | 20,96 | 20,96 | 20,96 | |
| 0,001252454 | 0,001305347 | 0,00100076 | 0,001002859 | 0,001000605 | 0,001000921 | 0,001000359 | 0,001000397 | 0,001000344 | 0,001001174 | |
| -4,47180097 | -5,222012911 | -3,756012138 | -3,894441536 | -4,052219222 | -4,180536264 | -3,6518555 | -3,617254519 | -3,662744203 | -3,6207356 | |
| 5,248893939 | 5,470492332 | 4,194384706 | 4,203247005 | 4,193832742 | 4,195229045 | 4,192573191 | 4,192758461 | 4,192528971 | 4,196237408 | |
| 11,5689532 | 11,27010202 | 11,62601711 | 11,51083275 | 11,37948269 | 11,27105412 | 11,79617804 | 11,75858269 | 11,69824367 | 11,75981419 | |
| 34,7068596 | 33,81030606 | 34,87805134 | 34,53249824 | 34,13844807 | 33,81316236 | 35,38853411 | 35,27574807 | 35,094731 | 35,27944258 | |
| 37,22841218 | 36,43278332 | 37,19332238 | 36,84869964 | 36,45456044 | 36,13092083 | 37,71487613 | 37,5939679 | 37,40965854 | 37,59852064 | |
| 0,141421356 | 0,141421356 | 0,141421356 | 0,141421356 | 0,141421356 | 0,141421356 | 0,141421356 | 0,141421356 | 0,141421356 | 0,141421356 | |
| 1,388552776 | 1,388552776 | 1,388552776 | 1,388552776 | 1,388552776 | 1,388552776 | 1,388552776 | 1,388552776 | 1,388552776 | 1,388552776 | |
| 39,5906648 | 38,84320915 | 39,48052317 | 39,13732076 | 38,74298263 | 38,41935948 | 40,01439535 | 39,88236144 | 39,6957237 | 39,88862213 | |
| 0,684429509 | 0,689314242 | 0,679175384 | 0,680008504 | 0,680926957 | 0,681734984 | 0,678429831 | 0,678368516 | 0,678661256 | 0,678388646 | |
| 1,001561434 | 1,001564679 | 1,001530479 | 1,001523203 | 1,001517623 | 1,001509791 | 1,001544843 | 1,001541001 | 1,001535434 | 1,001539248 | |
| 1,293744526 | 1,274562344 | 1,258202921 | 1,286371155 | 1,264676472 | 1,254821872 | 1,266704236 | 1,256318739 | 1,255752038 | 1,262298557 | |
| 0,011384263 | 0,011382262 | 0,011374181 | 0,011376149 | 0,011378879 | 0,011371914 | 0,011380714 | 0,011380785 | 0,01138001 | 0,011375985 | |
| 0,01 | 0,01 | 0,01 | 0,01 | 0,01 | 0,01 | 0,01 | 0,01 | 0,01 | 0,01 | |
| 0,1732 | 0,1732 | 0,1732 | 0,1732 | 0,1732 | 0,1732 | 0,1732 | 0,1732 | 0,1732 | 0,1732 | |
| -6,577448929 | -6,581084867 | -6,405335564 | -6,362530858 | -6,318022789 | -6,280008216 | -6,499871908 | -6,469277431 | -6,432537774 | -6,470662316 | |
| 1,291727579 | 1,272571178 | 1,256280211 | 1,284414731 | 1,262760079 | 1,252930209 | 1,264750396 | 1,254385729 | 1,253826869 | 1,260358553 | |
| -0,011366514 | -0,011364481 | -0,0113568 | -0,011358847 | -0,011361636 | -0,01135477 | -0,011363159 | -0,011363274 | -0,011362564 | -0,011358502 | |
| -0,04919094 | -0,059009491 | -0,068828041 | -0,078646592 | -0,088465143 | -0,098283694 | -0,108102245 | -0,117920796 | -0,127739346 | -0,137558797 | |
| -0,001700573 | -0,001700573 | -0,001700573 | -0,001700573 | -0,001700573 | -0,001700573 | -0,001700573 | -0,001700573 | -0,001700573 | -0,001700573 | |
| 6,703278779 | 6,703262608 | 6,527743318 | 6,491366368 | 6,443596282 | 6,404539703 | 6,622669137 | 6,590832373 | 6,554851133 | 6,59371129 | |
| 0,141421356 | 0,141421356 | 0,141421356 | 0,141421356 | 0,141421356 | 0,141421356 | 0,141421356 | 0,141421356 | 0,141421356 | 0,141421356 | |
| 1,388552776 | 1,388552776 | 1,388552776 | 1,388552776 | 1,388552776 | 1,388552776 | 1,388552776 | 1,388552776 | 1,388552776 | 1,388552776 | |
| 0,0553 | 0,0301 | 0,35 | 0,3871 | 0,4172 | 0,4438 | 0,238 | 0,2793 | 0,3199 | 0,2758 | |
| 1,001561434 | 1,001564679 | 1,001530479 | 1,001523203 | 1,001517623 | 1,001509791 | 1,001544843 | 1,001541001 | 1,001535434 | 1,001539248 | |
| 39,5906648 | 38,84320915 | 39,48052317 | 39,13732076 | 38,74298263 | 38,41935948 | 40,01439535 | 39,88236144 | 39,6957237 | 39,88862213 | |
| 0,01 | 0,01 | 0,01 | 0,01 | 0,01 | 0,01 | 0,01 | 0,01 | 0,01 | 0,01 | |
| 0,100498756 | 0,100498756 | 0,100498756 | 0,100498756 | 0,100498756 | 0,100498756 | 0,100498756 | 0,100498756 | 0,100498756 | 0,100498756 | |
| 1,057869622 | 0,331510767 | 40,14711146 | 49,82130337 | 58,94982012 | 67,72849749 | 18,33653194 | 25,25769796 | 33,27484355 | 24,63647445 | |
| 1,224224762 | 1,224380467 | 1,229217384 | 1,229285687 | 1,22986877 | 1,229771667 | 1,226566392 | 1,228484896 | 1,228890806 | 1,226876098 | |
| 0,016997134 | 0,005317039 | 0,662176486 | 0,82406368 | 0,977705805 | 1,125441072 | 0,299267733 | 0,414151198 | 0,547448862 | 0,40330261 | |
| -0,00259014 | -0,000811791 | -0,098699055 | -0,12248923 | -0,145001085 | -0,166581174 | -0,044981948 | -0,062057401 | -0,081782299 | -0,060451803 | |
| -0,017727685 | -0,005595788 | -0,670339683 | -0,832937182 | -0,98735148 | -1,135642143 | -0,305170951 | -0,420977669 | -0,555024775 | -0,41009817 | |
| -0,04890953 | -0,015327064 | -1,856161002 | -2,303437458 | -2,725485177 | -3,131358426 | -0,847770967 | -1,167764062 | -1,538428661 | -1,139042423 | |
| 0,000279725 | 8,58671E-05 | 0,005065425 | 0,006218019 | 0,006527928 | 0,007674333 | 0,003604691 | 0,003642871 | 0,004463922 | 0,004637227 | |
| 0,054791446 | 0,017180484 | 2,083970686 | 2,587224709 | 3,062696355 | 3,519874211 | 0,950495906 | 1,310069036 | 1,726622071 | 1,277477739 | |
| 6,845803627 | 6,845590083 | 6,991598205 | 7,124580537 | 7,268295593 | 7,43879843 | 6,83310089 | 6,861736738 | 6,919203419 | 6,85835671 | |
| 0,103497982 | 0,103453391 | 0,107875777 | 0,110462583 | 0,113303522 | 0,116455712 | 0,104253907 | 0,105098776 | 0,106435502 | 0,104995005 | |
| 0,006053545 | 0,005935889 | 0,006167947 | 0,006147559 | 0,00612258 | 0,006101742 | 0,006176734 | 0,006181657 | 0,006180883 | 0,00617928 | |
| 0,692210651 | 0,697034237 | 0,687689163 | 0,688922018 | 0,690289222 | 0,691610093 | 0,686393409 | 0,68646165 | 0,686956779 | 0,686465663 | |
| 0,0553 | 0,0301 | 0,35 | 0,3871 | 0,4172 | 0,4438 | 0,238 | 0,2793 | 0,3199 | 0,2758 | |
| 1,001561434 | 1,001564679 | 1,001530479 | 1,001523203 | 1,001517623 | 1,001509791 | 1,001544843 | 1,001541001 | 1,001535434 | 1,001539248 | |
| 39,5906648 | 38,84320915 | 39,48052317 | 39,13732076 | 38,74298263 | 38,41935948 | 40,01439535 | 39,88236144 | 39,6957237 | 39,88862213 | |
| 0,009858397 | 0,005513479 | 0,061407519 | 0,068501959 | 0,074597407 | 0,080038356 | 0,041326958 | 0,048578441 | 0,05584241 | 0,047971033 | |
| -0,001408342 | -0,00078764 | -0,008772503 | -0,009785994 | -0,010656772 | -0,011434051 | -0,005903851 | -0,006939777 | -0,007977487 | -0,006859005 | |
| -0,005939111 | -0,005428019 | -0,005580679 | -0,006545593 | -0,072564836 | -0,077949925 | -0,040053487 | -0,047077264 | -0,054140114 | -0,04649006 | |
| 0,013859433 | 0,00777936 | 0,086009869 | 0,096003125 | 0,104613552 | 0,11230791 | 0,057853736 | 0,068002163 | 0,078186744 | 0,067152843 | |
| 0,984095398 | 0,987498924 | 0,98044847 | 0,981025772 | 0,981662631 | 0,982223288 | 0,979932159 | 0,97988971 | 0,980092394 | 0,979903646 | |

| 16 | 17 | 18 | 19 | 20 | 21 |
|--------------|--------------|--------------|--------------|--------------|--------------|
| 0,873531749 | 0,870391013 | 0,88245207 | 0,925017811 | 0,985073102 | 0,970723326 |
| 1,047190929 | 1,041591587 | 1,05034045 | 1,097636695 | 1,160664208 | 1,142629734 |
| -0,173659179 | -0,171200574 | -0,167888381 | -0,172618884 | -0,175591106 | -0,171906407 |
| 4 | 4 | 4 | 4 | 1 | 2 |
| 6648,687653 | 6633,776863 | 6615,725425 | 6594,632027 | 6681,794158 | 6669,567844 |
| 6666,59338 | 6655,164725 | 6641,681226 | 6626,061658 | 6683,800941 | 6675,086638 |
| 96,41689383 | 96,42749753 | 96,42961085 | 96,42089773 | 96,37269483 | 96,31550558 |
| 1,341 | 1,418 | 1,308 | 1,3305 | 1,2525 | 1,2455 |
| 1,282 | 1,436 | 1,216 | 1,261 | 1,105 | 1,091 |
| 24 | 28 | 32,5 | 36,7 | 10,31 | 16,3 |
| 0,97234568 | 0,97336896 | 0,97452015 | 0,975594594 | 0,968843504 | 0,970375866 |
| 24,68257996 | 28,76607037 | 33,34974654 | 37,61808463 | 10,64155352 | 16,79761479 |
| 3,767026863 | 4,400265117 | 5,1155443 | 5,788990828 | 1,615925963 | 2,555449559 |
| 1,341 | 1,418 | 1,308 | 1,3305 | 1,2525 | 1,2455 |
| 1001,550526 | 1001,547689 | 1001,544431 | 1001,542243 | 1001,558739 | 1001,555943 |
| 1001,550526 | 1001,547689 | 1001,544431 | 1001,542243 | 1001,558739 | 1001,555943 |
| 6666,59338 | 6655,164725 | 6641,681226 | 6626,061658 | 6683,800941 | 6675,086638 |
| 109,0237931 | 110,5487581 | 108,3874082 | 108,8211851 | 107,239105 | 107,0442119 |

| | | | | | |
|-------------|-------------|-------------|-------------|-------------|-------------|
| 1,008738211 | 1,008766 | 1,008730796 | 1,008542048 | 1,008223462 | 1,008302497 |
| 6614,871012 | 6601,986074 | 6590,334677 | 6572,911056 | 6630,643939 | 6622,573578 |

| | | | | | |
|--------------|--------------|------------|--------------|--------------|--------------|
| 4191,037755 | 4191,064251 | 4191,0904 | 4191,097163 | 4190,932194 | 4190,9619 |
| -727,8121768 | -717,5126039 | -703,63538 | -723,4625155 | -735,8904204 | -720,4532041 |

| | | | | | |
|-------------|-------------|-------------|-------------|-------------|-------------|
| 49,82914552 | 49,82914552 | 49,82914552 | 49,82914552 | 49,82914552 | 49,82914552 |
|-------------|-------------|-------------|-------------|-------------|-------------|

| | | | | | |
|---|---|---|---|---|---|
| 0 | 0 | 0 | 0 | 0 | 0 |
| 0 | 0 | 0 | 0 | 0 | 0 |
| 0 | 0 | 0 | 0 | 0 | 0 |

| | | | | | |
|-------------|-------------|-------------|-------------|-------------|------------|
| 5936,887981 | 5934,302616 | 5936,528442 | 5899,277686 | 5944,582664 | 5951,94952 |
|-------------|-------------|-------------|-------------|-------------|------------|

| | | | | | |
|-------------|-------------|-------------|-------------|-------------|------------|
| 5936,887981 | 5934,302616 | 5936,528442 | 5899,277686 | 5944,582664 | 5951,94952 |
|-------------|-------------|-------------|-------------|-------------|------------|

| | | | | | |
|-------------|-------------|-------------|-------------|-------------|-------------|
| 1001,550526 | 1001,547689 | 1001,544431 | 1001,542243 | 1001,558739 | 1001,555943 |
| 4,151058316 | 4,839931513 | 5,60905585 | 6,366907906 | 1,787340261 | 2,817819474 |

| | | | | | |
|-------------|-------------|-------------|-------------|-------------|-------------|
| 1001,550526 | 1001,547689 | 1001,544431 | 1001,542243 | 1001,558739 | 1001,555943 |
| 6655,522126 | 6640,611317 | 6622,559856 | 6601,466444 | 6688,628688 | 6676,402354 |
| 109,6039858 | 110,3717506 | 109,29211 | 109,5046268 | 108,6895987 | 108,5635383 |
| 6535,784235 | 6520,148404 | 6503,223966 | 6481,965053 | 6569,698646 | 6557,635509 |

| | | | | | |
|-------------|-------------|-------------|-------------|------------|-------------|
| 40,83535295 | 40,07932454 | 41,15936513 | 40,93844774 | 41,7042947 | 41,77302456 |
|-------------|-------------|-------------|-------------|------------|-------------|

| | | | | | |
|-------------|-------------|-------------|-------------|-------------|-------------|
| 4,616378374 | 5,382472003 | 6,237812662 | 7,080617455 | 1,987695258 | 3,133687819 |
| 0,44221352 | 0,487601402 | 0,612609857 | 0,6836214 | 0,203859739 | 0,323200031 |
| 10,55769825 | 14,36662487 | 19,26750798 | 24,83390266 | 1,954686822 | 4,857770543 |

| | | | | | |
|-------------|-------------|-------------|-------------|-------------|-------------|
| 6587,177287 | 6574,594354 | 6563,650839 | 6547,737403 | 6613,357627 | 6604,266304 |
|-------------|-------------|-------------|-------------|-------------|-------------|

| | | | | | |
|------------|-------------|-------------|-------------|-------------|-------------|
| 0,90127952 | 0,902611218 | 0,904455247 | 0,900964306 | 0,898875125 | 0,901227971 |
|------------|-------------|-------------|-------------|-------------|-------------|

| | | | | | |
|-------------|-------------|-------------|-------------|-------------|-------------|
| 3388,089134 | 3382,75816 | 3375,477393 | 3367,773722 | 3396,2363 | 3391,816186 |
| 3382,563056 | 3375,491534 | 3365,925983 | 3355,485535 | 3398,659143 | 3392,482946 |
| 0,960361339 | 0,9559913 | 0,96639626 | 1,011327253 | 1,072868655 | 1,05667653 |
| 3381,505137 | 3375,796112 | 3369,055419 | 3361,241278 | 3390,086818 | 3385,701072 |
| 2,436765875 | 2,435195507 | 2,441226035 | 2,462508906 | 0,992536551 | 1,485361663 |

| | | | | | |
|-------------|-------------|-------------|-------------|-------------|-------------|
| 1,008738211 | 1,008766 | 1,008730796 | 1,008542048 | 1,008223462 | 1,008302497 |
| 4191,037755 | 4191,064251 | 4191,0904 | 4191,097163 | 4190,932194 | 4190,9619 |
| 1001,550526 | 1001,547689 | 1001,544431 | 1001,542243 | 1001,558739 | 1001,555943 |
| 4190,110073 | 4190,136011 | 4190,161247 | 4190,180696 | 4191,009097 | 4190,720094 |
| 1,002234875 | 1,002250135 | 1,00223381 | 1,002152645 | 1,008591408 | 1,00640678 |

| | | | | | |
|-------------|-------------|-------------|-------------|-------------|-------------|
| 0,996859625 | 0,996880717 | 0,996856335 | 0,996720354 | 0,996483772 | 0,996542042 |
| 4166,539541 | 4166,553775 | 4166,584127 | 4166,638789 | 4166,588095 | 4166,591575 |
| 1001,820237 | 1001,817616 | 1001,813956 | 1001,809906 | 1001,823653 | 1001,821562 |
| 4167,503615 | 4167,520888 | 4167,546101 | 4167,584047 | 4166,554541 | 4166,891891 |
| 0,992090167 | 0,992102399 | 0,992091419 | 0,992032608 | 0,996752541 | 0,995159647 |

| | | | | | |
|-------------|-------------|-------------|-------------|-------------|-------------|
| 670,8909892 | 669,6094423 | 668,494867 | 666,874115 | 673,5574051 | 672,6314718 |
| 0,998008559 | 1,00087502 | 1,003379188 | 1,007039286 | 0,992088194 | 0,994137437 |
| 24,63342606 | 28,79124127 | 33,4624416 | 37,8828891 | 10,55735961 | 16,69913771 |
| 0,999335745 | 1,000291588 | 1,00112513 | 1,002340944 | 0,997355745 | 0,998041981 |
| 4,148300955 | 4,841342781 | 5,615366765 | 6,381812484 | 1,782614078 | 2,812302129 |

| | | | | | |
|--------------|-------------|--------------|--------------|--------------|--------------|
| 16 | 17 | 18 | 19 | 20 | 21 |
| 0,002017476 | 0,002017532 | 0,002017462 | 0,002017084 | 0,002016447 | 0,002016605 |
| 1,920370256 | 1,906361856 | 1,907304509 | 1,910985406 | 1,924761609 | 1,908105299 |
| 0,011385785 | 0,011381729 | 0,011383069 | 0,011385723 | 0,01138136 | 0,011379532 |
| 0,01 | 0,01 | 0,01 | 0,01 | 0,01 | 0,01 |
| 0,1732 | 0,1732 | 0,1732 | 0,1732 | 0,1732 | 0,1732 |
| 1,001550526 | 1,001547689 | 1,001544431 | 1,001542243 | 1,001558739 | 1,001555943 |
| 13,22974202 | 13,20397215 | 13,18066935 | 13,14582211 | 13,26128788 | 13,24514716 |
| 1,937150857 | 1,923073025 | 1,923956796 | 1,927309136 | 1,940589812 | 1,923947337 |
| 9,9197E-05 | 9,91995E-05 | 9,91957E-05 | 9,91769E-05 | 9,91472E-05 | 9,91547E-05 |
| 0,011485277 | 0,011481501 | 0,011482453 | 0,011482981 | 0,011474955 | 0,01147401 |
| 0,001718093 | 0,001718135 | 0,00171807 | 0,001717744 | 0,00171723 | 0,00171736 |
| -1,27171E-05 | -1,4245E-05 | -1,20622E-05 | -1,25062E-05 | -1,09558E-05 | -1,08178E-05 |
| 13,37081757 | 13,3432839 | 13,32035244 | 13,28635745 | 13,40252885 | 13,38415598 |

| | | | | | |
|--------------|--------------|-------------|--------------|--------------|--------------|
| 20,96 | 20,96 | 20,96 | 20,96 | 20,95 | 20,95 |
| 0,001001934 | 0,001000318 | 0,001015242 | 0,001000674 | 0,001023972 | 0,001000914 |
| -3,639060884 | -3,587563019 | -3,5181769 | -3,617312577 | -3,679452102 | -3,602266021 |
| 4,199142331 | 4,19239816 | 4,25497166 | 4,193923124 | 4,291395711 | 4,19479118 |
| 11,87377596 | 11,86860523 | 11,87305688 | 11,79855537 | 11,88916533 | 11,90389904 |
| 35,62132789 | 35,60581569 | 35,61917065 | 35,39566612 | 35,66749598 | 35,71169712 |

| | | | | | |
|-------------|-------------|-------------|-------------|-------------|-------------|
| 37,95709573 | 37,93527003 | 37,94966601 | 37,71913348 | 38,01942881 | 38,04734836 |
| 0,141421356 | 0,141421356 | 0,141421356 | 0,141421356 | 0,141421356 | 0,141421356 |
| 1,388552776 | 1,388552776 | 1,388552776 | 1,388552776 | 1,388552776 | 1,388552776 |

| | | | | | |
|-------------|-------------|-------------|-------------|-------------|-------------|
| 40,26720698 | 40,23749515 | 40,24347175 | 40,01485228 | 40,33649496 | 40,35671477 |
| 0,678254451 | 0,678049263 | 0,677895712 | 0,678300877 | 0,678542082 | 0,678041953 |

| | | | | | |
|--------------|--------------|--------------|--------------|--------------|--------------|
| 1,001550526 | 1,001547689 | 1,001544431 | 1,001542243 | 1,001558739 | 1,001555943 |
| 1,28788327 | 1,264872362 | 1,264421213 | 1,272430386 | 1,296910504 | 1,270338487 |
| 0,011385785 | 0,011381729 | 0,011383069 | 0,011385723 | 0,01138136 | 0,011379532 |
| 15,01 | 16,01 | 17,01 | 18,01 | 19,01 | 20,01 |
| 0,1732 | 0,1732 | 0,1732 | 0,1732 | 0,1732 | 0,1732 |
| -6,542127019 | -6,527247217 | -6,509242738 | -6,488204742 | -6,575172488 | -6,563040621 |
| 1,285889464 | 1,262917758 | 1,262471413 | 1,270471011 | 1,294892106 | 1,268364983 |
| -0,011368159 | -0,011364141 | -0,011365516 | -0,011368191 | -0,011363647 | -0,011361853 |
| -0,147376448 | -0,157194999 | -0,16701355 | -0,176832101 | -0,186650652 | -0,196469202 |
| -0,001700573 | -0,001700573 | -0,001700573 | -0,001700573 | -0,001700573 | -0,001700573 |

| | | | | | |
|-------------|-------------|-------------|-------------|-------------|-------------|
| 6,668942165 | 6,650169907 | 6,632654121 | 6,613796117 | 6,704074082 | 6,687374975 |
| 0,141421356 | 0,141421356 | 0,141421356 | 0,141421356 | 0,141421356 | 0,141421356 |
| 1,388552776 | 1,388552776 | 1,388552776 | 1,388552776 | 1,388552776 | 1,388552776 |

| | | | | | |
|--------------|--------------|--------------|--------------|--------------|--------------|
| 0,168 | 0,196 | 0,2275 | 0,2569 | 0,07217 | 0,1141 |
| 1,001550526 | 1,001547689 | 1,001544431 | 1,001542243 | 1,001558739 | 1,001555943 |
| 40,26720698 | 40,23749515 | 40,24347175 | 40,01485228 | 40,33649496 | 40,35671477 |
| 0,01 | 0,01 | 0,01 | 0,01 | 0,01 | 0,01 |
| 0,100498756 | 0,100498756 | 0,100498756 | 0,100498756 | 0,100498756 | 0,100498756 |
| 9,112683684 | 12,36213413 | 16,56410162 | 21,29552593 | 1,701677346 | 4,216153005 |
| 1,225410428 | 1,226609475 | 1,224830563 | 1,225230598 | 1,223749998 | 1,223603359 |
| 0,147807775 | 0,201132748 | 0,269745112 | 0,347674637 | 0,027365616 | 0,068008788 |
| -0,022333555 | -0,030327022 | -0,040576436 | -0,05218386 | -0,004164855 | -0,010317798 |
| -0,151478332 | -0,205632147 | -0,275065918 | -0,35396358 | -0,028260296 | -0,069958999 |
| -0,421315693 | -0,57155074 | -0,765824448 | -0,984577055 | -0,078675327 | -0,19492956 |
| 0,00209362 | 0,002407223 | 0,004119295 | 0,005042885 | 0,000476374 | 0,001204098 |

| | | | | | |
|-------------|-------------|-------------|-------------|-------------|-------------|
| 0,472020029 | 0,640573754 | 0,858239002 | 1,103770099 | 0,088061917 | 0,218231292 |
|-------------|-------------|-------------|-------------|-------------|-------------|

| | | | | | |
|-------------|-------------|-------------|-------------|-------------|-------------|
| 6,828299299 | 6,82372137 | 6,830574916 | 6,847531404 | 6,846929459 | 6,833497477 |
| 0,103660476 | 0,103789238 | 0,104066701 | 0,104578589 | 0,103531819 | 0,103470956 |

| | | | | | |
|-------------|-------------|-------------|-------------|-------------|-------------|
| 0,006183951 | 0,006191433 | 0,006203089 | 0,006183456 | 0,006169835 | 0,006181446 |
| 0,686130158 | 0,685946797 | 0,685837061 | 0,686315351 | 0,686395072 | 0,685891485 |

| | | | | | |
|--------------|--------------|--------------|--------------|--------------|--------------|
| 0,168 | 0,196 | 0,2275 | 0,2569 | 0,07217 | 0,1141 |
| 1,001550526 | 1,001547689 | 1,001544431 | 1,001542243 | 1,001558739 | 1,001555943 |
| 40,26720698 | 40,23749515 | 40,24347175 | 40,01485228 | 40,33649496 | 40,35671477 |
| 0,029057408 | 0,033879521 | 0,039263391 | 0,044568355 | 0,012511382 | 0,019724736 |
| -0,004151058 | -0,004839932 | -0,005609056 | -0,006366908 | -0,00178734 | -0,002817819 |
| -0,028154738 | -0,03281712 | -0,038023549 | -0,043186792 | -0,012127856 | -0,019105998 |

| | | | | | |
|-------------|-------------|-------------|-------------|-------------|-------------|
| 0,040672515 | 0,047415295 | 0,054944205 | 0,062385694 | 0,017516111 | 0,027605153 |
| 0,979810747 | 0,979668721 | 0,979562451 | 0,979842885 | 0,980009876 | 0,979663662 |

Appendix D

Calibration reports

Calibration of the two pressure transducers Digiquartz, and the temperature sensors SBE38, in the following pages.



GE Hydro

Calibration report

Date: 2000-07-17

| | |
|-----------------------|--|
| Project: | Sintef Energiforskning A/S, Att. Terje Bryhni |
| Object/purpose: | DIQ Pressure transducers./ |
| Producer/type/ident.: | Paroscientific/9002K, 2000 psia/4544-1, 4544-2 |

REFERENCE EQUIPMENT:

| Type/Producer: | S/N: | Range: | Int.reg.No. |
|------------------------------|--------------|----------------|-------------|
| DW-tester/D&H | 2852 | 0- 600 [kPa] | ME 1 |
| DW-tester/D&H | 2821 | 0- 6000 [kPa] | ME 2 |
| DW-tester/D&H | 3185 | 0- 12000 [kPa] | ME 3 |
| Mercury manometer/W&T | AM 00757 | 0- 108 [kPa] | ME 4 |
| Barometric transducer/Sedeme | 45885 | 0- 108 [kPa] | ME 1005 |
| Transducers/Paroscientific | 21970, 16619 | 0- 2000 [kPa] | ME 102/103 |
| Portable calibrator/Druck | 600/1231-2 | 0- 600 [kPa] | ME 101 |
| Portable calibrator/Druck | 2925/89-11 | 0- 2000 [kPa] | ME 110 |

| |
|---|
| |
| x |
| |
| x |
| |
| |
| |

Pamb (ME 4) : 100.94 [kPa] a

Tamb : 22 ±1 [°C]

4544-1 102.58 [kPa] a

4544-2 103.28 [kPa] a

δp: 1.6 [kPa]

δp: 2.3 [kPa]

| #1 | #2 | #3 | #4 | #5 | #6 | #7 |
|-----------|---------|---------|-----------|---------|---------|-----------|
| Ref | | 4544-1 | | | 4544-2 | |
| ME 2+ME 4 | | #2-#1 | #3/#2*100 | | #5-#1 | #6/#5*100 |
| [kPa] a | [kPa] a | δ [kPa] | [%] MV | [kPa] a | δ [kPa] | [%] MV |
| 5011.86 | 5013.0 | 1.1 | 0.02 | 5013.7 | 1.8 | 0.04 |
| 5011.56 | 5012.7 | 1.1 | 0.02 | 5013.4 | 1.8 | 0.04 |
| 5011.26 | 5012.4 | 1.1 | 0.02 | 5013.1 | 1.9 | 0.04 |
| 5113.81 | 5114.9 | 1.1 | 0.02 | 5115.6 | 1.8 | 0.04 |
| 5113.41 | 5114.6 | 1.2 | 0.02 | 5115.3 | 1.9 | 0.04 |
| 5113.21 | 5114.3 | 1.1 | 0.02 | 5115.0 | 1.8 | 0.04 |
| 5214.45 | 5215.7 | 1.2 | 0.02 | 5216.3 | 1.9 | 0.04 |
| 5214.05 | 5215.2 | 1.1 | 0.02 | 5215.9 | 1.9 | 0.04 |
| 5213.65 | 5214.7 | 1.1 | 0.02 | 5215.5 | 1.8 | 0.04 |
| 5312.79 | 5313.9 | 1.1 | 0.02 | 5314.6 | 1.8 | 0.03 |
| 5312.09 | 5313.2 | 1.1 | 0.02 | 5314.0 | 1.9 | 0.04 |
| 5311.89 | 5312.9 | 1.0 | 0.02 | 5313.7 | 1.8 | 0.03 |

Average: 1.1 [kPa]

Average: 1.8 [kPa]

| | | | |
|-----------|-------------------------------|----------|--------------------|
| Date/sign | 2000-07-17 <i>[Signature]</i> | Approved | <i>[Signature]</i> |
|-----------|-------------------------------|----------|--------------------|

SEA-BIRD ELECTRONICS, INC.

1808 136th Place N.E., Bellevue, Washington, 98005 USA

Phone: (425) 643 - 9866 Fax (425) 643 - 9954 Email: seabird@seabird.com

SENSOR SERIAL NUMBER: 0316
CALIBRATION DATE: 16-Dec-08

SBE 38 TEMPERATURE CALIBRATION DATA
ITS-90 TEMPERATURE SCALE

ITS-90 COEFFICIENTS

a0 = -1.585645e-005
a1 = 2.759849e-004
a2 = -2.343142e-006
a3 = 1.552764e-007

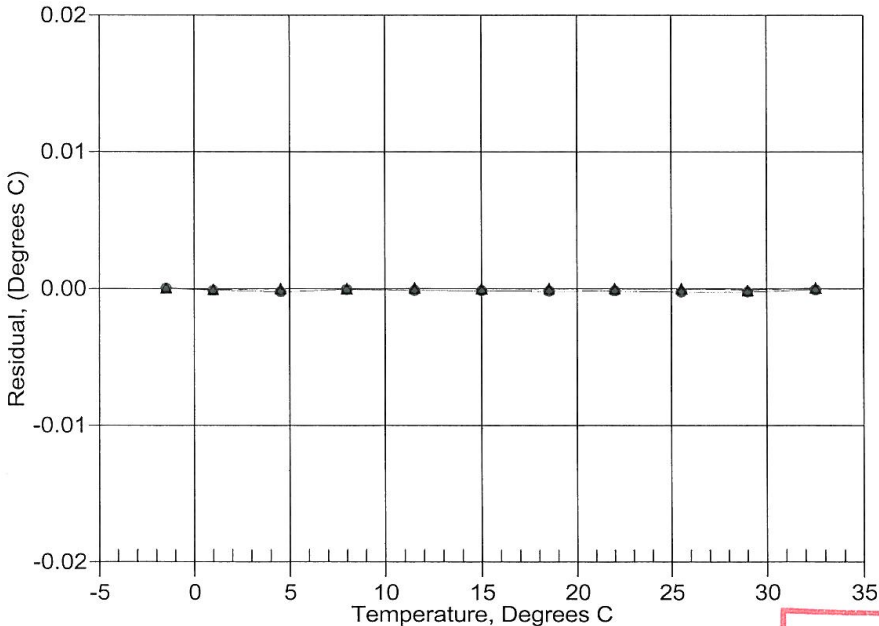
| BATH TEMP (ITS-90) | INSTRUMENT OUTPUT | INST TEMP (ITS-90) | RESIDUAL (ITS-90) |
|-----------------------|----------------------|-----------------------|----------------------|
| -1.50010 | 770364.2 | -1.50005 | 0.00005 |
| 0.99990 | 688193.2 | 0.99984 | -0.00006 |
| 4.49990 | 589347.5 | 4.49989 | -0.00001 |
| 7.99990 | 506346.4 | 7.99989 | -0.00001 |
| 11.49990 | 436411.6 | 11.49994 | 0.00004 |
| 14.99990 | 377294.3 | 14.99990 | 0.00000 |
| 18.49990 | 327159.3 | 18.49991 | 0.00001 |
| 21.99990 | 284509.9 | 21.99992 | 0.00002 |
| 25.49990 | 248118.9 | 25.49990 | -0.00000 |
| 29.00000 | 216976.0 | 28.99989 | -0.00011 |
| 32.49990 | 190247.5 | 32.49997 | 0.00007 |

$$\text{Temperature ITS-90} = 1/\{a_0 + a_1[\ln(n)] + a_2[\ln^2(n)] + a_3[\ln^3(n)]\} - 273.15 \text{ (}^\circ\text{C)}$$

Residual = instrument temperature - bath temperature

Date, Delta T (mdeg C)

- 11-Nov-06 -0.15
- ▲ 16-Dec-08 0.00



OAN
OLE A. NORDBY AS
Vækerovn. 210, 0751 OSLO
Tlf. 22 50 02 60 Fax 22 50 24 10

POST CRUISE
CALIBRATION

SEA-BIRD ELECTRONICS, INC.

1808 136th Place N.E., Bellevue, Washington, 98005 USA

Phone: (425) 643 - 9866 Fax (425) 643 - 9954 Email: seabird@seabird.com

SENSOR SERIAL NUMBER: 0196
CALIBRATION DATE: 12-Dec-08

SBE 38 TEMPERATURE CALIBRATION DATA
ITS-90 TEMPERATURE SCALE

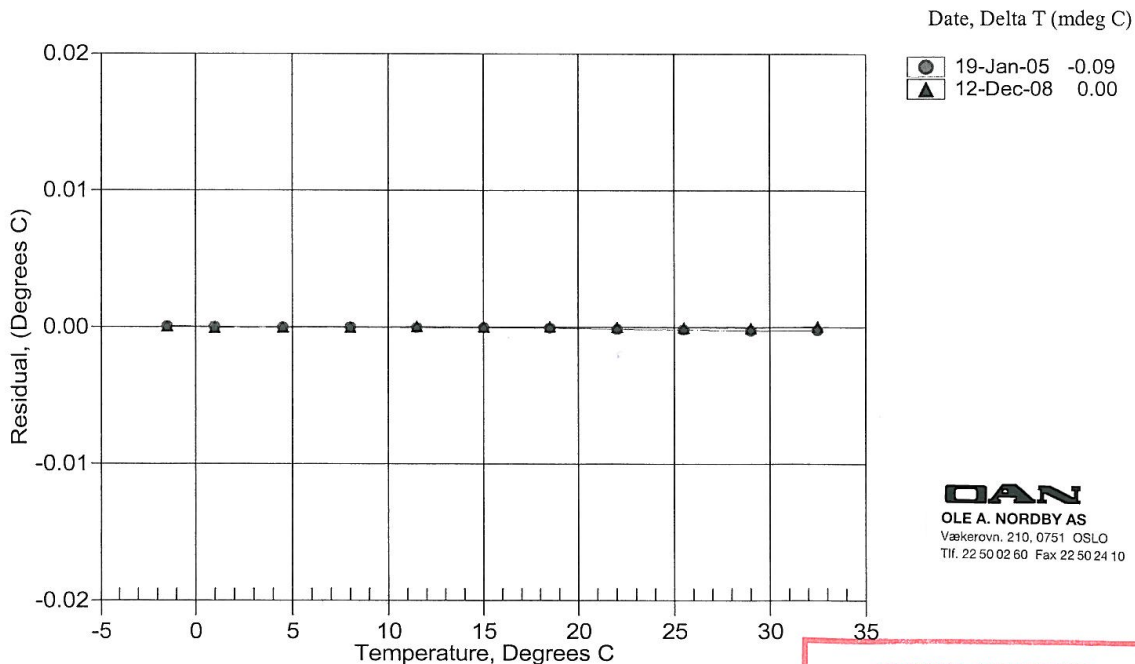
ITS-90 COEFFICIENTS

a0 = -7.325337e-005
a1 = 2.933706e-004
a2 = -3.642166e-006
a3 = 1.949100e-007

| BATH TEMP (ITS-90) | INSTRUMENT OUTPUT | INST TEMP (ITS-90) | RESIDUAL (ITS-90) |
|-----------------------|----------------------|-----------------------|----------------------|
| -1.50010 | 678484.0 | -1.50005 | 0.00005 |
| 0.99990 | 606776.7 | 0.99985 | -0.00005 |
| 4.49990 | 520396.9 | 4.49988 | -0.00002 |
| 7.99990 | 447747.5 | 7.99987 | -0.00003 |
| 11.49990 | 386440.8 | 11.49994 | 0.00004 |
| 14.99990 | 334540.9 | 14.99992 | 0.00002 |
| 18.49990 | 290464.7 | 18.49994 | 0.00004 |
| 21.99990 | 252919.2 | 21.99990 | 0.00000 |
| 25.49990 | 220841.0 | 25.49986 | -0.00004 |
| 28.99990 | 193354.3 | 28.99983 | -0.00007 |
| 32.49990 | 169734.4 | 32.49996 | 0.00006 |

$$\text{Temperature ITS-90} = 1/\{a_0 + a_1[\ln(n)] + a_2[\ln^2(n)] + a_3[\ln^3(n)]\} - 273.15 \text{ (}^\circ\text{C)}$$

Residual = instrument temperature - bath temperature



OAN
OLE A. NORDBY AS
V kerovn. 210, 0751 OSLO
Tlf. 22 50 02 60 Fax 22 50 24 10

POST CRUISE
CALIBRATION

SEA-BIRD ELECTRONICS, INC.

1808 136th Place N.E., Bellevue, Washington, 98005 USA

Phone: (425) 643 - 9866 Fax (425) 643 - 9954 Email: seabird@seabird.com

SENSOR SERIAL NUMBER: 0187
CALIBRATION DATE: 12-Dec-08

SBE 38 TEMPERATURE CALIBRATION DATA
ITS-90 TEMPERATURE SCALE

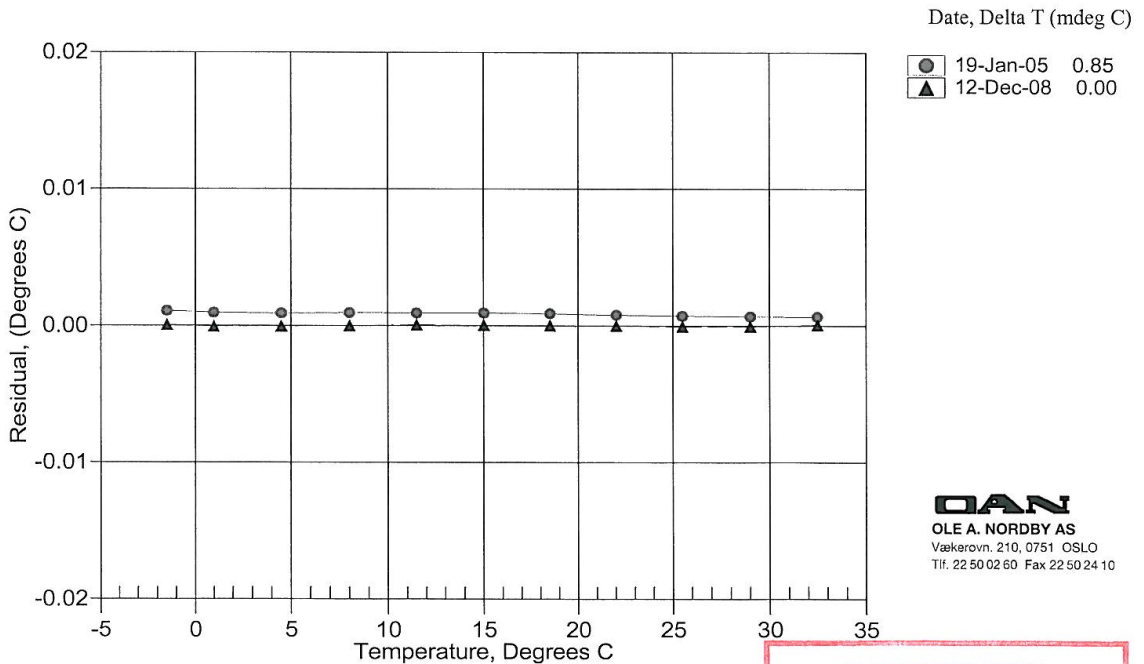
ITS-90 COEFFICIENTS

a0 = -7.292490e-005
a1 = 2.905139e-004
a2 = -3.548210e-006
a3 = 1.832022e-007

| BATH TEMP (ITS-90) | INSTRUMENT OUTPUT | INST TEMP (ITS-90) | RESIDUAL (ITS-90) |
|-----------------------|----------------------|-----------------------|----------------------|
| -1.50010 | 802275.1 | -1.50004 | 0.00006 |
| 0.99990 | 716036.3 | 0.99984 | -0.00006 |
| 4.49990 | 612410.8 | 4.49985 | -0.00005 |
| 7.99990 | 525504.3 | 7.99989 | -0.00001 |
| 11.49990 | 452371.7 | 11.49996 | 0.00006 |
| 14.99990 | 390628.2 | 14.99993 | 0.00003 |
| 18.49990 | 338330.4 | 18.49992 | 0.00002 |
| 21.99990 | 293894.8 | 21.99990 | 0.00000 |
| 25.49990 | 256024.7 | 25.49983 | -0.00007 |
| 28.99990 | 223653.0 | 28.99985 | -0.00005 |
| 32.49990 | 195901.4 | 32.49996 | 0.00006 |

$$\text{Temperature ITS-90} = 1 / \{a_0 + a_1[\ln(n)] + a_2[\ln^2(n)] + a_3[\ln^3(n)]\} - 273.15 \text{ (}^\circ\text{C)}$$

Residual = instrument temperature - bath temperature



OAN
OLE A. NORDBY AS
Vækerovn. 210, 0751 OSLO
Tlf. 22 50 02 60 Fax 22 50 24 10

**POST CRUISE
CALIBRATION**

SEA-BIRD ELECTRONICS, INC.

1808 136th Place N.E., Bellevue, Washington, 98005 USA

Phone: (425) 643 - 9866 Fax (425) 643 - 9954 Email: seabird@seabird.com

SENSOR SERIAL NUMBER: 0315
CALIBRATION DATE: 16-Oct-09

SBE 38 TEMPERATURE CALIBRATION DATA
ITS-90 TEMPERATURE SCALE

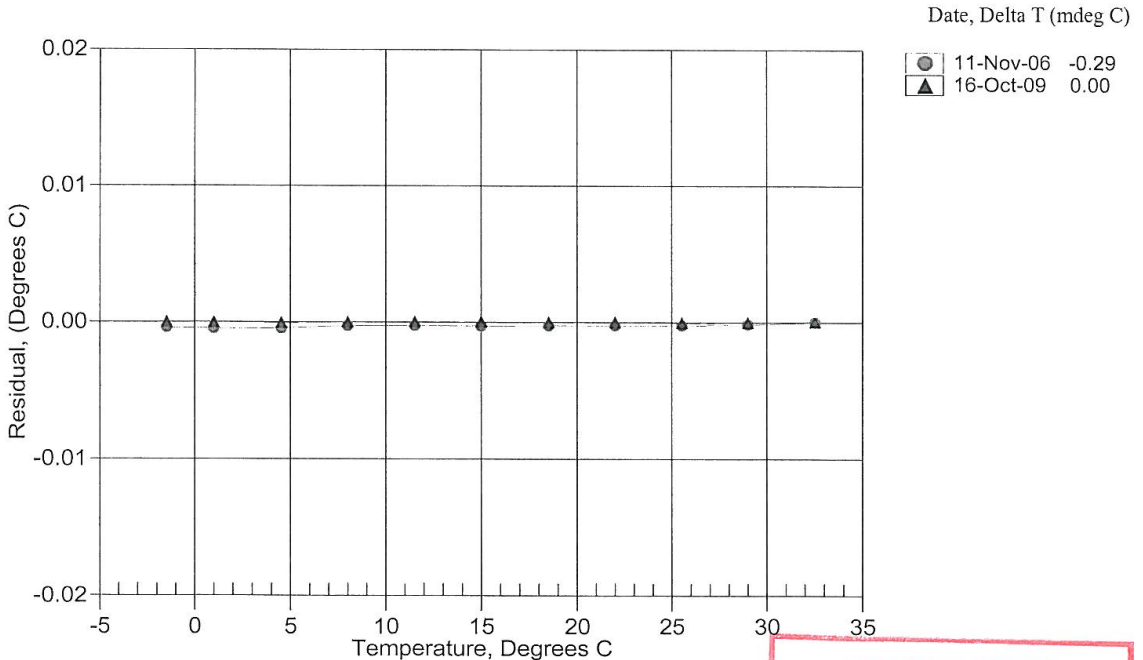
ITS-90 COEFFICIENTS

a0 = -4.501998e-005
a1 = 2.797438e-004
a2 = -2.596485e-006
a3 = 1.627054e-007

| BATH TEMP (ITS-90) | INSTRUMENT OUTPUT | INST TEMP (ITS-90) | RESIDUAL (ITS-90) |
|-----------------------|----------------------|-----------------------|----------------------|
| -1.50010 | 786653.6 | -1.50008 | 0.00002 |
| 0.99980 | 703050.8 | 0.99979 | -0.00001 |
| 4.49990 | 602427.7 | 4.49986 | -0.00004 |
| 7.99990 | 517882.3 | 7.99989 | -0.00001 |
| 11.49990 | 446605.0 | 11.49993 | 0.00003 |
| 14.99990 | 386317.5 | 14.99994 | 0.00004 |
| 18.49990 | 335162.8 | 18.49990 | 0.00000 |
| 21.99990 | 291621.9 | 21.99991 | 0.00001 |
| 25.49990 | 254450.9 | 25.49985 | -0.00005 |
| 28.99990 | 222623.6 | 28.99988 | -0.00002 |
| 32.49990 | 195294.5 | 32.49993 | 0.00003 |

Temperature ITS-90 = $1 / \{a_0 + a_1[\ln(n)] + a_2[\ln^2(n)] + a_3[\ln^3(n)]\} - 273.15$ (°C)

Residual = instrument temperature - bath temperature



**POST CRUISE
CALIBRATION**

SEA-BIRD ELECTRONICS, INC.

1808 136th Place N.E., Bellevue, Washington, 98005 USA

Phone: (425) 643 - 9866 Fax (425) 643 - 9954 Email: seabird@seabird.com

SENSOR SERIAL NUMBER: 0199
CALIBRATION DATE: 16-Oct-09

SBE 38 TEMPERATURE CALIBRATION DATA
ITS-90 TEMPERATURE SCALE

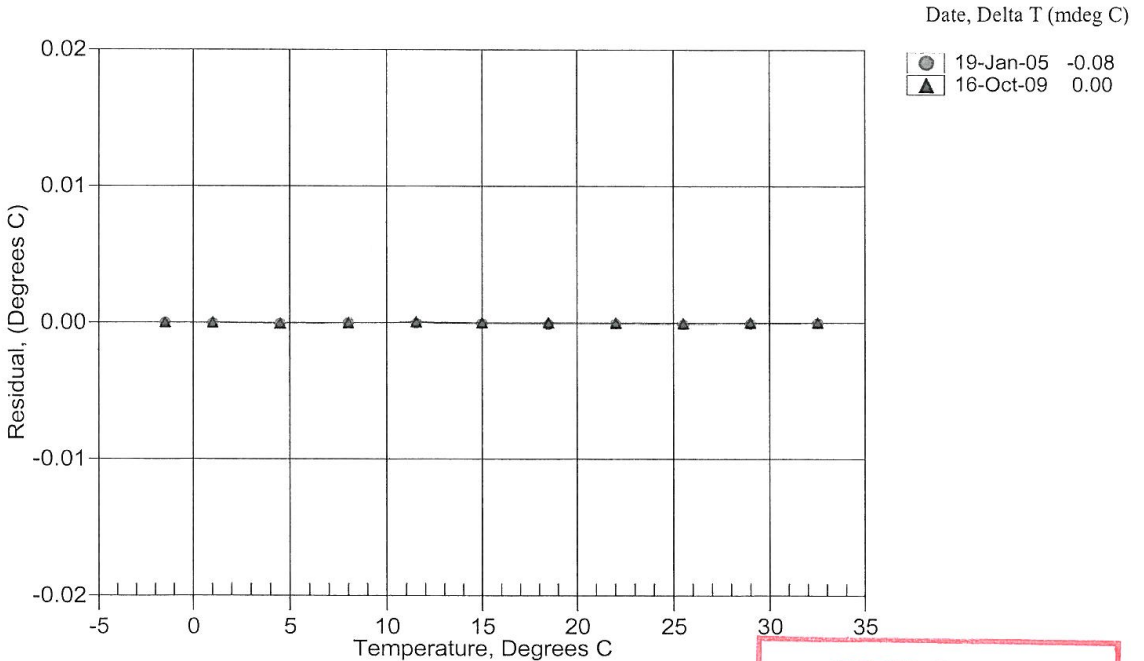
ITS-90 COEFFICIENTS

a0 = -5.194867e-005
a1 = 2.907533e-004
a2 = -3.517530e-006
a3 = 1.888905e-007

| BATH TEMP (ITS-90) | INSTRUMENT OUTPUT | INST TEMP (ITS-90) | RESIDUAL (ITS-90) |
|-----------------------|----------------------|-----------------------|----------------------|
| -1.50010 | 692122.6 | -1.50008 | 0.00002 |
| 0.99980 | 618428.4 | 0.99981 | 0.00001 |
| 4.49990 | 529750.1 | 4.49984 | -0.00006 |
| 7.99990 | 455258.2 | 7.99989 | -0.00001 |
| 11.49990 | 392473.0 | 11.49997 | 0.00007 |
| 14.99990 | 339384.6 | 14.99991 | 0.00001 |
| 18.49990 | 294349.9 | 18.49992 | 0.00002 |
| 21.99990 | 256030.5 | 21.99988 | -0.00002 |
| 25.49990 | 223326.5 | 25.49985 | -0.00005 |
| 28.99990 | 195332.5 | 28.99992 | 0.00002 |
| 32.49990 | 171303.1 | 32.49991 | 0.00001 |

$$\text{Temperature ITS-90} = 1 / \{ a_0 + a_1[\ln(n)] + a_2[\ln^2(n)] + a_3[\ln^3(n)] \} - 273.15 \text{ (}^\circ\text{C)}$$

Residual = instrument temperature - bath temperature



POST CRUISE
CALIBRATION

SEA-BIRD ELECTRONICS, INC.

1808 136th Place N.E., Bellevue, Washington, 98005 USA

Phone: (425) 643 - 9866 Fax (425) 643 - 9954 Email: seabird@seabird.com

SENSOR SERIAL NUMBER: 0242
CALIBRATION DATE: 17-Oct-09

SBE 38 TEMPERATURE CALIBRATION DATA
ITS-90 TEMPERATURE SCALE

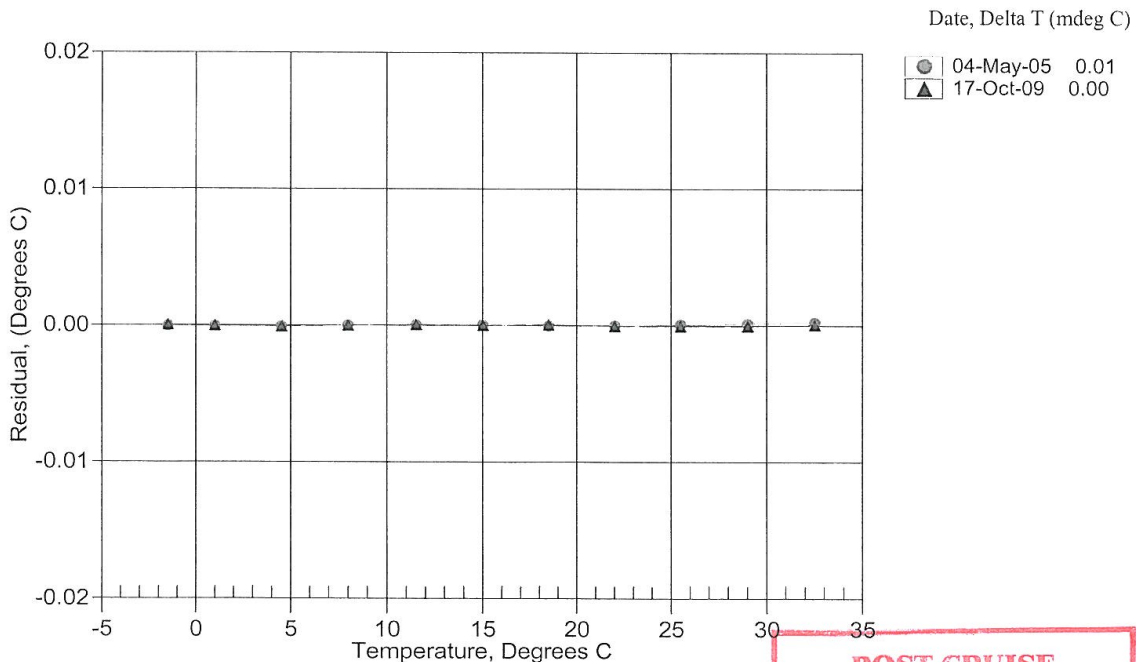
ITS-90 COEFFICIENTS

a0 = -3.417405e-005
a1 = 2.782890e-004
a2 = -2.508966e-006
a3 = 1.596827e-007

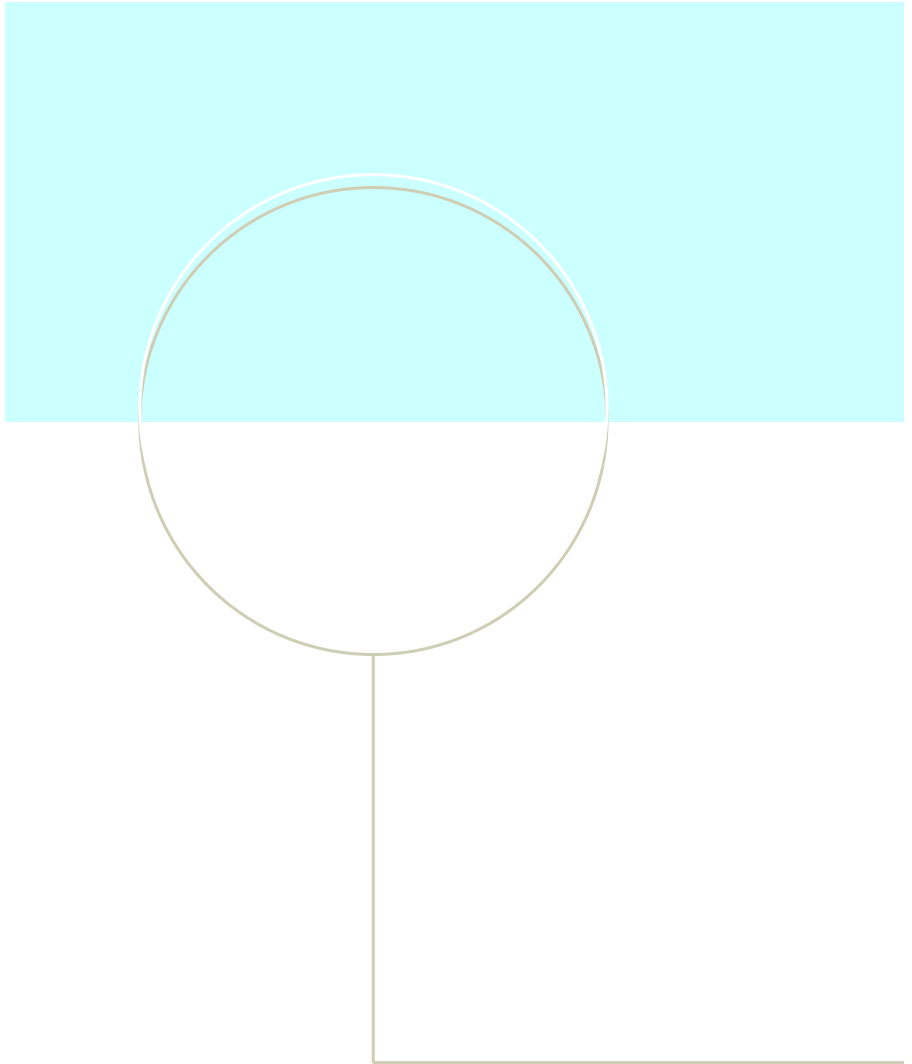
| BATH TEMP (ITS-90) | INSTRUMENT OUTPUT | INST TEMP (ITS-90) | RESIDUAL (ITS-90) |
|-----------------------|----------------------|-----------------------|----------------------|
| -1.50010 | 787543.6 | -1.50005 | 0.00005 |
| 0.99980 | 703651.8 | 0.99977 | -0.00003 |
| 4.49990 | 602713.8 | 4.49982 | -0.00008 |
| 7.99990 | 517935.4 | 7.99989 | -0.00001 |
| 11.49990 | 446489.2 | 11.49997 | 0.00007 |
| 14.99990 | 386082.5 | 14.99992 | 0.00002 |
| 18.49980 | 334844.5 | 18.49986 | 0.00006 |
| 21.99990 | 291247.6 | 21.99987 | -0.00003 |
| 25.49990 | 254041.2 | 25.49984 | -0.00006 |
| 28.99990 | 222194.5 | 28.99985 | -0.00005 |
| 32.49990 | 194857.1 | 32.49996 | 0.00006 |

Temperature ITS-90 = $1 / \{a_0 + a_1[\ln(n)] + a_2[\ln^2(n)] + a_3[\ln^3(n)]\} - 273.15$ (°C)

Residual = instrument temperature - bath temperature



**POST CRUISE
CALIBRATION**



NTNU – Trondheim
Norwegian University of
Science and Technology